Dual N⁶/C7-substituted 7-deazapurine and tricyclic ribonucleosides with affinity for G protein-coupled receptors

Dual N^6/C7-substituted 7-deazapurine and tricyclic ribonucleosides with affinity for G protein-coupled receptors

Simon Krols[1], Federica Matteucci[1], Kristof Van Hecke[2], Guy Caljon[3], Kenneth A. Jacobson[4], Serge Van Calenbergh[1*]

[1] Laboratory for Medicinal Chemistry, Faculty of Pharmaceutical Sciences, Ghent University, Ottergemsesteenweg 460, 9000 Ghent, Belgium

[2] XStruct, Department of Chemistry, Ghent University, Krijgslaan 281-S3, 9000 Ghent, Belgium

[3] Laboratory of Microbiology, Parasitology and Hygiene (LMPH), University of Antwerp, Universiteitsplein 1, B-2610 Wilrijk, Belgium

[4] Molecular Recognition Section, Laboratory of Bioorganic Chemistry, National Institute of Diabetes and Digestive and Kidney Diseases, National Institutes of Health, 9000 Rockville Pike, Bethesda, Maryland 20892, United States

ABSTRACT: Various purine-based nucleoside analogues have demonstrated unexpected affinity for non-purinergic G protein-coupled receptors (GPCRs), such as opioid and serotonin receptors. In this work we synthesized a small library of new 7-deazaadenosine and pyrazolo[3,4-*d*]pyrimidine riboside analogues, featuring dual C7 and N^6 modifications and assessed their affinity for various GPCRs. During the course of the synthesis of 7-ethynyl pyrazolo[3,4-*d*]pyrimidine ribosides, we observed the formation of an unprecedented tricyclic nucleobase, formed via a 6-*endo-dig* ring closure. The synthesis of this tricyclic nucleoside was optimized, and the substrate scope for such cyclisation further explored, since it might avail further exploration in the nucleoside field. From displacement experiments on a panel of GPCRs and transporters, combining C7 and N^6-modifications afforded non-cytotoxic nucleosides with micromolar and submicromolar affinity for different GPCRs, such as the 5-hydroxytryptamine $(5\text{-HT})_{2B}$, κ-opioid (KOR) and $\sigma_{1/2}$ receptor. These results corroborate that the novel nucleoside analogues reported here are potentially useful starting points for the further development of modulators of GPCRs and transmembrane proteins.

Keywords: Tricyclic nucleosides, GPCRs, 7-deazaadenosine, Tubericidin, , 6-endo-dig cyclisation, Triciribine

G protein-coupled receptors (GPCRs) are transmembrane receptors representing the largest membrane protein family, with approximately 800 known GPCRs.[1] They regulate a vast array of physiological functions by transducing various signals from the extracellular environment into the cell. Given GPCRs' important roles in a wide spectrum of diseases, including asthma, diabetes, cardiovascular and neurological disorders, they have been of long-standing interest as drug targets, resulting in over 475 approved GPCR-targeting drugs (accounting for approximately 34% of all FDA-approved drugs).[2–4] Adenosine (Figure 1A) and its corresponding nucleotide, ATP, are endogenous ligands for purinergic receptors[5], and various derivatives have been synthesized to modulate this class of GPCRs.[6,7] Examination of off-target

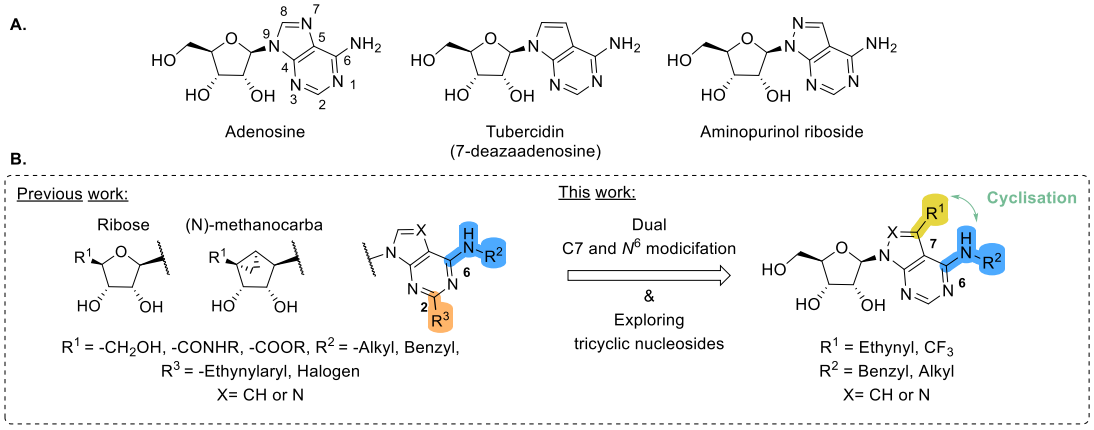

Figure 1. A) Chemical structures of adenosine, tubercidin and aminopurinol riboside. The purine base numbering is highlighted on adenosine. B) Earlier reported nucleosidic non-purinergic GPCR ligands (left) and combined C7 and N^6 substitutions on tubercidin and aminopurinol riboside explored in this work (right).

Scheme 1. Synthesis of 7-trifluoro- and 7-ethynyl-7-deazaadenosine nucleoside analogues

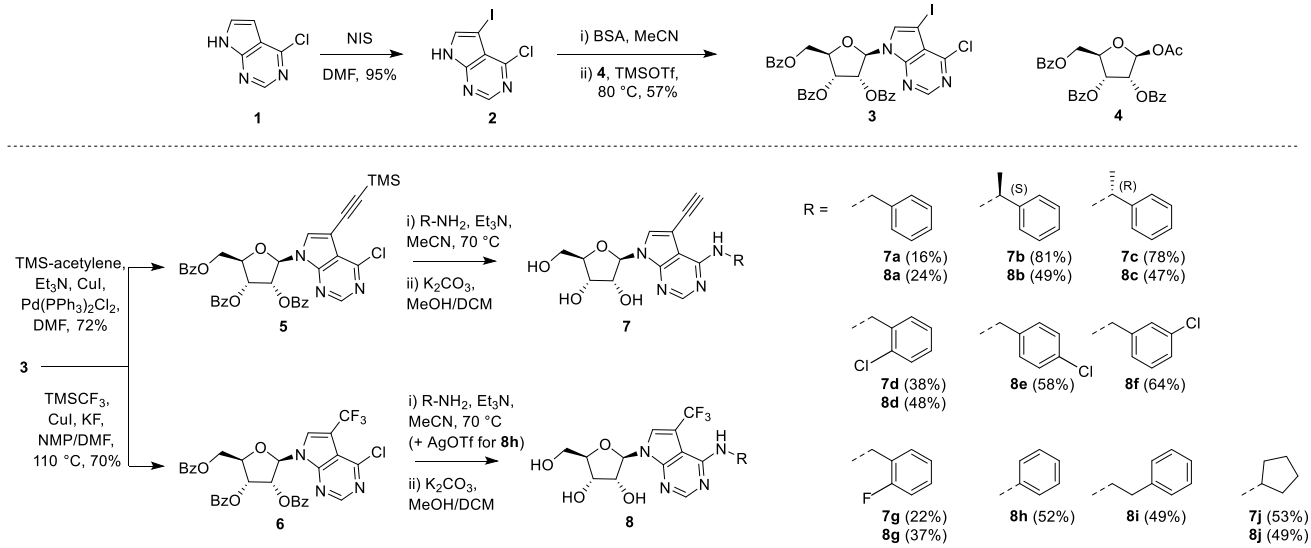

effects of reported adenosine receptor modulators has unveiled unexpected affinities for non-purinergic GPCRs, including serotonin (5-HT) and opioid receptors[8,9], as well as transporter proteins.[10] Further structure activity relationship studies have demonstrated the potential for enhancing affinity and selectivity for non-purinergic receptors. For instance, the incorporation of a bicyclo[3.1.0]hexane fused ring, also called (N)-methanocarba, in place of a ribose ring, greatly increased 5-HT_{2B} receptor affinity.[8] Switching 5'-amides into 5'-esters and incorporation of a 7-deazaadenine nucleobase increased selectivity for k-opioid receptors (KOR) over the A3 adenosine receptor.[11] Additionally, various C2 substitutions and N^6 substitution with selected alkyl or benzyl moieties influenced affinity for both purinergic and non-purinergic GPCRs.[12] These examples highlight the potential of utilizing nucleosides as GPCR binders with non-nucleoside endogenous ligands and the possibility of fine-tuning GPCR affinity of purine nucleosides by chemical modifications. In our pursuit of finding new entry points for modulating transmembrane proteins, we synthesized a small library of unique nucleoside analogues and screened these against a panel of different GPCR receptors and transporter proteins. The 7-deazaadenosine (tubercidin[13]) and pyrazolo[3,4-*d*]pyrimidine derivatives were designed as to comprise privileged N^6-benzyl and cyclopentyl substitutions, since these have been extensively shown to modulate GPCR affinity.[12] In contrast, C7-substituents on 7-deazapurine nucleosides have not been thoroughly studied in the context of GPCRs, although 7-ethynyl or 7-trifluoromethyl modifications provided potent anti-cancer, anti-parasitic and anti-viral agents.[14–18] This incited us to combine the aforementioned N^6-substitution patterns with a 7-CF_3 or a 7-ethynyl motif.

The synthesis of such dual N^6/C7 modified 7-deazaadenosine analogues **7** and **8** is depicted in **Scheme 1**. It started with the 5-iodination of commercially available 4-chloro-7*H*-pyrrolo[2,3-*d*]pyrimidine (**1**) with *N*-Iodosuccinimide (NIS), followed by modified Vorbrüggen glycosylation with 1-*O*-acetyl-tri-*O*-benzoylribofuranose (**4**).[19] The iodine in the resulting intermediate **3** was readily converted into a TMS-protected ethynyl group under Sonogashira conditions. Chlorine displacement by the appropriate amines delivered nucleosides **7a-d, g, j** after benzoyl removal with K_2CO_3 in MeOH. A 7-CF_3-group was installed via a cross-coupling reaction of **3** with *in situ*-formed $CuCF_3$.[20] Subsequent S_NAR with various amines went smoothly. Coupling of the less nucleophilic aniline was achieved upon addition of AgOTf. Finally, benzoyl protecting group removal delivered the desired analogues **8 a-j**. Besides 7-ethynyl-7-deazaadenosine analogues **7**, we explored the synthesis of related 7-ethynylaminopurinol derivatives (**Scheme 2**). Coupling of 3-iodo-4-chloro-*1H*-pyrazolo[3,4-*d*]pyrimidine under the Vorbrüggen conditions applied for the corresponding 7-deazapurine failed. This led us to perform the glycosylation with iodinated allopurinol **10**. Glycosylation with BF_3OEt_2 in refluxing nitromethane resulted in the desired *N*-9 glycosylated product **11**, albeit in low yields due to concomitant formation of substantial amounts of the *N*-8 regioisomer. Subsequent Sonogashira coupling, introduction of a 6-chloro group with $SOCl_2$ in DMF/$CHCl_3$ and S_NAR with benzylamine yielded **14**.

Scheme 2. Initial attempt towards 7-ethynyl-aminopurinol riboside analogues resulted in a 6-endo-dig-cyclisation.

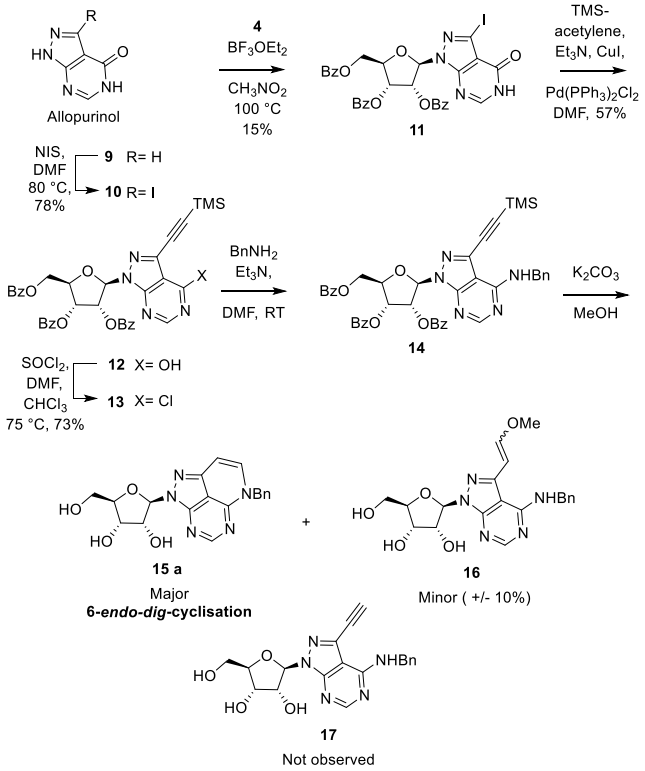

Scheme 3. Optimized synthesis route towards tricyclic nucleosides

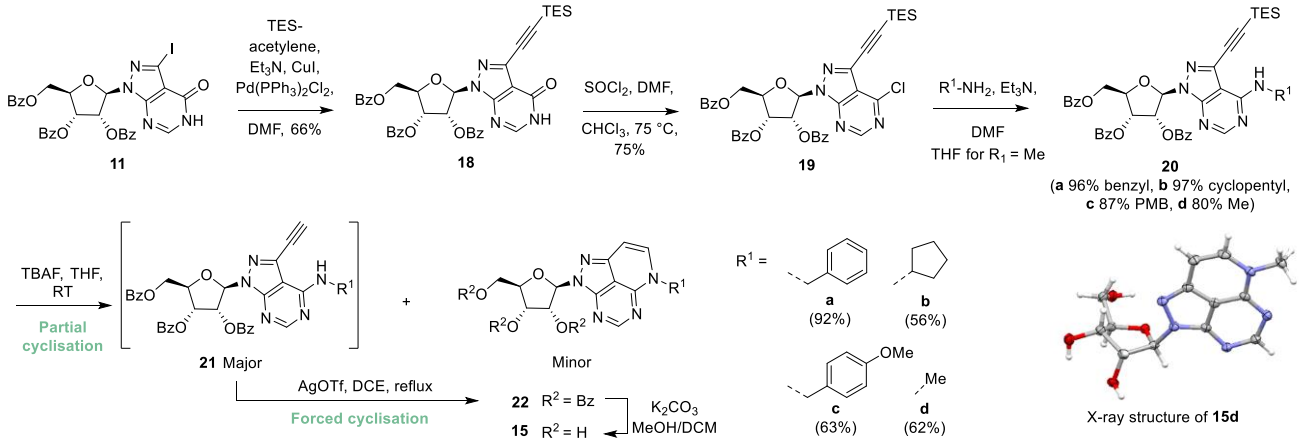

However, treatment with K_2CO_3 in MeOH to remove the TMS and benzoyl protecting groups did not afford the expected nucleoside **17**. Instead, the 6-*endo-dig* cyclised isomer **15a** was observed as the main product, together with an inseparable side product, presumed to be MeOH adduct **16** (Supporting Info.). This serendipitous finding encouraged us to elaborate on the synthesis of these tricyclic nucleosides (**Scheme 3**). Since TMS-removal was observed during Sonogashira coupling and the subsequent S_NAR, we opted for a more stable alkyne triethylsilyl (TES) protecting group. After introducing the TES-protected alkyne at position 7 and converting the 6-OH to a 6-Cl group, the latter was substituted with different primary amines. To prevent formation of MeOH adduct **16**, we removed the TES group with tetra-n-butylammonium fluoride (TBAF). This resulted in a mixture of ethynyl analogues **21** as the major products and around 20-30% of the corresponding cyclised isomers (**22**). The remaining ethynyl analogues **21** could be fully converted into the cyclised isomers **22** by treating the crude mixture with catalytic amounts of AgOTf in refluxing DCE. Finally, alcohol group deprotection delivered tricyclic nucleosides **15a-d**. An X-ray structure of methyl analogue **15d** unambiguously confirmed the formation of the 6-*endo-dig*-cyclised product (**Scheme 3**). Remarkably, efforts to cyclize the related N^6-benzyl-7-ethynyl-7-deazaadenosine (**7a**, Bz-protected), 7-ethynylallopurinol riboside (**23**) and 7-ethynylaminopurinol[21] (**25**) analogues were not successful (**Scheme 4**, **Table S3 and S4**), indicating that an electron withdrawing nitrogen at position 8 and an electron donating alkyl group on N^6 are required for cyclisation and that a 6-OH is not nucleophilic enough to undergo this transformation. Attempts to remove the p-methoxybenzyl (PMB) group of **22c** (R^1 = PMB) via hydrogenation, oxidation with DDQ/CAN or under acidic conditions (e.g., HCl, TFA) failed to afford the unsubstituted N^6-cyclised aminopurinol analogue **26** (**Table S5**). Since cyclisation of an aminopurinol **25** and allopurinol **23** riboside failed, we prepared the corresponding 6-thio analogue by treating intermediate **19** with thiourea. Upon TBAF removal of the TES group, spontaneous cyclisation occurred and afforded nucleoside **29** after benzoyl deprotection.

Scheme 4. Exploration of the scope of the 6-*endo-dig* cyclisation reaction.

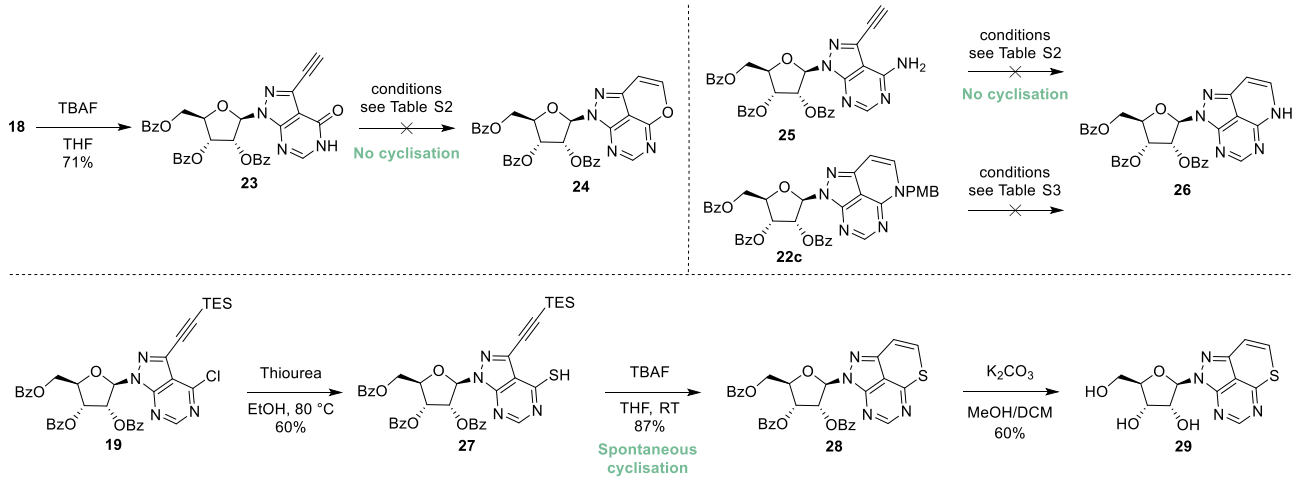

Incited by the previously reported activity of adenosine congeners against serotonin (5-HT), opioid receptors and noradrenaline and dopamine transporters,[8–10] we screened our analogues against a panel of related signalling proteins (total 45 targets). Hits were observed for receptors (5-HT_{1B}, 5-HT_{1D}, 5-HT_{2A}, 5-HT_{2B}, 5-HT_{2C}, 5-HT_6, 5-HT_{7A}, α_{2C}, M_5, DOR, KOR, MOR, σ_1, σ_2) and transporters (NET, DAT, TSPO) (**Table 1**, **Table S1** and **S2**). Combining a 7-ethynyl group with a N^6-benzyl substituent resulted in analogue **7a** with moderate affinity for $\boldsymbol{\sigma_1/\sigma_2}$. Interestingly, compound **15a**, the cyclised variant of **7a**, did not inhibit $\boldsymbol{\sigma_1/\sigma_2}$, but showed selective affinity for the 5-HT_{1D} receptor (K_i 2.6 µM). Derivative **8a**, which

features a 7-CF_3 and a N^6-benzyl substituent, displayed K_i values of 0.50 µM and 1.0 µM for the 5-HT_{2B} and 5-HT_6 receptor, respectively. The sub-micromolar 5-HT_{2B} affinity found for **8a**, led us to explore the effect of different substituted benzyl derivatives (**8b-g**). Introduction of a chlorine in para (**8e**) and ortho (**8d**) position of the phenyl ring gave a similar inhibitory binding activity for the 5-HT_{2B} receptor, but increased selectivity versus the 5-HT_6 receptor. Analogue **8f** with a chlorine in meta position and **8g** with a fluor in ortho also displayed promising 5-HT_{2B} receptor affinity (K_i values of 0.62 and 1.2 µM). The same applies to *R*-methylbenzyl derivative **8c** (K_i = 0.71 µM), while its *S*-diastereoisomer **8b** preferred KOR binding (K_i = 1.9 µM). Notably, while tubercidin and its C7-substituted analogues display strong cytotoxic effects,[14–16] non of our synthesized analogues proved toxic to MRC-5 fibroblasts, except for tricyclic *N*-Me derivative **15d** (**Table S2**). More extensive biological data can be found in supplementary **Tables S1** (7-deazaadenosine) and **S2** (tricyclic nucleosides).

Overall, we successfully synthesized a library of new 7-deazaadenosine ribonucleosides that combine a 7-ethynyl or 7-CF_3 modification with N^6 substituents and were able to identify new (sub)micromolar hits for different GPCRs such as 5-HT_{1D}, $_{2B}$, KOR, and $\sigma_{1/2}$. The structure activity relationship (SAR) of the discovered hits here can be potentially further developed by additional structural modification. For instance, we previously showed that incorporation of a bicyclo[3.1.0]hexane ring system in other nucleoside scaffolds with moderate 5-HT_{2B} binding, greatly increased binding affinity, pending further exploration of the series discovered here.[9,11] Moreover, the previous reported nucleoside based 5-HT_{2B} binders turned out to be antagonistic and it will be interesting to confirm this for the 5-HT_{2B} receptor binders (**8a**, **8d**, **8f**…) discovered here. Potent structurally distinct 5-HT_{2B} antagonists have been discovered recently via high-throughput screening[22] and might be of interest as antifibrotic agents or inflammatory conditions in lung or liver.[23–26] Additionally, we serendipitously discovered ribonucleosides with a tricyclic nucleobase and provide a practical synthesis route towards these analogues via a 6-*endo-dig* cyclisation. We studied it's the substrate scope and believe that this may catalyse the field to further develop nucleoside analogues with such unprecedented tricyclic nucleobases for other applications. In the tricyclic series, *N*-benzyl derivative **15a** showed only weak binding for the 5-HT_{1D} receptor. Of note, the structure of the tricyclic N-methyl analogue **15d** is reminiscent of that of the anti-cancer agent triciribine.[27–30] Furthermore, nucleotides with altered bases have been of long-standing interest in synthetic biology to expand the genetic alphabets, or to modify the shape/size, hydrophobicity, and pi-electron interactions in DNA and RNA duplex formation[31–33] and to visualize nucleic acid processes.[34] It might therefor be useful to study e.g. the base pairing capabilities of nucleos(t)ides with such a tricyclic scaffold.

Table 1. Binding inhibition at diverse targets (K_i, µM) and cytotoxicity in MRC-5 fibroblasts (CC_{50} in µM) of selected dual C7/N^6 7-deazaadenosine analogues and tricyclic analogue 15a.

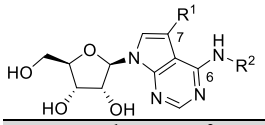

	R^1	R^2	5-HT_{1D}	5-HT_{2B}	5-HT_6	α_{2C}	KOR	σ_1	σ_2	MRC-5
7a			<	<	<	<	<	3.5 ±1.1	3.4 ±0.7	> 64
8a			<	0.50 ±0.10	1.0 ±0.2	2.5 ±1.3	1.8 ±0.3	3.3 ±1.0	<	> 64
8b			<	<	<	<	1.9 ±0.7	6.5 ±3.5	5.3 ±1.8	> 64
8c			<	0.71 ±0.10	<	<	<	<	1.8 ±0.1	41.8
8e		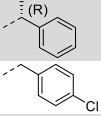	<	0.83 ±0.03	<	<	<	2.3 ±0.2	<	> 64
8d			2.5 ±1.0	0.55 ±0.15	<	<	<	3.4 ±1.4	3.4 ±1.1	> 64
8f			<	0.62 ±0.35	<	<	<	<	<	> 64
8g			<	1.2 ±0.3	<	<	<	<	<	> 64
15a	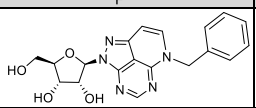		2.6 ±0.1	<	<	<	<	<	<	> 64

A primary radioligand binding screen was performed at each target protein using a fixed concentration of 10 µM (n=4). A K_i-value (represented in the table as mean ± SEM (µM)) was determined for analogues showing > 50% inhibition (n = 3). Analogues showing < 50% inhibition are indicated with '<'. The exact values can be found in **Table S1 and S2**. The cytotoxicity experiment was performed in duplicate.

ASSOCIATED CONTENT

Data availability

The data underlying this study are available in the published article and its Supporting Information.

Supporting Information

Detailed experimental procedures of chemical reactions and crystal X-ray data, characterization data and spectra (HRMS, NMR, LCMS) of intermediates and final compounds, detailed inhibition values and curves of final compounds on the receptors/transporters tested. (PDF)

AUTHOR INFORMATION

Corresponding Author

*Serge Van Calenbergh, Serge.VanCalenbergh@UGent.be,

Author Contributions

The manuscript was written through contributions of all authors. All authors have given approval to the final version of the manuscript.

Notes

The authors declare no competing financial interest.

Funding:. The research of the manuscript was supported/funded by FWO grant 1S80521N and by NIDDK Intramural Research grant ZIADK031117 (KAJ). We thank the special research fund (BOF) from UGhent (project BOF 24Y2023001501).

ACKNOWLEDGMENT

We thank Izet Karalic for technical assistance and measuring HRMS spectra, Dr. Bryan L. Roth (Univ. North Carolina at Chapel Hill) and National Institute of Mental Health's Psychoactive Drug Screening Program (Contract # HHSN-271-2008-00025-C) for screening data. We thank as well Veronique Van Speybroeck and Kuber Singh Rawat for their scientific contributions and Natascha Van Pelt and An Matheeussen for their help with performing cytotoxicity studies.

ABBREVIATIONS

ATP, Adenosine triphosphate; BSA, Bis(trimethylsilyl)acetamide; DAT, Dopamine transporter; FDA, Food and Drug administration; GPCR, G protein-coupled receptors; 5-HT, 5-Hydroxytryptamine; KOR, κ-Opioid receptor; MRC-5, Medical Research Council- cell strain 5; NET, Norepinephrine transporter; NIS, *N*-Iodosuccinimide; SAR, Structure activity relationship; TBAF, Tetra-n-butylammonium fluoride; TES, Triethylsilyl; TMS, Trimethylsilyl; TSPO, Translocator protein; PMB, para-methoxybenzyl;

REFERENCES

(1) Fredriksson, R.; Lagerström, M. C.; Lundin, L.-G.; Schiöth, H. B. The G-Protein-Coupled Receptors in the Human Genome Form Five Main Families. Phylogenetic Analysis, Paralogon Groups, and Fingerprints. *Mol Pharmacol* **2003**, *63* (6), 1256–1272. https://doi.org/10.1124/mol.63.6.1256.

(2) Hauser, A. S.; Attwood, M. M.; Rask-Andersen, M.; Schiöth, H. B.; Gloriam, D. E. Trends in GPCR Drug Discovery: New Agents, Targets and Indications. *Nat Rev Drug Discov* **2017**, *16* (12), 829–842. https://doi.org/10.1038/nrd.2017.178.

(3) Rask-Andersen, M.; Masuram, S.; Schiöth, H. B. The Druggable Genome: Evaluation of Drug Targets in Clinical Trials Suggests Major Shifts in Molecular Class and Indication. *Annu Rev Pharmacol Toxicol* **2014**, *54* (1), 9–26. https://doi.org/10.1146/annurev-pharmtox-011613-135943.

(4) Sriram, K.; Insel, P. A. G Protein-Coupled Receptors as Targets for Approved Drugs: How Many Targets and How Many Drugs? *Mol Pharmacol* **2018**, *93* (4), 251–258. https://doi.org/10.1124/mol.117.111062.

(5) Fredholm, B. B.; IJzerman, A. P.; Jacobson, K. A.; Klotz, K. N.; Linden, J. International Union of Pharmacology. XXV. Nomenclature and Classification of Adenosine Receptors. *Pharmacol Rev* **2001**, *53* (4), 527–552.

(6) Jacobson, K. A.; IJzerman, A. P.; Müller, C. E. Medicinal Chemistry of P2 and Adenosine Receptors: Common Scaffolds Adapted for Multiple Targets. *Biochem Pharmacol* **2021**, *187*, 114311. https://doi.org/10.1016/j.bcp.2020.114311.

(7) Jacobson, K. A.; Gao, Z.-G. Adenosine Receptors as Therapeutic Targets. *Nat Rev Drug Discov* **2006**, *5* (3), 247–264. https://doi.org/10.1038/nrd1983.

(8) Tosh, D. K.; Ciancetta, A.; Warnick, E.; Crane, S.; Gao, Z.-G.; Jacobson, K. A. Structure-Based Scaffold Repurposing for G Protein-Coupled Receptors: Transformation of Adenosine Derivatives into 5HT $_{2B}$ /5HT $_{2C}$ Serotonin Receptor Antagonists. *J Med Chem* **2016**, *59* (24), 11006–11026. https://doi.org/10.1021/acs.jmedchem.6b01183.

(9) Tosh, D. K.; Calkins, M. M.; Ivancich, M. S.; Bock, H. A.; Campbell, R. G.; Lewicki, S. A.; Chen, E.; Gao, Z.-G.; McCorvy, J. D.; Jacobson, K. A. Structure Activity Relationships of 5-HT2B and 5-HT2C Serotonin Receptor Antagonists: N6, C2 and 5′-Modified (N)-Methanocarba-Adenosine Derivatives. *Eur J Med Chem* **2023**, *259*, 115691. https://doi.org/10.1016/j.ejmech.2023.115691.

(10) Tosh, D. K.; Janowsky, A.; Eshleman, A. J.; Warnick, E.; Gao, Z.-G.; Chen, Z.; Gizewski, E.; Auchampach, J. A.; Salvemini, D.; Jacobson, K. A. Scaffold Repurposing of Nucleosides (Adenosine Receptor Agonists): Enhanced Activity at the Human Dopamine and Norepinephrine Sodium Symporters. *J Med Chem* **2017**, *60* (7), 3109–3123. https://doi.org/10.1021/acs.jmedchem.7b00141.

(11) Tosh, D. K.; Ciancetta, A.; Mannes, P.; Warnick, E.; Janowsky, A.; Eshleman, A. J.; Gizewski, E.; Brust, T. F.; Bohn, L. M.; Auchampach, J. A.; Gao, Z.-G.; Jacobson, K. A. Repurposing of a Nucleoside Scaffold from Adenosine Receptor Agonists to Opioid Receptor Antagonists. *ACS Omega* **2018**, *3* (10), 12658–12678. https://doi.org/10.1021/acsomega.8b01237.

(12) Jacobson, K. A.; IJzerman, A. P.; Müller, C. E. Medicinal Chemistry of P2 and Adenosine Receptors: Common Scaffolds Adapted for Multiple Targets. *Biochem Pharmacol* **2021**, *187*, 114311. https://doi.org/10.1016/j.bcp.2020.114311.

(13) Acs, G.; Reich, E.; Mori, M. Biological and Biochemical Properties of the Analogue Antibiotic Tubercidin. *Proceedings of the National Academy of Sciences* **1964**, *52* (2), 493–501. https://doi.org/10.1073/pnas.52.2.493.

(14) Nauš, P.; Caletková, O.; Konečný, P.; Džubák, P.; Bogdanová, K.; Kolář, M.; Vrbková, J.; Slavětínská, L.; Tloušťová, E.; Perlíková, P.; Hajdúch, M.; Hocek, M. Synthesis, Cytostatic, Antimicrobial, and Anti-HCV Activity of 6-Substituted 7-(Het)Aryl-7-Deazapurine Ribonucleosides. *J Med Chem* **2014**, *57* (3), 1097–1110. https://doi.org/10.1021/jm4018948.

(15) Bourderioux, A.; Nauš, P.; Perlíková, P.; Pohl, R.; Pichová, I.; Votruba, I.; Džubák, P.; Konečný, P.; Hajdúch, M.; Stray, K. M.; Wang, T.; Ray, A. S.; Feng, J. Y.; Birkus, G.; Cihlar, T.; Hocek, M. Synthesis and Significant Cytostatic Activity of 7-Hetaryl-7-Deazaadenosines. *J Med Chem* **2011**, *54* (15), 5498–5507. https://doi.org/10.1021/jm2005173.

(16) Nauš, P.; Perlíková, P.; Bourderioux, A.; Pohl, R.; Slavětínská, L.; Votruba, I.; Bahador, G.; Birkuš, G.; Cihlář, T.; Hocek, M. Sugar-Modified Derivatives of Cytostatic 7-(Het)Aryl-7-Deazaadenosines: 2′-C-Methylribonucleosides, 2′-Deoxy-2′-Fluoroarabinonucleosides, Arabinonucleosides and 2′-Deoxyribonucleosides. *Bioorg Med Chem* **2012**, *20* (17), 5202–5214. https://doi.org/10.1016/j.bmc.2012.07.003.

(17) Bouton, J.; Ferreira De Almeida Fiuza, L.; Cardoso Santos, C.; Mazzarella, M. A.; De Nazaré Correia Soeiro, M.; Maes, L.; Karalic, I.; Caljon, G.; Van Calenbergh, S. Revisiting Pyrazolo[3,4-d]Pyrimidine Nucleosides as Anti- Trypanosoma Cruzi and Antileishmanial Agents. *J Med Chem* **2021**, *64* (7), 4206–4238. https://doi.org/10.1021/acs.jmedchem.1c00135.

(18) Tsukamoto, Y.; Hiono, T.; Yamada, S.; Matsuno, K.; Faist, A.; Claff, T.; Hou, J.; Namasivayam, V.; vom Hemdt, A.; Sugimoto, S.; Ng, J. Y.; Christensen, M. H.; Tesfamariam, Y. M.; Wolter, S.; Juranek, S.; Zillinger, T.; Bauer, S.; Hirokawa, T.; Schmidt, F. I.; Kochs, G.; Shimojima, M.; Huang, Y.-S.; Pichlmair, A.; Kümmerer,

B. M.; Sakoda, Y.; Schlee, M.; Brunotte, L.; Müller, C. E.; Igarashi, M.; Kato, H. Inhibition of Cellular RNA Methyltransferase Abrogates Influenza Virus Capping and Replication. *Science (1979)* **2023**, *379* (6632), 586–591. https://doi.org/10.1126/science.add0875.

(19) Hulpia, F.; Bouton, J.; Campagnaro, G. D.; Alfayez, I. A.; Mabille, D.; Maes, L.; de Koning, H. P.; Caljon, G.; Van Calenbergh, S. C6–O-Alkylated 7-Deazainosine Nucleoside Analogues: Discovery of Potent and Selective Anti-Sleeping Sickness Agents. *Eur J Med Chem* **2020**, *188*. https://doi.org/10.1016/j.ejmech.2019.112018.

(20) Cottet, F.; Schlosser, M. Trifluoromethyl-Substituted Pyridines Through Displacement of Iodine by in Situ Generated (Trifluoromethyl)Copper. *European J Org Chem* **2002**, *2002* (2), 327–330. https://doi.org/10.1002/1099-0690(20021)2002:2<327::AID-EJOC327>3.0.CO;2-V.

(21) Zheng, Y.; Beal, P. A. Synthesis and Evaluation of an Alkyne-Modified ATP Analog for Enzymatic Incorporation into RNA. *Bioorg Med Chem Lett* **2016**, *26* (7), 1799–1802. https://doi.org/10.1016/j.bmcl.2016.02.038.

(22) Bender, A. M.; Valentine, M. S.; Bauer, J. A.; Days, E.; Lindsley, C. W.; Merryman, W. D. Identification of Potent, Selective, and Peripherally Restricted Serotonin Receptor 2B Antagonists from a High-Throughput Screen. *Assay Drug Dev Technol* **2023**, *21* (3), 89–96. https://doi.org/10.1089/adt.2022.116.

(23) Stasi, C.; Milani, S.; Galli, A. Gut-Liver The Role of Serotonin and Its Pathways in Hepatic Fibrogenesis. In *The Complex Interplay Between Gut-Brain, Gut-Liver, and Liver-Brain Axes*; Elsevier, 2021; pp 129–155. https://doi.org/10.1016/B978-0-12-821927-0.00005-X.

(24) Ebrahimkhani, M. R.; Oakley, F.; Murphy, L. B.; Mann, J.; Moles, A.; Perugorria, M. J.; Ellis, E.; Lakey, A. F.; Burt, A. D.; Douglass, A.; Wright, M. C.; White, S. A.; Jaffré, F.; Maroteaux, L.; Mann, D. A. Stimulating Healthy Tissue Regeneration by Targeting the 5-HT2B Receptor in Chronic Liver Disease. *Nat Med* **2011**, *17* (12), 1668–1673. https://doi.org/10.1038/nm.2490.

(25) Löfdahl, A.; Tornling, G.; Wigén, J.; Larsson-Callerfelt, A.-K.; Wenglén, C.; Westergren-Thorsson, G. Pathological Insight into 5-HT2B Receptor Activation in Fibrosing Interstitial Lung Diseases. *Int J Mol Sci* **2020**, *22* (1), 225. https://doi.org/10.3390/ijms22010225.

(26) Löfdahl, A.; Wenglén, C.; Rydell-Törmänen, K.; Westergren-Thorsson, G.; Larsson-Callerfelt, A.-K. Effects of 5-Hydroxytryptamine Class 2 Receptor Antagonists on Bronchoconstriction and Pulmonary Remodeling Processes. *Am J Pathol* **2018**, *188* (5), 1113–1119. https://doi.org/10.1016/j.ajpath.2018.01.006.

(27) Schram, K. H.; Townsend, L. B. The Synthesis of 6-Amino-4-Methyl-8-(β-D-Ribofuranosyl) (4-H,8-H)Pyrrolo-[4,3,2-de]Pyrimido[4,5-c]Pyridazine, a New Tricyclic Nucleoside. *Tetrahedron Lett* **1971**, *12* (49), 4757–4760. https://doi.org/10.1016/S0040-4039(01)87546-8.

(28) Yang, L.; Dan, H. C.; Sun, M.; Liu, Q.; Sun, X.; Feldman, R. I.; Hamilton, A. D.; Polokoff, M.; Nicosia, S. V.; Herlyn, M.; Sebti, S. M.; Cheng, J. Q. Akt/Protein Kinase B Signaling Inhibitor-2, a Selective Small Molecule Inhibitor of Akt Signaling with Antitumor Activity in Cancer Cells Overexpressing Akt. *Cancer Res* **2004**, *64* (13), 4394–4399. https://doi.org/10.1158/0008-5472.CAN-04-0343.

(29) Wotring, L. L.; Townsend, L. B.; Jones, L. M.; Borysko, K. Z.; Gildersleeve, D. L.; Parker, W. B. *Dual Mechanisms of Inhibition of DNA Synthesis by Triciribine1*; 1990; Vol. 50. http://aacrjournals.org/cancerres/article-pdf/50/16/4891/2440492/cr0500164891.pdf.

(30) Kawasaki, A. M.; Wotring, L. L.; Townsend, L. B. Synthesis and Cytotoxicity Studies of 8-Amino-6-Methyl-2-.Beta.-D-Ribofuranosyl-1,2,3,5,6,7-Hexaazaacenaphthylene (7-Aza-TCN) and the Corresponding 2'-Deoxy- and Arabinonucleoside Analogues. *J Med Chem* **1990**, *33* (12), 3170–3176. https://doi.org/10.1021/jm00174a012.

(31) Kimoto, M.; Hirao, I. Genetic Alphabet Expansion Technology by Creating Unnatural Base Pairs. *Chem Soc Rev* **2020**, *49* (21), 7602–7626. https://doi.org/10.1039/D0CS00457J.

(32) Malyshev, D. A.; Romesberg, F. E. The Expanded Genetic Alphabet. *Angewandte Chemie International Edition* **2015**, *54* (41), 11930–11944. https://doi.org/10.1002/anie.201502890.

(33) Marx, A.; Betz, K. The Structural Basis for Processing of Unnatural Base Pairs by DNA Polymerases. *Chemistry – A European Journal* **2020**, *26* (16), 3446–3463. https://doi.org/10.1002/chem.201903525.

(34) Wypijewska del Nogal, A.; Füchtbauer, A. F.; Bood, M.; Nilsson, J. R.; Wranne, M. S.; Sarangamath, S.; Pfeiffer, P.; Rajan, V. S.; El-Sagheer, A. H.; Dahlén, A.; Brown, T.; Grøtli, M.; Wilhelmsson, L. M. Getting DNA and RNA out of the Dark with 2CNqA: A Bright Adenine Analogue and Interbase FRET Donor. *Nucleic Acids Res* **2020**, *48* (14), 7640–7652. https://doi.org/10.1093/nar/gkaa525.

Dual N^6/C7-substituted 7-deazapurine and tricyclic ribonucleosides with affinity for G protein-coupled receptors

Simon Krols[1], Federica Matteucci[1], Kristof Van Hecke[2], Guy Caljon[3], Kenneth A. Jacobson[4], Serge Van Calenbergh[1]

[1] Laboratory for Medicinal Chemistry, Faculty of Pharmaceutical Sciences, Ghent University, Belgium

[2] XStruct, Department of Chemistry, Ghent University, Krijgslaan 281 (S3), 9000 Ghent, Belgium

[3] Laboratory of Microbiology, Parasitology and Hygiene (LMPH), University of Antwerp, Universiteitsplein 1, B-2610 Wilrijk, Belgium

[4] Molecular Recognition Section, Laboratory of Bioorganic Chemistry, National Institute of Diabetes and Digestive and Kidney Diseases, National Institutes of Health, 9000 Rockville Pike, Bethesda, Maryland 20892, United States

Supplementary Information

Contents

In this work, no unexpected or unusually high safety hazards were encountered

Biological data

Radioligand binding assay

Screening of the analogues at 45 receptors, channels and transporters was performed by the PDSP. A complete list of the interactions tested is (human unless noted): $5HT_{1A}$, $5HT_{1B}$, $5HT_{1D}$, $5HT_{1E}$, $5HT_{2A}$, $5HT_{2B}$, $5HT_{2C}$, $5HT_3$, $5HT_{5A}$, $5HT_6$, $5HT_7$, α_{1A}, α_{1B}, α_{1D}, α_{2A}, α_{2B}, α_{2C}, β_1, β_2, β_3, BZP rat brain site, D_1, D_2, D_3, D_4, D_5, $GABA_A$, H_1, H_2, H_3, H_4, M_1, M_2, M_5, δ-opioid receptor (DOR), κ-opioid receptor (KOR), μ-opioid receptor (MOR), σ_1, σ_2, DAT, NET, SERT. The only hits among these signaling proteins are shown in Tables 1, S1 and S2. For targets not shown in the tables, the % inhibition at 10 μM was <50% for all compounds. Detailed experimental procedures can be found on the PDSP website: http://pdsp.med.unc.edu/ (binding assays). In brief, a primary radioligand binding assay was carried out at a single concentration of 10 μM in quadruplicate in the presence of the human recombinant receptors, coming from stably or transiently transfected cell lines. Compounds showing a minimum of 50% inhibition at 10 μM are tagged for secondary radioligand binding assays to determine full response concentration curves at specific targets. In secondary binding assays, selected compounds were usually tested at 11 concentrations (0.1, 0.3, 1, 3, 10, 30, 100, 300 nM, 1, 3, 10 μM) and in triplicate. Binding assays were carried out in appropriate binding buffers with a final volume of 0.125 mL. The concentration of the hot ligand was usually close to the K_d. Total binding and nonspecific binding were determined in the respectively absence and presence of 10 μM of the reference compound. Reactions were stopped by vacuum filtration onto 0.3% polyethyleneimine (PEI) soaked 96-well filter mats using a 96-well Filtermate harvester, followed by three washes with cold wash buffers. Scintillation cocktail was then melted onto the microwave-dried filters on a hot plate and radioactivity was counted in a Microbeta counter.

Cytotoxicity in MRC-5 cells

MRC-5_{SV2}cells were cultured in MEM + Earl's salts-medium, supplemented with L-glutamine, $NaHCO_3$, and 5% inactivated fetal calf serum. All cultures and assays were conducted at 37°C under an atmosphere of 5% CO_2. Assays were performed in sterile 96-well microtiter plates, each well containing 10μL of the watery compound dilutions together with 190μL of MRC-5_{SV2} inoculum (1.5×10^5 cells/mL). Cell growth was compared to untreated control wells (100% cell growth) and medium-control wells (0% cell growth). After 3 days incubation, cell viability was assessed fluorimetrically after addition of 50 μL of resazurin per well. After 4 h at 37°C, fluorescence was measured (λ_{ex} 550 nm, λ_{em} 590 nm). The results were expressed as % reduction in cell growth/viability compared to control wells, and an average CC_{50} value was determined based on 2 independent replicates.

Table S1. Binding inhibition of 7-deazaadenosine analogues and other nucleoside analogues at diverse targets (Ki, μM, or % inhibition at 10 μM) and cytotoxicity in MRC-5 fibroblasts (CC_{50} (μM))[a,b]

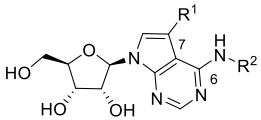

	R¹	R²	5-HT$_{1B}$	5-HT$_{1D}$	5-HT$_{2A}$	5-HT$_{2B}$	5-HT$_{2C}$	5-HT$_{6}$	5-HT$_{7A}$	α_{2C}	M_5	DOR	KOR	MOR	NET	DAT	σ_1	σ_2	TPSO	MRC-5
Ref	H		4%	-7%	4%	15%	5.3	28%	13%	-4%	-12%	6%	36%	-7%	12%	39%	25%	2.8	49%	ND
7a			-8%	21%	9%	19%	26%	25%	41%	27%	17%	12%	19%	6%	9.2 ±0.8	-19%	3.5 ±1.1	3.4 ±0.7	-18%	> 64
7j			3%	-14%	6%	19%	13%	19%	15%	22%	25%	17%	9%	-2%	51%[c]	11%	42%	41%	-21%	> 64
8a			14%	2%	14%	**0.50 ±0.10**	34%	**1.0 ±0.2**	15%	2.5 ±1.3	-2%	5%	1.8 ±0.3	-6%	35%	10%	3.3 ±1.0	35%	45%	> 64
8b			23%	23%	41%	49%	9%	37%	6%	26%	5.6 ±0.5	4%	1.9 ±0.7	6%	25%	4%	6.5 ±3.5	5.3 ±1.8	45%	37.3
8c			25%	27%	23%	**0.71 ±0.10**	21%	41%	1%	42%	9%	11%	22%	8%	27%	-11%	-11%	1.8 ±0.1	7%	41.8
8d			25%	2.5 ±1.0	18%	**0.55 ±0.15**	28%	30%	4%	18%	16%	3%	5%	16%	23%	5%	3.4 ±1.4	3.4 ±1.1	48%	> 64
8e			6%	15%	42%	**0.83 ±0.03**	47%	26%	4%	-2%	0%	21%	5%	45%	8.0 ±1.2	7.3 ±1.2	2.3 ±0.2	37%	37%	> 64
8f		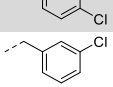	6%	5%	18%	**0.62 ±0.35**	30%	14%	15%	-1%	-9%	18%	16%	21%	4%	5.7	48%	10%	5%	> 64
8g			28%	30%	7.5 ±2.5	1.2 ±0.3	24%	25%	6%	26%	3%	5%	12%	9%	19%	-3%	6%	41%	-13%	> 64
8h			1%	2%	-5%	43%	-17%	18%	7%	33%	8%	-1%	17%	-3%	29%	12%	26%	50%	27%	> 64
8i		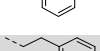	11%	13%	-8%	25%	-19%	34%	7%	25%	27%	1%	15%	7%	29%	8%	16%	29%	14%	52.7
8j			6%	-1%	3%	36%	22%	7%	21%	9%	-2%	6%	43%	4%	45%	18%	-6%	31%	7%	> 64
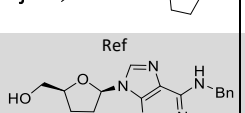			13%	-3%	-3%	3%	13%	15%	5%	-6%	9%	7%	9%	-16%	6%	2%	-18%	18%	38%	ND

[a] *A Ki value (represented in the table as mean ± SEM (µM)) was determined for analogues showing % inhibition > 50%. Ki-values lower than 1 µM are highlighted in bold. % Inhibition at 10 µM is shown for analogues with a % inhibition < 50%.*

[b] *Compounds **7b-j** were not included in the screen since only moderate activity of benzyl-analogue **7a** was observed.*

[c] *Although the primary binding showed > 50% inhibition at 10 µM, the full curves indicated Ki >10 µM*

Table S2. Binding inhibition of tricyclic at diverse targets (K_i, µM, or % inhibition at 10 µM) and cytotoxicity in MRC-5 fibroblasts (IC_{50} (µM)).

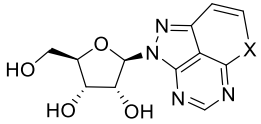

	X	5-HT_{1B}	5-HT_{1D}	5-HT_{2A}	5-HT_{2B}	5-HT_{2C}	5-HT_6	5-HT_{7A}	α_{2C}	M_5	DOR	KOR	MOR	NET	DAT	σ_1	σ_2	TPSO	MRC-5
15a	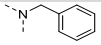	16%	2.6 ±0.1	14%	7%	-28%	13%	48%	30%	37%	0%	>10,0[a]	8%	>10,0[a]	-13%	15%	25%	-15%	> 64
15b		4%	20%	12%	0%	-4%	14%	40%	13%	8%	0%	13%	-3%	-3%	-4%	30%	31%	-10%	> 64
15c	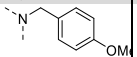	-6%	-2%	14%	6%	14%	16%	4%	13%	12%	7%	-1%	14%	12%	-18%	35%	22%	4%	> 64
15d		5%	-6%	11%	4%	-9%	6%	4%	8%	6%	18%	-2%	37%	5%	28%	25%	5%	-87%	2.95
29		-7%	-6%	-8%	-17%	6%	-8%	8%	16%	0%	-5%	16%	4%	5%	-43%	43%	14%	-34%	> 64

A primary radioligand binding screen was performed at each target protein using a fixed concentration of 10 µM. A K_i value (represented in the table as mean ± SEM (µM)) was determined for analogues showing % inhibition > 50%. % Inhibition at 10 µM is shown for analogues with a % inhibition < 50%.

[a] *Although the primary binding showed > 50% inhibition at 10 µM, the full curves indicated Ki >10 µ*

Full binding curves

Representative secondary binding results from PDSP. Test compound in red, reference ligand in black. Each radioligand is used at 0.5 – 1.0x its K_d value. The binding is performed in 96-well plates in the dark at room temperature for 90 minutes. Complete procedures can be found at: https://pdsp.unc.edu/pdspweb/content/PDSP%20Protocols%20II%202013-03-28.pdf

Compound 7a

Sigma$_1$, radioligand [^{3}H]pentazocine(+), HEKT cells.

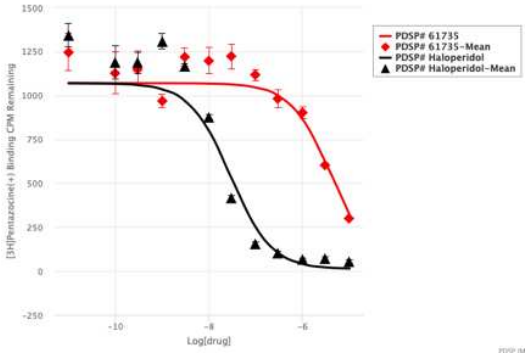

Sigma$_2$, radioligand [^{3}H]DTC, HEKT cells.

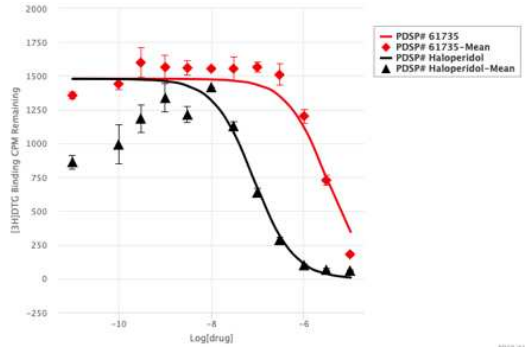

Compound 8a

5-HT$_{2B}$, radioligand [^{3}H]LSD, stable HEK cells.

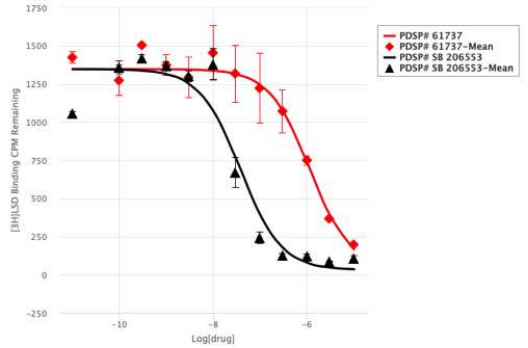

5-HT$_6$, radioligand [^{3}H]LSD, stable HEK cells.

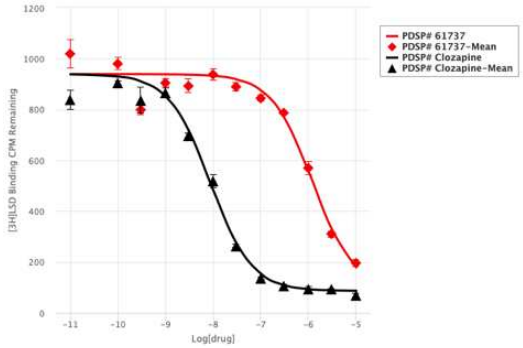

KOR, radioligand [^{3}H]U69593, stable HEK cells

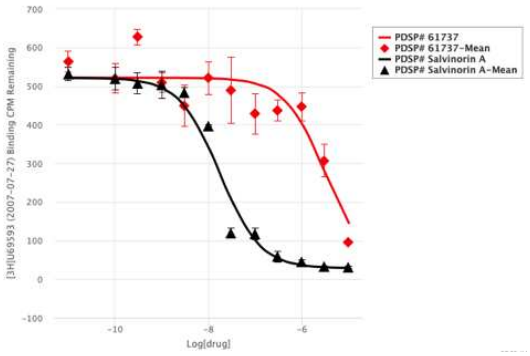

Compound 8b

sigma$_2$, radioligand [^{3}H]DTC, HEKT cells.

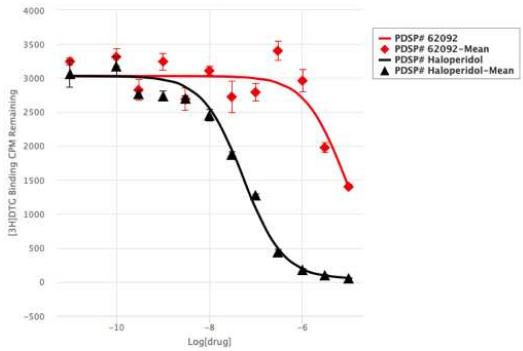

KOR, radioligand [^{3}H]U69593, stable HEK cells.

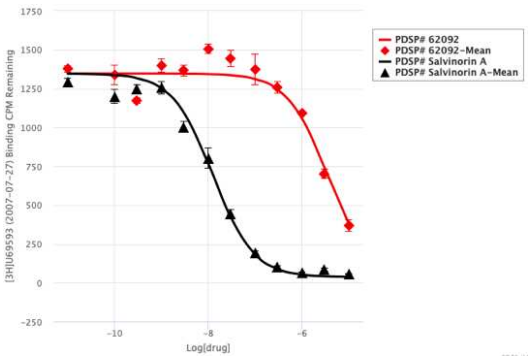

Compound 8c

sigma$_2$, radioligand [^{3}H]DTC, HEKT cells.

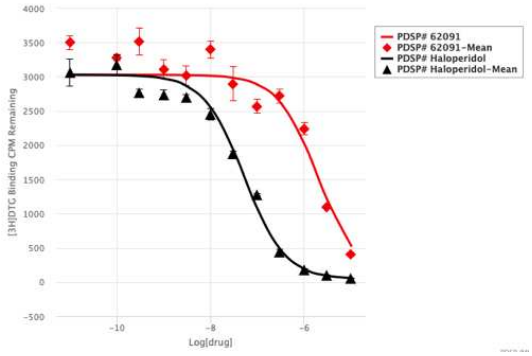

5-HT$_{2B}$, radioligand [3H]LSD, stable HEK cells

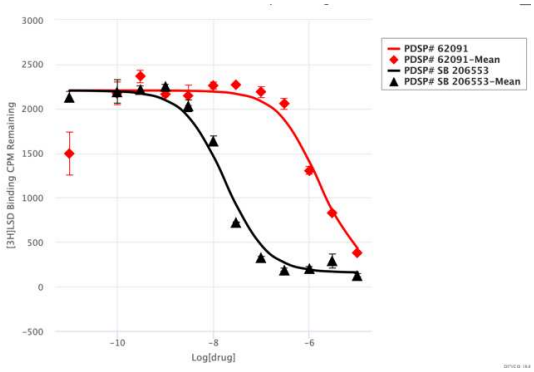

Compound 8d

sigma$_1$, radioligand [^{3}H]pentazocine(+), HEKT cells.

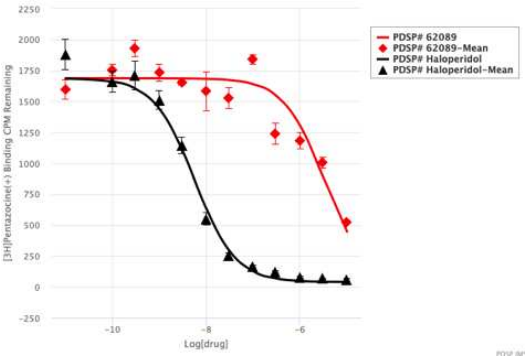

sigma$_2$, radioligand [^{3}H]DTC, HEKT cells.

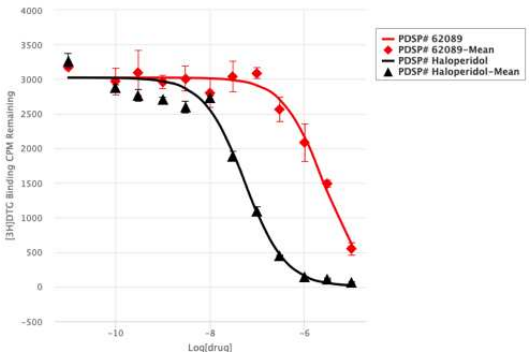

5-HT_{1D}, radioligand [^{3}H]GR125743, HEKT cells

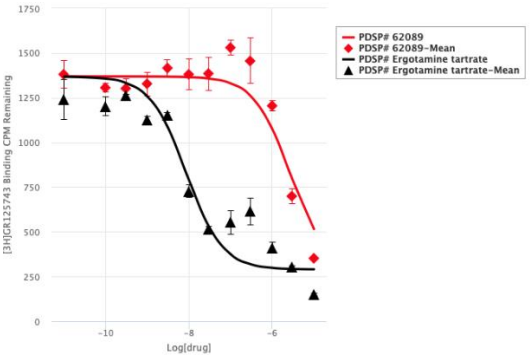

5-HT_{2B}, radioligand [^{3}H]LSD, stable HEK cells.

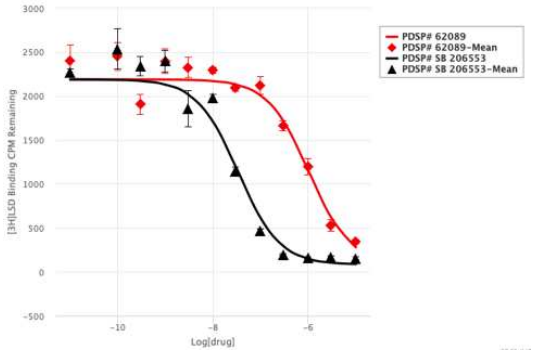

Compound 8e

sigma$_1$, radioligand [^{3}H]pentazocine(+), HEKT cells

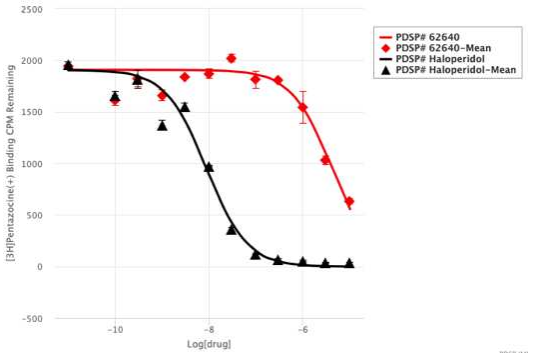

DAT, radioligand [^{3}H]WIN35428, stable HEK cells

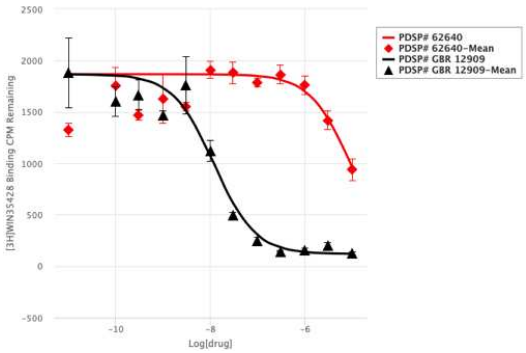

5-HT_{2B}, radioligand [^{3}H]LSD, stable HEK cells

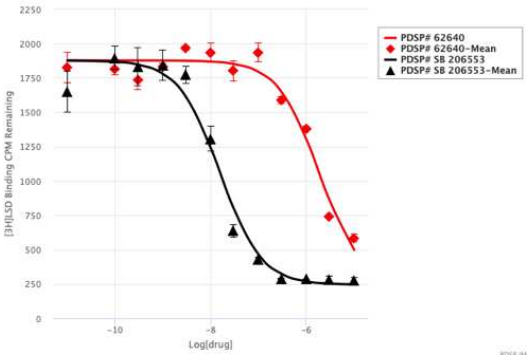

NET, radioligand [^{3}H]WIN35428 , stable HEK cells

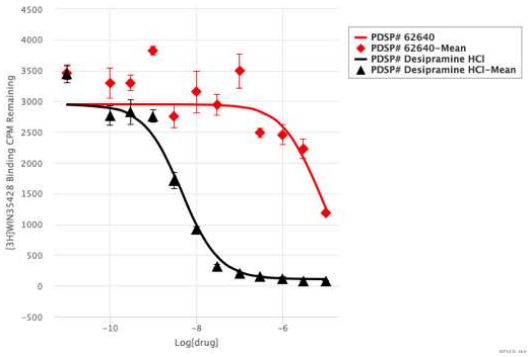

Compound 8f

5-HT$_{2B}$, radioligand [^{3}H]LSD, stable HEK cells

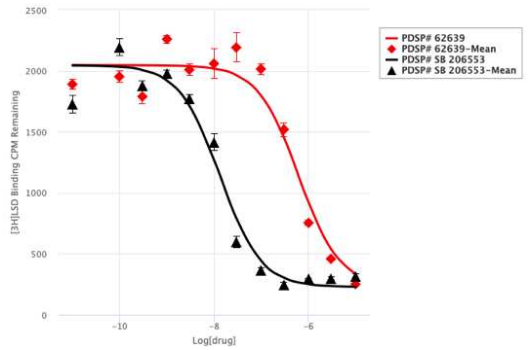

Compound 8g

5-HT$_{2B}$, radioligand [^{3}H]LSD, stable HEK cells

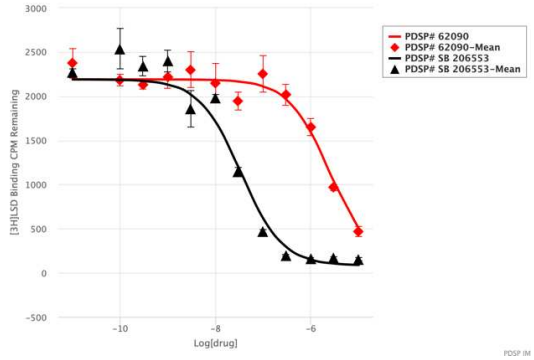

Compound 15a

5-HT_{1D}, radioligand [^{3}H]GR125743, HEKT cells

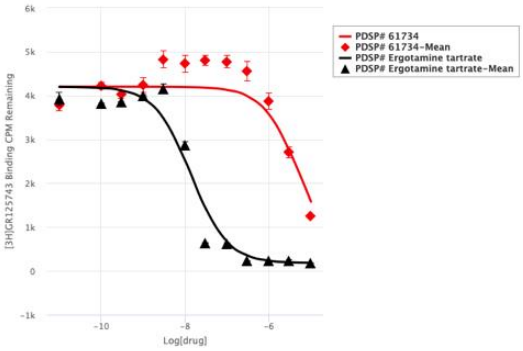

Experimental details

In this work, no unexpected or unusually high safety hazards were encountered

General

All reactions described were performed in a fume hood. Additionally, all reactions were carried out under a nitrogen atmosphere and at room temperature (ca 20 °C) unless explicitly stated otherwise.

Reactions were monitored by TLC analysis using Machery Nagel ALUGRAM Xtra SIL G UV254 sheets. Visualization of material on the TLC plate was carried out by inspection under UV light (254 nm) and/or staining the plates with one of the following spray reagents: A: a solution of $(NH_4)_6Mo_7O_{24}{\cdot}4H_2O$ (25 gL^{-1}) and $(NH_4)_4Ce(SO_4)_4{\cdot}2H_2O$ (10 gL^{-1}) in 10% aqueous sulfuric acid (v/v) followed by heating with a heat gun; B: an aqueous solution of KMn04 (20 gL^{-1}) and K_2CO_3 (10 gL^{-1}).

Column chromatography was performed on a Reveleris X2 automated flash chromatography system (Grace/Büchi) using disposable 60Å silica gel cartridges (Agela).

LC-MS analysis for reaction monitoring and purity analyses were carried out on a Waters Autopurification system equipped with a Waters CORTECS column (4.6x100 mm, C18, 2.7µm) and using a water/acetonitrile/trifluoroacetic acid linear gradient. Peak detection was achieved using mass spectrometry (ESI-MD) and a photo-diode-array detector (PDA)

Nuclear magnetic resonance analyses including ^{1}H- and ^{13}C- spectra were carried out on a Bruker Avance Neo 400MHz spectrometer equipped with an autosampler and using TOPSPIN/ICON-NMR. Chemical shifts are given in ppm (δ) relative to the solvent peak. NMR solvents included $CDCl_3$ (7.26 ppm in ^{1}H NMR, 77.16 ppm in ^{13}C NMR) or DMSO-d6 (2.50 ppm in ^{1}H NMR and 39.52 ppm in ^{13}C NMR) and were all purchased from Euriso-Top (Saint Aubin, France). The purine nomenclature was used in the characterization of proton and carbon NMR spectra, while systematic nomenclature was used to name the synthesized compounds.

High-resolution mass spectrometry was performed on a Waters Premier XE HRMS system that is calibrated using a solution of Le-enkephalin. Infusion of the analyte into the HRMS system was done as a solution (0.5 $ngmL^{-1}$) in UPLC grade water and acetonitrile.

All solvents utilized (HPLC grade or equivalent or superior purity) were purchased from ChemLab (Zedelgem, Belgium) and used as received. All building blocks and reagents were were purchased from common chemical suppliers including but not limited to: Fluorochem (Glossop, Derbyshire UK), Apollo Scientific (Bredbury/Stockport Cheshire UK), Sigma-Aldrich (Diegem, Belgium), and Fisher Scientific (Merelbeke, Belgium).

All obtained final compounds had purity > 95%, as assayed by analytical HPLC (UV) using a linear gradient Water/ MeCN 0 -> 98 % + 0.02 % TFA in 10 min on a Waters CORTECS column (4.6x100 mm, C18, 2.7µm).

Synthesis of intermediates

General procedure A: S_NAR on pyrrolopyrimidines

The 6-chloro substrate (1 eq) was dissolved in MeCN and the primary amine (1.2 eq) and Et_3N (1.2 eq) were added. The reaction mixture was heated to 70 °C and stirred for 4 to 7h. EA was added, washed with brine twice, dried over Na_2SO_4 and evaporated. Purification via flash column chromatography (PE/EA 0 → 30%) delivered the desired intermediate. The intermediates were, without further characterisation, used in the next step (benzoyl deprotection via general procedure B).

General procedure B: Benzoyl deprotection

The protected nucleoside (1 eq) was dissolved in a 1/1 mixture of DCM/MeOH and K_2CO_3 (0.5 eq) was added. When LCMS indicated that the reaction was finished, the reaction mixture was filtered over celite and extensively flushed with DCM and MeOH. The final products were obtained after flash column chromatography using DCM/MEOH (0 → 10% MeOH).

General procedure C: TBAF-mediated ethynyl deprotection followed by cyclisation

The TES-protected ethynyl derivative (1 eq) was dissolved in THF and TBAF (1M in THF, 1.1 eq) was added. After 1h, H_2O was added and extracted with EA. The organic layer was washed with brine, dried over Na_2SO_4, filtered and evaporated. The crude mixture was redissolved in DCE, AgOTf (0.2 eq) was added and stirred for 16h at 84°C. Evaporation of the RM on celite, followed by flash column chromatography (PE/EA 30 → 100%) delivered the cyclised intermediate.

Synthesis of 4-chloro-5-iodo-7*H*-pyrrolo[2,3-*d*]pyrimidine (2)

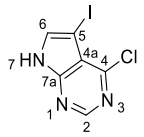

4-chloro-7H-pyrrolo[2,3-*d*]pyrimidine **1** (5 g, 32.6 mmol, 1 eq) and N-iodosuccinimide (7.69 g, 34.2 mmol, 1.05 eq) were dissolved in DMF (50 mL). The reaction mixture was stirred at room temperature overnight in the dark. Next, the reaction mixture was cooled to 0 °C and ice-cold water was added. The precipitate was filtered and dried *in vacuo* (8.75 g, 97% yield).

In all NMR characterizations, the purine nomenclature was used.

^{1}H NMR (DMSO-d6, 400MHz): δ = 7.93 (s, 1H, H-8), 8.59 (s, 1H, H-2), 12.94 (s, 1H, NH) ppm.

^{13}C NMR (DMSO-d6, 100MHz): δ = 51.66 (C-7), 115.77 (C-5), 133.85 (CH-8), 150.47 (CH-2), 150.72 (C-4), 151.50 (C-6) ppm.

HRMS (ESI): calculated for $C_6H_2ClIN_3$ ($[M-H]^+$): 277.89872, found: 279.8989

Synthesis of 4-chloro-5-iodo-N7-(2', 3', 5'-tri-O-benzoyl-β-D-ribofuranosyl)-pyrrolo[2,3-*d*]pyrimidine (3)

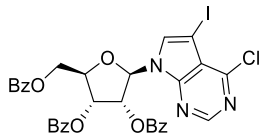

6-chloro-7-iodo-7-deazapurine **2** (8.75 g, 31.3 mmol, 1.1 eq) was dissolved in acetonitrile (300 mL), BSA (7.99 mL, 32.7 mmol, 1.15 eq) was added and stirred at room temperature for 30 min. 1-*O*-acetyl-2,3,5-tri-*O*-benzoyl-β-D-ribofuranose (14.35 g, 28.45 mmol, 1 eq) and TMSOTf (5.4 mL, 29.9 mmol, 1.05 eq) were added. After 30 min of stirring at room temperature the RM was heated to 80°C for 2 h. EtOAc was added and was washed with sat. $NaHCO_3$ and brine. The organic phase was dried over Na_2SO_4, filtered and concentrated under reduced pressure. The residue was purified via column chromatography (PE/EA 10% -> 25%) and delivered the product as a white foam (11.34 g, 55% yield).

^{1}H NMR ($CDCl_3$, 400MHz): δ = 4.68 (dd, J= 12.2, 3.6 Hz, 1H, H-5'), 4.80 (m, 1H, H-4'), 4.90 (dd, J= 12.3, 3.3 Hz, 1H, H-5'), 6.11 (m, 1H, H-3'), 6.15 (m, 1H, H-2'), 6.67 (d, J= 5.4 Hz, 1H, H-1'), 7.33-7.44 (m, 4H,

Bz), 7.47 (m, 6H, H-8 & Bz), 7.92 (dd, J= 8.5, 1.3 Hz, 2H, Bz), 7.99 (dd, J= 8.4, 1.4 Hz, 2H, Bz), 8.11 (dd, J= 8.5, 1.4 Hz, 2H, Bz), 8.58 (s, 1H, H-2) ppm.

^{13}C NMR ($CDCl_3$, 100MHz): δ = 53.80 (C-7), 63.61 (CH_2-5'), 71.57 (CH-3'), 74.29 (CH-2'), 80.81 (CH-4'), 86.93 (CH-1'), 117.94 (C-5), 128.51 (C-Bz), 128.66 (CH-Bz), 128.71 (CH-Bz), 128.80 (C-Bz), 128.97 (CH-Bz), 129.40 (C-Bz), 129.84 (CH-Bz), 129.97 (CH-Bz), 129.98 (CH-Bz), 132.15 (CH-8), 133.74 (CH-Bz), 133.92 (CH-Bz), 133.95 (CH-Bz), 151.14 (C-4), 151.39 (CH-2), 153.27 (C-6), 165.20 (C=O-Bz), 165.50 (C=O-Bz), 166.24 (C=O-Bz) ppm.

HRMS (ESI): calculated for $C_{32}H_{24}ClIN_3O_7$ ($[M+H]^+$): 724.03418, found: 724.0345.

Synthesis of 4-chloro-5-(trimethylsilyl)ethynyl-N7-(2', 3', 5'-tri-O-benzoyl-β-D-ribofuranosyl)-pyrrolo[2,3-*d*]pyrimidine (5)

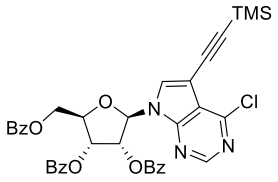

Compound **3** (11.34 g, 15.67 mmol, 1 eq) was dissolved in DMF (78 mL) and triethylamine (21.84 mL, 156.7 mmol, 10 eq) and trimethylsilylacetylene (21.71 mL, 156.7 mmol, 10 eq) were added. The solution was purged with argon for 5 min before the addition of CuI (0.30 g, 1.57 mmol, 0.1 eq) and $Pd(PPh_3)_2Cl_2$ (0.55 g, 0.78 mmol, 0.05 eq). EA was added after 1h and washed twice with brine. The organic phase was then dried over Na_2SO_4, filtered and concentrated under reduced pressure. The residue was purified via column chromatography (PE/EA 0 -> 15%) and yielded the pure product as a slightly yellow foam (7.79 g, 72% yield).

^{1}H NMR ($CDCl_3$, 400MHz): δ = 0.25 (s, 9H, H-TMS), 4.69 (dd, J= 12.1, 3.7 Hz, 1H, H-5'), 4.80 (m, 1H, H-4'), 4.86 (dd, J= 12.1, 3.1 Hz, 1H, H-5'), 6.09 (m, 1H, H-3'), 6.15 (m, 1H, H-2'), 6.64 (d, J= 5.3 Hz, 1H, H-1'), 7.33-7.43 (m, 4H, Bz), 7.45-7.63 (m, 6H, Bz, H-8), 7.91 (d, J= 7.4 Hz, 2H, Bz), 7.99 (dd, J= 7.4 Hz, 2H, Bz), 8.11 (dd, J= 7.4 Hz, 2H, Bz), 8.58 (s, 1H, H-2) ppm.

^{13}C NMR ($CDCl_3$, 100MHz): δ = -0.16 (CH_3, TMS), 63.66 (CH_2-5'), 71.53 (CH-3'), 74.23 (CH-2'), 80.70 (CH-4'), 86.99 (CH-1'), 95.60 (C-ethynyl), 99.14 (C-ethynyl), 99.30 (C-7), 117.83 (C-5), 128.50 (C-Bz), 128.66 (CH-Bz), 128,71 (CH-Bz), 128.81 (C-Bz), 128.87 (CH-Bz), 129.44 (C-Bz), 129.86 (CH-Bz), 129.98 (2x CH-Bz), 130.69 (CH-8), 133.64 (CH-Bz), 133.91 (CH-Bz), 133.94 (CH-Bz), 150.98 (C-4), 152.05 (CH-2), 153.79 (C-6), 165.17 (C=O-Bz), 165.49 (C=O-Bz), 166.28 (C=O-Bz) ppm.

HRMS (ESI): calculated for $C_{37}H_{33}ClN_3O_7Si$ ($[M+H]^+$): 694.17708, found: 694.1771.

Synthesis of 4-chloro-5-trifluoromethyl-N7-(2', 3', 5'-tri-O-benzoyl-β-D-ribofuranosyl)-pyrrolo[2,3-*d*]pyrimidine (6)

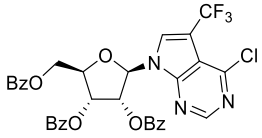

CuI (4.74 g, 24.87 mmol, 3 eq) and KF (4.13 g, 24.86 mmol, 3 eq) are added to a mixture of NMP/DMF 1:1 (40 mL), previously purged with argon. Then, $TMSCF_3$ (3.68 mL, 24.87 mmol, 3 eq) is added to the solution dropwise in the course of 1 h. Compound **3** (6 g, 8.29 mmol, 1 eq) was dissolved in NMP/DMF 1:1 (40 mL, purged with argon), and added to the reaction mixture. After 1h heating at 110°C, EA (80

mL) and water (100 mL) were added followed by filtration of the mixture over celite. The filtrate was washed with brine and dried over Na_2SO_4. The residue was purified via column chromatography (PE/EA 5 -> 30%) and afforded **6** as a slightly yellow foam (3.85 g, 70% yield).

^{1}H NMR ($CDCl_3$, 400MHz): δ = 4.71 (dd, J= 12.3, 3.6 Hz, 1H, H-5'), 4.84 (m, 1H, H-4'), 4.91 (dd, J= 12.3, 3.0 Hz, 1H, H-5'), 6.11-6.15 (m, 1H, H-3'), 6.16-6.22 (m, 1H, H-2'), 6.68 (d, J= 5.4 Hz, 1H, H-1'), 7.34 – 7.51 (m, 6H, H-Bz), 7.52 - 7.65 (m, 3H, H-Bz), 7.83 (s, 1H, H-8), 7.92 (dd, J= 8.3;1.3 Hz, 2H, H-Bz), 8.01 (dd, J= 8.4;1.3 Hz, 2H, H-Bz), 8.10 (dd, J= 8.4; 1.2 Hz, 2H, H-Bz), 8.66 (s, 1H, H-2) ppm.

^{13}C NMR ($CDCl_3$, 100MHz): δ = 63.53 (CH_2-5'), 71.56 (CH-3'), 74.36 (CH-2'), 81.12 (CH-4'), 87.54 (CH-1'), 107.23 (q, $^2J_{(C,F)}$ = 39.28 Hz, C-7), 114.36 (C-5), 121.87 (q, $^1J_{(C,F)}$ = 267.32 Hz, CF_3), 127.82 (q, $^3J_{(C,F)}$ = 5.92 Hz, CH-8), 128.41 (C-Bz), 128.70 (CH-Bz), 128.75 (CH-Bz), 128.88 (CH-Bz), 129.28 (C-Bz), 129.77 (CH-Bz), 129.99 (2x CH-Bz), 133.80 (CH-Bz), 133.98 (CH-Bz), 134.03 (CH-Bz), 152.15 (C-4), 152.43 (CH-2), 152.76 (C-6), 165.21 (C=O-Bz), 165.49 (C=O-Bz), 166.24 (C=O-Bz) ppm. One C-Bz missing.

^{19}F NMR (CDCl3, 377MHz): δ = -56.16 ppm.

HRMS (ESI): calculated for $C_{33}H_{24}ClF_3N_3O_7$ ($[M+H]^+$): 666.12498, found: 666.1247.

Synthesis of 3-iodo-allopurinol (10)

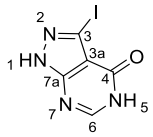

Allopurinol (10 g, 73.47 mmol, 1 eq) and *N*-iodosuccinimide (18.18 g, 80.82 mmol, 1.1 eq) were dissolved in DMF (100 mL). The reaction mixture was stirred at 80°C in the dark. After 16 h, the reaction mixture was cooled to 0°C and ice-cold water (100 mL) and 2M solution of $Na_2S_2O_3$ (100 mL) were added. Filtrating the precipitate delivered the product as a white solid (19.25 g, 78%) after it was dried *in vacuo*.

^{1}H NMR ($CDCl_3$, 400MHz): δ = 8.01 (s, 1H), 12.09 (br s, 1H), 13.81 (br s, 1H) ppm.

HRMS (ESI): calculated for $C_5H_2IN_4O$ ($[M-H]^+$): 260.92792, found: 260.9277.

Synthesis of 3-iodo-4-oxo -N1-(2', 3', 5'-tri-O-benzoyl-β-D-ribofuranosyl)-pyrazolo[3,4-*d*]pyrimidine (11)

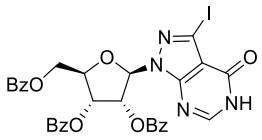

Iodinated allopurinol (5 g, 19.08 mmol, 1 eq) and 1-*O*-acetyl-2,3,5-tri-*O*-Benzoyl-β-D-ribofuranose (12.52 g, 24.81 mmol, 1.3 eq) were added in a previously oven-dried flask under argon atmosphere. Dry nitromethane (40 mL) was added and heated to 100°C. Next, boron trifluoride etherate (3.06 mL, 24.81 mmol, 1.3 eq) was added and stirred for 80 min. The reaction mixture was concentrated, purified via column chromatography (DCM/MeOH 0 -> 5%) and delivered the product as a white foam (1.85 g, 15%).

^{1}H NMR ($CDCl_3$, 400MHz): δ = 4.65 (dd, J= 12.1, 4.6 Hz, 1H, H-5'), 4.78 (dd, J= 12.1, 3.6 Hz, 1H, H-5'), 4.82 – 4.88 (m, 1H, H-4'), 6.24 (t, J=5.7 Hz, 1H, H-3'), 6.36 (dd, J= 3.1; 5.4 Hz, 1H, H-2'), 6.68 (d, J= 3.1

Hz, 1H, H-1'), 7.33 – 7.50 (m, 6H, H-Bz), 7.52 – 7.62 (m, 3H, H-Bz), 7.93 – 8.01 (m, 4H, H-Bz), 8.03 (s, 1H, H-2), 8.05 – 8.13 (m, 2H, H-Bz), 11.62 (s, 1H, 6-OH) ppm.

^{13}C NMR ($CDCl_3$, 100MHz): δ = 63.82 (CH_2-5'), 71.86 (CH-3'), 74.74 (CH-2'), 80.60 (CH-4'), 87.55 (CH-1'), 93.33 (C-7), 109.53 (C-5), 128.62 - 128.67 - 128.71 (3 x CH-Bz), 128.81 – 128.93 – 129.67 (3x C-Bz), 129.93 – 130.01 – 130.05 (CH-Bz), 133.31 – 133.73 – 133.87 (CH-Bz), 147.70 (CH-2), 153.68 (C-4), 158.86 (C-6), 165.23 – 165.38 – 166.43 (C=O Bz) ppm.

HRMS (ESI): calculated for $C_{31}H_{24}IN_4O_8$ ([M+H]$^+$): 707.06338, found: 707.0638.

Synthesis of 4-oxo-3-((triethylsilyl)ethynyl)-N1-(2', 3', 5'-tri-O-benzoyl-β-D-ribofuranosyl)-pyrazolo[3,4-*d*]pyrimidine (18)

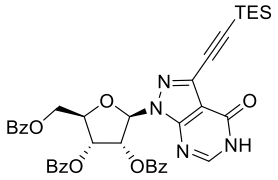

Compound **11** (1.85 g, 2.62 mmol, 1 eq) was dissolved in DMF (13 mL) and triethylamine (1.10 mL,7.86 mmol, 3 eq) and triethylsilylacetylene (0.99 mL, 7.86 mmol, 3 eq) were added. The solution was purged with argon for 5 min before the addition of CuI (0.05 g, 0.26 mmol, 0.1 eq) and $Pd(PPh_3)_2Cl_2$ (0.09 g, 0.13 mmol, 0.05 eq). EA was added after 1h and washed twice with brine. The organic phase was then dried over Na_2SO_4, filtered and concentrated under reduced pressure. The residue was purified via column chromatography (PE/EA 20 -> 100%) and yielded the pure product as an off-white foam (1.38 g, 73% yield).

^{1}H NMR ($CDCl_3$, 400MHz): δ = 0.77 (q, J= 7.9Hz, 6H, CH_3-CH_2-Si), 1.12 (t, J= 7.9 Hz, 9H, CH_3-CH_2-Si), 4.76 (dd, J= 12.0, 4.9 Hz, 1H, H-5'), 4.86 (dd, J= 12.0, 3.6 Hz, 1H, H-5'), 4.84 (m, 1H, H-4'), 6.24 (t, J= 5.9 Hz, 1H, H-3'), 6.37 (dd, J=5.2, 2.9 Hz, 1H, H-2'), 6.73 (d, J= 2.8 Hz, 1H, H-1'), 7.33 – 7.47 (m, 6H, CH-Bz), 7.49 – 7.62 (m, 3H, CH-Bz), 7.91 (s, 1H, H-2), 7.93 – 8.00 (m, 4H, CH-Bz), 8.10 (d, J= 7.3Hz, 2H, H-Bz), 12.00 (br s, 1H, 6-NH) ppm.

^{13}C NMR ($CDCl_3$, 100MHz): δ = 4.37 (CH_3-CH_2-Si), 7.60 (CH_3-CH_2-Si), 64.00 (CH_2-5'), 71.97 (CH-3'), 74.75 (CH-2'), 80.53 (CH-4'), 87.82 (CH-1'), 95.90 (C-ethynyl), 99.79 (C-ethynyl), 108.05 (C-5), 128.59 – 128.61 – 128.65 (CH-Bz), 128.88 – 128.98 – 129.68 (C-Bz), 129.33 – 130-01 – 130.04 (CH-Bz), 132.66 (C-7), 130.19 – 133.68 – 133.82 (CH-Bz), 147.61 (CH-2), 153.17 (C-4), 158.59 (C-6), 165.21 - 165.36 - 166.43 (C=O Bz) ppm.

HRMS (ESI): calculated for $C_{39}H_{39}N_4O_8Si$ ([M+H]$^+$): 719.25318, found: 719.2534.

Synthesis of 4-chloro-3-((triethylsilyl)ethynyl)-N1-(2', 3', 5'-tri-O-benzoyl-β-D-ribofuranosyl)-pyrazolo[3,4-*d*]pyrimidine (19)

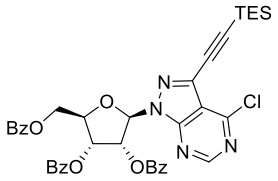

Compound **18** (2.5 g, 3.48 mmol, 1 eq) was dissolved in chloroform (35 mL). Then, DMF (2 mL) and thionyl chloride (3.5 mL) were added. After 1h stirring at 75°C, the solution was cooled to 0°C and ice and saturated $NaHCO_3$ solution were added. Organic layer was washed twice with sat. $NaHCO_3$, dried

over Na_2SO_4, filtered and concentrated under reduced pressure. The residue was purified via column chromatography (PE/EA 0 -> 30%) and afforded **19** as a white foam (1.8 g, yield of 70%).

^{1}H NMR ($CDCl_3$, 400MHz): δ = 0.78 (q, J= 7.8Hz, TES), 1.09 (t, J= 7.9 Hz, TES), 4.65 (dd, J= 12.1, 4.8 Hz, 1H, H-5'), 4.77 (dd, J= 12.1, 3.8 Hz, 1H, H-5'), 4.86 (m, 1H, H-4'), 6.25 (t, J= 5.9 Hz, 1H, H-3'), 6.44 (dd, J=3.4; 5.4 Hz, 1H, H-2'), 6.87 (d, J= 3.3 Hz, 1H, H-1'), 7.34 – 7.59 (m, 9H, CH-Bz), 7.94 – 8.00 (m, 4H, CH-Bz), 8.09 (d, J= 7.4Hz, 2H, H-Bz), 8.74 (s, 1H, H-2) ppm.

^{13}C NMR ($CDCl_3$, 100MHz): δ = 4.22 (CH_3-CH_2-Si), 7.59 (CH_3-CH_2-Si), 63.87 (CH_2-5'), 71.91 (CH-3'), 74.46 (CH-2'), 80.64 (CH-4'), 87.94 (CH-1'), 94.99 (C-ethynyl), 102.14 (C-ethynyl), 114.85 (C-5), 128.61 – 128.64 – 128.66 (CH-Bz), 128.93, (C-Bz), 129.63 (C-Bz), 130.0 (C-7, via HMBC) , 129.89 (CH-Bz) – 130-00 (2x CH-Bz), 130.21 (C-Bz), 133.24 – 133.76 – 133.88 (CH-Bz), 154.22 (C-4), 155.69 (CH-2), 156.02 (C-6), 165.20 - 165.40 - 166.36 (C=O Bz) ppm.

HRMS (ESI): calculated for $C_{39}H_{38}ClN_4O_7Si$ ($[M+H]^+$): 737.21928, found: 737.2187

Synthesis of 4-methylamino-3-((triethylsilyl)ethynyl)-N1-(2', 3', 5'-tri-O-benzoyl-β-D-ribofuranosyl)-pyrazolo[3,4-*d*]pyrimidine (22d)

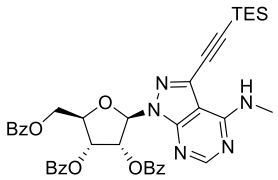

Chlorine **19** (500 mg, 0.68 mmol, 1 eq) was dissolved in THF (3mL) and Et_3N (1.5 eq, 1.02 mmol, 0.14 mL) and 2M methylamine in THF (1.5 eq, 0.51 mL) were added. After 1 h, the mixture was filtered and the filtrate evaporated. Purification (Toluene/EA 0 -> 25%) delivered 400 mg of the product as a white foam.

^{1}H NMR ($CDCl_3$, 400MHz): δ = 0.78 (q, J= 7.9 Hz, 6H, TES), 1.10 (t, J=7.2 Hz, 9H, TES), 3.16 (d, J= 5.0 Hz, 3H, Me), 4.65 (dd, J= 4.9; 12.0 Hz, 1H, H5'), 4.73 (dd, J= 3.9; 12.0 Hz, 1H, H5'), 4.78- 4.85 (m, 1H, H4'), 6.22 (q, J= 4.8 Hz, 1H, NH), 6.27 (t, J=5.7 Hz, 1H, H3'), 6.42 (dd, J= 3.5; 5.4 Hz, 1H, H2'), 6.81 (d, J= 3.4 Hz, 1H, H1'), 7.31-7.45 (m, 6H, H-Bz), 7.49-7.58 (m, 3H, H-Bz), 7.91-8.00 (m, 4H, H-Bz), 8.08-8.14 (m, 2H, H-Bz), 8.42 (s, 1H, H2) ppm.

^{13}C NMR ($CDCl_3$, 100MHz): δ = 4.30 (3 x CH_2, TES), 7.64 (3 x CH_3, TES), 27.69 (CH_3, Me), 64.24 (CH_2-5'), 72.13 (CH-3'), 74.52 (CH-2'), 80.33 (CH-4'), 87.24 (CH-1'), 97.83 (C-ethynyl), 100.20 (C-ethynyl), 103.05 (C-5), 128.26 (C-Bz), 128.53- 128.56- 128.59 (3x CH-Bz), 128.98 (C-Bz), 129.06 (C-Bz), 129.78 (C-7), 129.93- 130.01- 130.08 (3x CH-Bz), 133.08- 133.61- 133.70 (CH-Bz), 154.10 (C-6/4), 157.47 (CH-2), 157.78 (C-6/4), 165.18- 165.40- 166.43 (3x C=O, Bz) ppm.

HRMS (ESI): calculated for $C_{40}H_{42}N_5O_7Si$ ($[M+H]^+$): 732.28480, found: 732.2841

Synthesis of 4-(cyclopentylamino)-3-((triethylsilyl)ethynyl)-N1-(2', 3', 5'-tri-O-benzoyl-β-D-ribofuranosyl)-pyrazolo[3,4-*d*]pyrimidine (22b)

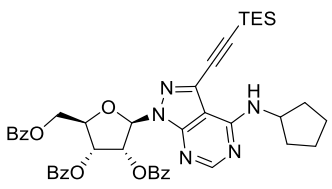

Chlorine **19** (1.02 g, 1.38 mmol, 1 eq) was dissolved in DMF (10 mL) and Et_3N (1.1 eq, 1.52 mmol, 0.21 mL) and cyclopentylamine (1.1 eq, 1.52 mmol, 0.15 mL) were added. After stirring 1h, the mixture was diluted with EA and washed 2 times with brine. After drying the organic phase over Na_2SO_4 and evaporation, the crude was purified via flash column chromatography (PE/EA 5 -> 30%). This delivered 0.99 g (yield: 97%) of the product as a white foam and was used in the next step without detailed characterization.

^{1}H NMR ($CDCl_3$, 400MHz): δ = 0.78 (q, J= 7.9 Hz, 6H, TES), 1.09 (t, J=7.9 Hz, 9H, TES), 1.53 (m, 2H, Cyclopentyl), 1.75 (m, 4H, cyclopentyl), 2.21 (m, 2H, cyclopentyl), 4.60-4.75 (m, 3H, 2x H5', CH-cyclopentyl), 4.81 (m, 1H, H4'), 6.22-6.31 (m, 2H, H3', NH), 6.42 (dd, J= 3.6; 5.2 Hz, 1H, H2'), 6.79 (d, J= 3.5 Hz, 1H, H1'), 7.32-7.45 (m, 6H, H-Bz), 7.49-7.58 (m, 3H, H-Bz), 7.91-7.98 (m, 4H, H-Bz), 8.08-8.13 (m, 2H, H-Bz), 8.41 (s, 1H, H2) ppm.

Synthesis of 4-(benzylamino)-3-((triethylsilyl)ethynyl)-N1-(2', 3', 5'-tri-O-benzoyl-β-D-ribofuranosyl)-pyrazolo[3,4-*d*]pyrimidine (22a)

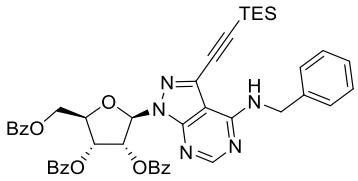

Chlorine **19** (1.8 g, 2.44 mmol, 1 eq) was dissolved in DMF (10 mL) and Et_3N (1.1 eq, 2.69 mmol, 0.38 mL) and benzylamine (1.1 eq, 2.69 mmol, 0.30 mL) were added. After 15 min, the mixture was diluted with EA and washed 2 times with brine. After drying the organic phase over Na_2SO_4 and evaporation, the crude was purified via flash column chromatography (PE/EA 5 -> 40%). This delivered 1.9 g (yield: 96%) of the product as a white foam and was used in the next step without further characterization.

Synthesis of 4-(p-methoxybenzylamino)-3-((triethylsilyl)ethynyl)-N1-(2', 3', 5'-tri-O-benzoyl-β-D-ribofuranosyl)-pyrazolo[3,4-*d*]pyrimidine (22c)

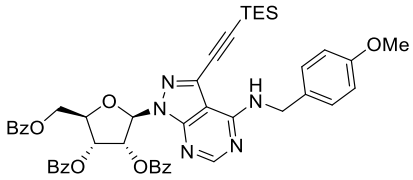

Chlorine **19** (1.5 g, 2.07 mmol, 1 eq) was dissolved in DMF (15 mL) and Et_3N (1.1 eq, 2.28 mmol, 0.32 mL) and paramethoxybenzylamine (1.1 eq, 2.28 mmol, 0.30 mL) were added. After 30 min, the mixture was diluted with EA and washed 2 times with brine. After drying over Na_2SO_4 and evaporation, the crude was purified via flash column chromatography (PE/EA 5 -> 50%). This delivered 1.5 g (yield: 87%) of the product as a white foam and was used in the next step without further characterization.

Synthesis of 3-ethynyl-4-oxo-N1-(2', 3', 5'-tri-O-benzoyl-β-D-ribofuranosyl)-pyrazolo[3,4-*d*]pyrimidine (23)

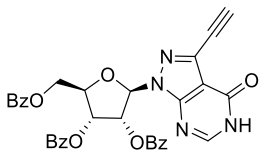

TES-protected intermediate **18** (500 mg, 0.7 mmol, 1 eq) was dissolved in THF and TBAF (1M in THF; 0.77mL, 0.77mmol, 1.1 eq) was added. After 1 h, H_2O was added, the mixture extracted with DCM (x2)

and the organic layer dried over Na_2SO_4. Flash column chromatography (PE/EA 40 -> 100 %) delivered the product (300 mg) in 71% yield. No cyclisation occurred as determined via LCMS and ^{1}H NMR (presence of NH and H-ethynyl).

^{1}H NMR ($CDCl_3$, 400MHz): δ 3.46 (s, 1H, Ethynyl), 4.65 (dd, J= 4.7; 12.1 Hz, 1H, H5'), 4.78 (dd, J= 3.7; 12.2 Hz, 1H, H5'), 4.83-4.88 (m, 1H, H4'), 6.29 (m, 1H, H3'), 6.32 – 6.36 (m, 1H, H2'), 6.74 (d, J= 2.6 Hz, 1H, H1'), 7.34-7.47 (m, 6H, H-Bz), 7.51-7.60 (m, 3H, H-Bz), 7.93-8.02 (m, 4H, H-Bz), 8.05 (d, J= 2.7Hz, 1H, H-2), 8.08- 8.12 (m, 2H, H-Bz), 11.94 (br s, 1H, NH) ppm.

Synthesis of 4-mercapto-3-((triethylsilyl)ethynyl)-N1-(2', 3', 5'-tri-O-benzoyl-β-D-ribofuranosyl)-pyrazolo[3,4-*d*]pyrimidine (27)

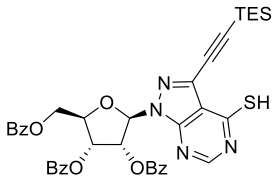

Chlorine **19** (0.33 g, 0.46 mmol, 1 eq) was dissolved in EtOH (5 mL) and thiourea (0.070 g, 0.91, 2eq) was added. After 2 h stirring at 80°C under reflux, the mixture was evaporated on celite and purified via flash column chromatography (PE/EA 10 -> 50%). This delivered 0.40 g (yield: 91%) of the product as a slightly yellow foam.

^{1}H NMR ($CDCl_3$, 400MHz): δ = 0.78 (q, J= 7.9Hz, CH_3-CH_2-Si), 1.10 (t, J= 7.9 Hz, CH_3-CH_2-Si), 4.65 (dd, J= 12.1, 4.8 Hz, 1H, H-5'), 4.76 (dd, J= 12.1, 3.7 Hz, 1H, H-5'), 4.81-4.87 (m, 1H, H-4'), 6.24 (m, 1H, H-3'), 6.36 (dd, J=5.4, 3.1 Hz, 1H, H-2'), 6.67 (d, J= 3.1 Hz, 1H, H-1'), 7.33 – 7.47 (m, 6H, CH-Bz), 7.50- 7.59 (m, 3H, CH-Bz), 7.79 (s, 1H, H-2), 7.93 – 8.00 (m, 4H, CH-Bz), 8.06- 8.11 (m, 2H, H-Bz), 10.70 (br s, 6-SH) ppm.

^{13}C NMR ($CDCl_3$, 100MHz): δ = 4.28 (CH_3-CH_2-Si), 7.68 (CH_3-CH_2-Si), 63.87 (CH_2-5'), 71.91 (CH-3'), 74.63 (CH-2'), 80.64 (CH-4'), 88.03 (CH-1'), 95.84 (C-ethynyl), 101.61 (C-ethynyl), 118.15 (C-5), 128.62 (CH-Bz), 128.66 (2 x CH-Bz), 128.82 – 128.96 – 129.6 (C-Bz), 129.94 – 130-02 – 130.04 (CH-Bz), 133.25 - 133.72 – 133.86 (CH-Bz), 134.70 (C-7), 145.84 (CH-2), 147.48 (C-4), 165.22 - 165.36 - 166.43 (C=O Bz), 178.77 (C6) ppm.

Synthesis of N1-(2', 3', 5'-tri-O-benzoyl-β-D-ribofuranosyl)-5-thia-1,2,6,8-tetraazaacenaphtylene (28)

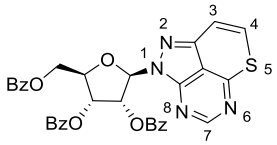

Intermediate **27** (220 mg, 0.299 mmol, 1eq) is dissolved in THF (5.5 mL) and TBAF (0.36 mL 1M, 0.36 mmol, 1.1 eq) was added. After 1h stirring at RT, H_2O was added and extracted with EA (x2). After drying over Na_2SO_4 the crude was purified via flash column chromatography (T/EA 0 -> 30%) and delivered the product as a white foam (160 mg, 87%).

The systematic numbering of acenaphtylene ring is highlighted. In the NMR characterization, the purine nomenclature is used.

^{1}H NMR ($CDCl_3$, 400MHz): δ = 4.59-4.64 (m, 1H, H5'), 4.79- 4.89 (m, 2H, H5', H4'), 6.34 (m, 1H, H3'), 6.37-6.41 (m, 1H, H2'), 6.73 (d, J= 3.0 Hz, 1H, H1'*), 6.91 (d, J= 9.8 Hz), 7.05 (d, J= 9.8 Hz),* 7.34-7.43 (m,

6H, H-Bz), 7.51-7.61 (m, 3H, H-Bz), 7.94-8.00 (m, 4H, H-Bz), 8.08-8.13 (m, 2H, H-Bz), 8.62 (s, 1H, H2) ppm.

^{13}C NMR ($CDCl_3$, 100MHz): δ = 63.83 (CH_2-5'), 72.00 (CH-3'), 74.85 (CH-2'), 80.50 (CH-4'), 87.65 (CH-1'), 114.98 (C-5), *118.50 (CH),* 128.48 - 128.63 – 128.67 (3 x CH-Bz), *129.13 (CH),* 128.82 – 128.95 – 129.81 (C-Bz), 129.95 – 130.02 – 130.04 (CH-Bz), 133.28 – 133.75 – 133.86 (CH-Bz), 144.32 (C-7), 151.41 (C-4), 157.19 (C-2), 164.15 (C-6), 165.28 - 165.47 - 166.28 (C=O Bz) ppm.

Initial synthesis of cyclised nucleoside 15a, side product 16 & its NMR-analysis

Synthesis of 4-oxo-3-((trimethylsilyl)ethynyl)-N1-(2', 3', 5'-tri-O-benzoyl-β-D-ribofuranosyl)-pyrazolo[3,4-*d*]pyrimidine (12)

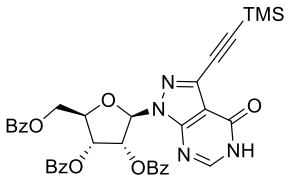

Iodinated allopurinol riboside **11** (1.83 g, 2.59 mmol, 1 eq) was dissolved in DMF (7 mL) and triethylamine (3.61 mL, 25.9 mmol, 10 eq) and trimethylsilylacetylene (3.59 mL, 25.9 mmol, 10 eq) were added. The solution was purged with argon for 5 minutes before the addition of CuI (0.050 g, 0.26 mmol, 0.1 eq) and $Pd(PPh_3)_2Cl_2$ (0.091 g, 0.13 mmol, 0.05 eq). EA was added after 4 h and the organic layer washed twice with brine. The organic phase was then dried over Na_2SO_4, filtered and concentrated under reduced pressure. The residue was purified via column chromatography (PE/EA 15 -> 100%) and yielded the pure product as a slightly yellow foam (1.0 g, 57% yield).

^{1}H NMR ($CDCl_3$, 400MHz): δ 0.34 (s, 9H, TMS), 4.66 (dd, J= 4.8; 12.1 Hz, 1H, H5'), 4.76 (dd, J= 3.7; 12.2 Hz, 1H, H5'), 4.84 (m, 1H, H4'), 6.28 (m, 1H, H3'), 6.33 – 6.37 (m, 1H, H2'), 6.72 (d, J= 2.8 Hz, 1H, H1'), 7.32-7.47 (m, 6H, H-Bz), 7.50-7.60 (m, 3H, H-Bz), 7.93-8.02 (m, 5H, H-Bz, H2), 8.08- 8.11 (m, 2H, H-Bz), 11.73 (s, 1H, NH) ppm.

Synthesis of 4-chloro-3-((trimethylsilyl)ethynyl)-N1-(2', 3', 5'-tri-O-benzoyl-β-D-ribofuranosyl)-pyrazolo[3,4-*d*]pyrimidine (13)

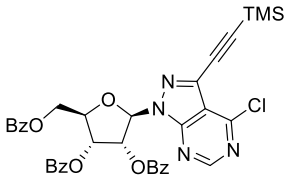

Compound **12** (1 g, 1.48 mmol, 1 eq) was dissolved in chloroform (14 mL). Then, DMF (0.75 mL) and thionyl chloride (1.48 mL) were added. After 1.5 h stirring at 75°C, the solution was cooled to 0°C and ice and saturated $NaHCO_3$ solution were added. The organic layer was washed twice with sat. $NaHCO_3$, dried over Na_2SO_4, filtered and concentrated under reduced pressure. The residue was purified via column chromatography (PE/EA 0 -> 20%) and afforded **13** as a white foam (0.75 g, yield of 73%).

^{1}H NMR ($CDCl_3$, 400MHz): δ 0.34 (s, 9H, TMS), 4.64 (dd, J= 4.8; 12.0 Hz, 1H, H5'), 4.76 (dd, J= 3.6; 12.1 Hz, 1H, H5'), 4.83- 4.89 (m, 1H, H4'), 6.28 (m, 1H, H3'), 6.40 (dd, J= 3.1; 5.4 Hz, 1H, H2'), 6.88 (d, J= 3.1 Hz, 1H, H1'), 7.34-7.48 (m, 6H, H-Bz), 7.52-7.60 (m, 3H, H-Bz), 7.93-7.99 (m, 4H, H-Bz), 8.07- 8.11 (m, 2H, H-Bz), 8.75 (s, 1H, H2) ppm.

Synthesis of 4-benzylamino-3-((trimethylsilyl)ethynyl)-N1-(2', 3', 5'-tri-O-benzoyl-β-D-ribofuranosyl)-pyrazolo[3,4-*d*]pyrimidine (14)

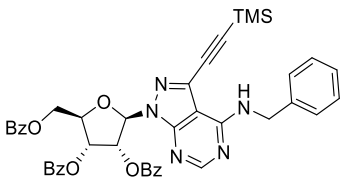

Chlorine **13** (300 mg, 0.43 mmol, 1 eq) was dissolved in DMF (5 mL) and Et_3N (0.060 mL, 0.43 mmol, 1.0 eq) and benzylamine (0.048 mL, 0.43 mmol, 1 eq) were added. After stirring 1 h, the mixture was diluted with EA and washed 2 times with brine. After drying the organic layer over Na_2SO_4 and evaporation, the crude was purified via flash column chromatography (PE/EA 5 -> 40%). This delivered 0.120 g (yield: 63%) of the product as a white foam and was used in the next step (deprotection) without detailed characterization.

Synthesis of 5-benzyl-1-(β-D-ribofuranosyl)-1,2,5,6,8-pentazaacenaphtylene 15a (& side product 16)

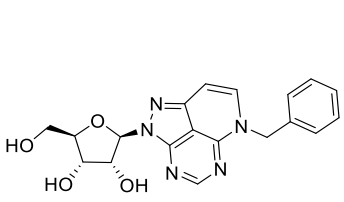

15a

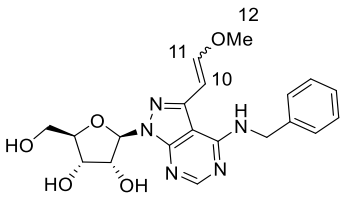

16

Intermediate **14** (0.12 g, 0,15 mmol, 1 eq) was dissolved in MeOH (2 mL) and DCM (2 mL) followed by addition of K_2CO_3 (10 mg, 0.075 mmol, 0.5 eq). After 6h, the reaction mixture was filtered and the filtrate purified via flash column chromatography (DCM/MeOH 0 -> 10%).

^{1}H NMR analysis revealed the absence of the NH- and ethynyl- proton and the presence of two doublets (Italics), matching with the 6-endo dig cyclized product 25:

^{1}H NMR (DMSO-d6, 400MHz): δ = 3.42-3.50 (m, 1H, H-5'), 3.55-3.62 (m, 1H, H-5'), 3.91 (dd, J= 9.3; 4.5 Hz, 1H, H4'), 4.20 (dd, J= 9.6; 5.0 Hz, 1H, H-3'), 4.64 (dd, J= 10.63; 5.1Hz, 1H, H-2'), 4.87 (dd, J= 6.5; 5.2 Hz, 1H, 5'-OH), 5.12 (d, J= 5.4 Hz, 1H, 3'-OH), 5.20 (s, 2H, CH_2-benzyl), 5.37 (d, J= 6.0 Hz, 1H, 2'-OH), 5.92 (d, J= 4.9 Hz, 1H, H-1'), *6.51 (d, J= 7.6 Hz, 1H),* 7.26-7.37 (m, 5H, H-phe),*7.40 (d, J= 7.6 Hz, 1H),* 8.39 (s, 1H, H-2) ppm.

LCMS and NMR analysis showed the presence of a side material, presumed to be MeOH adduct **26**.

^{1}H NMR:

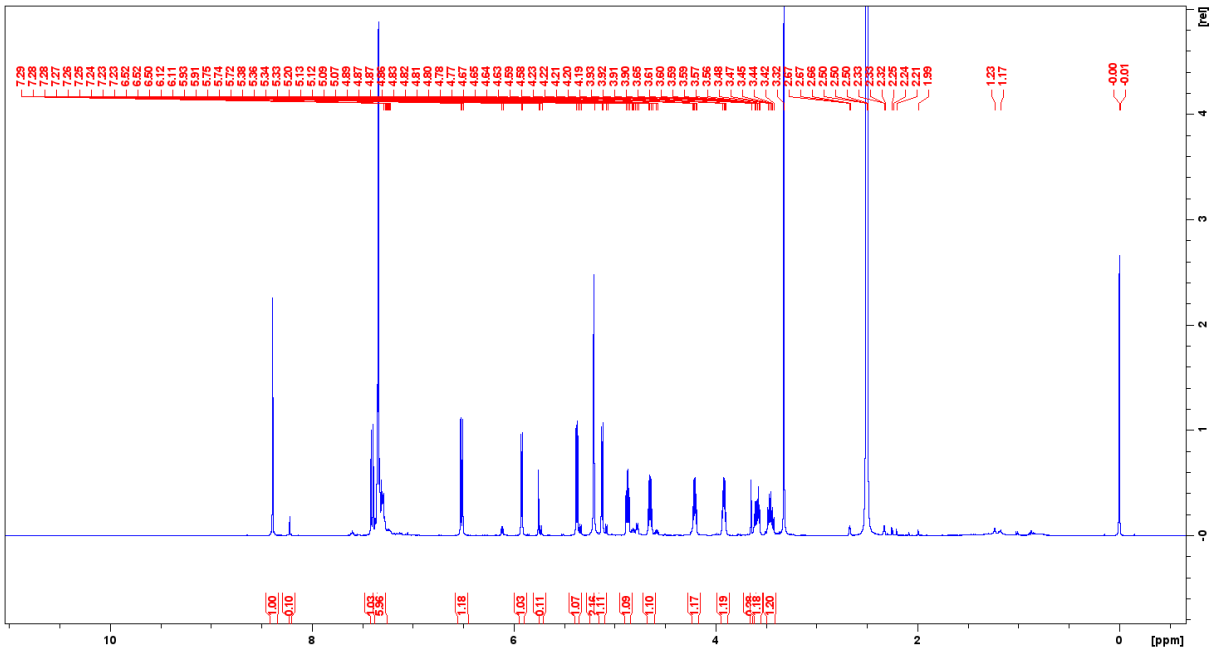

Indications for the formation of MeOH adduct **16** (+/- 10%):

^{1}H NMR (DMSO-d6, 400MHz): δ = 3.65 (s, 3H, OMe), 5.73 (d, J= 7.0 Hz, 1H, H-10), 6.51 (d, J= 7.1 Hz, 1H, H-11) ppm

^{13}C NMR ($CDCl_3$, 100MHz): δ = 60.48 (CH_3, OMe), 95.48 (CH, C10), 151.19 (CH, C11) ppm

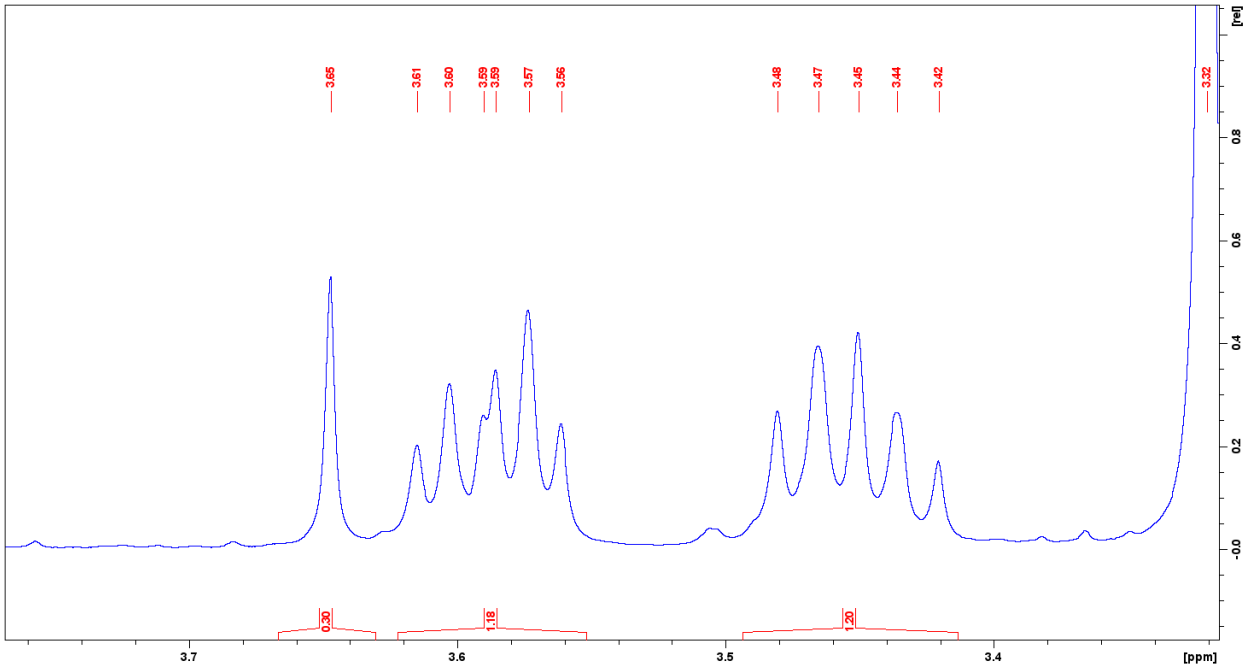

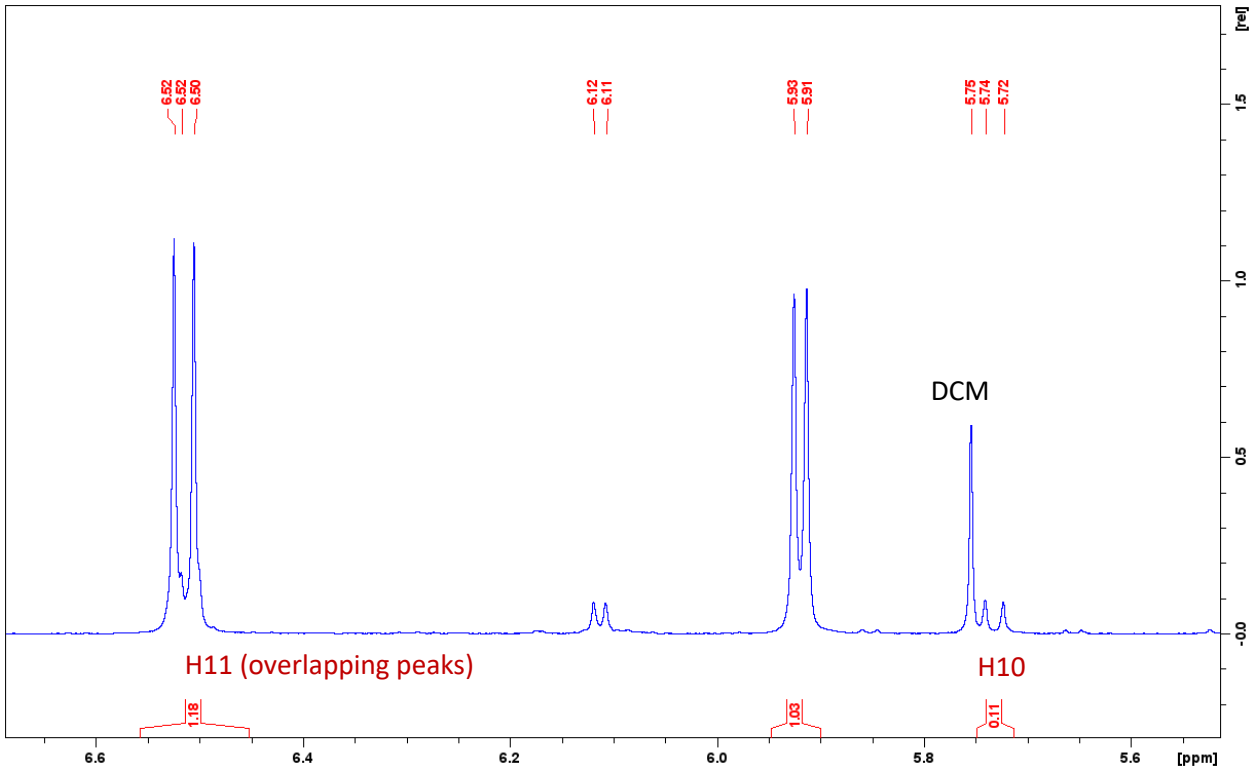
6.52
6.52
6.50
6.12
6.11
5.93
5.91
5.75
5.74
5.72
DCM
H11 (overlapping peaks)
H10
1.18
1.00
0.11
6.6
6.4
6.2
6.0
5.8
5.6
[ppm]
[rel]
1.5
1.0
0.5
-0.0

HMBC- analysis:

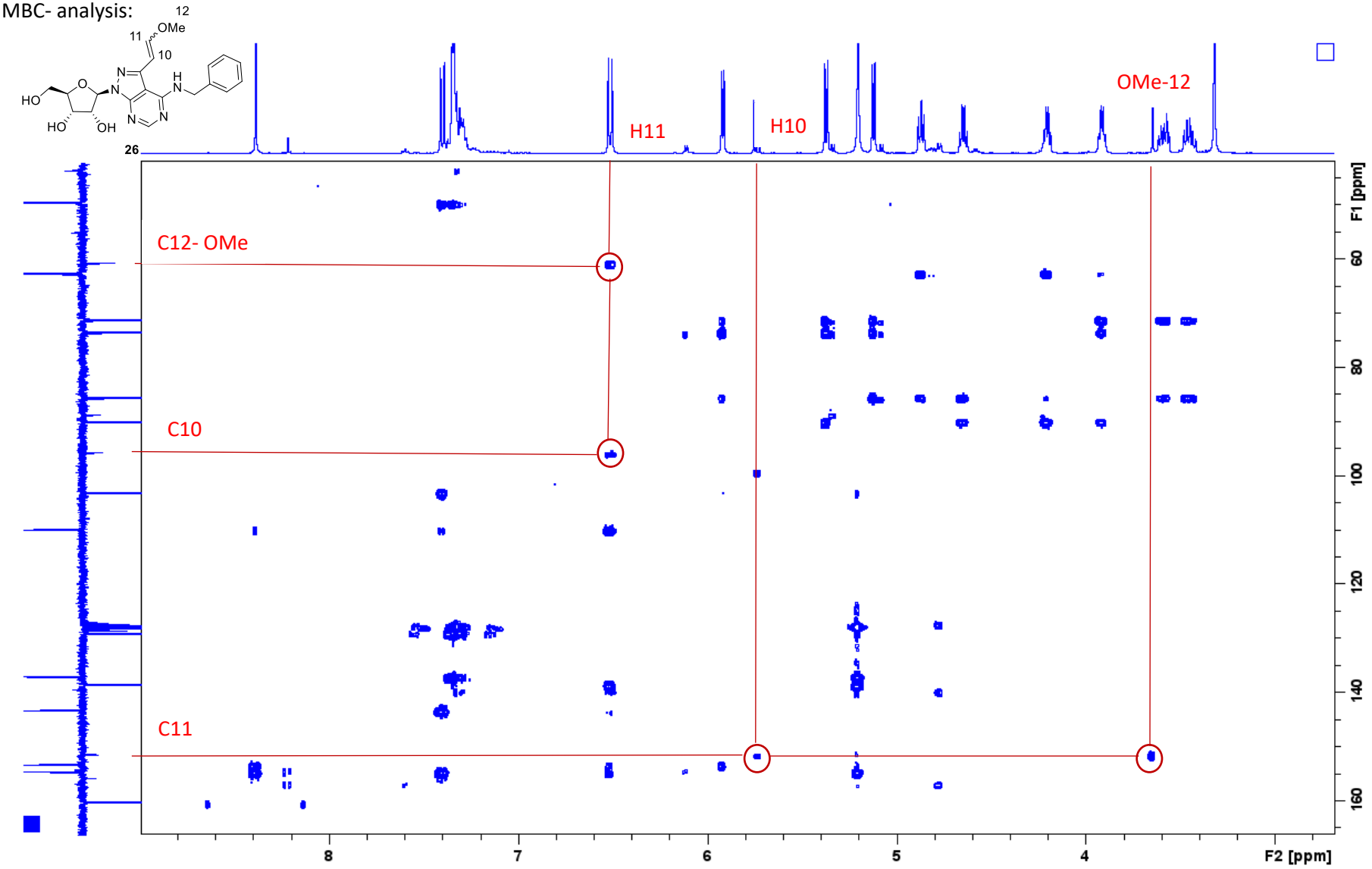

Synthesis of final nucleosides

Synthesis of 4-benzylamino-5-ethynyl-N7-(β-D-ribofuranosyl)-pyrrolo[2,3-*d*]pyrimidine (7a)

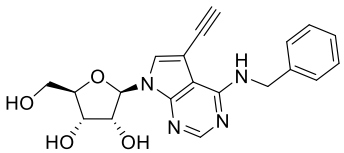

Compound **7a** was synthesized according to general procedure A (starting with 890 mg of **5**), followed by general procedure B. This delivered 76 mg of the product in 16 % yield over 2 steps.

^{1}H NMR (DMSO-d6, 400MHz): δ = 3.50-3.57 (m, 1H, H-5'), 3.60-3.68 (m, 1H, H-5'), 3.91 (m, 1H, H4'), 4.09 (m, 1H, H-3'), 4.29 (s, 1H, H-ethynyl), 4.39 (dd, J= 11.4; 6.0Hz, 1H, H-2'), 4.75- 4.86 (m, 2H, CH_2-benzyl), 5.13 (d, J= 4.8 Hz, 1H, 3'-OH), 5.18 (t, J= 5.5Hz, 1H, 5'-OH), 5.35 (d, J = 6.3 Hz, 1H, 2'-OH), 6.04 (d, J= 6.1 Hz, 1H, H-1'), 6.81 (t, J= 6.1 Hz, 1H, NH), 7.20-7.37 (m, 5H, H-phe),7.86 (s, 1H, H-8), 8.20 (s, 1H, H-2) ppm.

^{13}C NMR (DMSO-d6, 100MHz): δ = 43.27 (CH_2-benzyl), 61.47 (C-5'), 70.48 (C-3'), 74.03 (C-2'), 77.16 (C-ethynyl), 83.47 (CH-ethynyl), 85.29 (C-4'), 87.27 (C-1'), 93.59 (C-7), 102.62 (C-5), 126.78 (CH-phe), 126.94 (CH-phe), 127.63 (C-8), 128.39 (CH-Phe), 139.65 (C-Phe), 149.05 (C4), 152.62 (C2), 156.27 (C-6) ppm.

HRMS (ESI): calculated for $C_{20}H_{21}N_4O_4$ ($[M+H]^+$): 381.15573, found: 381.1555.

Synthesis of 4-(((S)-1-phenylethyl)amino)-5-ethynyl-N7-(β-D-ribofuranosyl)-pyrrolo[2,3-*d*]pyrimidine (7b)

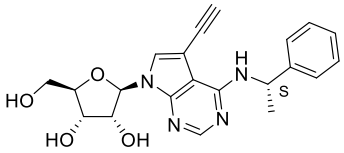

Compound **7b** was synthesized according to general procedure A (starting with 1.0 g of **5**), followed by general procedure B. This delivered 370 mg of the product in 81 % yield over 2 steps.

^{1}H NMR (DMSO-d6, 400MHz): δ = 1.55 (d, J= 6.8Hz, 3H, CH_3), 3.49-3.57 (m, 1H, H-5'), 3.59-3.68 (m, 1H, H-5'), 3.91 (m, 1H, H4'), 4.09 (m, 1H, H-3'), 4.36 (dd, J= 11.4; 6.0Hz, 1H, H-2'), 4.47 (s, 1H, H-ethynyl), 5.12 (d, J= 5.0 Hz, 1H, 3'-OH), 5.16 (t, J= 5.5Hz, 1H, 5'-OH), 5.34 (d, J = 6.2 Hz, 1H, 2'-OH), 5.43 (m, 1H, CH-benzyl), 6.02 (d, J= 6.1 Hz, 1H, H-1'), 6.45 (d, J= 8.0 Hz, 1H, NH), 7.21-7.46 (m, 5H, H-phe),7.88 (s, 1H, H-8), 8.18 (s, 1H, H-2) ppm.

^{13}C NMR (DMSO-d6, 100MHz): δ = 22.92 (CH_3), 49.16 (CH-benzyl), 61.44 (C-5'), 70.44 (C-3'), 74.10 (C-2'), 77.54 (C-ethynyl), 83.62 (CH-ethynyl), 85.29 (C-4'), 87.23 (C-1'), 93.29 (C-7), 102.61 (C-5), 125.69 (CH-Phe), 126.95 (CH-phe), 127.51 (C-8), 128.39 (CH-Phe), 144.16 (C-Phe), 149.92 (C4), 152.70 (C2), 155.60 (C-6) ppm.

HRMS (ESI): calculated for $C_{21}H_{23}N_4O_4$ ($[M+H]^+$): 395.17138, found: 381.1711.

Synthesis of 4-(((R)-1-phenylethyl)amino)-5-ethynyl-N7-(β-D-ribofuranosyl)-pyrrolo[2,3-*d*]pyrimidine (7c)

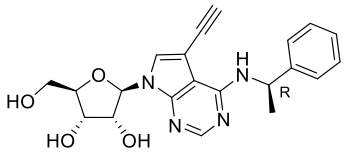

Compound **7c** was synthesized according to general procedure A (starting with 1.0 g of **5**), followed by general procedure B. This delivered 350 mg of the product in 78 % yield over 2 steps.

^{1}H NMR (DMSO-d6, 400MHz): δ = 1.55 (d, J= 6.8Hz, 3H, CH_3), 3.49-3.57 (m, 1H, H-5'), 3.59-3.68 (m, 1H, H-5'), 3.90 (m, 1H, H4'), 4.09 (m, 1H, H-3'), 4.38 (dd, J= 11.4; 6.0Hz, 1H, H-2'), 4.47 (s, 1H, H-ethynyl), 5.13 (d, J= 4.8 Hz, 1H, 3'-OH), 5.17 (t, J= 5.6Hz, 1H, 5'-OH), 5.35(d, J = 6.4 Hz, 1H, 2'-OH), 5.44 (m, 1H, CH-benzyl), 6.02 (d, J= 6.0 Hz, 1H, H-1'), 6.46 (d, J= 8.0 Hz, 1H, NH), 7.21-7.47 (m, 5H, H-phe),7.88 (s, 1H, H-8), 8.18 (s, 1H, H-2) ppm.

^{13}C NMR (DMSO-d6, 100MHz): δ = 22.93 (CH_3), 49.18 (CH-benzyl), 61.44 (C-5'), 70.44 (C-3'), 74.10 (C-2'), 77.52 (C-ethynyl), 83.63 (CH-ethynyl), 85.31 (C-4'), 87.33 (C-1'), 93.30 (C-7), 102.68 (C-5), 125.71 (CH-Phe), 126.99 (CH-phe), 127.59 (C-8), 128.60 (CH-Phe), 144.10 (C-Phe), 148.93 (C4), 152.70 (C2), 155.60 (C-6) ppm.

HRMS (ESI): calculated for $C_{21}H_{23}N_4O_4$ ($[M+H]^+$): 395.17138, found: 381.1715.

Synthesis of 4-((2-chlorobenzyl)amino)-5-ethynyl-N7-(β-D-ribofuranosyl)-pyrrolo[2,3-*d*]pyrimidine (7d)

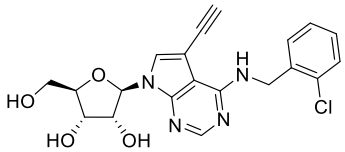

Compound **7c** was synthesized according to general procedure A (starting with 1 g of **5**), followed by general procedure B. This delivered 180 mg of the product in 38 % yield over 2 steps.

^{1}H NMR (DMSO-d6, 400MHz): δ = 3.50 – 3.59 (m, 1H, H-5'), 3.59 – 3.69 (m, 1H, H-5'), 3.90 (dd, J= 6.9, 3.5 Hz, 1H, H-4'), 4.09 (m, 1H, H-3'), 4.33 (s, 1H, H-ethynyl), 4.39 (dd, J= 11.1, 5.7 Hz, 1H, H-2'), 4.85 (d, J= 6.5 Hz, 2H, CH_2-benzyl), 5.13 (d, J= 4.4 Hz, 1H, 3'-OH), 5.17 (t, J= 5.5 Hz, 1H, 5'-OH), 5.35 (d, J= 6.0 Hz, 1H, 2'-OH), 6.04 (d, J= 6.0, 1H, H-1'), 6.93 (t, J= 6.2, 1H, NH), 7.26 – 7.37 (m, 3H, H-phe), (7.45 - 7.49 (m, 1H, H-phe), 7.88 (s, 1H, H-8), 8.18 (s, 1H, H-2) ppm.

^{13}C NMR (DMSO-d6, 100MHz): δ = 41.57 (CH_2-benzyl), 61.46 (C-5'), 70.47 (C-3'), 74.04 (C-2'), 77.04 (C-ehtynyl), 83.58 (CH-ethynyl), 85.30 (C-4'), 87.25 (C-1'), 93.64 (C-7), 102.84 (C-5), 127.21 (CH-phe), 127.70 (C8), 128.58 (2 x CH-phe), 129.21 (CH-phe), 132.03 (C-phe), 136.57 (C-phe), 149.09 (C-4), 152.58 (C-2), 156.11 (C-6) ppm.

HRMS (ESI): calculated for $C_{20}H_{20}ClN_4O_4$ ($[M+H]^+$): 415.11678, found: 415.1164.

Synthesis of 5-ethynyl-4-((2-fluorobenzyl)amino)-N7-(β-D-ribofuranosyl)-pyrrolo[2,3-*d*]pyrimidine (7g)

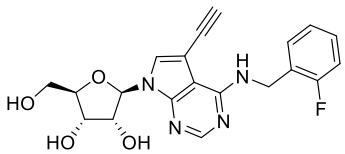

Compound **7g** was synthesized according to general procedure A (starting with 1 g of **5**), followed by general procedure B. This delivered 117 mg of the product in 22 % yield over 2 steps.

^{1}H NMR (DMSO-d6, 400MHz): δ = 3.50 – 3.59 (m, 1H, H-5'), 3.59 – 3.69 (m, 1H, H-5'), 3.90 (m, 1H, H-4'), 4.09 (m, 1H, H-3'), 4.32 (s, 1H, H-ethynyl), 4.38 (dd, J= 11.4, 6.0 Hz, 1H, H-2'), 4.84 (d, J= 6.2 Hz, 2H, CH_2-benzyl), 5.13 (d, J= 4.8 Hz, 1H, 3'-OH), 5.17 (t, J= 5.4 Hz, 1H, 5'-OH), 5.35 (d, J= 6.3 Hz, 1H, 2'-OH), 6.04 (d, J= 6.0, 1H, H-1'), 6.83 (t, J= 6.2, 1H, NH), 7.11 – 7.23 (m, 2H, H-phe), 7.26 – 7.38 (m, 2H, H-phe), 7.88 (s, 1H, H-8), 8.20 (s, 1H, H-2) ppm.

^{13}C NMR (DMSO-d6, 100MHz): δ = 37.57 (d, $^{3}J_{(C,F)}$ = 4.5 Hz, CH_2-benzyl), 61.47 (C-5'), 70.47 (C-3'), 74.05 (C-2'), 77.06 (C-ethynyl) 83.51 (CH-ethynyl), 85.29 (C-4'), 87.25 (C-1'), 93.61 (C-7), 102.77 (C-5), 115.12 (d, $^{2}J_{(C,F)}$ = 21.0 Hz, CH-phe), 124.37 (d, $^{4}J_{(C-F)}$ = 3.4 Hz, CH-phe), 126.33 (d, $^{2}J_{(C,F)}$ = 14.5 Hz, C-phe),127.72 (C-8), 128.79 (d, $^{3}J_{(C,F)}$ = 8.1 Hz, CH-phe), 128.92 (d, $^{3}J_{(C,F)}$ = 4.5 Hz, CH-phe), 149.08 (C-4), 152.57 (C-2), 156.17 (C-6), 160.19 (d, $^{1}J_{(C,F)}$ = 243.7 Hz, C-phe) ppm.

^{19}F NMR (DMSO-d6, 377MHz): δ = -119.22 ppm

HRMS (ESI): calculated for $C_{20}H_{20}FN_4O_4$ ([M+H]$^+$): 399.14628, found: 399.1464

Synthesis of 4-(cyclopentylamino)-5-ethynyl-N7-(β-D-ribofuranosyl)-pyrrolo[2,3-*d*]pyrimidine (7j)

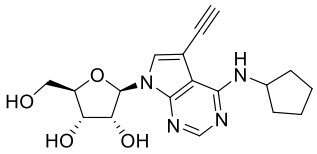

Compound **7j** was synthesized according to general procedure A (starting with 0.4 g of **5**), followed by general procedure B. This delivered 110 mg of product **7j** in 53 % yield over 2 steps.

^{1}H NMR (DMSO-d6, 400MHz): δ = 1.44-1.56 (m, 2H, H-cyclopentyl), 1.57-1.76 (m, 4H, H-cyclopentyl), 1.97-2.08 (m, 2H, H-cyclopentyl), 3.50-3.57 (m, 1H, H-5'), 3.60-3.67 (m, 1H, H-5'), 3.89-3.92 (m, 1H, H4'), 4.08 (m, 1H, H-3'), 4.36 (dd, J= 11.2; 5.8 Hz, 1H, H-2'), 4.42- 4.52 (m, 2H, H-cyclopentyl, H-ethynyl), 5.12 (d, J= 4.8 Hz, 1H, 3'-OH), 5.19 (t, J= 5.2Hz, 1H, 5'-OH), 5.34 (d, J = 6.4 Hz, 1H, 2'-OH), 6.00 (d, J= 6.0 Hz, 1H, H-1'), 6.12 (d, J= 7.3 Hz, 1H, NH), 7.83 (s, 1H, H-8), 8.21 (s, 1H, H-2) ppm.

^{13}C NMR (DMSO-d6, 100MHz): δ= 23.17 (CH_2-cyclopentyl), 32.69 (CH_2 cyclopentyl), 32.74 (CH2 cyclopentyl), 51.71 (CH cyclopentyl), 61.48 (C-5'), 70.47 (C-3'), 74.04 (C-2'), 77.56 (C-ethynyl), 83.42 (CH-ethynyl), 85.29 (C-4'), 87.32 (C-1'), 93.27 (C-7), 102.62 (C-5), 127.27 (C-8), 148.75 (C4), 152.79 (C2), 156.10 (C-6) ppm.

HRMS (ESI): calculated for $C_{18}H_{23}N_4O_4$ ([M+H]$^+$): 359.17139, found: 359.1711.

Synthesis of 4-benzylamino-5-trifluoromethyl-N7-(β-D-ribofuranosyl)-pyrrolo[2,3-*d*]pyrimidine (8a)

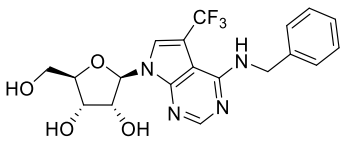

Compound **8a** was synthesized according to general procedure A (starting with 0.77 g of **6**), followed by general procedure B. This delivered 120 mg of the product in 24 % yield over 2 steps

^{1}H NMR (DMSO-d6, 400MHz): δ = 3.53-3.61 (m, 1H, H-5'), 3.63-3.71 (m, 1H, H-5'), 3.93 (m, 1H, H-4'), 4.12 (dd, J= 8.5; 4.8 Hz, 1H, H-3'), 4.41 (dd, J= 11.2; 5.8 Hz, 1H, H-2'), 4.83 (m, 2H, CH_2-benzyl), 5.15 (d, J= 4.9 Hz, 1H, 3'-OH), 5.20 (t, J= 5.4 Hz, 1H, 5'-OH), 5.41 (d, J= 6.2 Hz, 1H, 2'-OH), 6.13 (d, J= 5.9 Hz, 1H, H-1'), 6.56 (t, J= 5.7Hz, 1H, NH), 7.18-7.25 (m, 1H, H-phe), 7.27-7.35 (m, 4H, H-phe), 8.24 (s, 1H, H-8), 8.29 (s, 1H, H-2) ppm.

^{13}C NMR (DMSO-d6, 100MHz): δ = 43.73 (CH_2-benzyl), 61.20 (C-5'), 70.24 (C-3'), 74.11 (C-2'), 85.35 (C-4'), 87.36 (C-1'), 98.48 (C5), 103.14 (q, ^{2}J(C,F) = 37.1, C-7), 123.58 (q, ^{1}J(C,F) = 265.7 Hz, CF_3), 124.19 (q, ^{3}J(C,F) = 6.2 Hz, C8), 126.63 (CH-phe), 126.83 (CH-phe), 128.28 (CH-phe), 139.78 (C-phe), 150.89 (C-4), 152.82 (CH-2),154.81 (C-6) ppm.

^{19}F NMR (DMSO-d6, 377MHz): δ = -53.30 ppm

HRMS (ESI): calculated for $C_{19}H_{20}F_3N_4O_4$ ([M+H]$^+$): 425.14312, found: 425.1435.

Synthesis of 4-(((S)-1-phenylethyl)amino)-5-trifluoromethyl-N7-(β-D-ribofuranosyl)-pyrrolo[2,3-*d*]pyrimidine (8b)

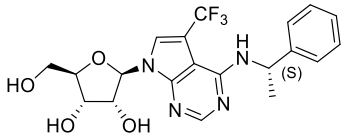

Compound **8b** was synthesized according to general procedure A (starting with 0.79 g of **6**), followed by general procedure B. This delivered 257 mg of the product in 49 % yield over 2 steps

^{1}H NMR (DMSO-d6, 400MHz): δ = 1.56 (d, J= 6.9 Hz, 3H, CH_3), 3.52 – 3.61 (m, 1H, H-5'), 3.63 – 3.72 (m, 1H, H-5'), 3.93 (dd, J= 6.7, 3.2 Hz, 1H, H-4'), 4.11 (dd, J= 8.7, 4.9 Hz, 1H, H-3'), 4.39 (dd, J= 11.4, 6.0 Hz, 1H, H-2'), 5.15 (d, J= 4.9 Hz, 1H, 3'-OH), 5.18 (t, J= 5.5 Hz, 1H, 5'-OH), 5.40 (d, J= 6.1 Hz, 1H, 2'-OH), 5.50 (m, 1H, CH-benzyl), 5.67 (d, J= 6.2 Hz, 1H, NH), 6.12 (d, J= 5.8, 1H, H-1'), 7.20 – 7.43 (m, 5H, H-phe), 8.28 (s, 1H, H-8), 8.30 (s, 1H, H-2) ppm.

^{13}C NMR (DMSO-d6, 100MHz): δ = 22.65 (CH_3), 49.56 (CH benzyl), 61.15 (C-5'), 70.19 (C-3'), 74.19 (C-2'), 85.36 (C-4'), 87.35 (C-1'), 98.59 (C-5), 102.66 (q, $^{2}J_{(C-F)}$ = 37.09 Hz, C-7), 123.78 (q, $^{1}J_{(C-F)}$ = 265.60 Hz, CF_3), 124.63 (q, $^{3}J_{(C-F)}$ = 6.21 Hz, C-8), 125.67 (CH phe), 126.97, (CH phe), 128.55 (CH phe) 144.08 (C phe), 150.84 (C-4), 152.88 (C-2), 154.01 (C-6) ppm.

^{19}F NMR (DMSO-d6, 377MHz): δ = - 48.22 ppm.

HRMS (ESI): calculated for $C_{20}H_{22}F_3N_4O_4$ ([M+H]$^+$): 439.15878, found: 439.1586

Synthesis of 4-(((R)-1-phenylethyl)amino)-5-trifluoromethyl-N7-(β-D-ribofuranosyl)-pyrrolo[2,3-*d*]pyrimidine (8c)

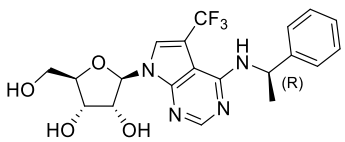

Compound **8c** was synthesized according to general procedure A(starting with 0.79 g of **6**), followed by general procedure B. This delivered 242 mg of the product in 47 % yield over 2 steps.

^{1}H NMR (DMSO-d6, 400MHz): δ = 1.56 (d, J= 6.9 Hz, 3H, CH_3), 3.52 – 3.61 (m, 1H, H-5'), 3.63 – 3.72 (m, 1H, H-5'), 3.93 (dd, J= 7.0, 3.5 Hz, 1H, H-4'), 4.06 – 4.14 (m, 1H, H-3'), 4.42 (dd, J= 11.3, 5.8 Hz, 1H, H-2'), 5.14 – 5.22 (m, 2H, 3' and 5'-OH), 5.42 (d, J= 6.2 Hz, 1H, 2'-OH), 5.50 (m, 1H, CH-benzyl), 5.67 (d, J=

6.0 Hz, 1H, NH), 6.11 (d, J= 5.8, 1H, H-1') , 7.20 – 7.43 (m, 5H, H-phe), 8.28 (s, 1H, H-8), 8.31 (s, 1H, H-2) ppm.

^{13}C NMR (DMSO-d6, 100MHz): δ = 22.67 (CH_3), 49.58 (CH benzyl), 61.16 (C-5'), 70.20 (C-3'), 74.11 (C-2'), 85.37 (C-4'), 87.43 (C-1'), 98.66 (C-5), 102.66 (q, $^2J_{(C-F)}$ = 37.05 Hz, C-7), 123.78 (q, $^1J_{(C-F)}$ = 265.6 Hz, CF_3), 124.69 (q, $^3J_{(C-F)}$ = 6.1 Hz, C-8), 125.70 (CH-phe), 127.02 (CH-phe), 128.58 (CH-phe), 144.02 (C-phe), 150.85 (C-4), 152.90 (C-2), 154.04 (C-6) ppm.

^{19}F NMR (DMSO-d6, 377MHz): δ = -52.98 ppm.

HRMS (ESI): calculated for $C_{20}H_{22}F_3N_4O_4$ ($[M+H]^+$): 439.15878, found: 439.1587.

Synthesis of 4-((2-chlorobenzyl)amino)-5-trifluoromethyl-N7-(β-D-ribofuranosyl)-pyrrolo[2,3-*d*]pyrimidine (8d)

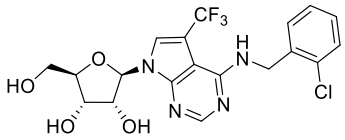

Compound **8d** was synthesized according to general procedure A (starting with 0.75 g of **6**), followed by general procedure B. This delivered 249 mg of the product in 48 % yield over 2 steps

^{1}H NMR (DMSO-d6, 400MHz): δ = 3.53 – 3.61 (m, 1H, H-5'), 3.64 – 3.72 (m, 1H, H-5'), 3.93 (m, 1H, H-4'), 4.11 (dd, J= 8.5, 4.9 Hz, 1H, H-3'), 4.42 (dd, J= 11.4, 5.5 Hz, 1H, H-2'), 4.88 (d, J= 5.9 Hz, 2H, CH_2-benzyl), 5.16 (d, J= 5.0 Hz, 1H, 3'-OH), 5.19 (t, J= 5.7 Hz, 1H, 5'-OH), 5.42 (d, J= 6.3 Hz, 1H, 2'-OH), 6.13 (d, J= 5.9, 1H, H-1'), 6.62 (t, J= 5.9, 1H, NH), 7.22 – 7.32 (m, 3H, H-phe), 7.43 – 7.49 (m, 1H, H-phe), 8.27 (s, 1H, H-8), 8.28 (s, 1H, H-2) ppm.

^{13}C NMR (DMSO-d6, 100MHz): δ = 42.02 (CH_2-benzyl), 61.20 (C-5'), 70.25 (C-3'), 74.14 (C-2'), 85.38 (C-4'), 87.39 (C-1'), 98.60 (C-5), 103.17 (q, $^2J_{(C-F)}$ = 37.4 Hz, C-7), 123.57 (q, $^1J_{(C-F)}$ = 265.88 Hz, CF_3), 124.38 (q, $^3J_{(C,F)}$ = 6.1 Hz, C-8), 127.14 – 127.97 – 128.38 – 129.15 (4x CH-phe), 131.86 (C-phe), 136.62 (C-phe), 150.95 (C-4), 152.82 (C-2), 154.71 (C-6) ppm.

^{19}F NMR ($CDCl_3$, 377MHz): δ = -53.33 ppm.

HRMS (ESI): calculated for $C_{19}H_{19}ClF_3N_4O_4$ ($[M+H]^+$): 459.10418, found: 459.1043.

Synthesis of 4-((4-chlorobenzyl)amino)-5-trifluoromethyl-N7-(β-D-ribofuranosyl)-pyrrolo[2,3-*d*]pyrimidine (8e)

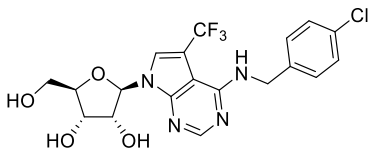

Compound **8e** was synthesized according to general procedure A (starting with 0.25g of **6**), followed by general procedure B. This delivered 99 mg of the product in 58 % yield over 2 steps.

^{1}H NMR (DMSO-d6, 400MHz): δ = 3.52 – 3.61 (m, 1H, H-5'), 3.63 – 3.70 (m, 1H, H-5'), 3.93 (m, 1H, H-4'), 4.08 – 4.14 (m, 1H, H-3'), 4.42 (dd, J= 11.2, 5.8 Hz, 1H, H-2'), 4.73-4.88 (m, 2H), 5.13 – 5.21 (m, 2H, 3' and 5'-OH), 5.40 (d, J= 6.2 Hz, 1H, 2'-OH), 6.12 (d, J= 5.9, 1H, H-1'), 6.69 (t, J= 5.78, 1H, NH), 7.31 – 7.40 (m, 4H, H-phe), 8.23 (s, 1H, H-8), 8.27 (s, 1H, H-2) ppm.

^{13}C NMR (DMSO-d6, 100MHz): δ = 43.15 (CH_2 benzyl), 61.19 (CH_2-5'), 70.23 (CH-3'), 74.10 (CH-2'), 85.35 (CH-4'), 87.34 (CH-1'), 98.49 (C-5), 103.18 (q, $^2J_{(C-F)}$ = 37.2 Hz, C-7), 123.53 (q, $^1J_{(C-F)}$ = 265.9 Hz, CF_3), 124.21 (q, $^3J_{(C-F)}$ = 6.17 Hz, C-8), 128.19 (2x CH-phe), 128.73 (2x CH-phe), 131.08 (C-phe), 138.99 (C-phe), 150.90 (C-4), 152.76 (CH-2), 154.70 (C-6) ppm.

^{19}F NMR (DMSO-d6, 377MHz): δ = -53.33 ppm.

HRMS (ESI): calculated for $C_{19}H_{19}ClF_3N_4O_4$ ([M+H]$^+$): 459,10415, found: 459.1042.

Synthesis of 4-((3-chlorobenzyl)amino)-5-trifluoromethyl-N7-(β-D-ribofuranosyl)-pyrrolo[2,3-*d*]pyrimidine (8f)

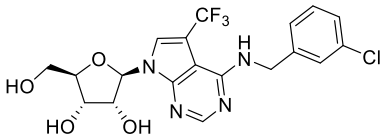

Compound **8f** was synthesized according to general procedure A (starting with 0.25 g of **6**), followed by general procedure B. This delivered 110 mg of the product in 64 % yield over 2 steps.

^{1}H NMR (DMSO-d6, 400MHz): δ = 3.52 – 3.61 (m, 1H, H-5'), 3.63 – 3.70 (m, 1H, H-5'), 3.93 (m, 1H, H-4'), 4.08 – 4.14 (m, 1H, H-3'), 4.41 (dd, J= 11.2, 5.8 Hz, 1H, H-2'), 4.74-4.88 (m, 2H), 5.12 – 5.21 (m, 2H, 3' and 5'-OH), 5.41 (d, J= 6.2 Hz, 1H, 2'-OH), 6.12 (d, J= 5.8, 1H, H-1'), 6.73 (t, J= 5.8, 1H, NH), 7.25 – 7.38 (m, 4H, H-phe), 8.25 (s, 1H, H-8), 8.28 (s, 1H, H-2) ppm.

^{13}C NMR (DMSO-d6, 100MHz): δ = 43.27 (CH_2 benzyl), 61.17 (CH_2-5'), 70.22 (CH-3'), 74.11 (CH-2'), 85.33 (CH-4'), 87.36 (CH-1'), 98.50 (C-5), 103.17 (q, $^2J_{(C-F)}$ = 37.2 Hz, C-7), 123.53 (q, $^1J_{(C-F)}$ = 265.8 Hz, CF_3), 124.26 (q, $^3J_{(C-F)}$ = 6.2 Hz, C-8), 125.53 (CH-phe), 126.53 (CH-Phe), 126.68 (CH-phe), 130.15 (CH-phe), 132.88 (C-phe), 142.69 (C-phe), 150.92 (C-4), 152.76 (CH-2), 154.67 (C-6) ppm.

^{19}F NMR (DMSO-d6, 377MHz): δ = -53.38 ppm.

HRMS (ESI): calculated for $C_{19}H_{19}ClF_3N_4O_4$ ([M+H]$^+$): 459.10418, found: 459.1044.

Synthesis of 4-((2-fluorobenzyl)amino)-5-trifluoromethyl-N7-(β-D-ribofuranosyl)-pyrrolo[2,3-*d*]pyrimidine (8g)

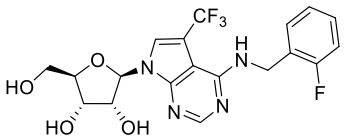

Compound **8g** was synthesized according to general procedure A (starting with 0.75 g of **6**), followed by general procedure B. This delivered 185 mg of product in 37% yield over 2 steps.

^{1}H NMR (DMSO-d6, 400MHz): δ = 3.52 – 3.61 (m, 1H, H-5'), 3.63 – 3.72 (m, 1H, H-5'), 3.93 (dd, J= 6.6, 3.2 Hz, 1H, H-4'), 4.11 (dd, J= 9.3, 5.1 Hz, 1H, H-3'), 4.41 (dd, J= 11.4, 5.9 Hz, 1H, H-2'), 4.87 (d, J= 5.9 Hz, 2H, CH_2-benzyl), 5.16 (d, J= 4.9 Hz, 1H, 3'-OH), 5.19 (t, J= 5.5 Hz, 1H, 5'-OH), 5.41 (d, J= 6.0 Hz, 1H, 2'-OH), 6.13 (d, J= 5.9, 1H, H-1'), 6.56 (t, J= 5.8, 1H, NH), 7.08 – 7.33 (m, 4H, H-phe), 8.26 (s, 1H, H-8), 8.29 (s, 1H, H-2) ppm.

^{13}C NMR (DMSO-d6, 100MHz): δ = 38.03 (d, $^3J_{(C,F)}$ = 4.6 Hz, CH_2-benzyl), 61.18 (C-5'), 70.23 (C-3'), 74.12 (C-2'), 85.36 (C-4'), 87.36 (C-1'), 98.59 (C-5), 103.13 (q, $^2J_{(C-F)}$ = 37.3 Hz, C-7), 115.08 (d, $J_{(C-F)}$ = 21.0 Hz,

CH-phe), 123.56 (q, $^{1}J_{(C-F)}$ = 265.94 Hz, CF_3), 124.29 (d, $J_{(C-F)}$ = 3.3 Hz, CH-phe), 124.36 (C-8), 126.42 (d, $^{2}J_{(C-F)}$ = 14.4 Hz, C-Phe), 128.49; 128.54; 128.62 (m, 2 x CH-phe), 150.91 (C-4), 152.80 (C-2), 154.73 (C-6), 160.14 (d, $^{1}J_{(C,F)}$= 243.52 Hz, C-phe) ppm.

^{19}F NMR (DMSO-d6, 377MHz): δ = - 119.32 (F-phe), -53.36 (CF_3) ppm.

HRMS (ESI): calculated for $C_{19}H_{19}F_4N_4O_4$ ($[M+H]^+$): 443.13368, found: 443.1333.

Synthesis of 4-phenylamino-5-trifluoromethyl-N7-(β-D-ribofuranosyl)-pyrrolo[2,3-*d*]pyrimidine (8h)

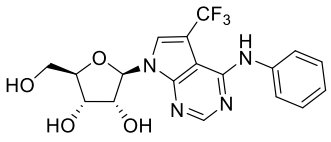

Compound **8h** was synthesized according to general procedure A (starting with 0.56 g of **6**), however, AgOTf (1eq) was added as well. Benzoyl group deprotection using general procedure B delivered 120 mg of the product in 52% yield over 2 steps.

^{1}H NMR (DMSO-d6, 400MHz): δ = 3.54 – 3.63 (m, 1H, H-5'), 3.65 – 3.74 (m, 1H, H-5'), 3.96 (m, 1H, H-4'), 4.10 – 4.17 (m, 1H, H-3'), 4.43 (dd, J= 11.2, 5.7 Hz, 1H, H-2'), 5.15 – 5.22 (m, 2H, 3' and 5'-OH), 5.45 (d, J= 6.2 Hz, 1H, 2'-OH), 6.19 (d, J= 5.7, 1H, H-1'), 7.13 (t, J= 7.4 Hz, 1H, H-phe), 7.34 – 7.47 (m, 3H, H-phe, NH), 7.69 (d, J= 7.7Hz, 2H, H-phe), 8.42 (s, 1H, H-8), 8.47 (s, 1H, H-2) ppm.

^{13}C NMR (DMSO-d6, 100MHz): δ = 61.10 (CH_2-5'), 70.15 (CH-3'), 74.24 (CH-2'), 85.39 (CH-4'), 87.36 (CH-1'), 99.69 (C-5), 102.86 (q, $^{2}J_{(C-F)}$ = 37.1 Hz, C-7), 121.67 (CH, phe), 123.62 (q, $^{1}J_{(C-F)}$ = 266.0 Hz, CF_3), 123.76 (CH, phe), 125.67 (q, $^{3}J_{(C-F)}$ = 6.3 Hz, C-8), 128.75 (CH-phe), 138.62 (C-phe), 151.39 (C-4), 152.44 (CH-2), 152.88 (C-6) ppm.

^{19}F NMR (DMSO-d6, 377MHz): δ = -52.66 ppm.

HRMS (ESI): calculated for $C_{18}H_{18}F_3N_4O_4$ ($[M+H]^+$): 411.12747, found: 411.1278.

Synthesis of 4-phenethylamino-5-trifluoromethyl-N7-(β-D-ribofuranosyl)-pyrrolo[2,3-*d*]pyrimidine (8i)

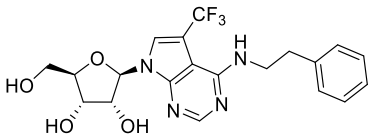

Compound **8i** was synthesized according to general procedure A (starting with 0.45 g of **6**), followed by general procedure B. This delivered 150 mg of the product in 49% yield over 2 steps.

^{1}H NMR (DMSO-d6, 400MHz): δ = 2.92 (t, J= 7.1Hz, 2H), 3.52 – 3.59 (m, 1H, H-5'), 3.63 – 3.71 (m, 1H, H-5'), 3.78-3.86 (m, 2H), 3.92 (m, 1H, H-4'), 4.07 – 4.13 (m, 1H, H-3'), 4.40 (dd, J= 11.2, 5.9 Hz, 1H, H-2'), 5.15 (d, J= 4.89Hz, 1H, 3'-OH), 5.19 (t, J= 5.39Hz, 1H, 5'-OH), 5.40 (d, J= 6.2 Hz, 1H, 2'-OH), 5.88 (t, J= 4.9Hz, 1H, NH), 6.12 (d, J= 5.9, 1H, H-1'), 7.18-7.33 (m, 5H, H-phe), 8.19 (s, 1H, H-8), 8.35 (s, 1H, H-2) ppm.

^{13}C NMR (DMSO-d6, 100MHz): δ = 34.73 (CH2), 41.92 (CH2), 61.19 (CH_2-5'), 70.22 (CH-3'), 74.09 (CH-2'), 85.33 (CH-4'), 87.30 (CH-1'), 98.46 (C-5), 102.97 (q, $^{2}J_{(C-F)}$ = 37.1 Hz, C-7), 123.50 (q, $^{1}J_{(C-F)}$ = 266.0 Hz, CF_3), 124.08 (q, $^{3}J_{(C-F)}$ = 6.4 Hz, C-8), 126.19 (CH, phe), 128.39 (2 x CH-phe), 128.69 (2 x CH-phe), 139.16 (C-phe), 150.77 (C-4), 152.94 (CH-2), 154.79 (C-6) ppm.

^{19}F NMR (DMSO-d6, 377MHz): δ = -53.36 ppm.

HRMS (ESI): calculated for $C_{20}H_{22}F_3N_4O_4$ ([M+H]$^+$): 439.15877, found: 439.1581.

Synthesis of 4-cyclopentylamino-5-trifluoromethyl-N7-(β-D-ribofuranosyl)-pyrrolo[2,3-*d*]pyrimidine (8j)

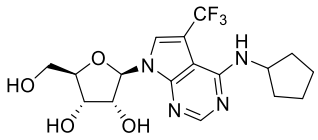

Compound **8j** was synthesized according to general procedure A (starting with 0.75 g of **6**), followed by general procedure B. This delivered 225 mg of the product in 49% yield over 2 steps.

^{1}H NMR (DMSO-d6, 400MHz): δ = 1.44 – 1.74 (m, 6H, H, CH_2-cyclopentyl), 1.98 – 2.10 (m, 2H, CH_2-cyclopentyl), 3.52 – 3.61 (m, 1H, H-5'), 3.63 – 3.71 (m, 1H, H-5'), 3.93 (dd, J= 7.0, 3.5 Hz, 1H, H-4'), 4.11 (dd, J= 8.5, 4.6 Hz, 1H, H-3'), 4.40 (dd, J= 11.2, 5.7 Hz, 1H, H-2'), 4.53 (m, CH-cyclopentyl), 5.15 (d, J= 4.9 Hz, 1H, 3'-OH), 5.19 (t, J= 5.0 Hz, 1H, 5'-OH), 5.33 (d, J= 5.4 Hz, 1H, NH), 5.40 (d, J= 6.1 Hz, 2'-OH), 6.12 (d, J= 5.9, 1H, H-1'), 8.24 (s, 1H, H-8), 8.34 (s, 1H, H-2) ppm.

^{13}C NMR (DMSO-d6, 100MHz): δ = 23.17 (2x CH_2-cyclopentyl), 32.59 (CH_2-cyclopentyl), 32.64 (CH_2-cyclopentyl), 52.16 (CH-cyclopentyl), 61.17 (C-5'), 70.20 (C-3'), 74.13 (C-2'), 85.35 (C-4'), 87.39 (C-1'), 98.61 (C-5), 102.63 (q, $^2J_{(C-F)}$ = 36.92 Hz, C-7), 123.76 (q, $^1J_{(C-F)}$ = 265.94 Hz, CF_3), 124.41 (q, $^3J_{(C-F)}$ = 6.23 Hz, C-8), 150.69 (C-4), 152.97 (C-2), 154.54 (C-6) ppm.

^{19}F NMR (DMSO-d6, 377MHz): δ = -53.10 ppm.

HRMS (ESI): calculated for $C_{17}H_{22}F_3N_4O_4$ ([M+H]$^+$): 403,15878, found: 403.1589.

Synthesis of 5-benzyl-1-(β-D-ribofuranosyl)-1,2,5,6,8-pentazaacenaphtylene (15a)

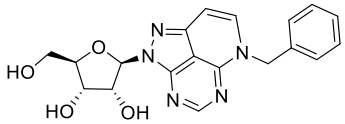

Nucleoside **15a** was synthesized according to general procedure C (starting with 0.14 g of **22a**), followed by general procedure B. This delivered 70 mg of the product in 76% yield over 2 steps.

^{1}H NMR (DMSO-d6, 400MHz): δ = 3.42-3.50 (m, 1H, H-5'), 3.55-3.62 (m, 1H, H-5'), 3.91 (dd, J= 9.3; 4.5 Hz, 1H, H4'), 4.20 (dd, J= 9.6; 5.0 Hz, 1H, H-3'), 4.64 (dd, J= 10.63; 5.1Hz, 1H, H-2'), 4.87 (dd, J= 6.5; 5.2 Hz, 1H, 5'-OH), 5.12 (d, J= 5.4 Hz, 1H, 3'-OH), 5.20 (s, 2H, CH_2-benzyl), 5.37 (d, J= 6.0 Hz, 1H, 2'-OH), 5.92 (d, J= 4.9 Hz, 1H, H-1'), *6.51 (d, J= 7.6 Hz, 1H),* 7.26-7.37 (m, 5H, H-phe),*7.40 (d, J= 7.6 Hz, 1H),* 8.39 (s, 1H, H-2) ppm.

^{13}C NMR (DMSO-d6, 100MHz): δ = 49.37 (CH_2-benzyl), 62.31 (C-5'), 70.87 (C-3'), 73.17 (C-2'), 85.28 (C-4'), 89.75 (C-1'), *102.82 (CH),* 109.65 (C-5), 127.45 (CH-phe), 127.73 (CH-phe), 128.75 (CH-phe), 136.84 (C-phe), *138.29 (CH),* 143.06 (C-7), 153.13 (C-4), 154.40 (C-6), 160.01 (C-2) ppm.

HRMS (ESI): calculated for $C_{19}H_{20}N_5O_4$ ([M+H]+): 382.15098, found: 382.1509.

Synthesis of 5-cyclpentyl-1-(β-D-ribofuranosyl)-1,2,5,6,8-pentazaacenaphtylene (15b)

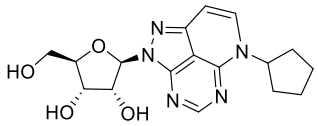

Nucleoside **15b** was synthesized according to general procedure C (starting with 0.99 g of **22b**), followed by general procedure B. This delivered 96 mg of the product in 21 % yield over 2 steps.

^{1}H NMR (DMSO-d6, 400MHz): δ = 1.57 – 1.73 (m, 2H, cyclopentyl), 1.75 – 1.92 (m, 4H, cyclopentyl), 1.97 - 2.11 (m, 2H, cyclopentyl), 3.39 – 3.49 (m, 1H, H-5'), 3.53 – 3.64 (m, 1H, H-5'), 3.91 (dd, J= 9.5, 4.5 Hz, 1H, H-4'), 4.20 (dd, J= 9.6, 5.0 Hz, 1H, H-3'), 4.61 (dd, J=10.6, 5.1 Hz, 1H, H-2'), 4.88 (dd, J= 6.5, 5.2 Hz, 1H, 5'-OH), 5.02 – 5.11 (m, 1H, C-CH-cyclopentyl), 5.11 (d, J= 5.5, 1H, 3'-OH), 5.36 (d, J= 5.9 Hz, 1H, 2-OH'), 5.92 (d, J= 4.8 Hz, 1H, H-1'), *6.48 (d, J= 7.8 Hz, 1H), 7.39 (d, J= 7.9 Hz, 1H),* 8.36 (s, 1H, H-2) ppm.

^{13}C NMR (DMSO-d6, 100MHz): δ = 23.81 (CH2-cyclopentyl), 30.67 (CH2-cyclopentyl), 56.11 (C-CH-cyclopentyl), 62.35 (C-5'), 70.89 (C-3'), 73.22 (C-2'), 85.40 (C-4'), 89.73 (C-1'), *102.98 (CH),* 109.60 (C-5), *134.73 (CH),* 143.00 (C-7), 153.40 (C-4), 154.47 (C-6), 159.78 (C-2) ppm.

HRMS (ESI): calculated for $C_{17}H_{23}N_5O_4$ ([M+H]+): 360.16668, found: 360.1665.

Synthesis of 5-(4-methoxybenzyl)-1-(β-D-ribofuranosyl)-1,2,5,6,8-pentazaacenaphtylene (15c)

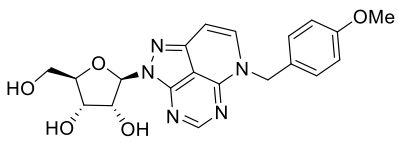

Nucleoside **15c** was synthesized according to general procedure C (starting with 0.99 g of **22c**), followed by general procedure B. This delivered 135 mg of product in 42 % yield over 2 steps.

^{1}H NMR (DMSO-d6, 400MHz): δ = 3.41-3.50 (m, 1H, H-5'), 3.55-3.63 (m, 1H, H-5'), 3.71 (s, 3H, OMe), 3.91 (m, 1H, H4'), 4.20 (dd, J= 9.6; 5.0 Hz, 1H, H-3'), 4.64 (dd, J= 10.7; 5.2Hz, 1H, H-2'), 4.87 (dd, J= 6.5; 5.3 Hz, 1H, 5'-OH), 5.12 (m, 3H, 3'-OH, CH_2-Bz), 5.37 (d, J= 6.0 Hz, 1H, 2'-OH), 5.91 (d, J= 4.9 Hz, 1H, H-1'), *6.49 (d, J= 7.6 Hz, 1H),* 6.90 (d, J= 8.7Hz, 2H, PMB), 7.31 (d, J= 8.7Hz, 2H, PMB),*7.39 (d, J= 7.6 Hz, 1H),* 8.39 (s, 1H, H-2) ppm.

^{13}C NMR (DMSO-d6, 100MHz): δ = 48.85 (CH2-benzyl), 55.08 (CH_3-Ome), 62.32 (C-5'), 70.87 (C-3'), 73.17 (C-2'), 85.68 (C-4'), 89.75 (C-1'), *102.76 (CH)*, 109.66 (C-5), 114.13 (2x CH-PMB), 128.76 (C, PMB), 129.15 (2x CH-PMB), *138.10 (CH),* 143.08 (C-7), 153.12 (C-4), 154.33 (C-6), 158.88 (C-PMB), 160.00 (C-2) ppm.

HRMS (ESI): calculated for $C_{20}H_{22}N_5O_5$ ([M+H]+): 412,16155, found: 412.1614.

Synthesis of 5-methyl-1-(β-D-ribofuranosyl)-1,2,5,6,8-pentazaacenaphtylene (15d)

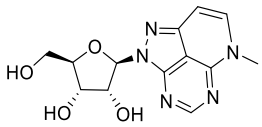

Nucleoside **15d** was synthesized according to general procedure C (starting with 0.34 g of **22d**), followed by general procedure B. This delivered 70 mg of the product in 44 % yield over 2 steps. (The protons/carbons of the cyclised ethynyl group are highlighted in italics, the purine numbering is followed in the NMR characterization)

^{1}H NMR (DMSO-d6, 400MHz): δ = 3.41 – 3.49 (m, 1H, H-5'), 3.51 (s, 3H, Me), 3.55 – 3.64 (m, 1H, H-5'), 3.91 (m, 1H, H-4'), 4.20 (dd, J= 9.7, 5.0 Hz, 1H, H-3'), 4.63 (dd, J=10.6, 5.1 Hz, 1H, H-2'), 4.90 (dd, J= 6.5, 5.2 Hz, 1H, 5'-OH), 5.12 (d, J= 5.4, 1H, 3'-OH), 5.37 (d, J= 5.9 Hz, 1H, 2-OH'), 5.91 (d, J= 4.8 Hz, 1H, H-1'), *6.45 (d, J= 7.6 Hz, 1H), 7.29 (d, J= 7.6 Hz, 1H),* 8.37 (s, 1H, H-2) ppm.

^{13}C NMR (DMSO-d6, 100MHz): δ =34.09 (CH3), 62.33 (CH_2-5'), 70.88 (CH-3'), 73.21 (CH-2'), 85.24 (CH-4'), 89.73 (CH-1'), *102.06 (CH),* 109.66 (C-5), *139.20 (CH),* 143.26 (C-7), 152.92 (C-4), 154.55 (C-6), 160.00 (CH-2) ppm.

HRMS (ESI): calculated for $C_{13}H_{16}N_5O_4$ ([M+H]+): 306.11968, found: 306.1194.

Synthesis of 1-(β-D-ribofuranosyl)-5-thia-1,2,6,8-tetraazaacenaphtylene (29)

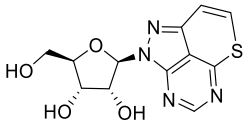

Intermediate **28** (0.16 g, 0.26 mmol, 1 eq) was dissolved in MeOH (4 mL) and K_2CO_3 (11 mg, 0.08 mmol, 0.3 eq) was added. After 3h, the reaction mixture was filtered and the filtrate purified via flash column chromatography (DCM/MeOH 0 -> 10%). This delivered 48 mg of the product in 60% yield.

^{1}H NMR (DMSO-d6, 400MHz): δ = 3.41 – 3.48 (m, 1H, H-5'), 3.54 – 3.62 (m, 1H, H-5'), 3.92 (dd, J= 9.9, 4.7 Hz, 1H, H-4'), 4.22 (dd, J= 9.9, 5.0 Hz, 1H, H-3'), 4.65 (dd, J=10.5, 5.1 Hz, 1H, H-2'), 4.77 (t, J= 5.9 Hz, 1H, 5'-OH), 5.18 (d, J= 5.5, 1H, 3'-OH), 5.44 (d, J= 5.9 Hz, 1H, 2'-OH), 6.02 (d, J= 4.8 Hz, 1H, H-1'), *7.39 (d, J= 9.7 Hz, 1H)*, *7.43 (d, J= 9.8 Hz, 1H),* 8.65 (s, 1H, H-2) ppm.

^{13}C NMR (DMSO-d6, 100MHz): δ = 62.13 (C-5'), 70.70 (C-3'), 73.11 (C-2'), 85.35 (C-4'), 89.11 (C-1'), 114.19 (C-5), *117.79 (CH), 129.93 (CH),* 142.93 (C-7), 151.02 (C-4), 158.10 (C-2), 164.35 (C-6).

HRMS (ESI): calculated for $C_{12}H_{13}N_4O_4S$ ([M+H]+): 309.06518, found: 309.0652.

Crystal X-Ray data

Experimental

Compound **15d** was crystalized from DCM via evaporation and a suitable crystal of **15d** was selected and mounted on a LithoLoop on a Rigaku Oxford Diffraction SuperNova Dual source (Cu at zero) diffractometer with an Atlas CCD detector using ω scans and CuKα (λ = 1.54184 Å) radiation. The crystal was kept at 100 K during data collection. The images were interpreted and integrated with the program CrysAlisPro [1]. Using Olex2 [2], the structure was solved with the SHELXT structure solution program using Intrinsic Phasing and refined with the SHELXL refinement package using Least Squares minimization [3,4].

Crystal structure determination

Crystal Data for $C_{13}H_{15}N_5O_4$ (MW = 305.30 g/mol): orthorhombic, space group $P2_12_12_1$ (no. 19), a = 7.62230(10) Å, b = 8.09260(10) Å, c = 21.8352(2) Å, V = 1346.89(3) Å^3, Z = 4, T = 100(2) K, μ(Cu Kα) = 0.968 mm^{-1}, *Dcalc* = 1.506 g/cm^3, 14126 reflections measured (8.098° ≤ 2Θ ≤ 147.114°), 2689 unique (R_{int} = 0.0360, R_{sigma} = 0.0225) which were used in all calculations. The final R_1 was 0.0259 (I > 2σ(I)) and wR_2 was 0.0656 (all data).

CCDC **2280787** contains the supplementary crystallographic data for this paper. These data can be obtained free of charge from The Cambridge Crystallographic Data Centre via www.ccdc.cam.ac.uk/structures.

Table S3: Conditions tested to cyclise N^6-benzyl-7-ethynyl-7-deazaadenosine

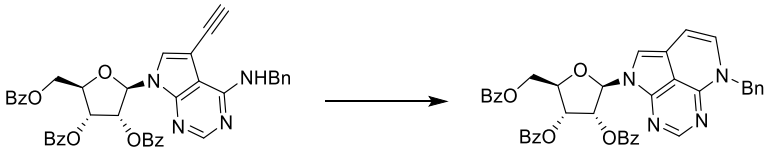

Entry	Reagent	Solvent	Conditions	Result
1	Ag OTf (0.2 eq)	DCE	84°C	No reaction
2	Cu $(OTf)_2$ (0.2 eq)	DCE	84°C	Alkyn-Alkyn cross coupling (Eglinton Reaction)
3	Cu $(OAc)_2$ (0.2 eq)	MeCN	82°C	Alkyn-Alkyn cross coupling
4	CuI (0.2 eq)	THF	66°C	No reaction
5	NaH (1 eq)	DMF	0°C -> RT	Complex mixture

All reactions were performed on a 0.5 mmol scale, monitored via LCMS and TLC.

Table S4: Conditions tested to cyclise 7-ethynyl-aminopurinol and allopurinol riboside

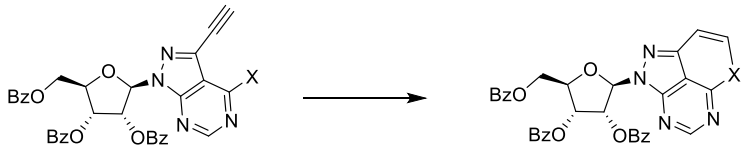

X= NH_2 or OH

Entry	X	Reagent	Solvent	Conditions	Result
1	OH	Ag OTf (0.2 eq)	DCE	84°C	No reaction
2	OH	Cu $(OAc)_2$ (0.2 eq)	MeCN	82°C	Alkyne-Alkyne cross coupling
3	OH	DBU (1 eq)	DCE	84°C	No reaction
4	OH	KOtBu (1 eq)	DMF	100°C	No reaction
5	NH_2	Ag OTf (0.2 eq)	DCE	84°C	No reaction

All reactions were performed on a 0.5 mmol scale.

Table S5: Attempts to remove the PMB protecting group

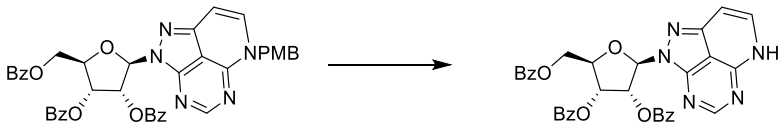

Entry	Reagent	Solvent	Conditions	Result
1	TFA	DCM (1/1)	RT	No reaction
2	4M HCl	Dioxane	90°C	Glycosidic bound cleavage
3	DDQ (1.1 eq)	DCM/H_2O	RT	No reaction
4	CAN (1.1 eq)	MeCN/H_2O	RT	No reaction
5	Pd/C 10%; H_2	Formic acid	RT	No reaction

All reactions were performed on a 0.5 mmol scale.

^{1}H & ^{13}C NMR spectra of intermediates

Compound 5 (4-chloro-5-(trimethylsilyl)ethynyl-N7-(2', 3', 5'-tri-O-benzoyl-β-D-ribofuranosyl)-pyrrolo[2,3-*d*]pyrimidine)

^{1}H NMR ($CDCl_3$), 400MHz)

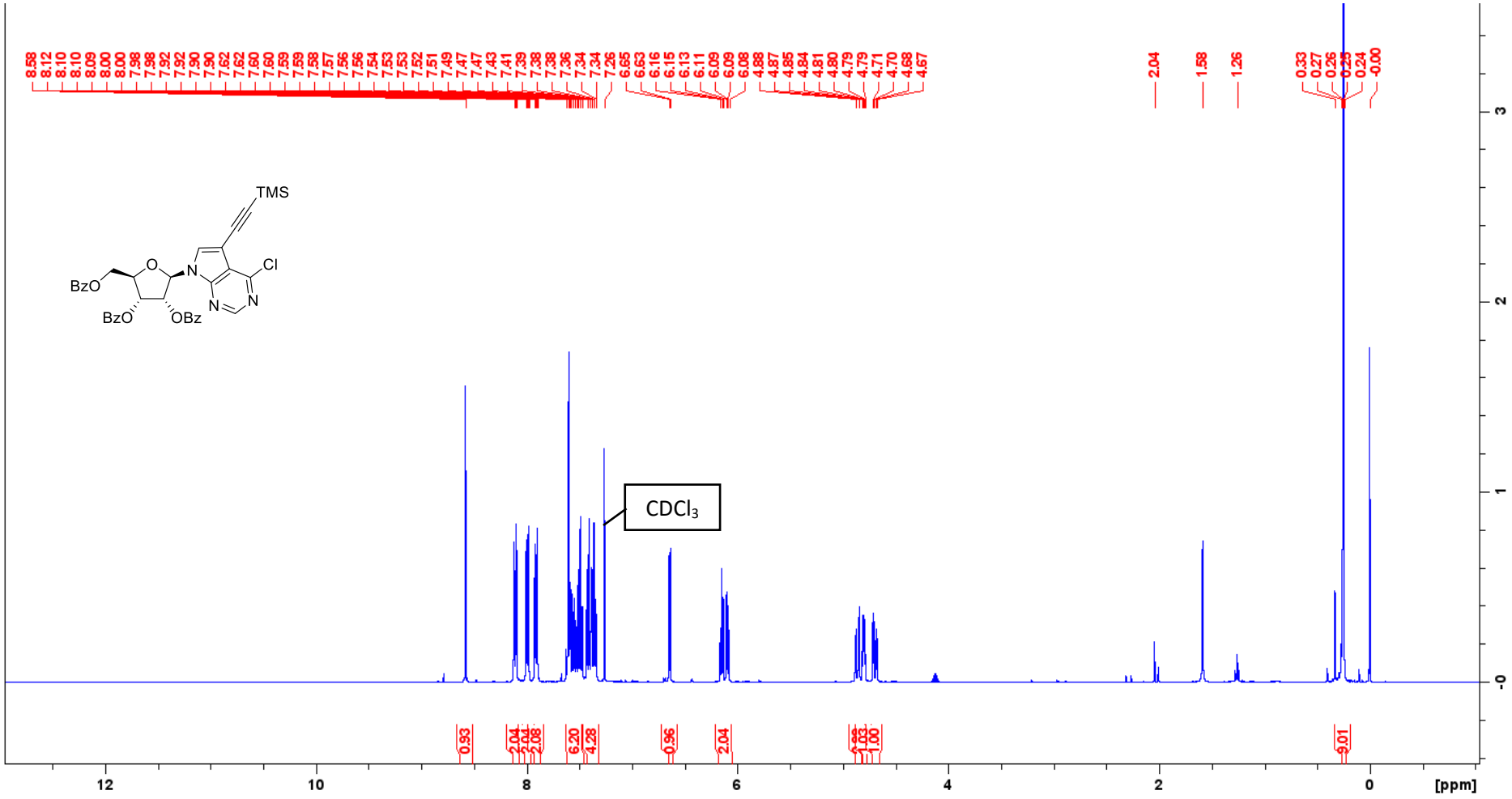

^{13}C NMR ($CDCl_3$, 100MHz)

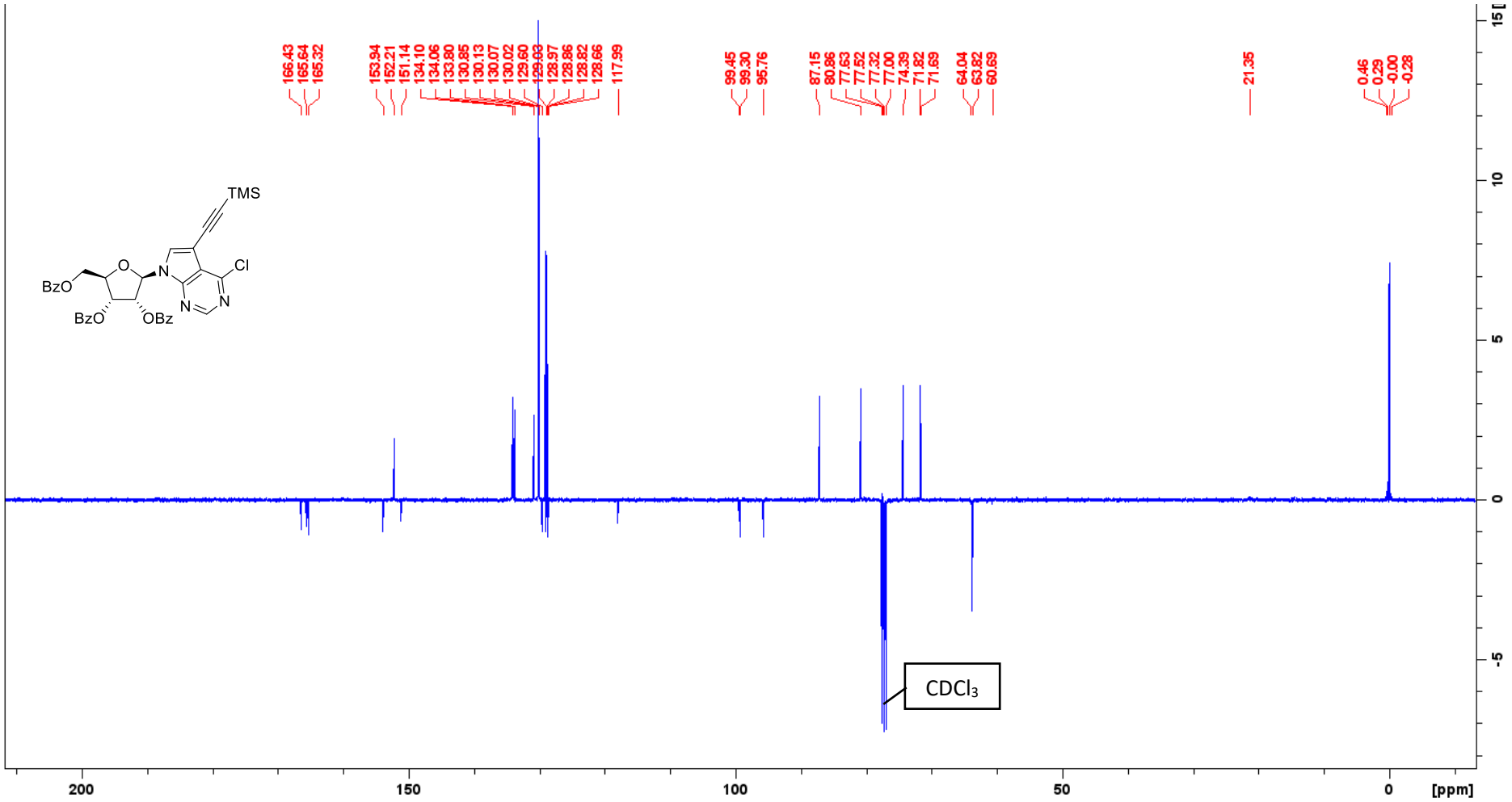

Compound 11 (3-iodo-4-oxo -N1-(2', 3', 5'-tri-O-benzoyl-β-D-ribofuranosyl)-pyrazolo[3,4-*d*]pyrimidine)

^{1}H NMR ($CDCl_3$), 400MHz)

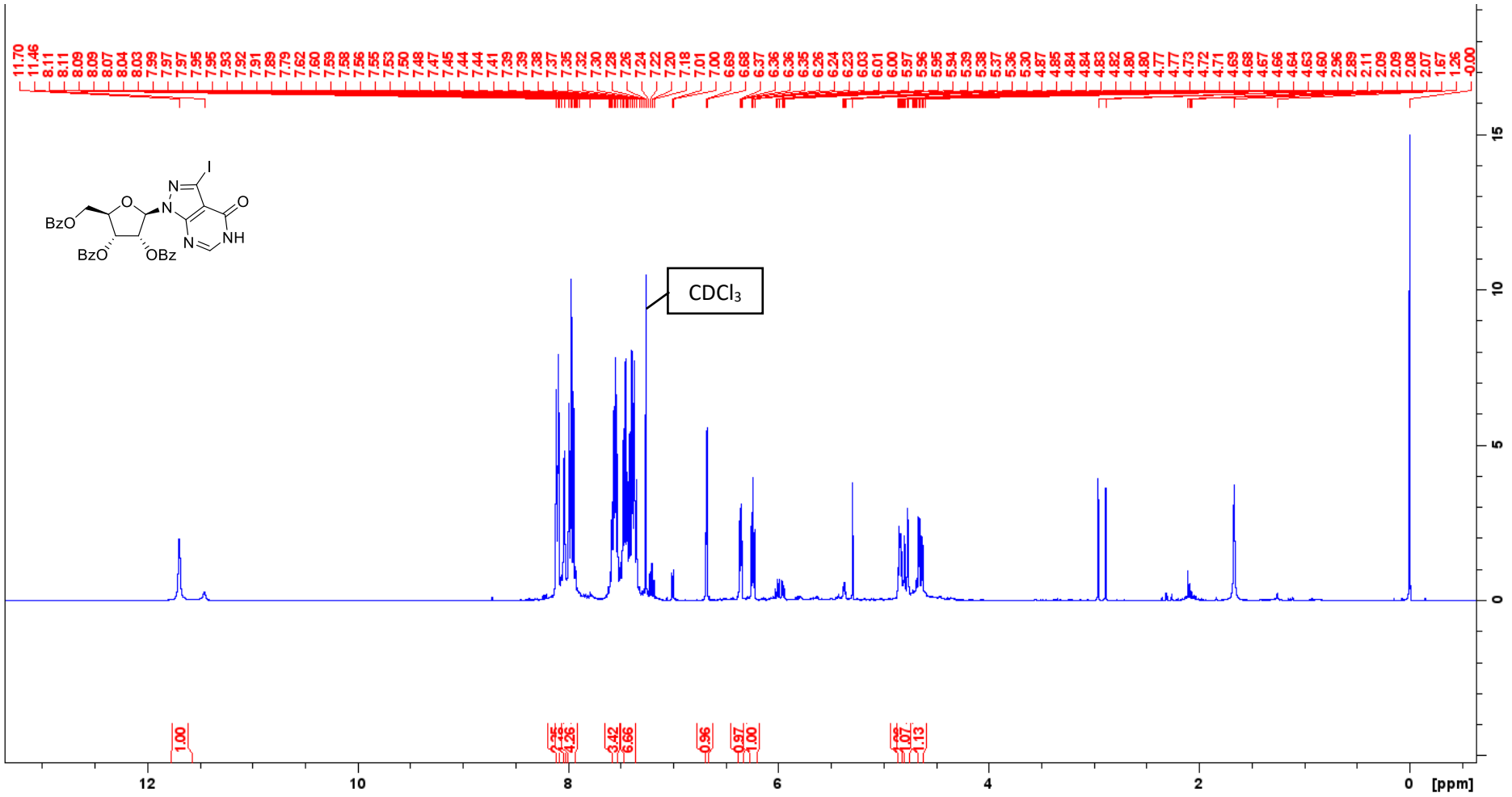

^{13}C NMR ($CDCl_3$, 100MHz)

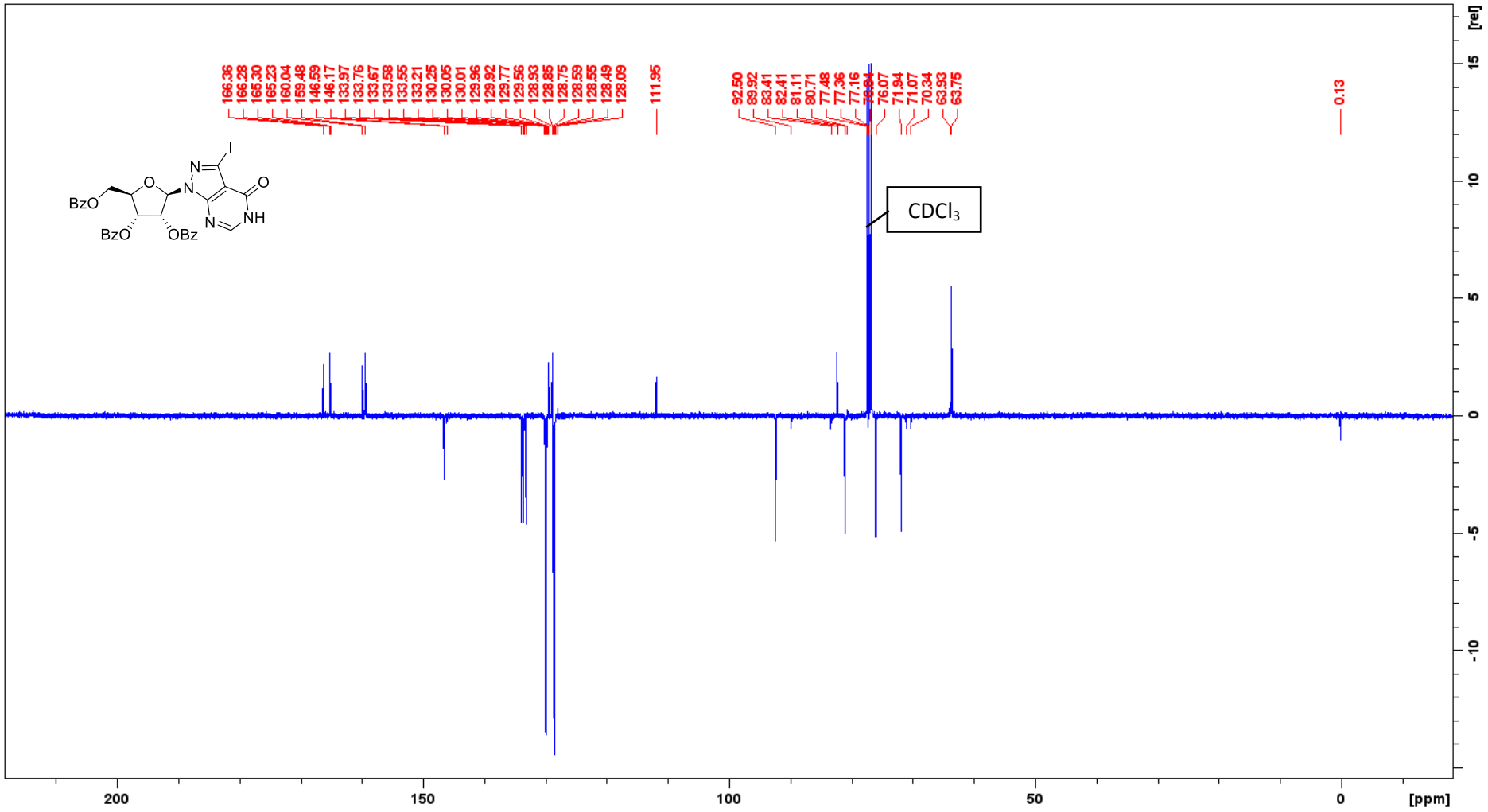

Compound 18 (4-oxo-3-((triethylsilyl)ethynyl)-N1-(2', 3', 5'-tri-O-benzoyl-β-D-ribofuranosyl)-pyrazolo[3,4-*d*]pyrimidine)

^{1}H NMR ($CDCl_3$), 400MHz)

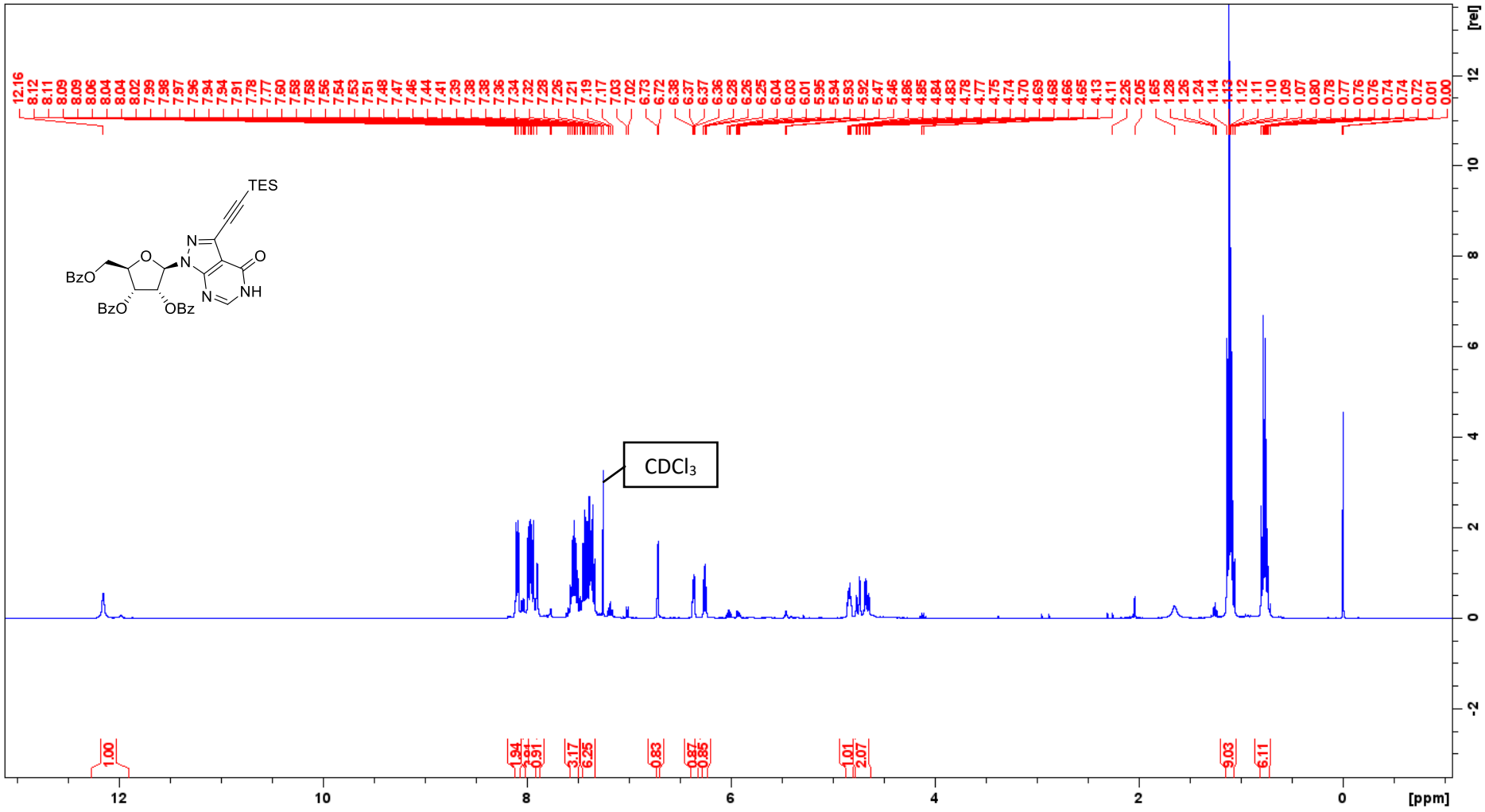

^{13}C NMR ($CDCl_3$, 100MHz)

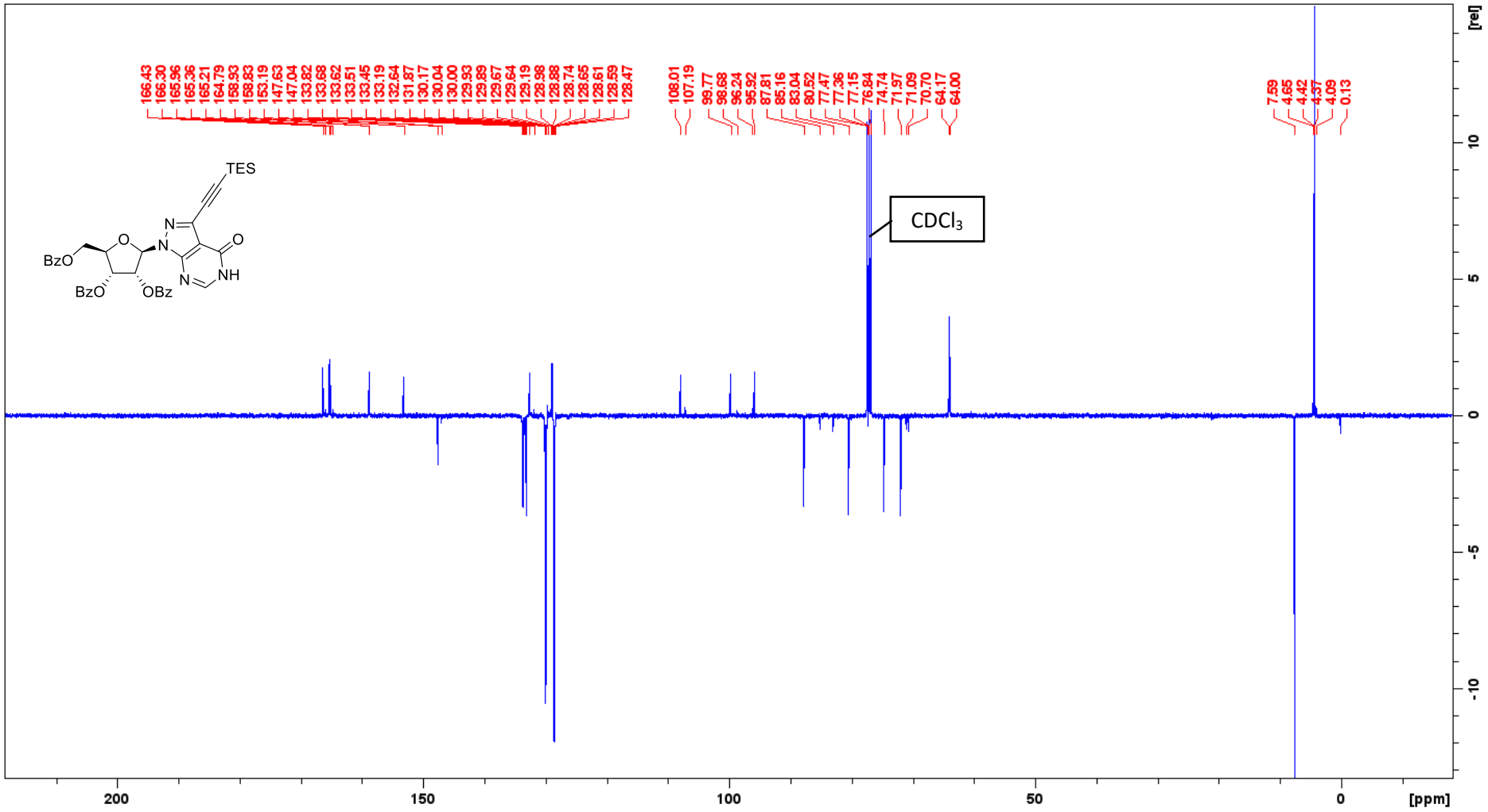

Compound 19 (4-chloro-3-((triethylsilyl)ethynyl)-N1-(2', 3', 5'-tri-O-benzoyl-β-D-ribofuranosyl)-pyrazolo[3,4-*d*]pyrimidine)

^{1}H NMR ($CDCl_3$), 400MHz)

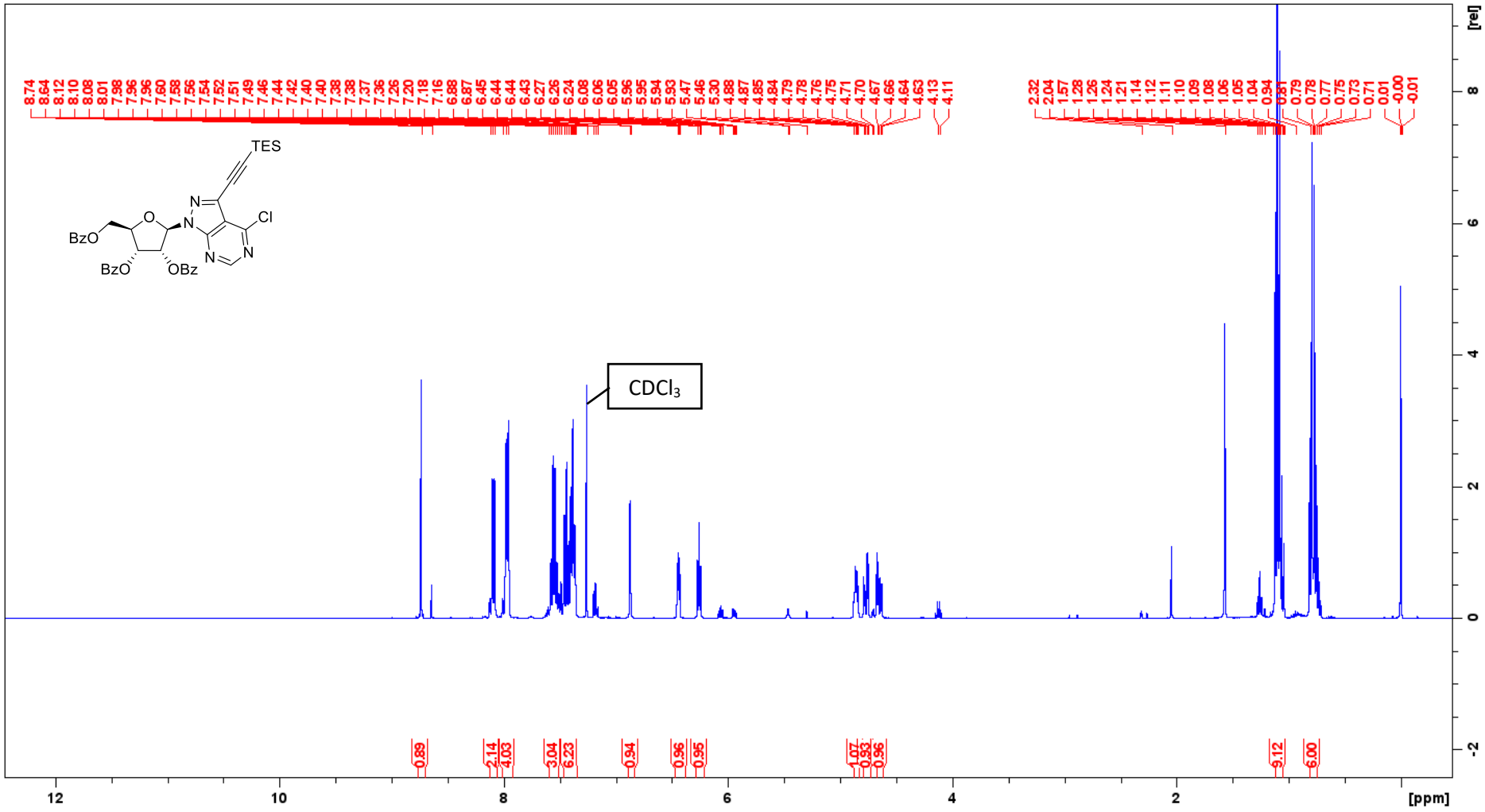

^{13}C NMR ($CDCl_3$, 100MHz)

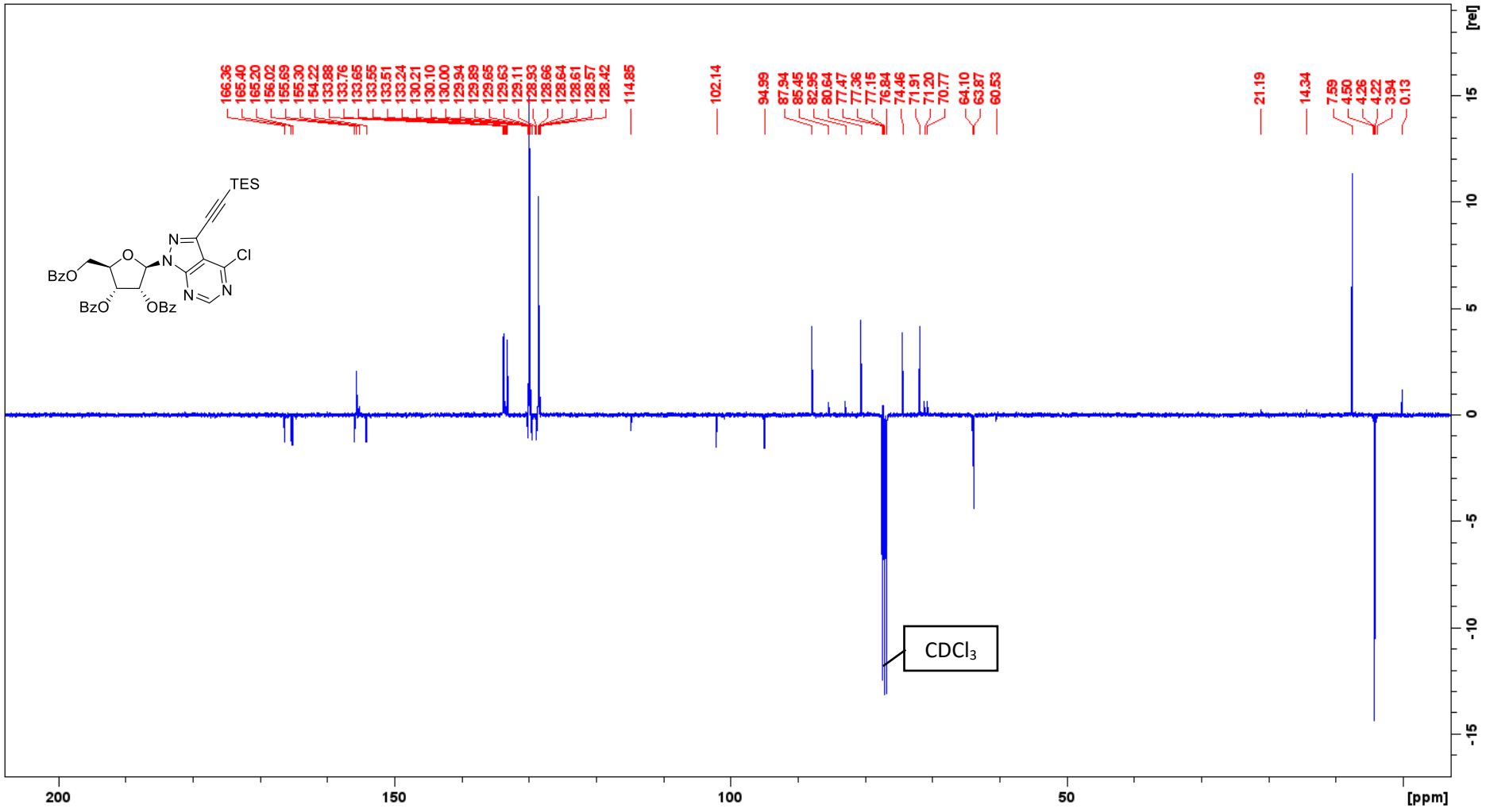

^{1}H & ^{13}C NMR spectra of final compounds

Compound **4-benzylamino-5-ethynyl-N7-(β-D-ribofuranosyl)-pyrrolo[2,3-*d*]pyrimidine (7a)**

^{1}H NMR (DMSO-d6, 400MHz)

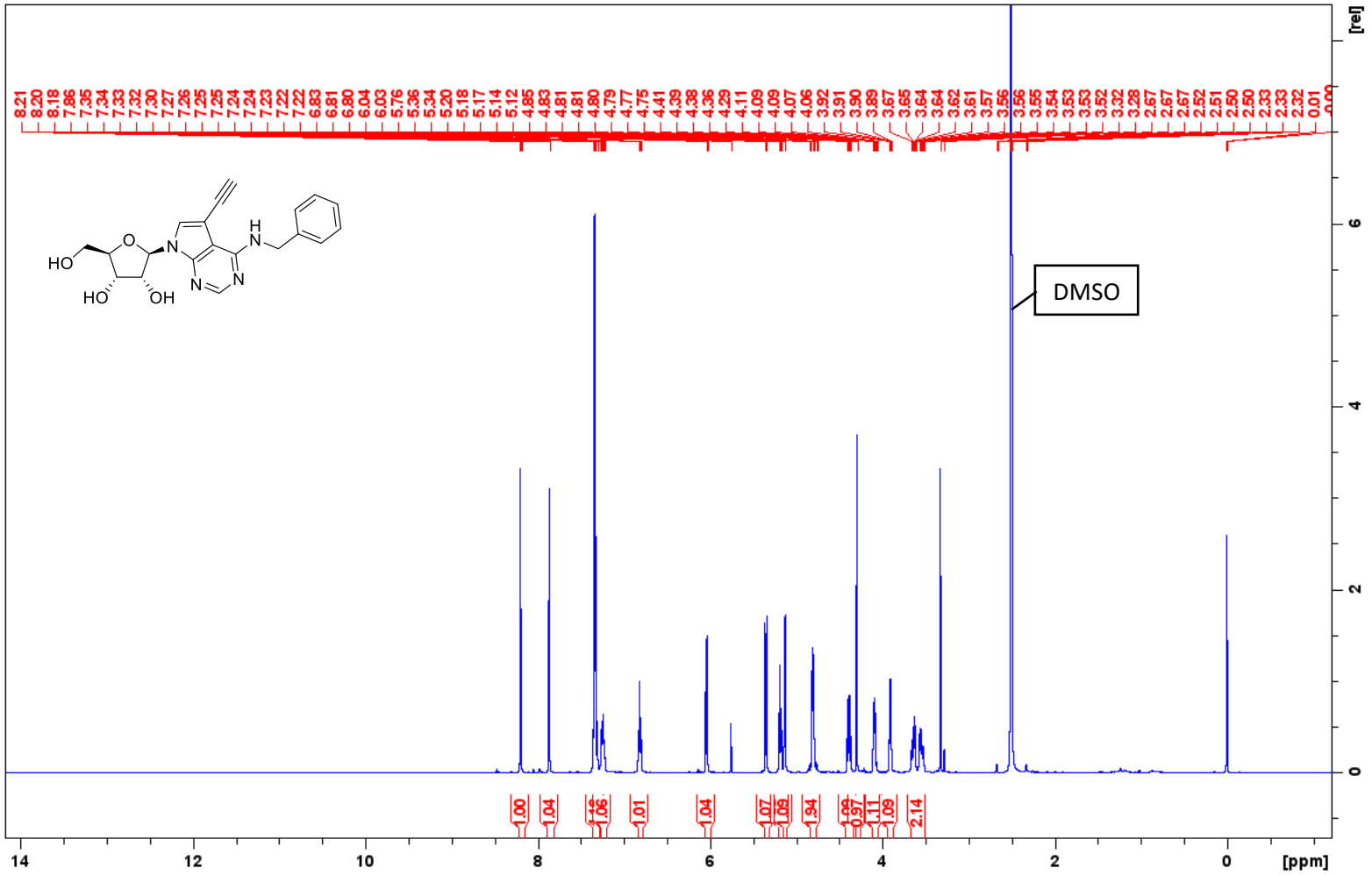

^{13}C NMR (DMSO-d6, 100MHz)

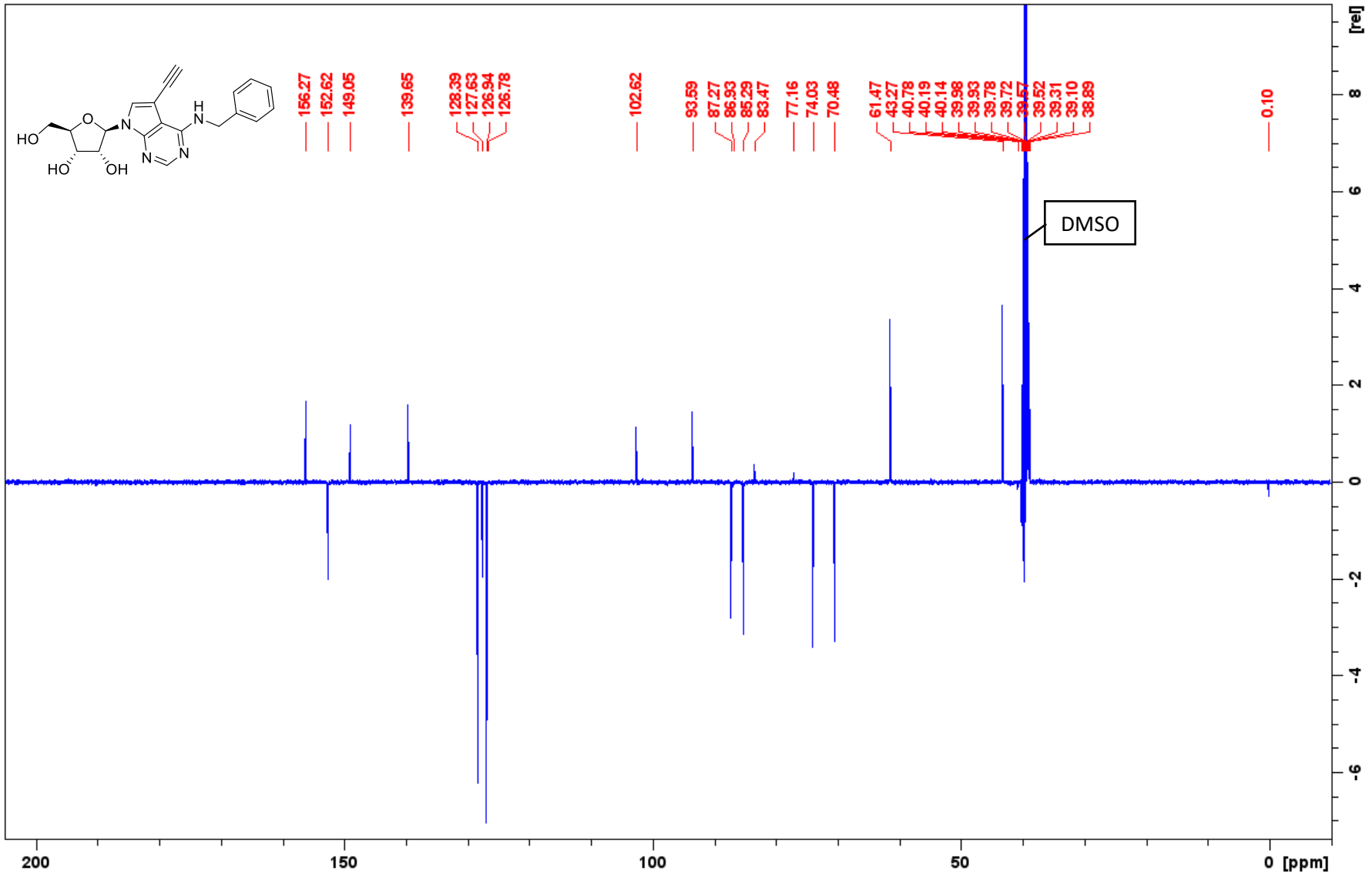

Compound **4-(((S)-1-phenylethyl)amino)-5-ethynyl-N7-(β-D-ribofuranosyl)-pyrrolo[2,3-*d*]pyrimidine (7b)**

^{1}H NMR (DMSO-d6, 400MHz)

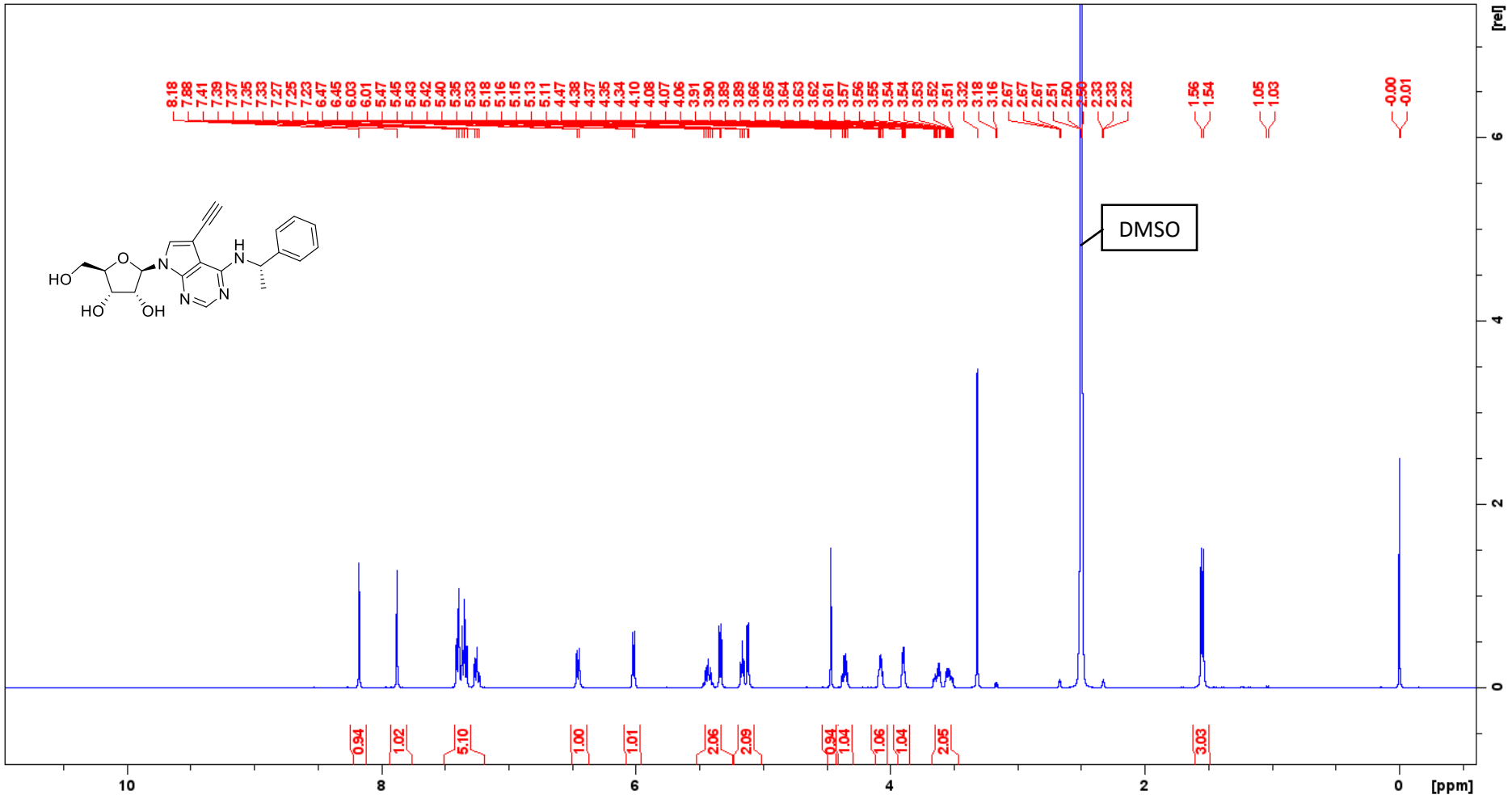

^{13}C NMR (DMSO-d6, 100MHz)

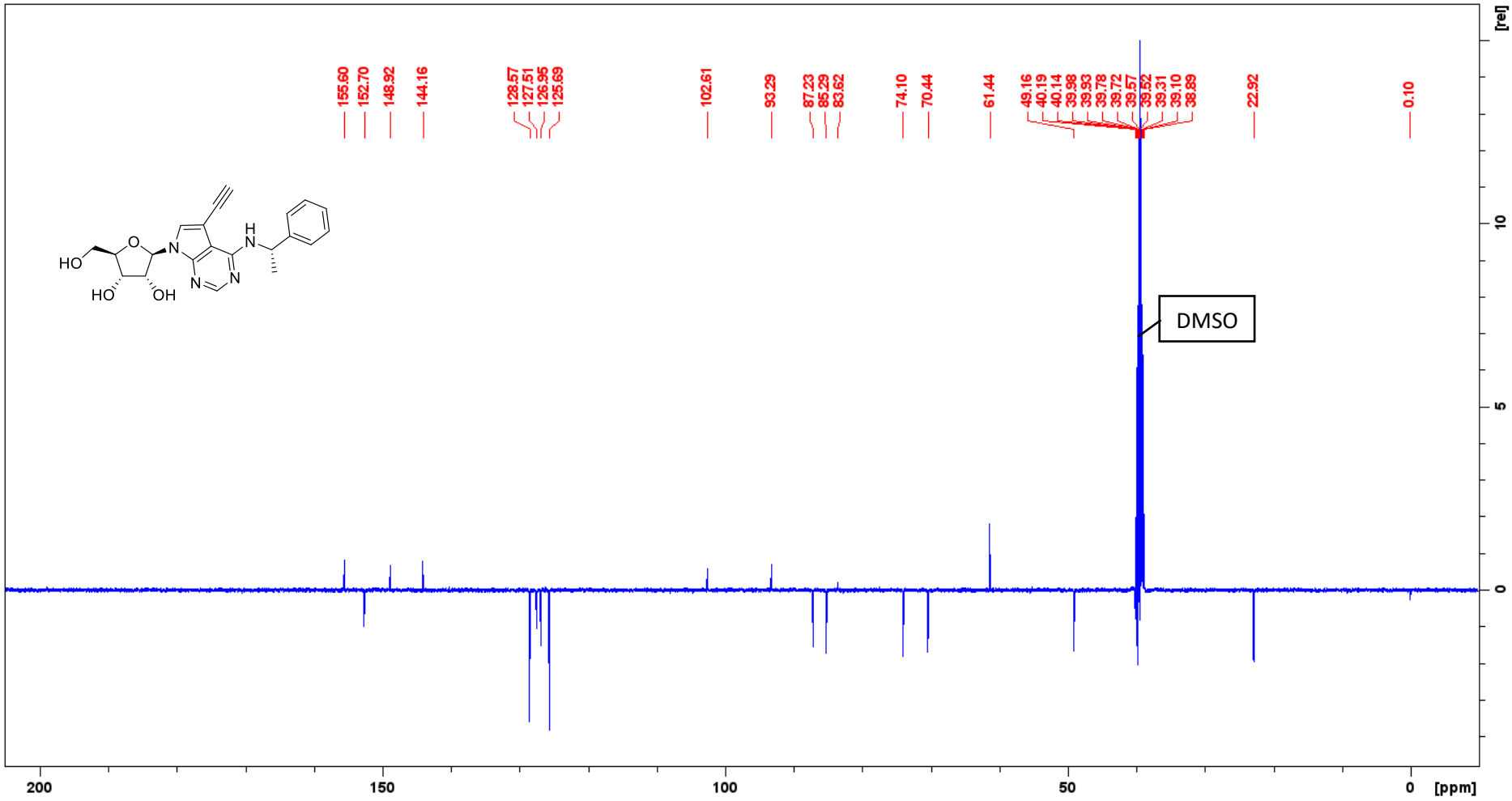

Compound **4-(((R)-1-phenylethyl)amino)-5-ethynyl-N7-(β-D-ribofuranosyl)-pyrrolo[2,3-*d*]pyrimidine (7c)**

^{1}H NMR (DMSO-d6, 400MHz)

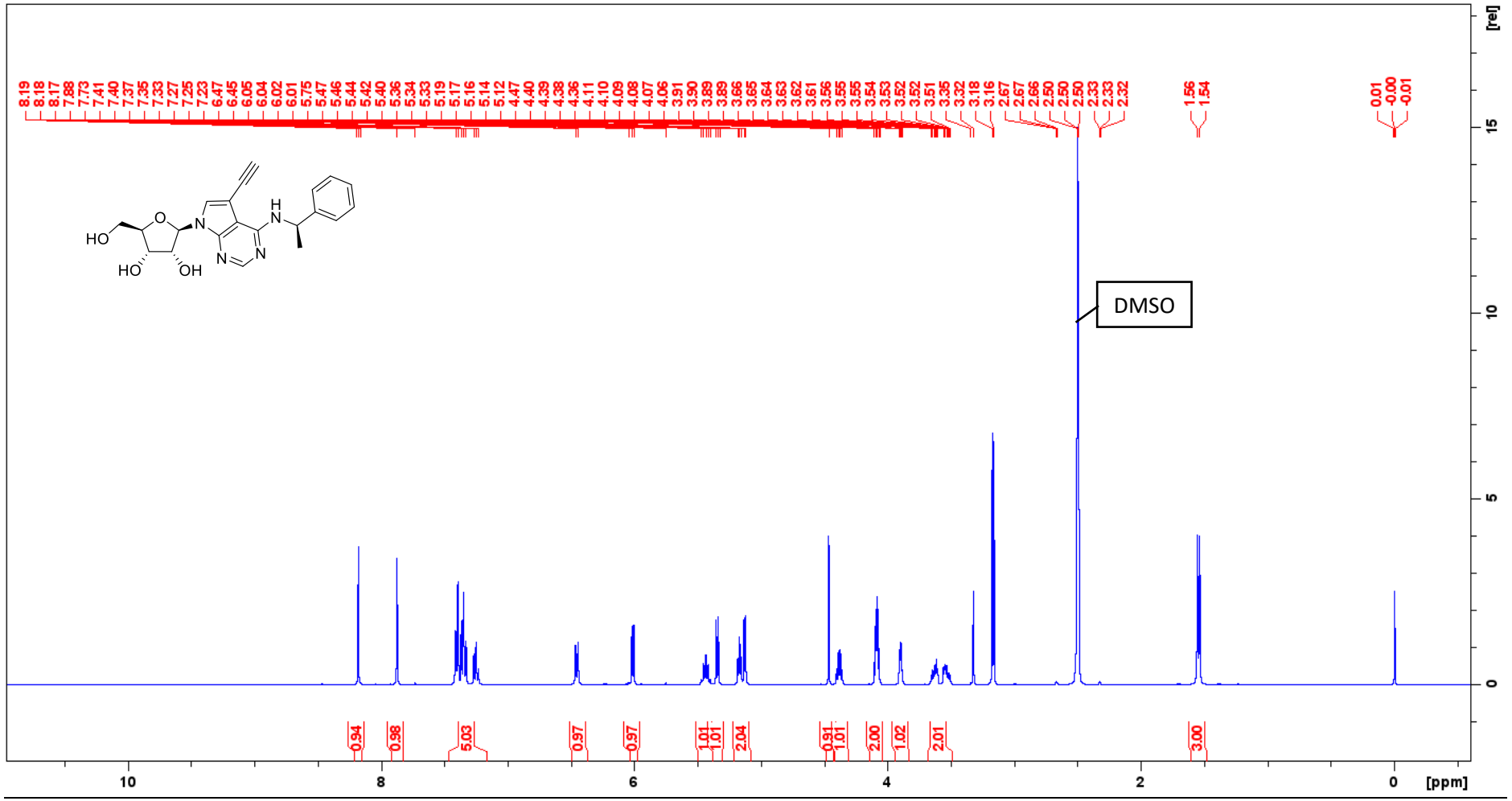

^{13}C NMR (DMSO-d6, 100MHz)

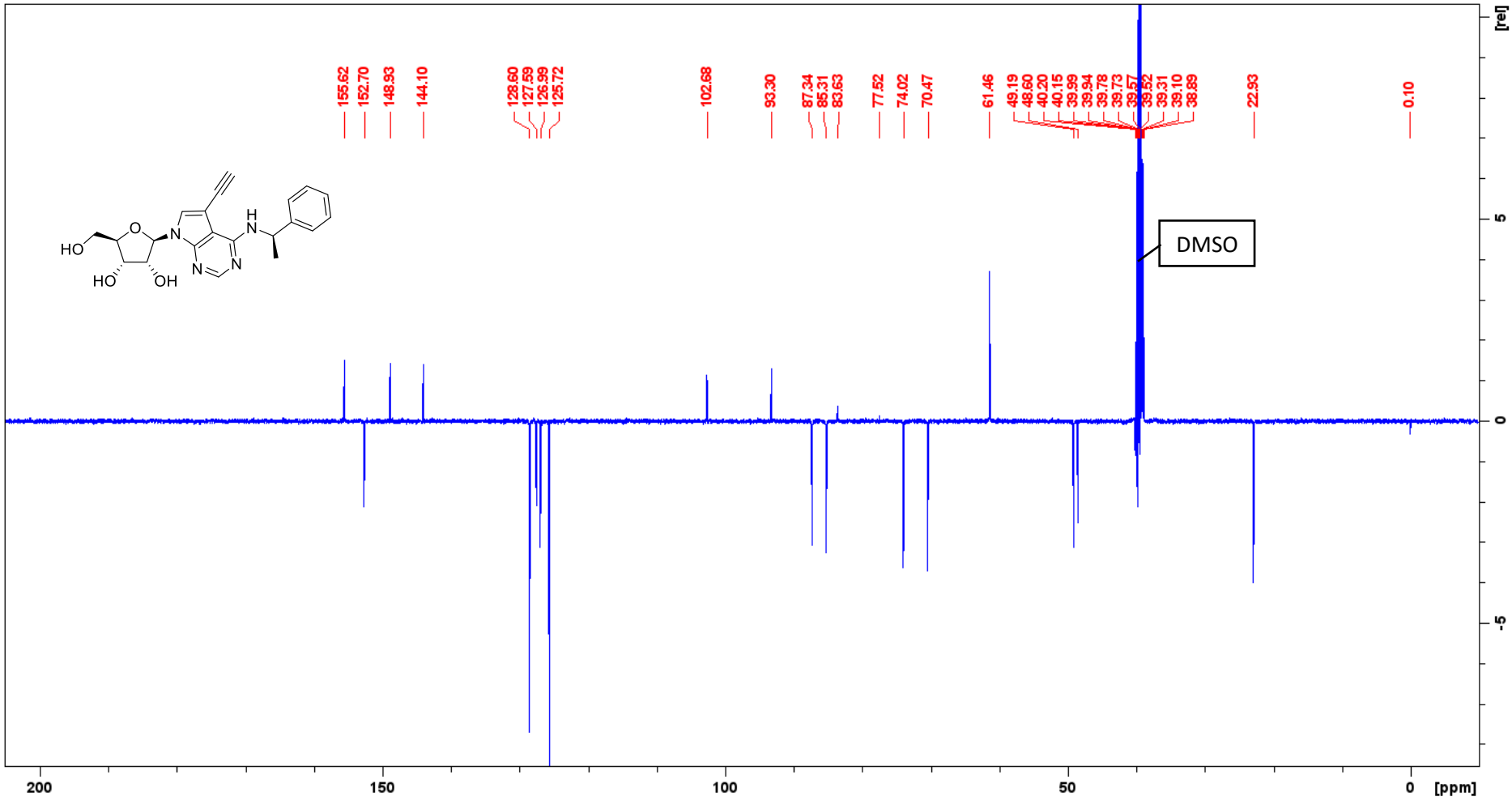

Compound **4-((2-chlorobenzyl)amino)-5-ethynyl-N7-(β-D-ribofuranosyl)-pyrrolo[2,3-*d*]pyrimidine (7d)**

^{1}H NMR (DMSO-d6, 400MHz)

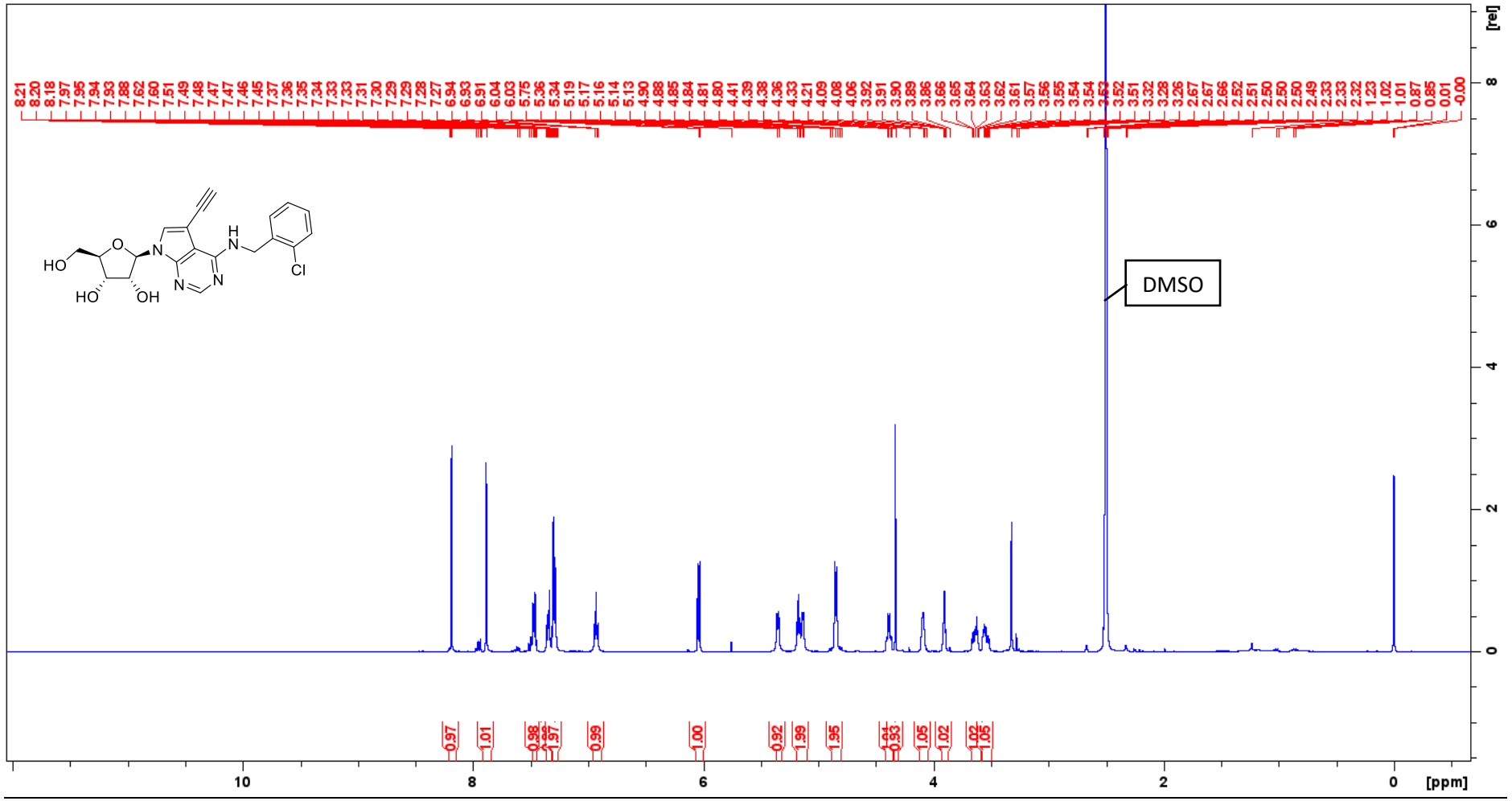

^{13}C NMR (DMSO-d6, 100MHz)

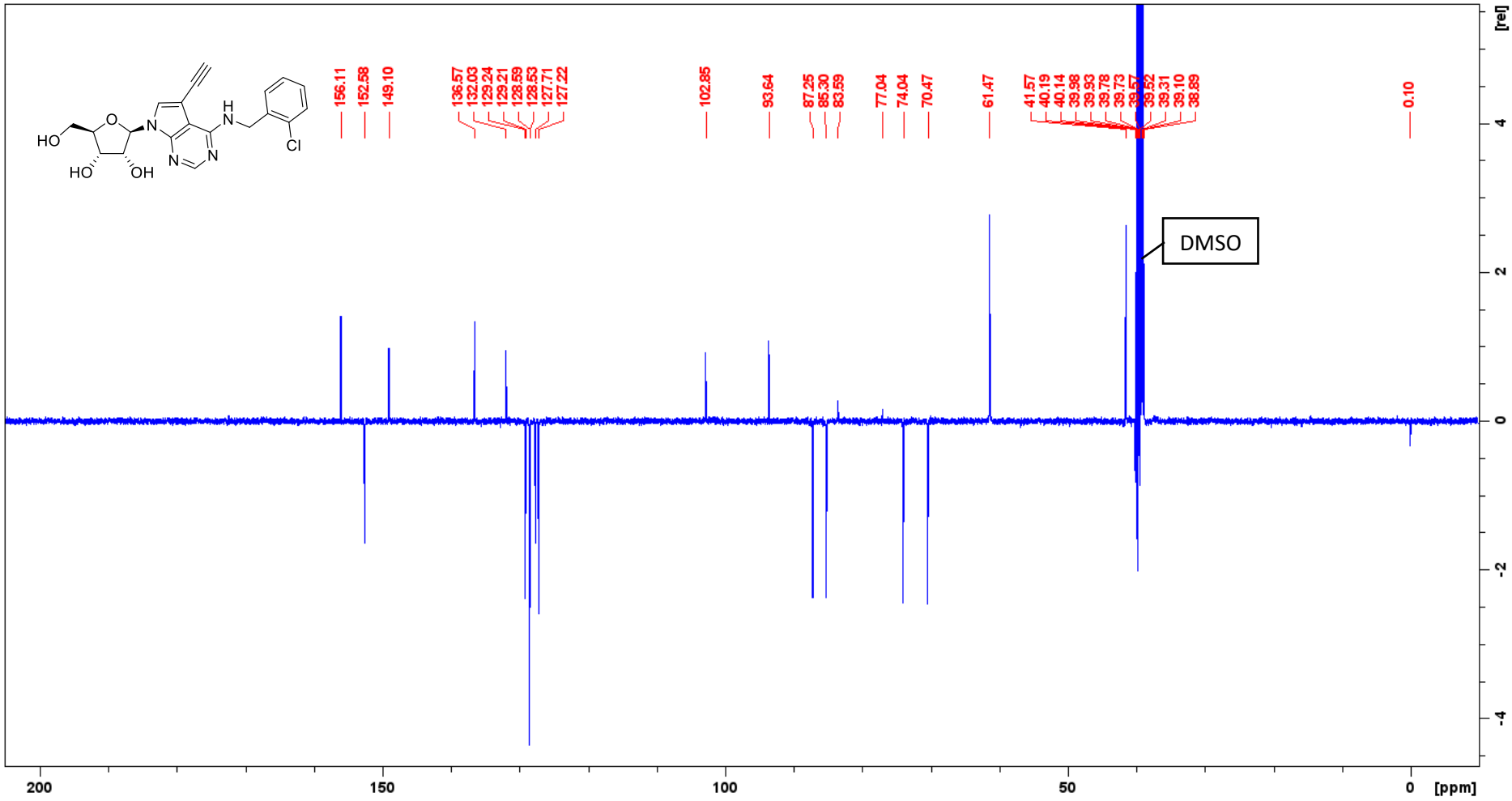

Compound **5-ethynyl-4-((2-fluorobenzyl)amino)-N7-(β-D-ribofuranosyl)-pyrrolo[2,3-*d*]pyrimidine (7g)**

^{1}H NMR (DMSO-d6, 400MHz)

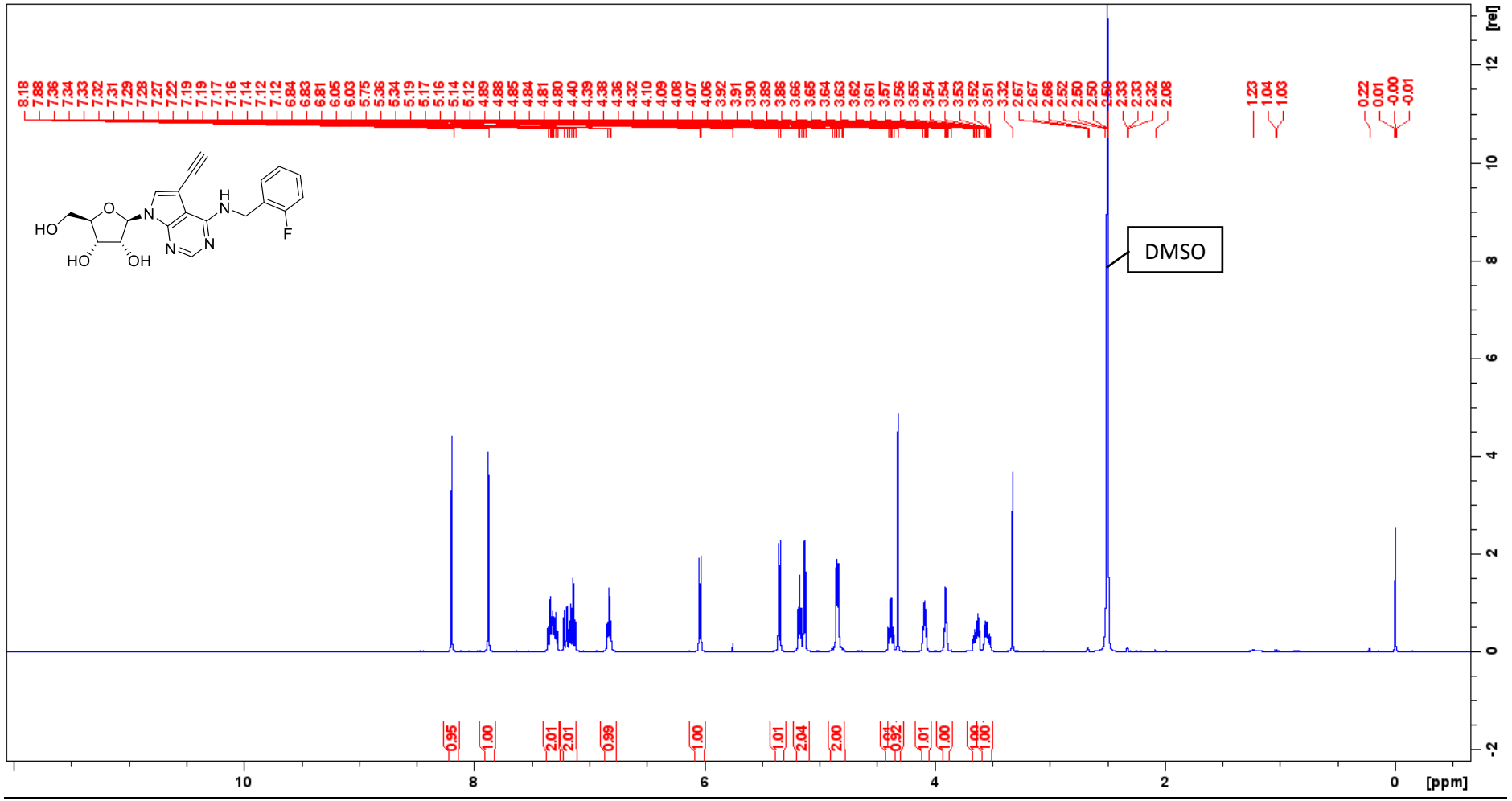

^{13}C NMR (DMSO-d6, 100MHz)

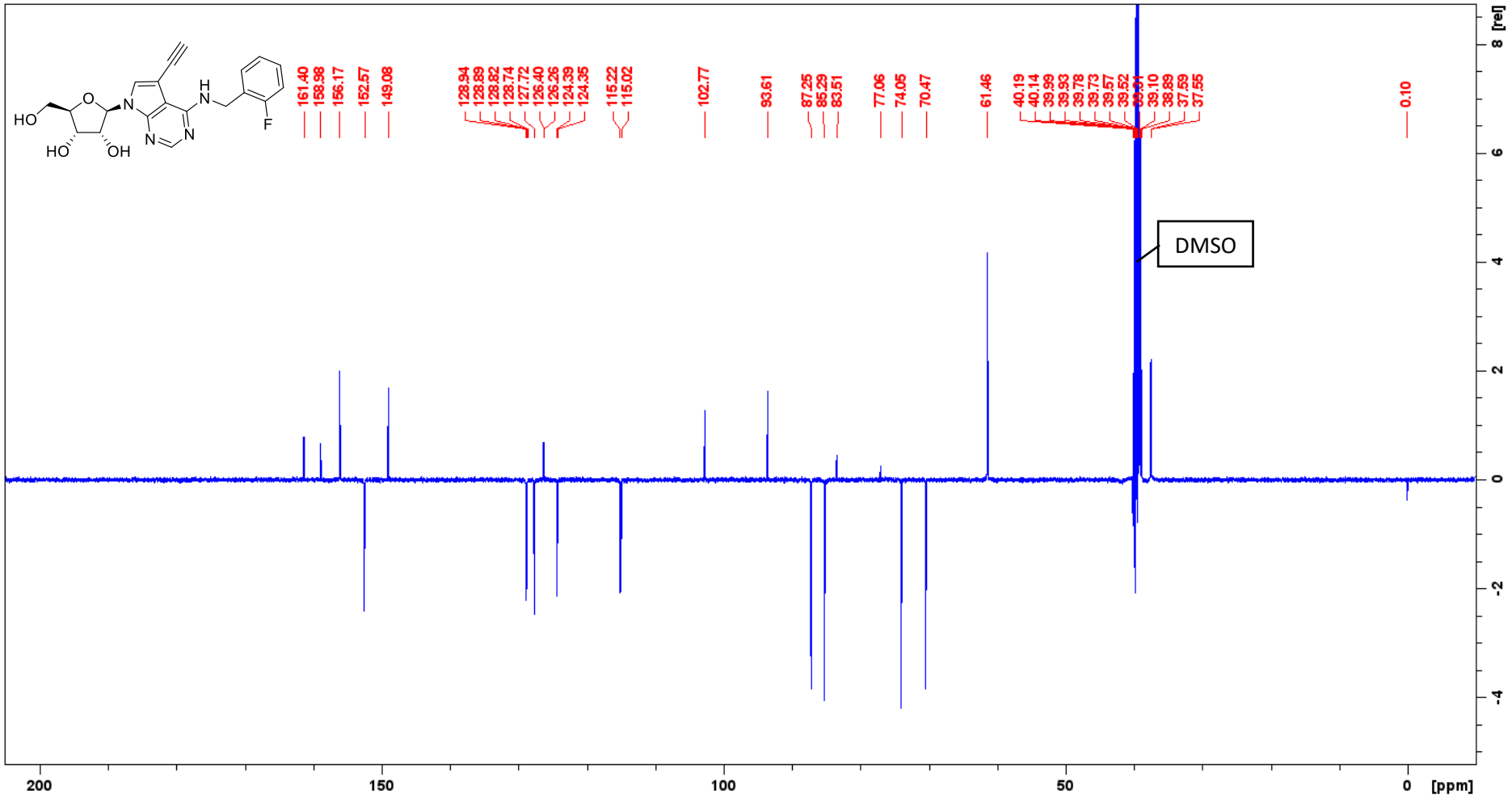

Compound **4-(cyclopentylamino)-5-ethynyl-N7-(β-D-ribofuranosyl)-pyrrolo[2,3-*d*]pyrimidine (7j)**

^{1}H NMR (DMSO-d6, 400MHz)

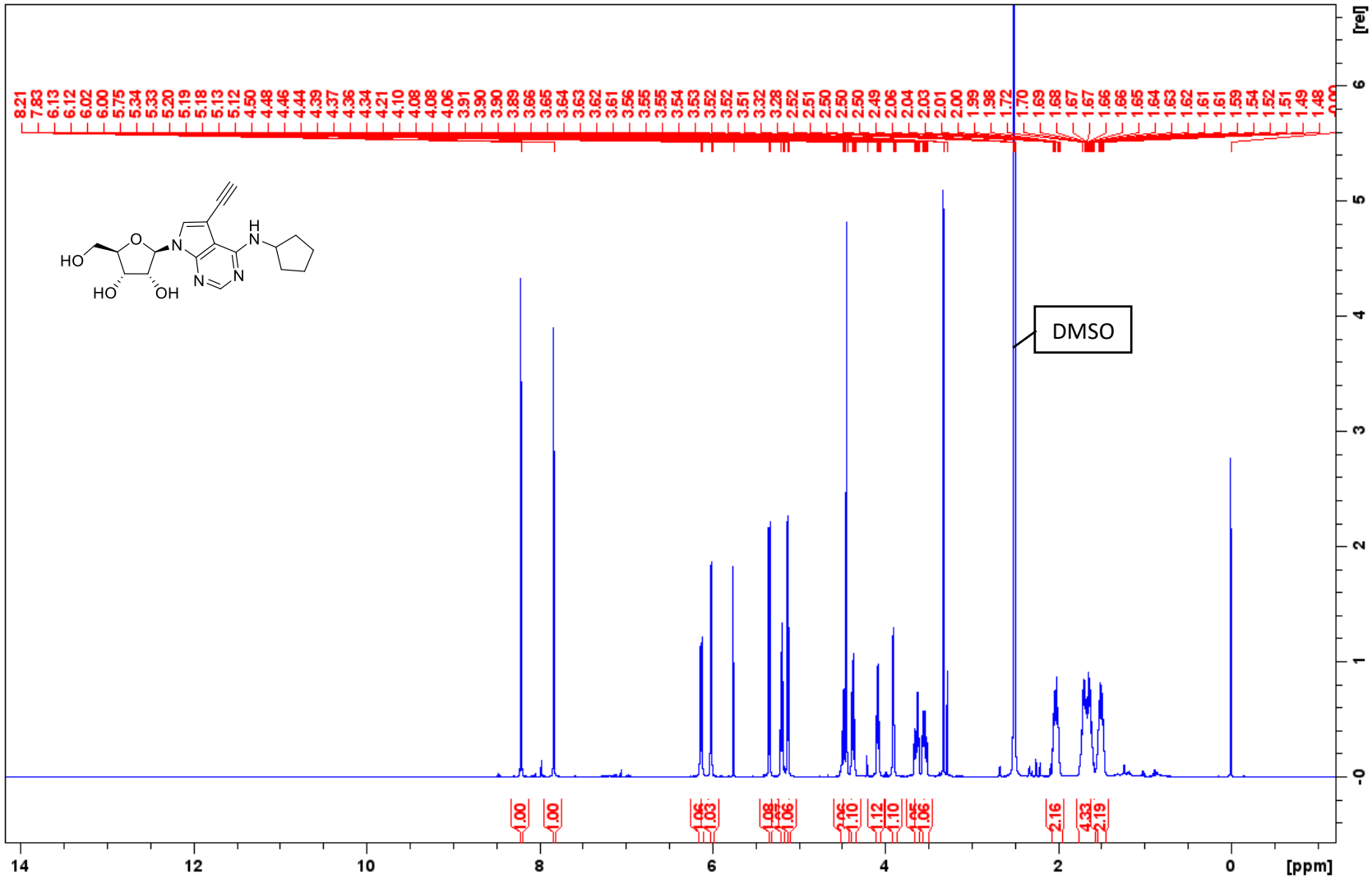

^{13}C NMR (DMSO-d6, 100MHz)

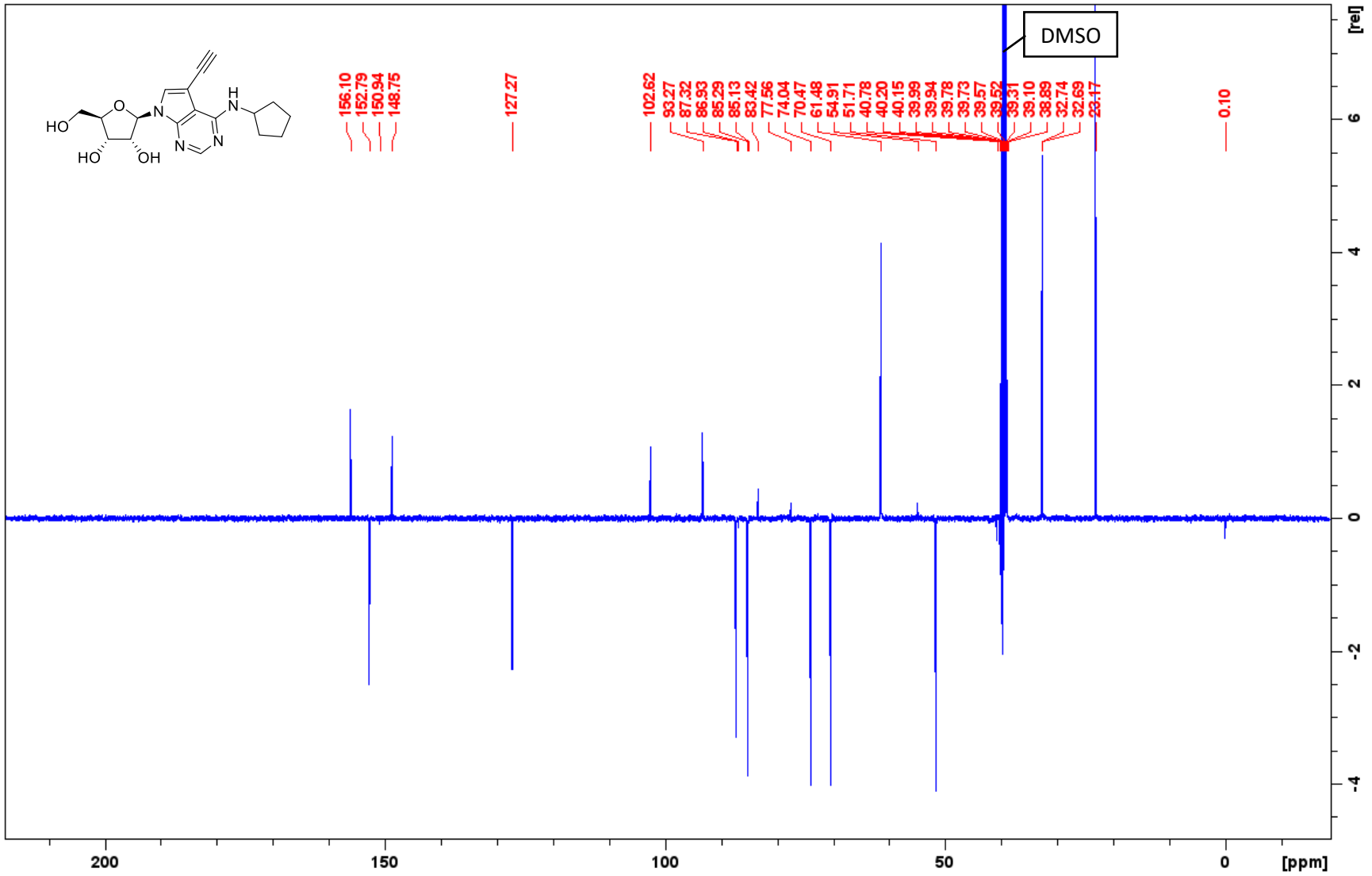

Compound **4-benzylamino-5-trifluoromethyl-N7-(β-D-ribofuranosyl)-pyrrolo[2,3-*d*]pyrimidine (8a)**

^{1}H NMR (DMSO-d6, 400MHz)

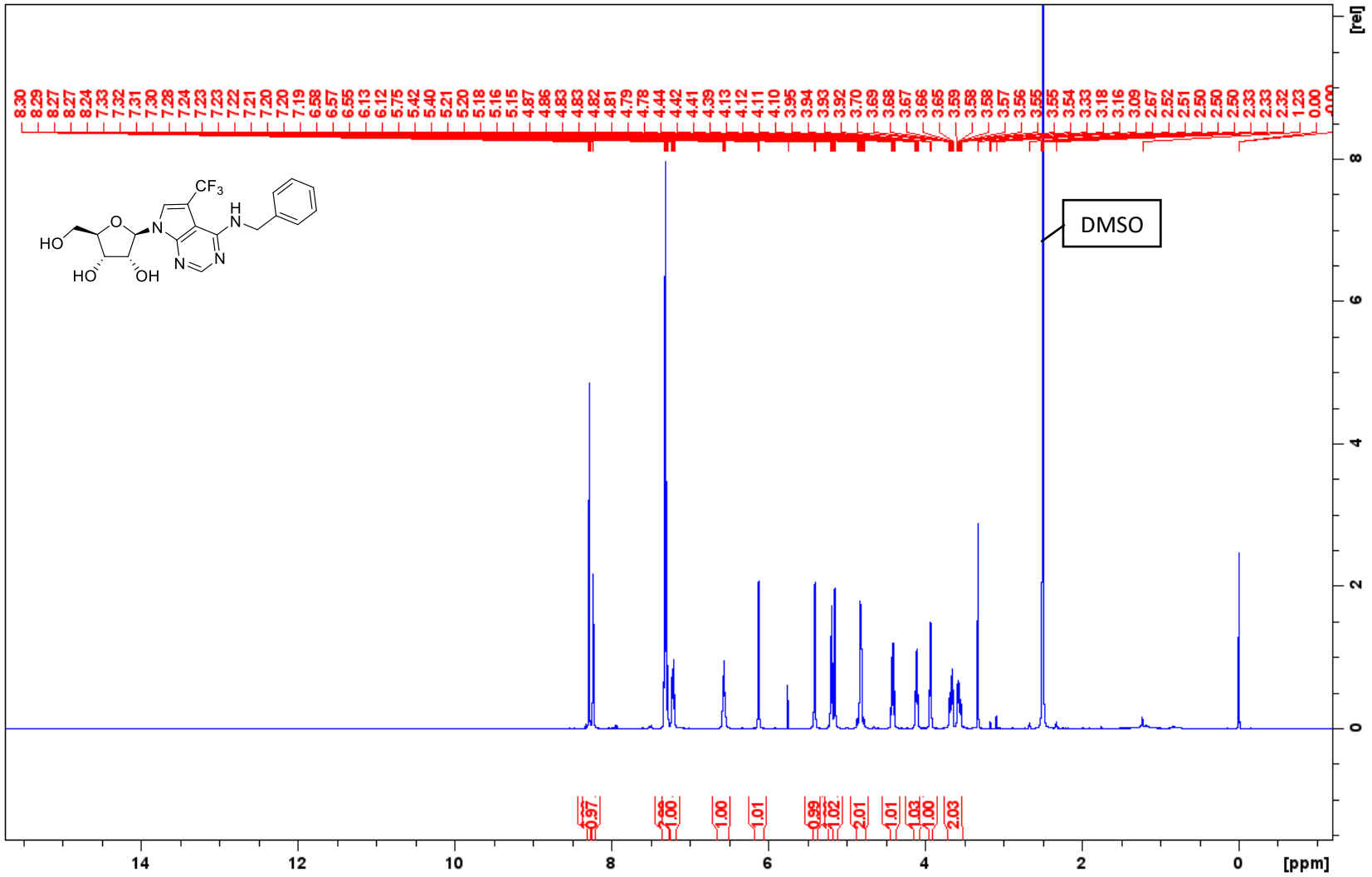

^{13}C NMR (DMSO-d6, 100MHz)

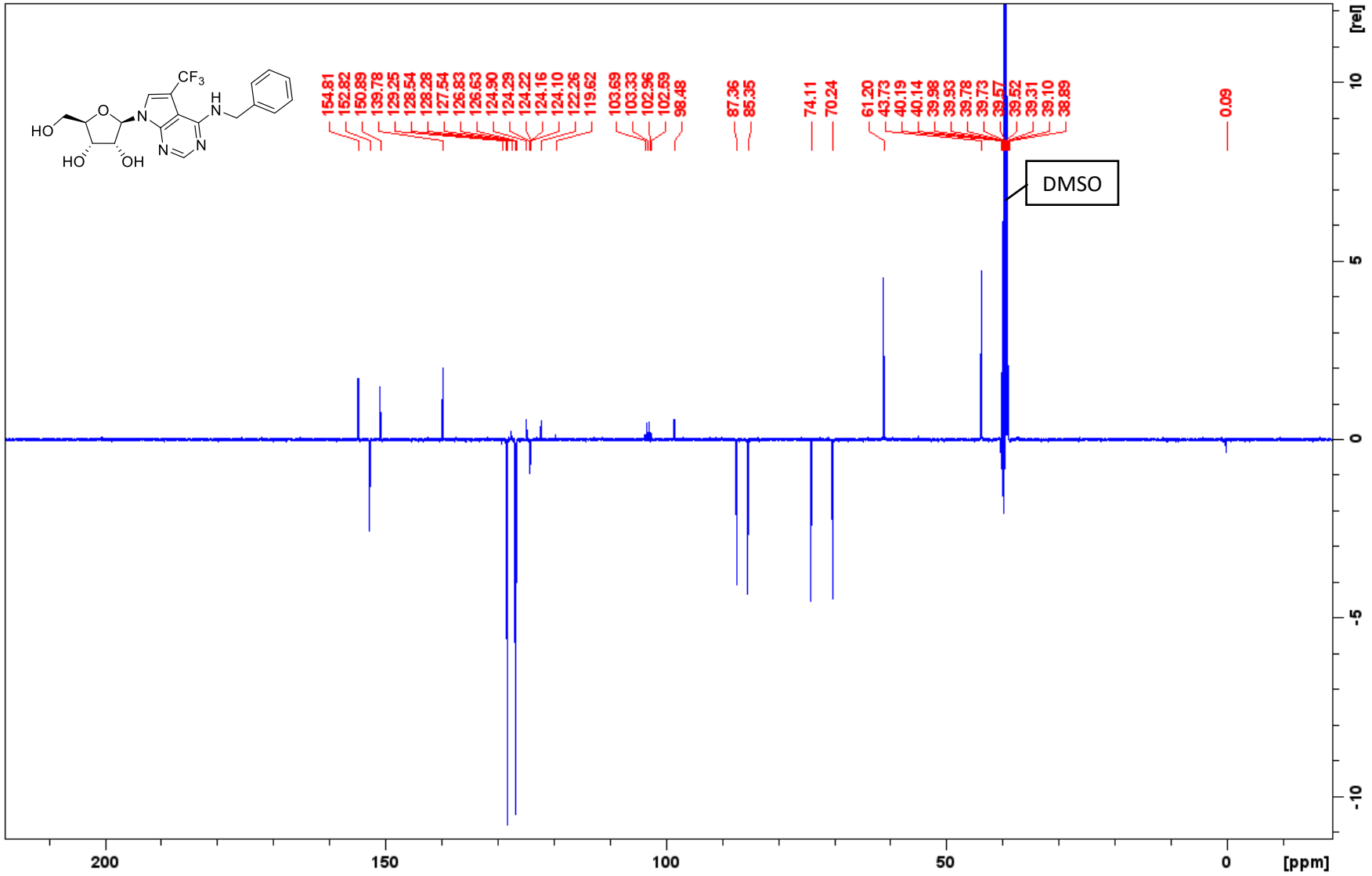

Compound **4-(((S)-1-phenylethyl)amino)-5-trifluoromethyl-N7-(β-D-ribofuranosyl)-pyrrolo[2,3-*d*]pyrimidine (8b)**

^{1}H NMR (DMSO-d6, 400MHz)

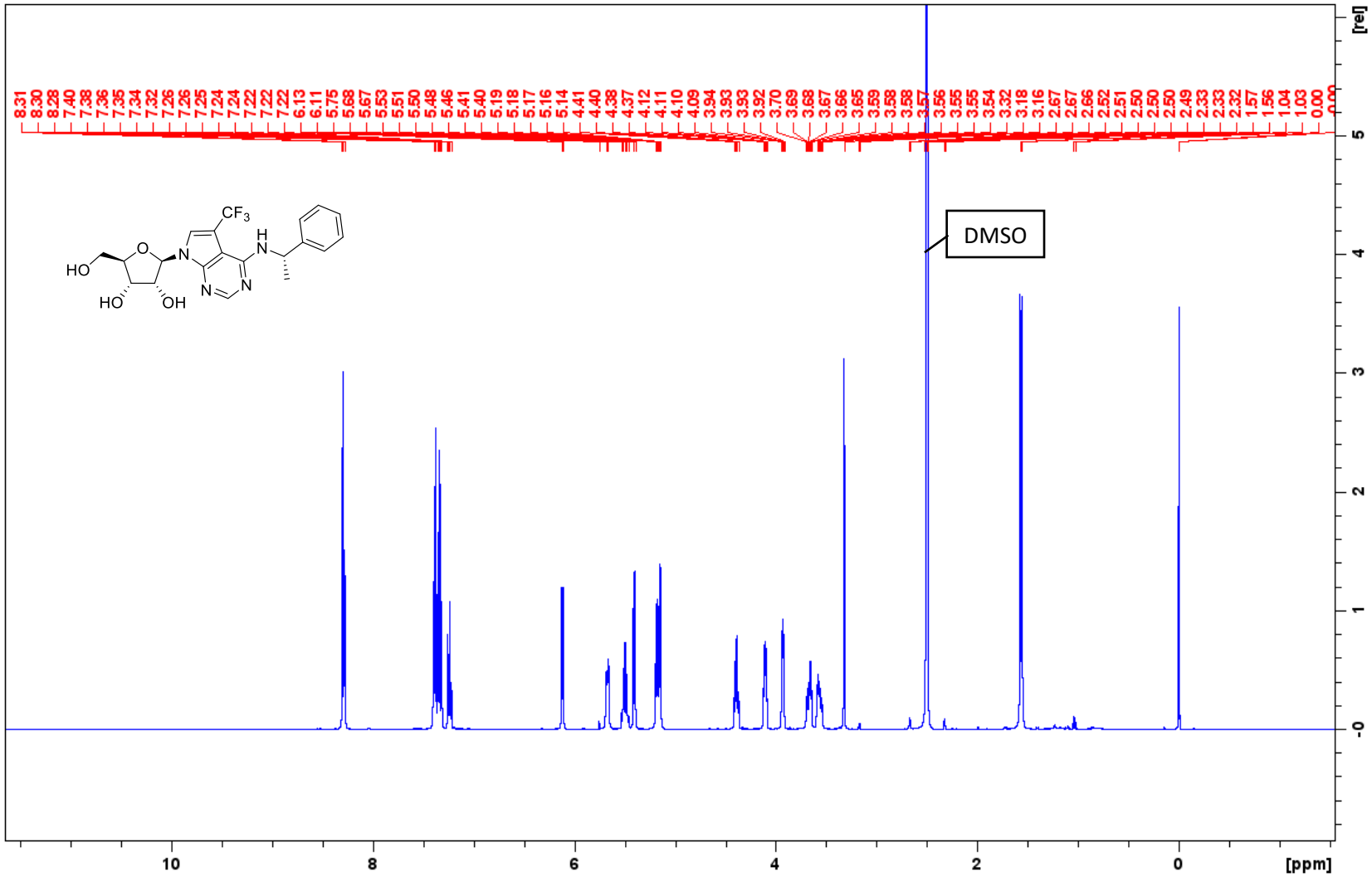

^{13}C NMR (DMSO-d6, 100MHz)

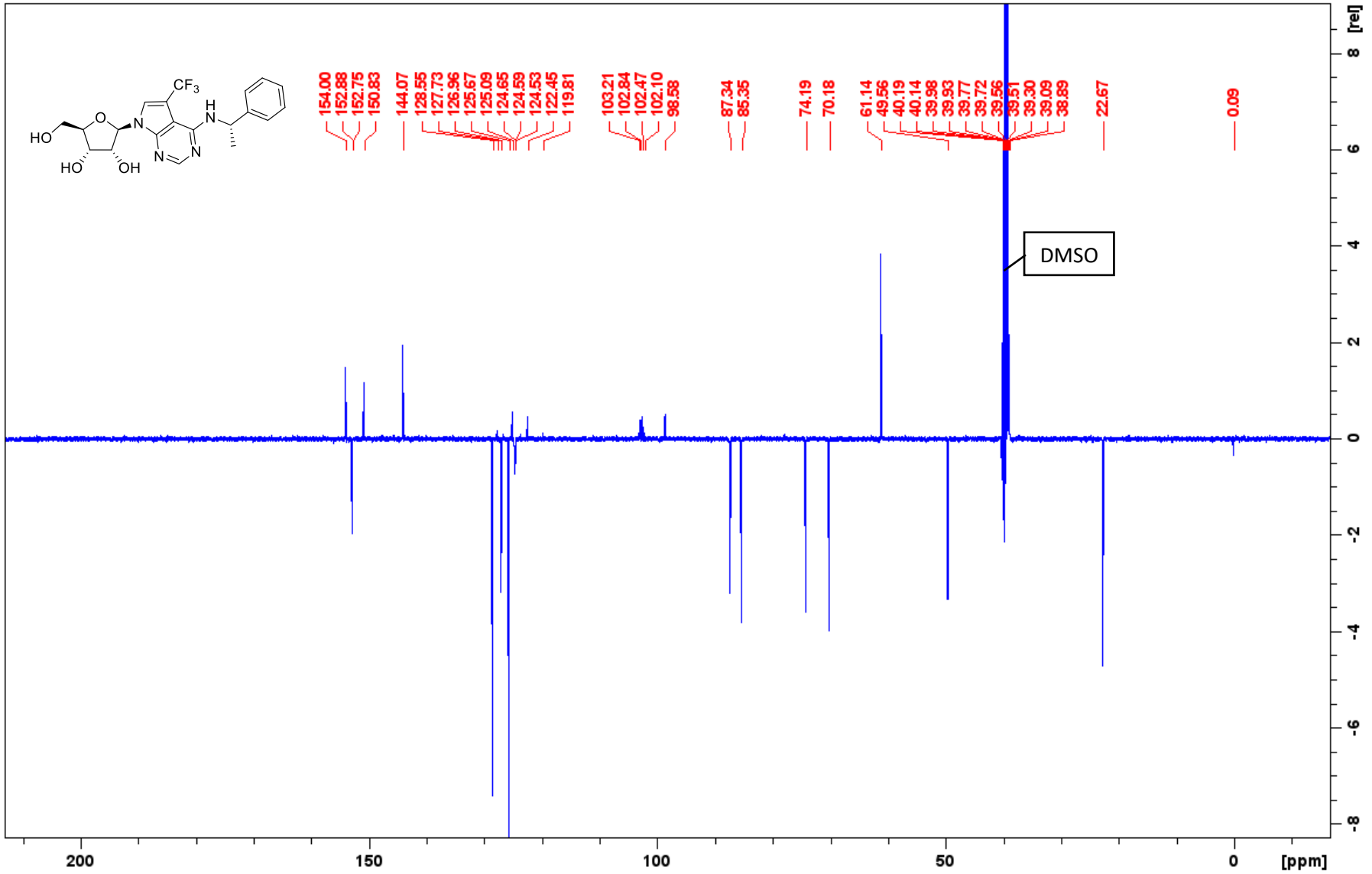

Compound **4-(((R)-1-phenylethyl)amino)-5-trifluoromethyl-N7-(β-D-ribofuranosyl)-pyrrolo[2,3-*d*]pyrimidine (8c)**

^{1}H NMR (DMSO-d6, 400MHz)

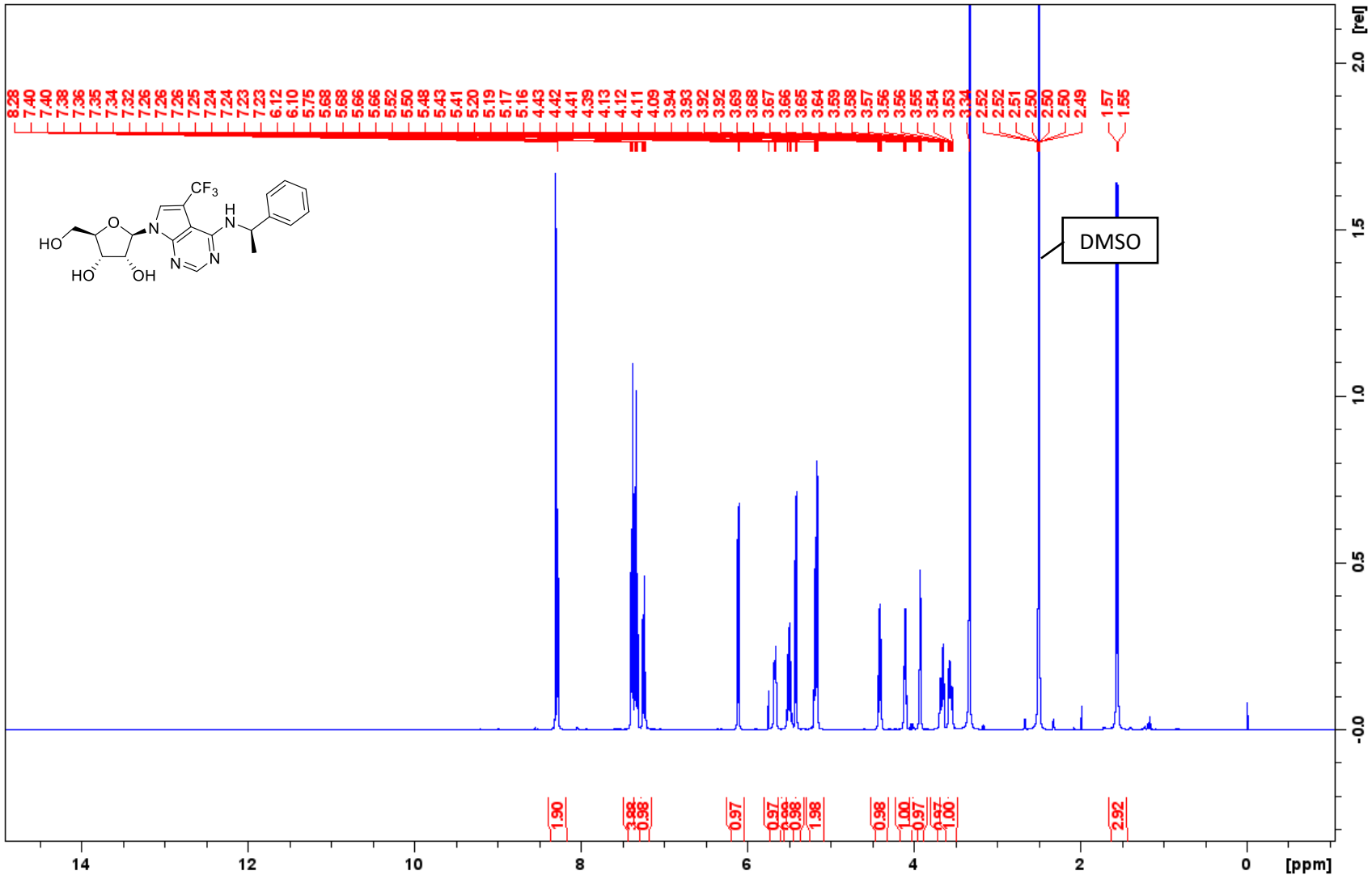

^{13}C NMR (DMSO-d6, 100MHz)

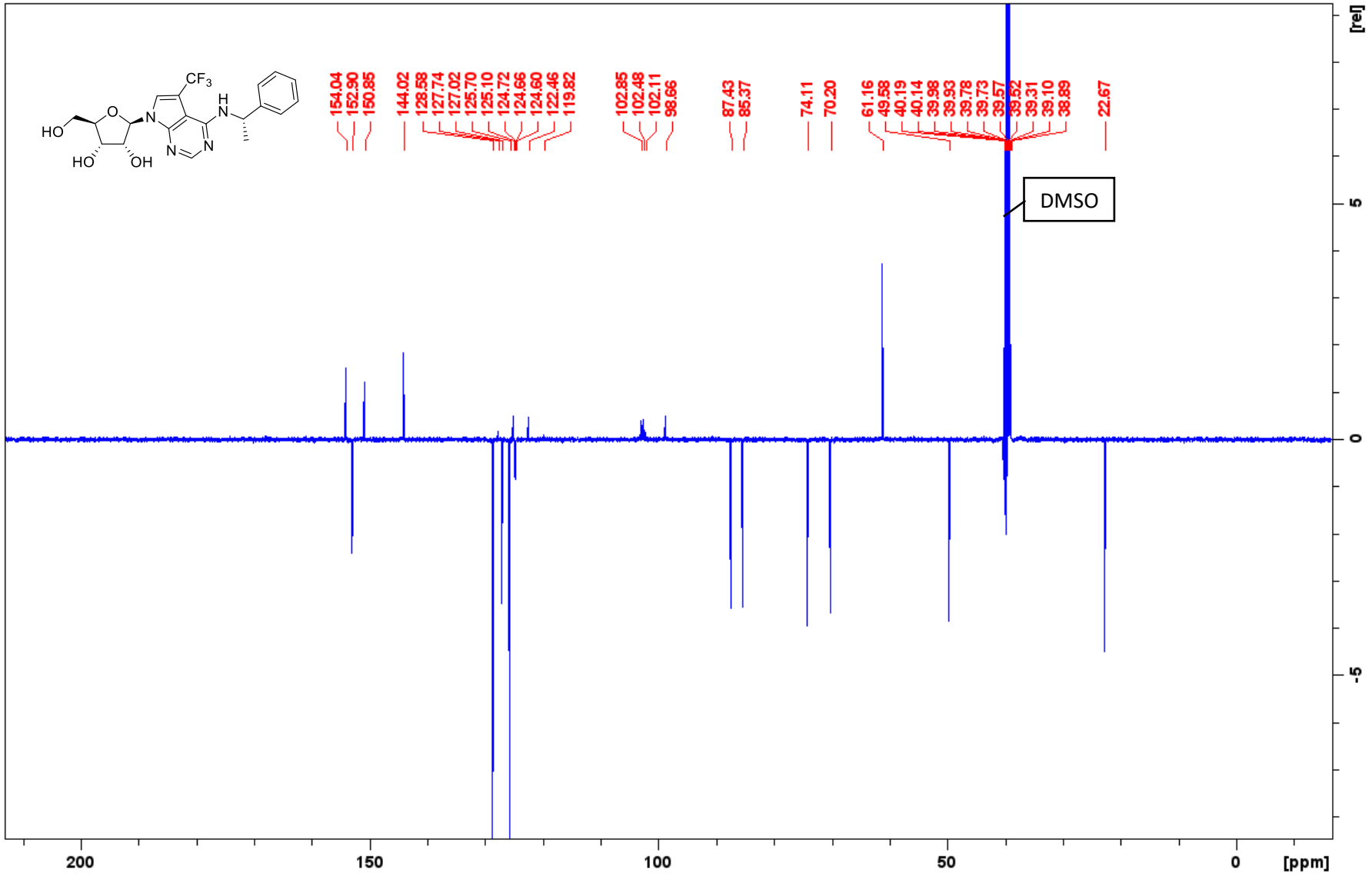

Compound **4-((2-chlorobenzyl)amino)-5-trifluoromethyl-N7-(β-D-ribofuranosyl)-pyrrolo[2,3-*d*]pyrimidine (8d)**

^{1}H NMR (DMSO-d6, 400MHz)

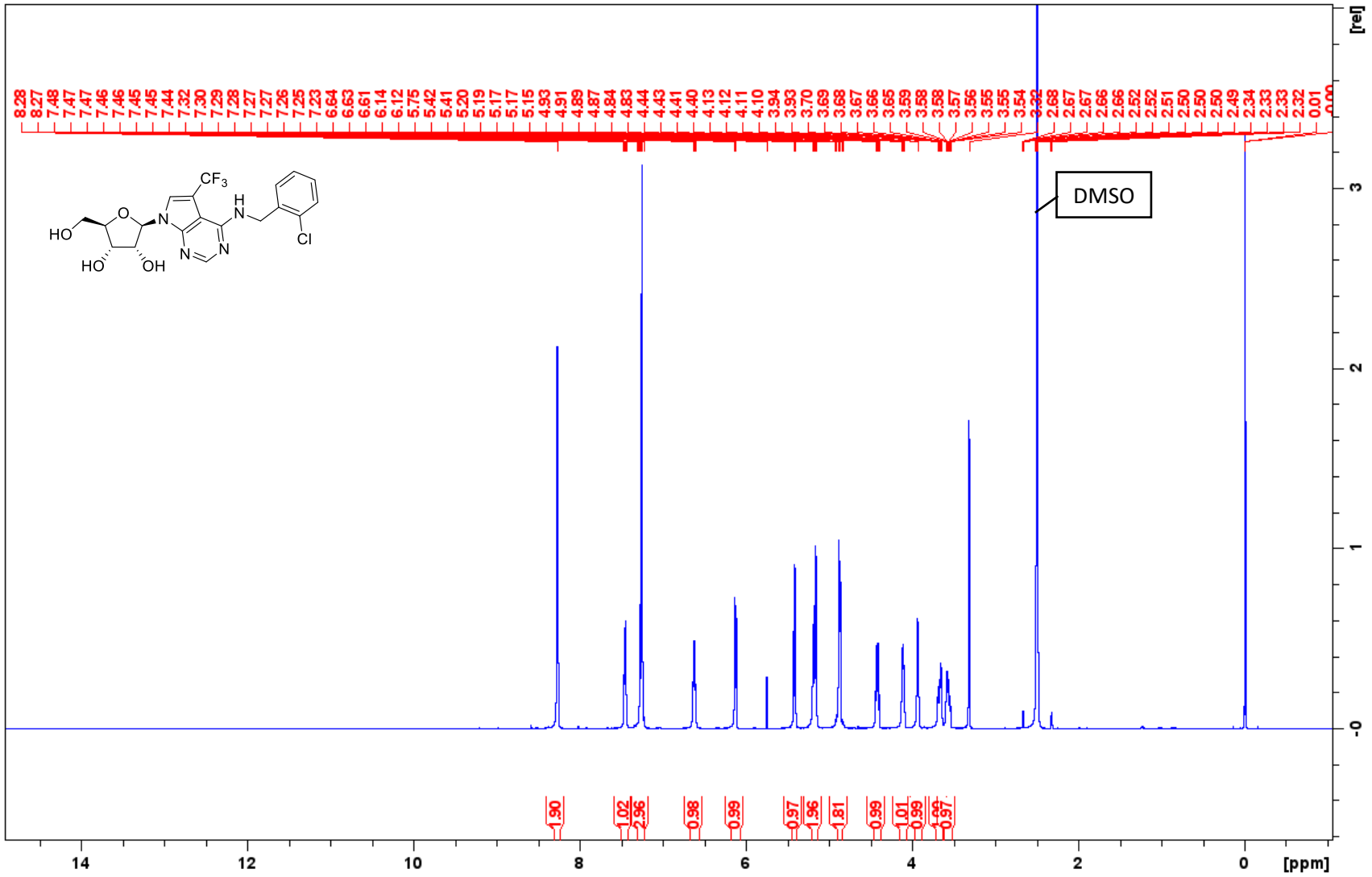

^{13}C NMR (DMSO-d6, 100MHz)

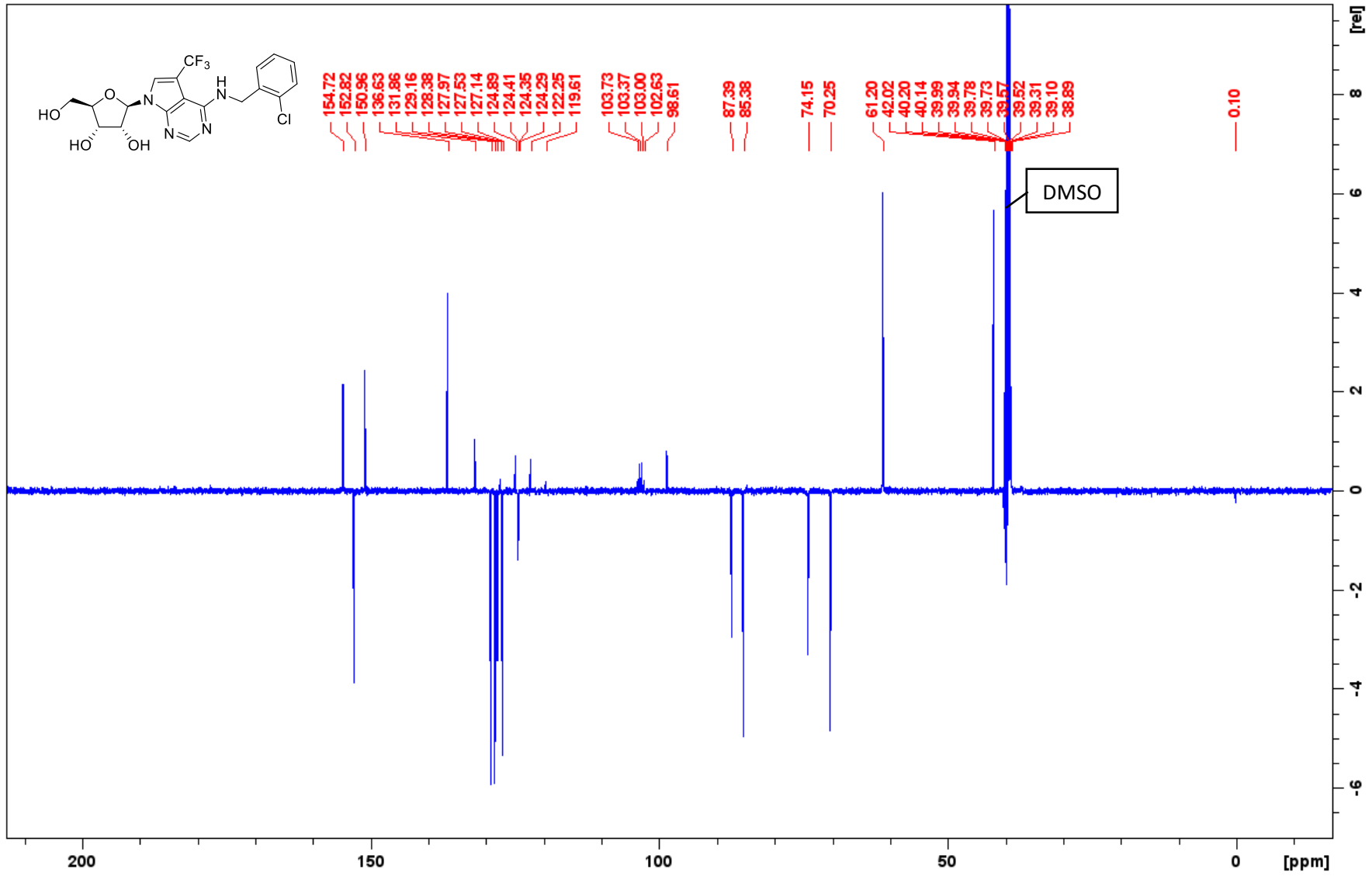

Compound **4-((4-chlorobenzyl)amino)-5-trifluoromethyl-N7-(β-D-ribofuranosyl)-pyrrolo[2,3-*d*]pyrimidine (8e)**

^{1}H NMR (DMSO-d6, 400MHz)

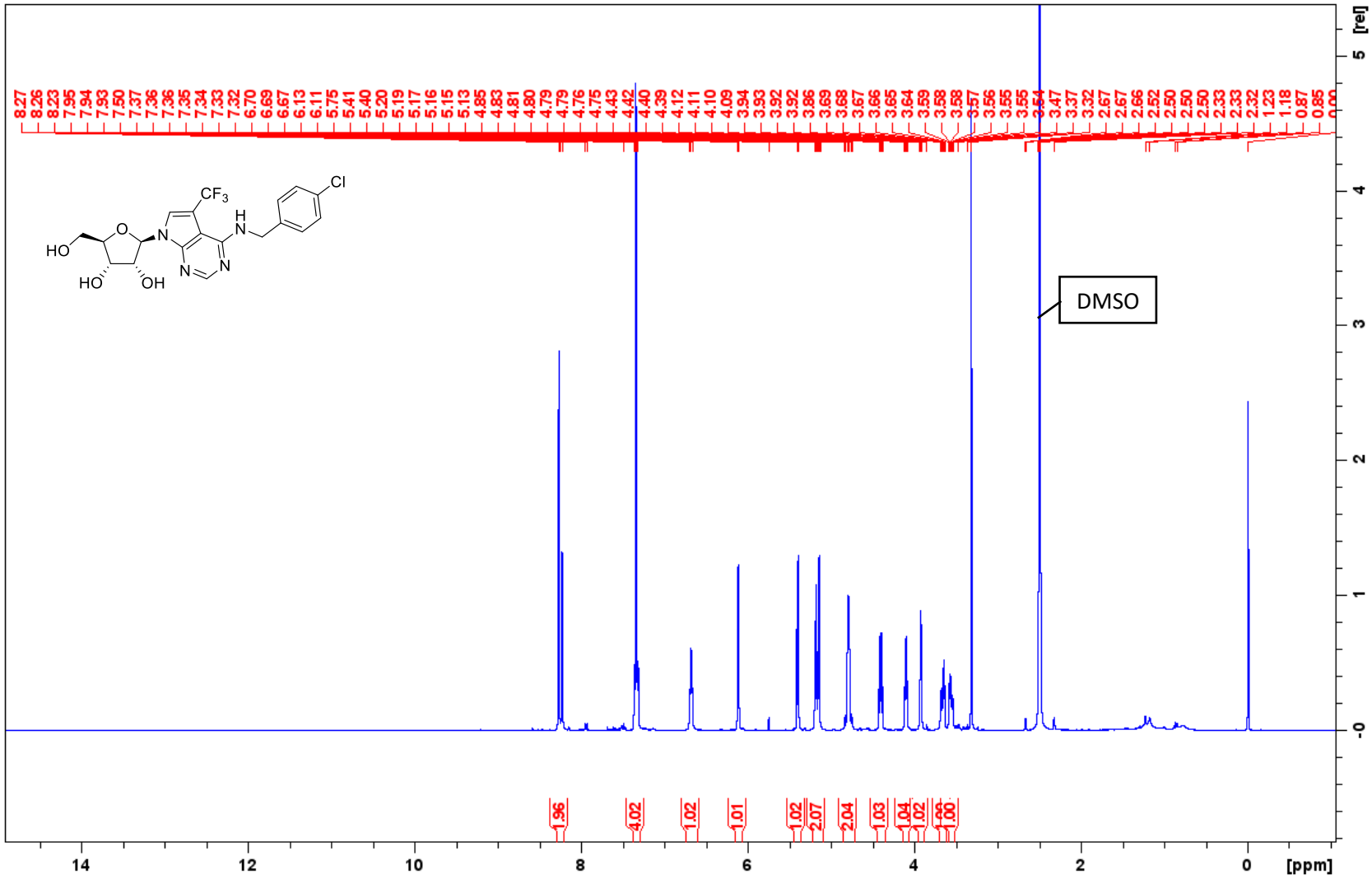

^{13}C NMR (DMSO-d6, 100MHz)

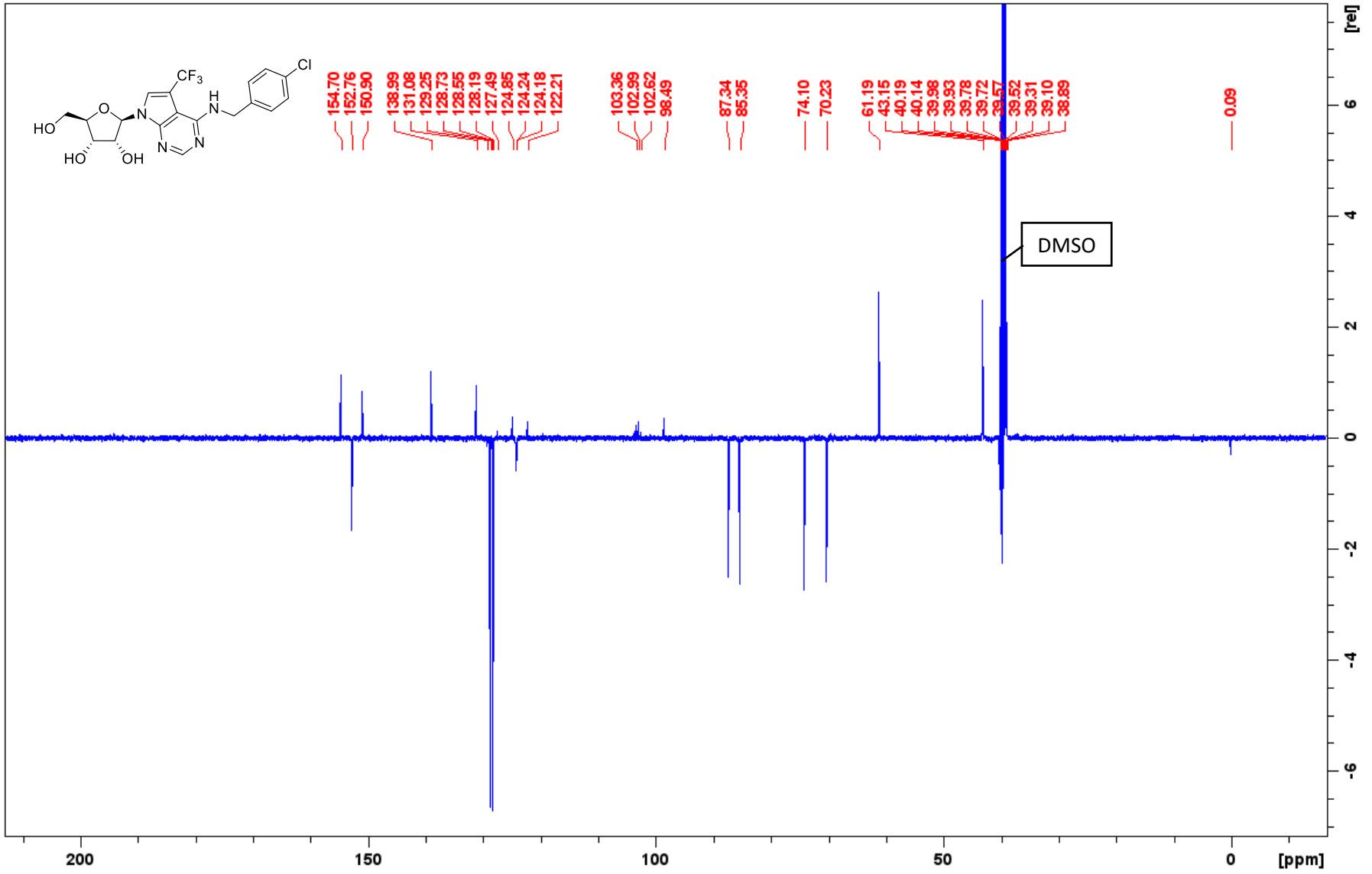

Compound **4-((3-chlorobenzyl)amino)-5-trifluoromethyl-N7-(β-D-ribofuranosyl)-pyrrolo[2,3-*d*]pyrimidine (8f)**

^{1}H NMR (DMSO-d6, 400MHz)

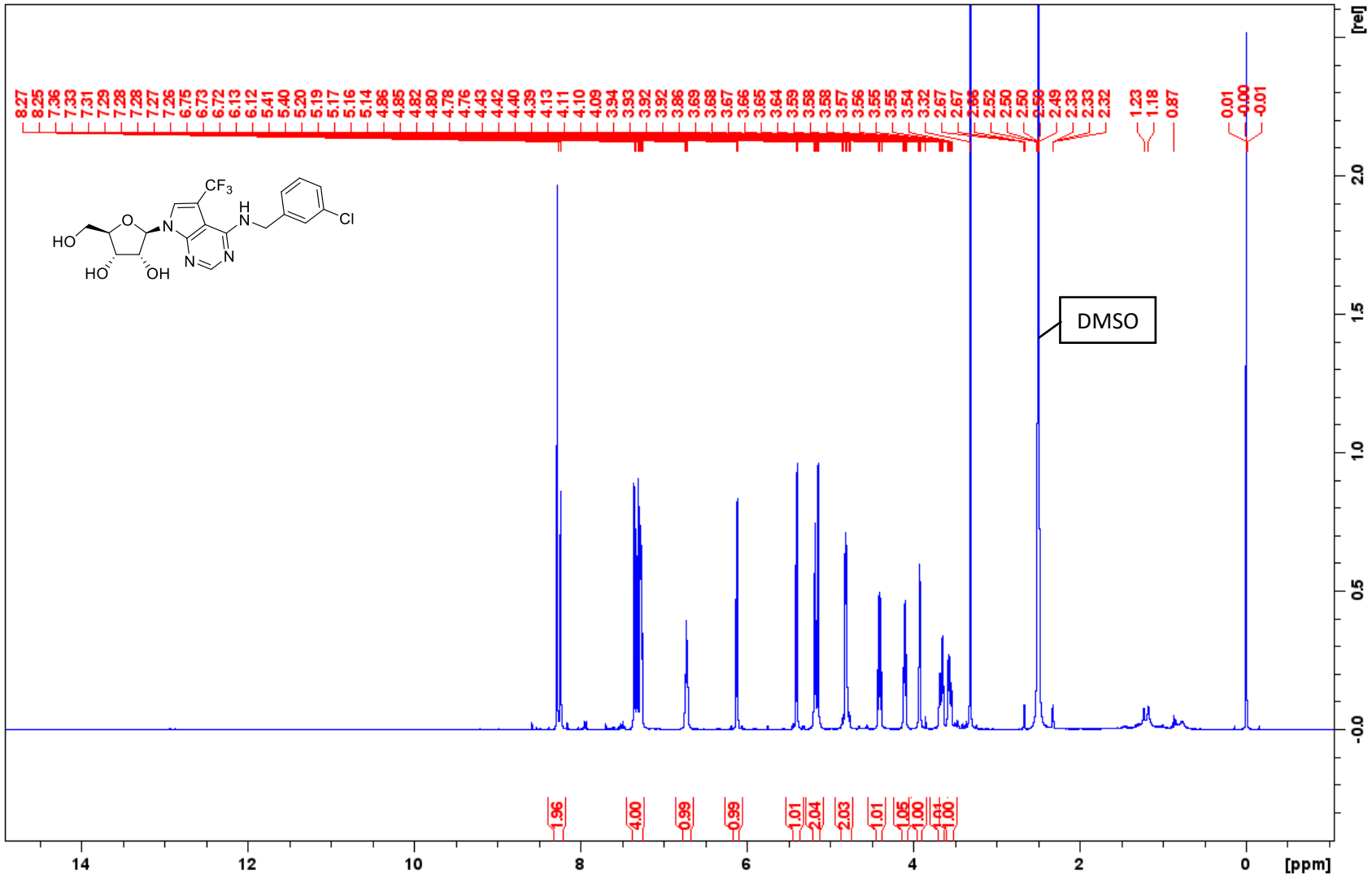

^{13}C NMR (DMSO-d6, 100MHz)

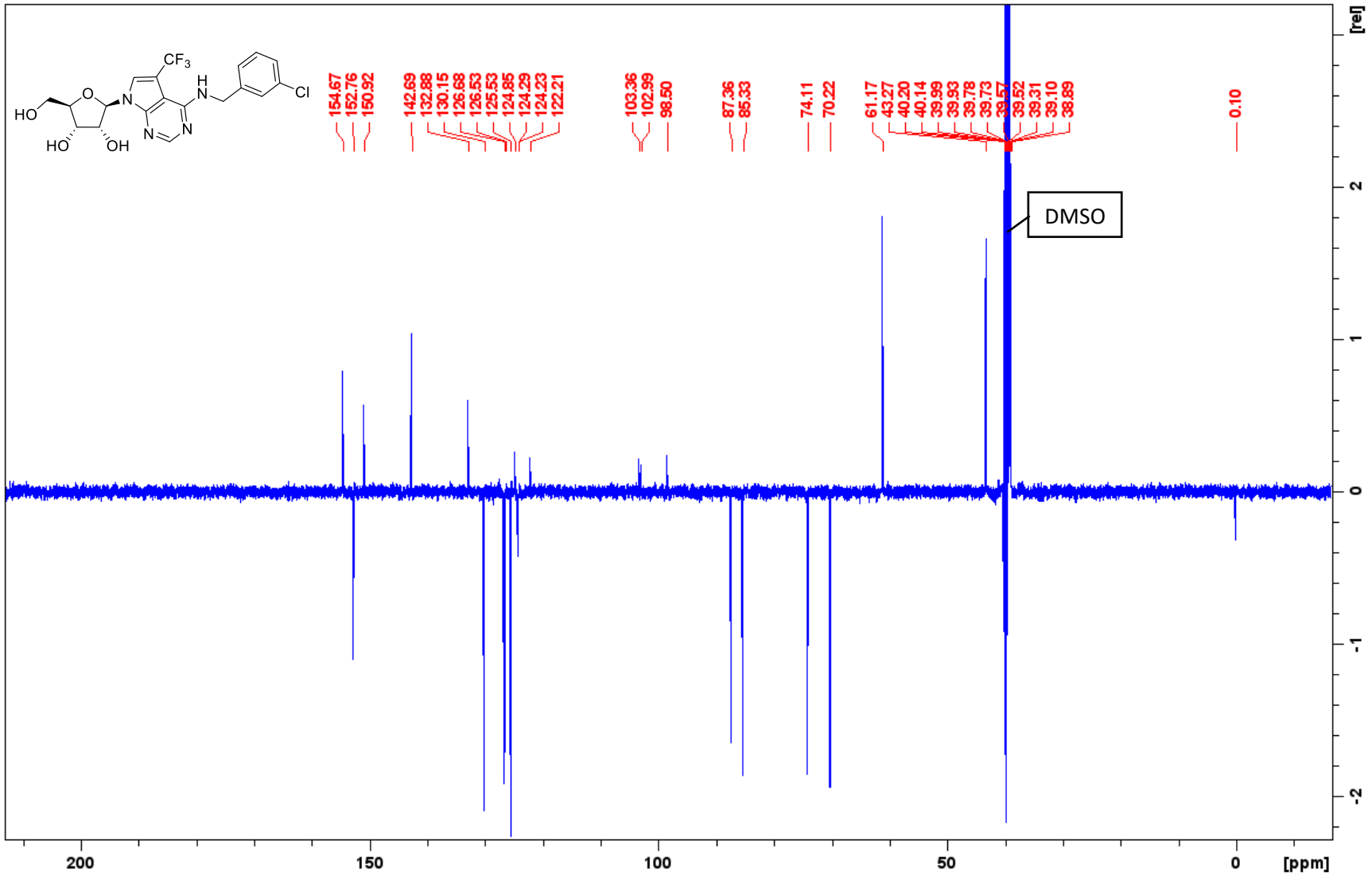

Compound **4-((2-fluorobenzyl)amino)-5-trifluoromethyl-N7-(β-D-ribofuranosyl)-pyrrolo[2,3-*d*]pyrimidine (8g)**

^{1}H NMR (DMSO-d6, 400MHz)

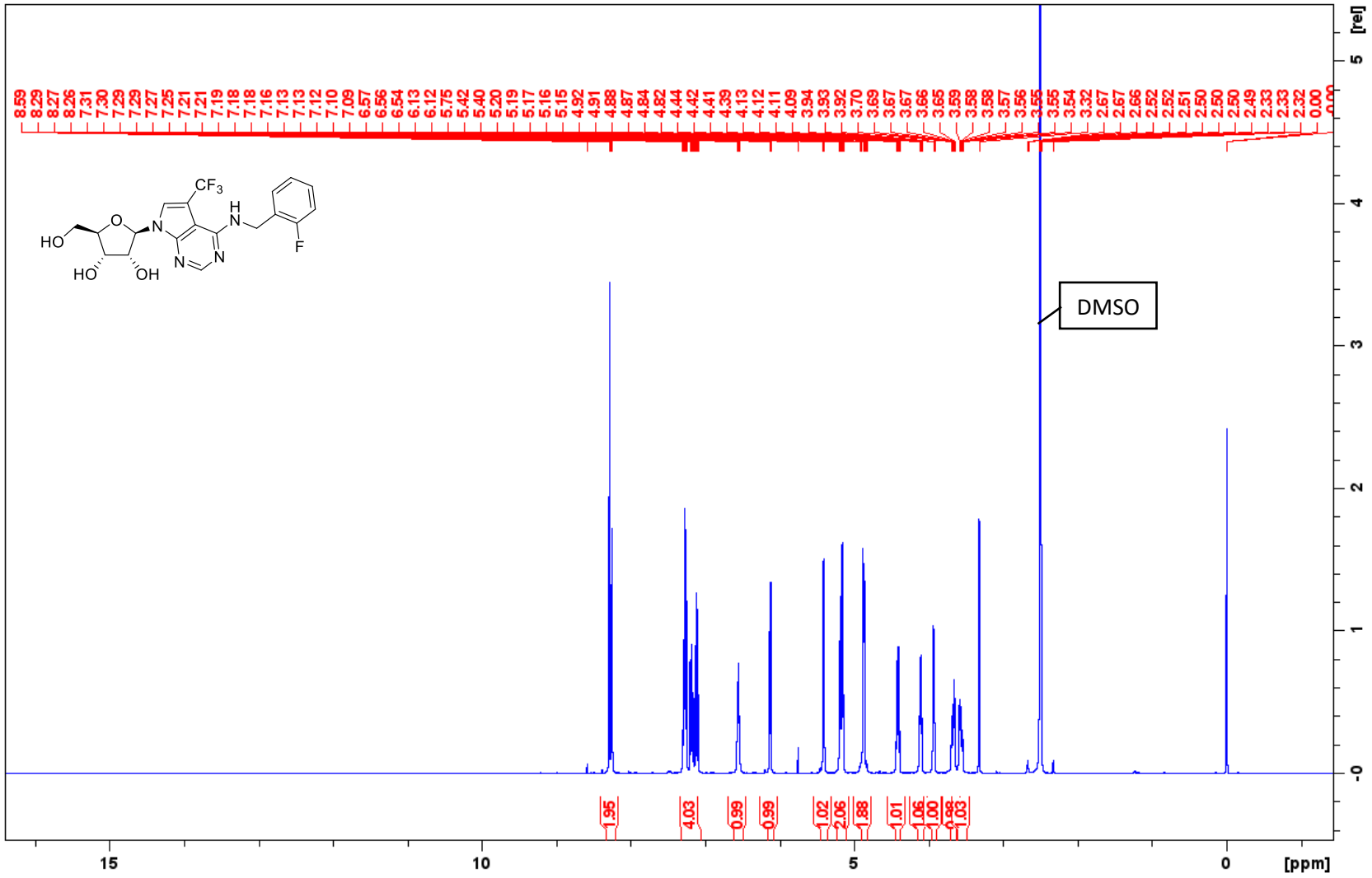

^{13}C NMR (DMSO-d6, 100MHz)

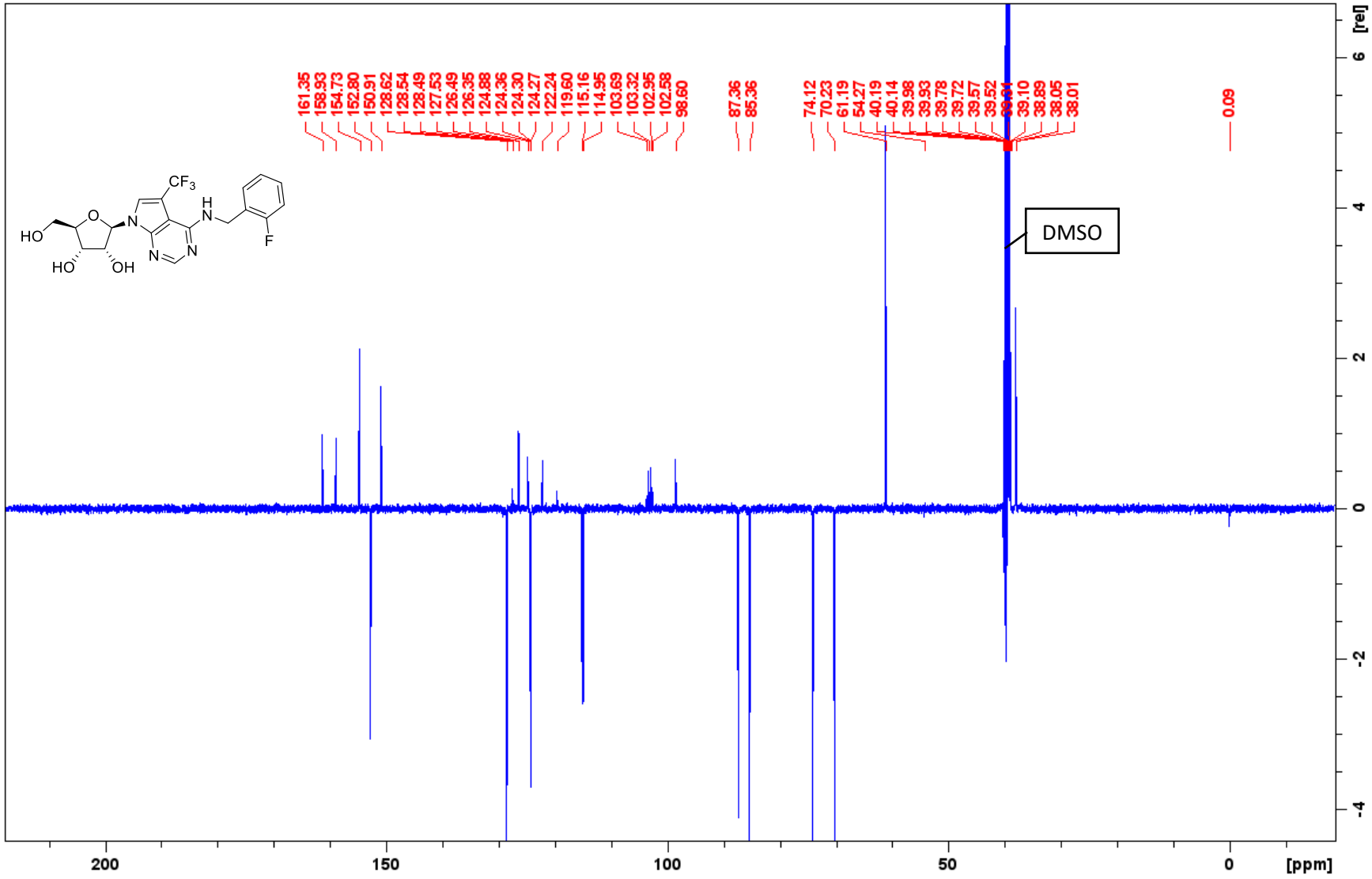

Compound **4-phenylamino-5-trifluoromethyl-N7-(β-D-ribofuranosyl)-pyrrolo[2,3-*d*]pyrimidine (8h)**

^{1}H NMR (DMSO-d6, 400MHz)

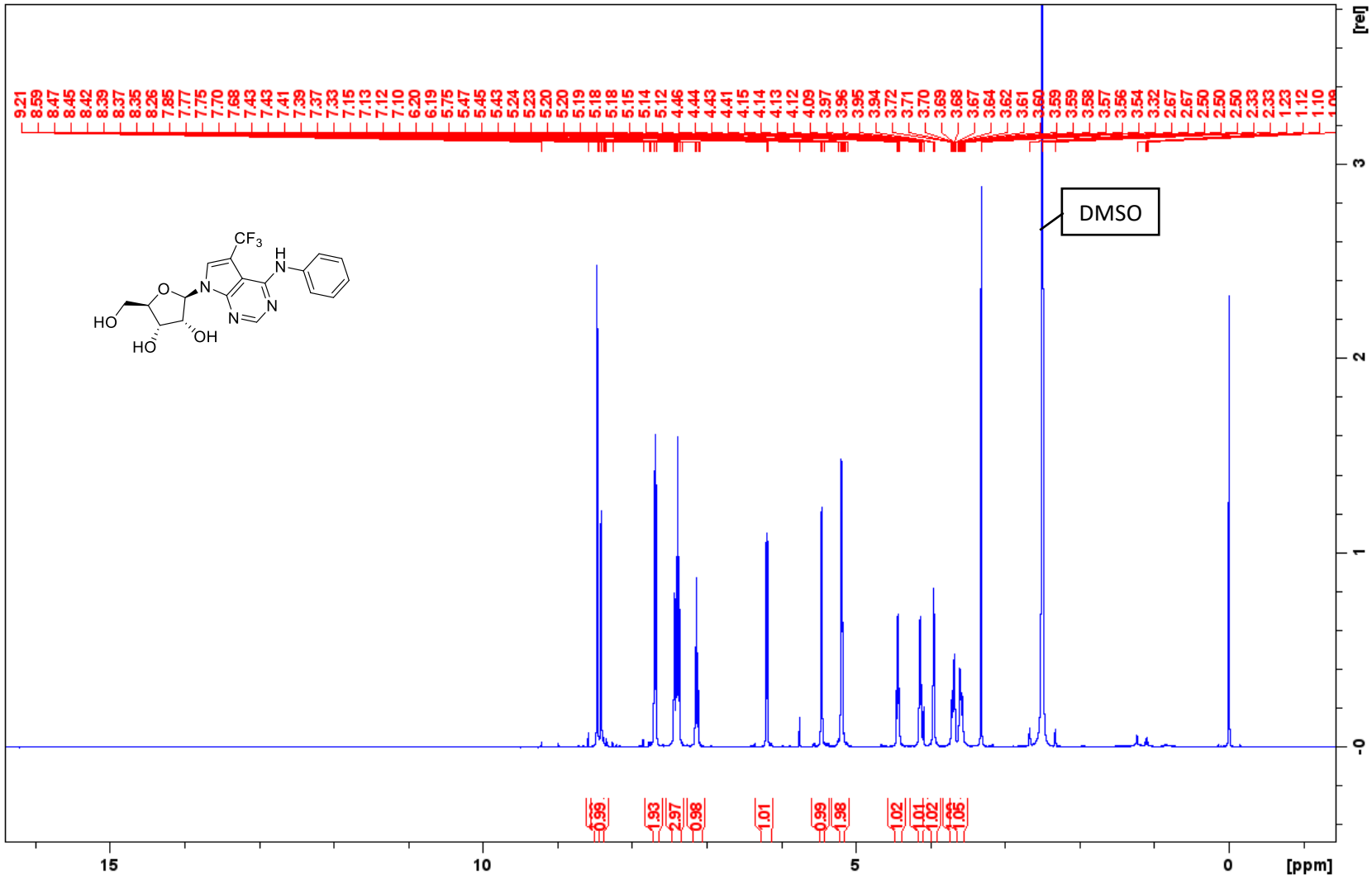

^{13}C NMR (DMSO-d6, 100MHz)

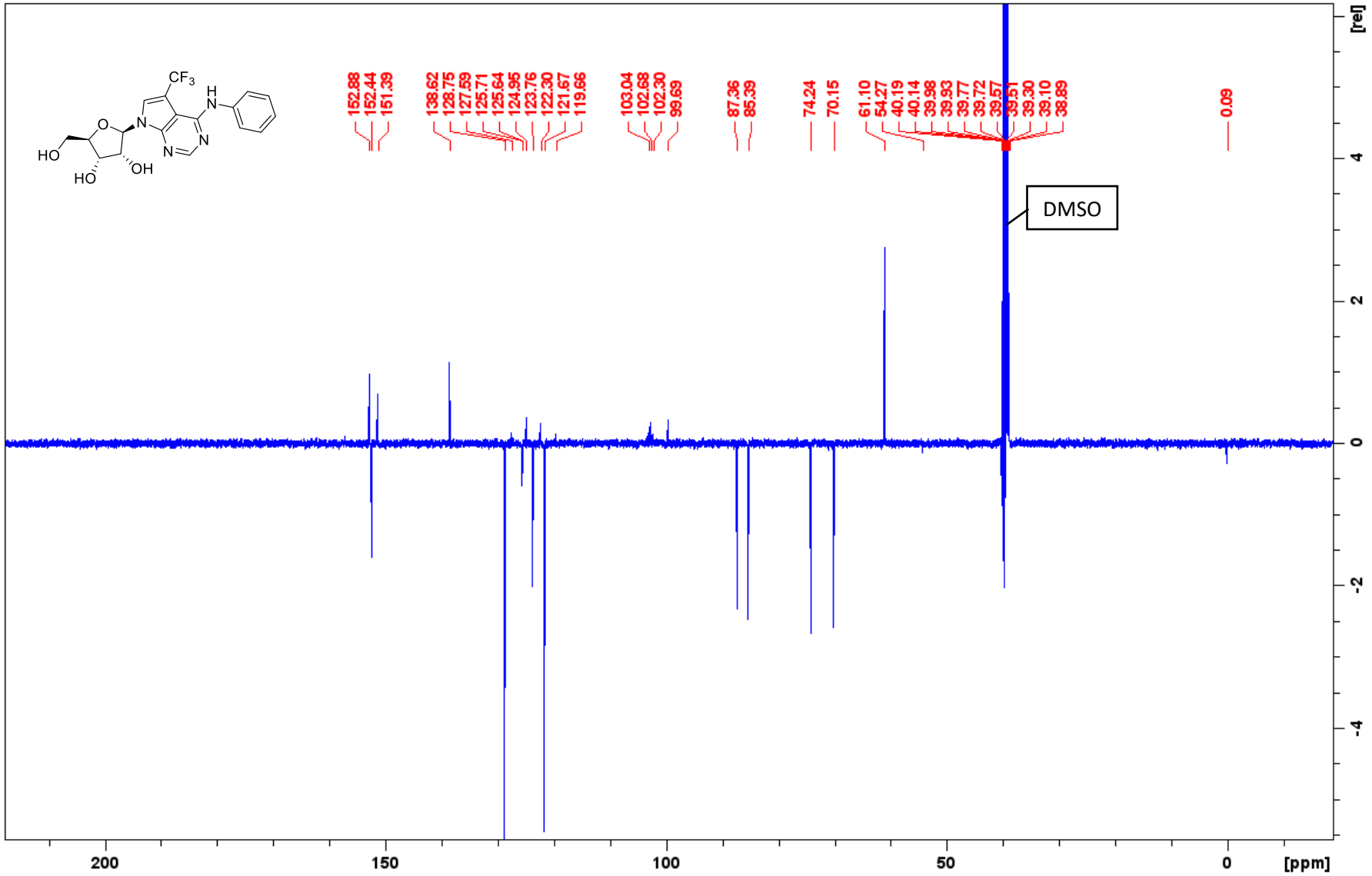

Compound **4-phenethylamino-5-trifluoromethyl-N7-(β-D-ribofuranosyl)-pyrrolo[2,3-*d*]pyrimidine (8i)**

^{1}H NMR (DMSO-d6, 400MHz)

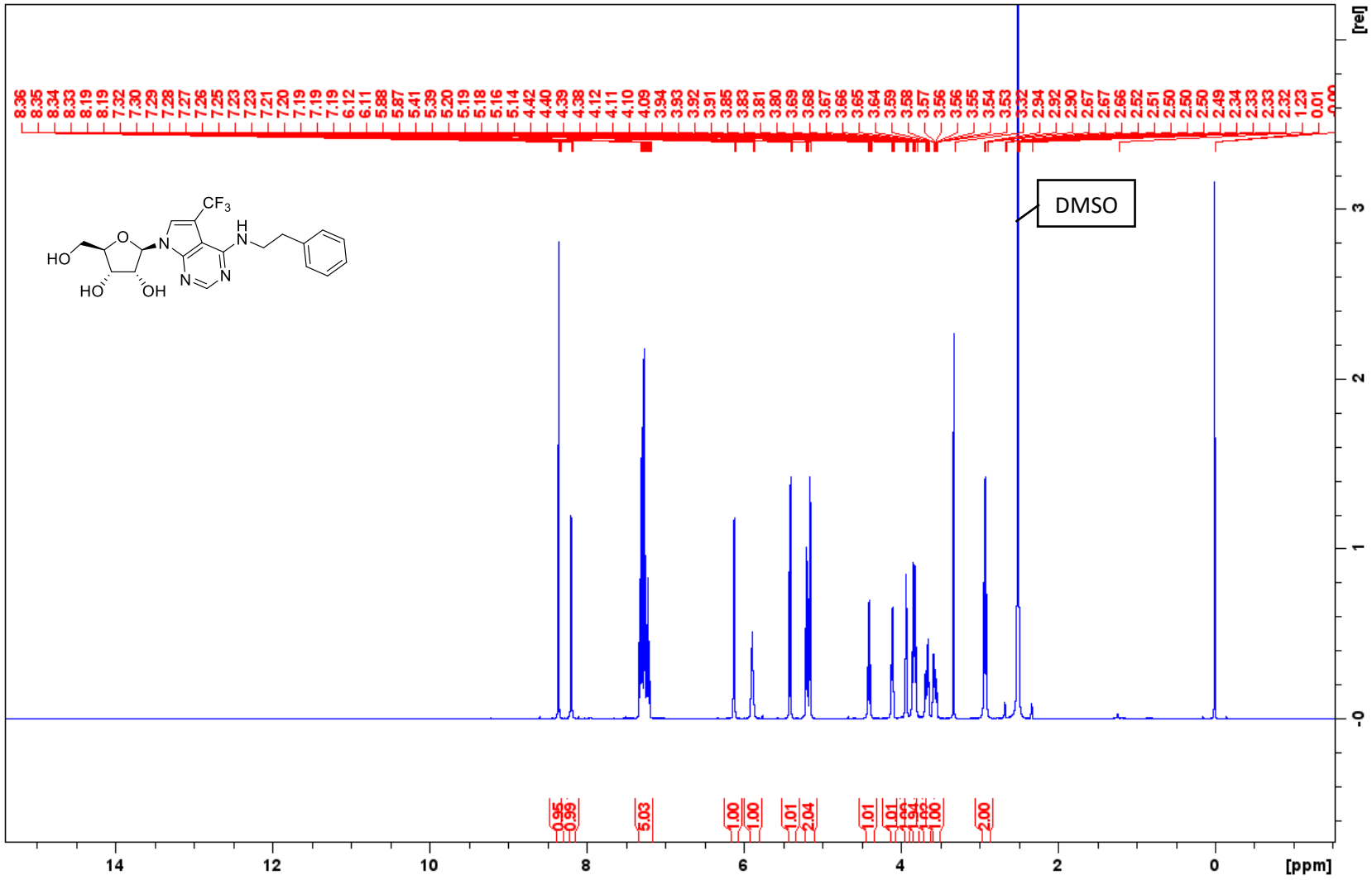

^{13}C NMR (DMSO-d6, 100MHz)

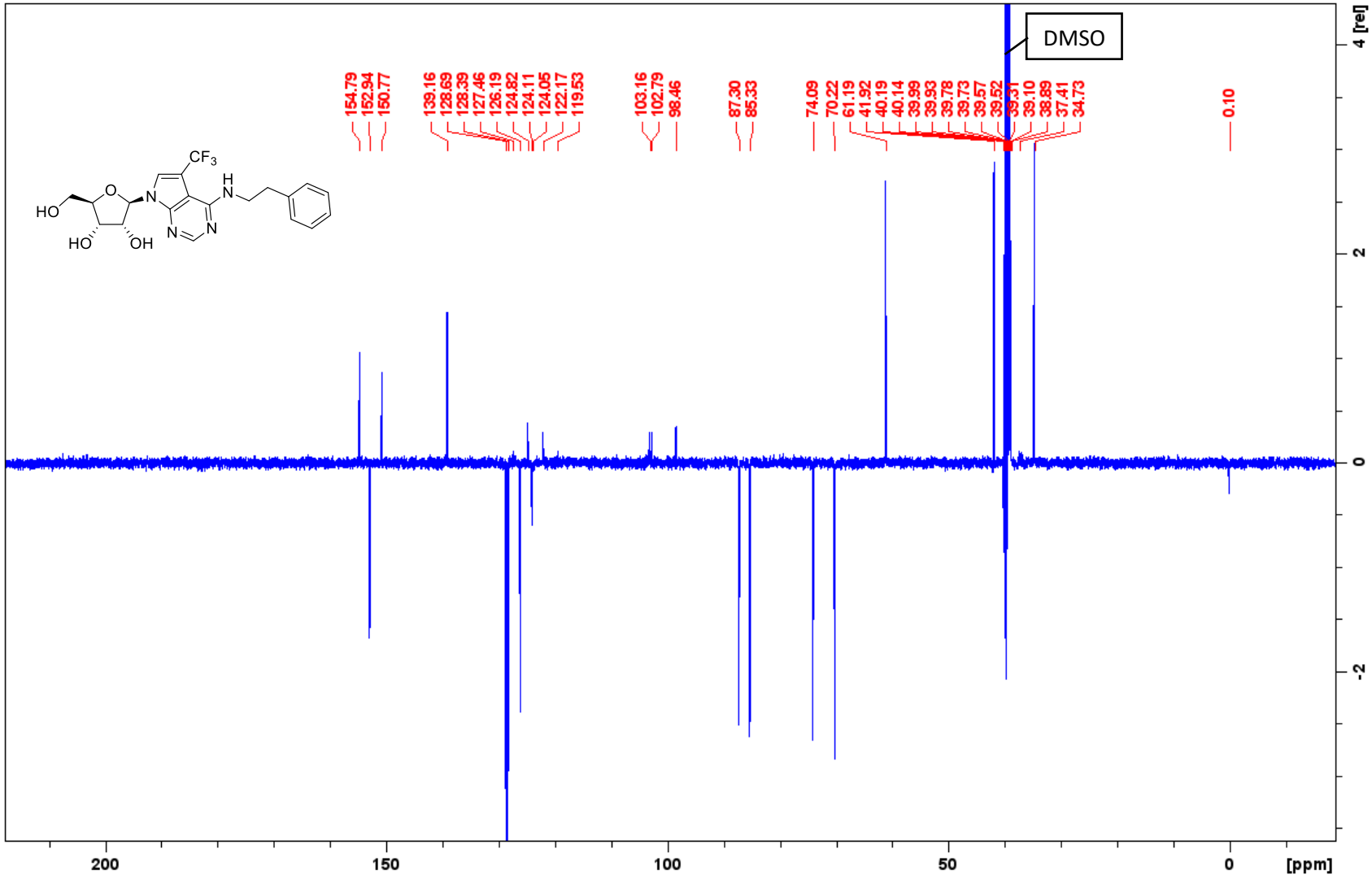

Compound **4-cyclopentylamino-5-trifluoromethyl-N7-(β-D-ribofuranosyl)-pyrrolo[2,3-*d*]pyrimidine (8j)**

^{1}H NMR (DMSO-d6, 400MHz)

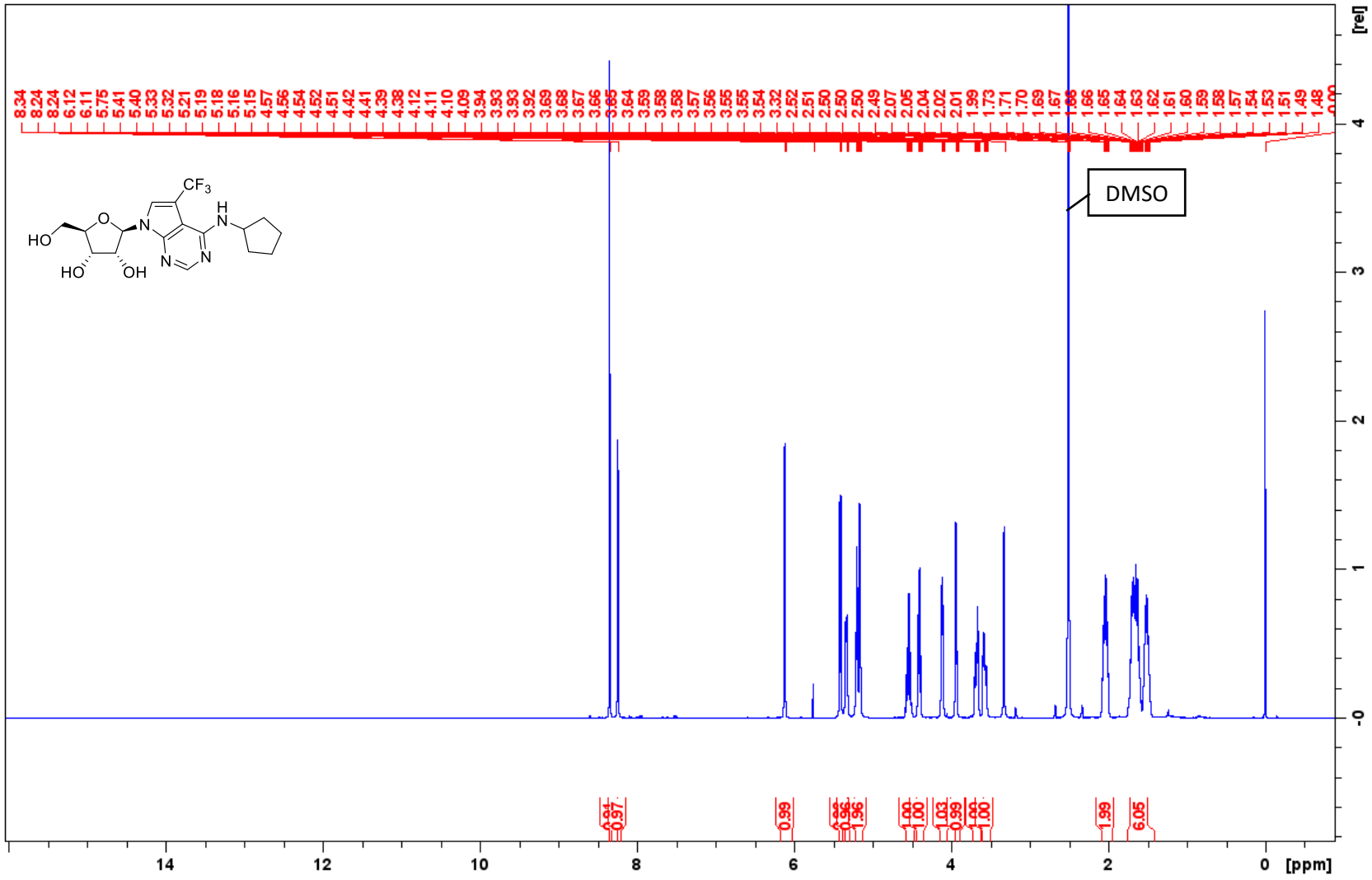

^{13}C NMR (DMSO-d6, 100MHz)

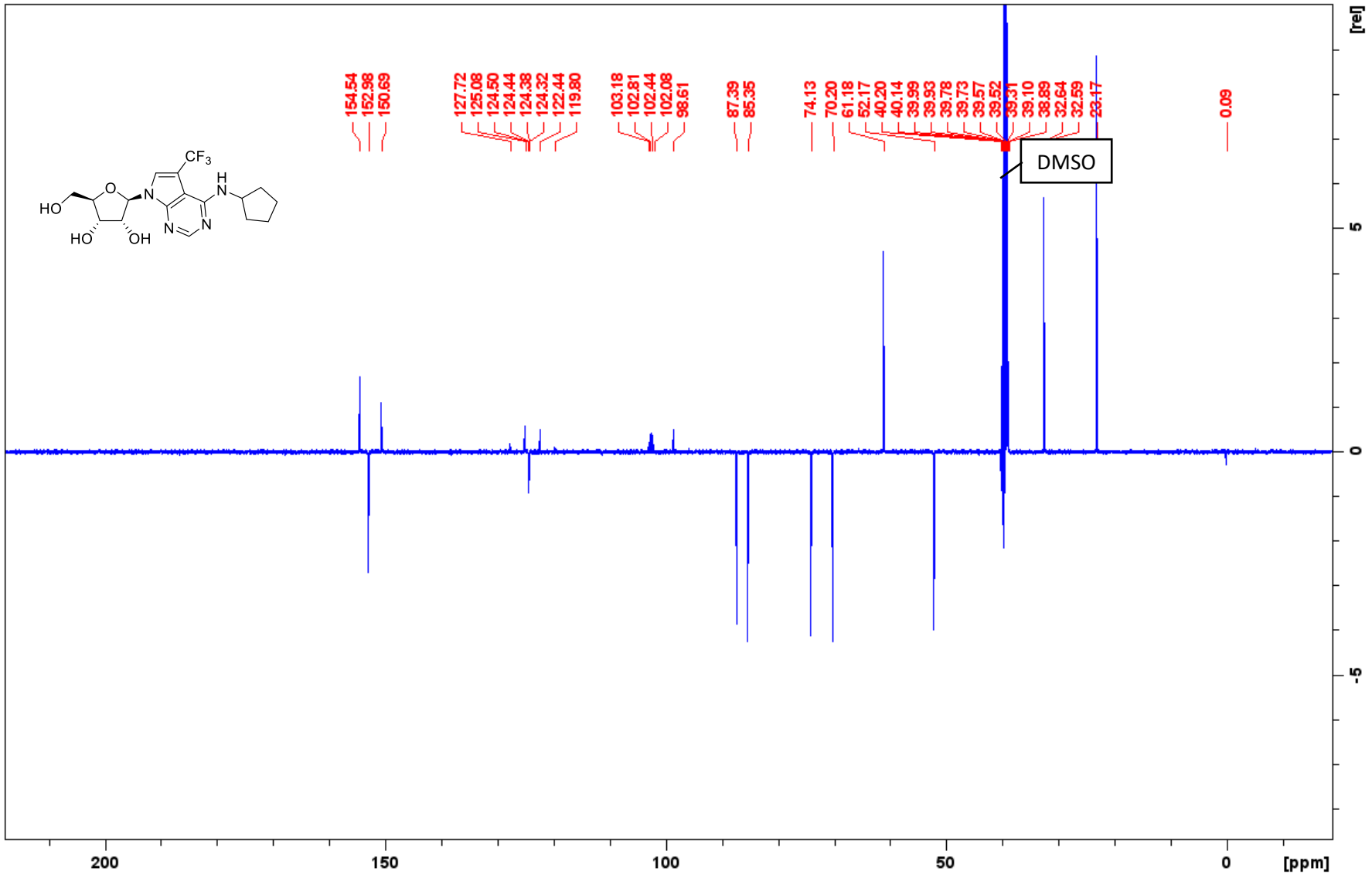

Compound **5-benzyl-1-(β-D-ribofuranosyl)-1,2,5,6,8-pentazaacenaphtylene (15a)**

^{1}H NMR (DMSO-d6, 400MHz)

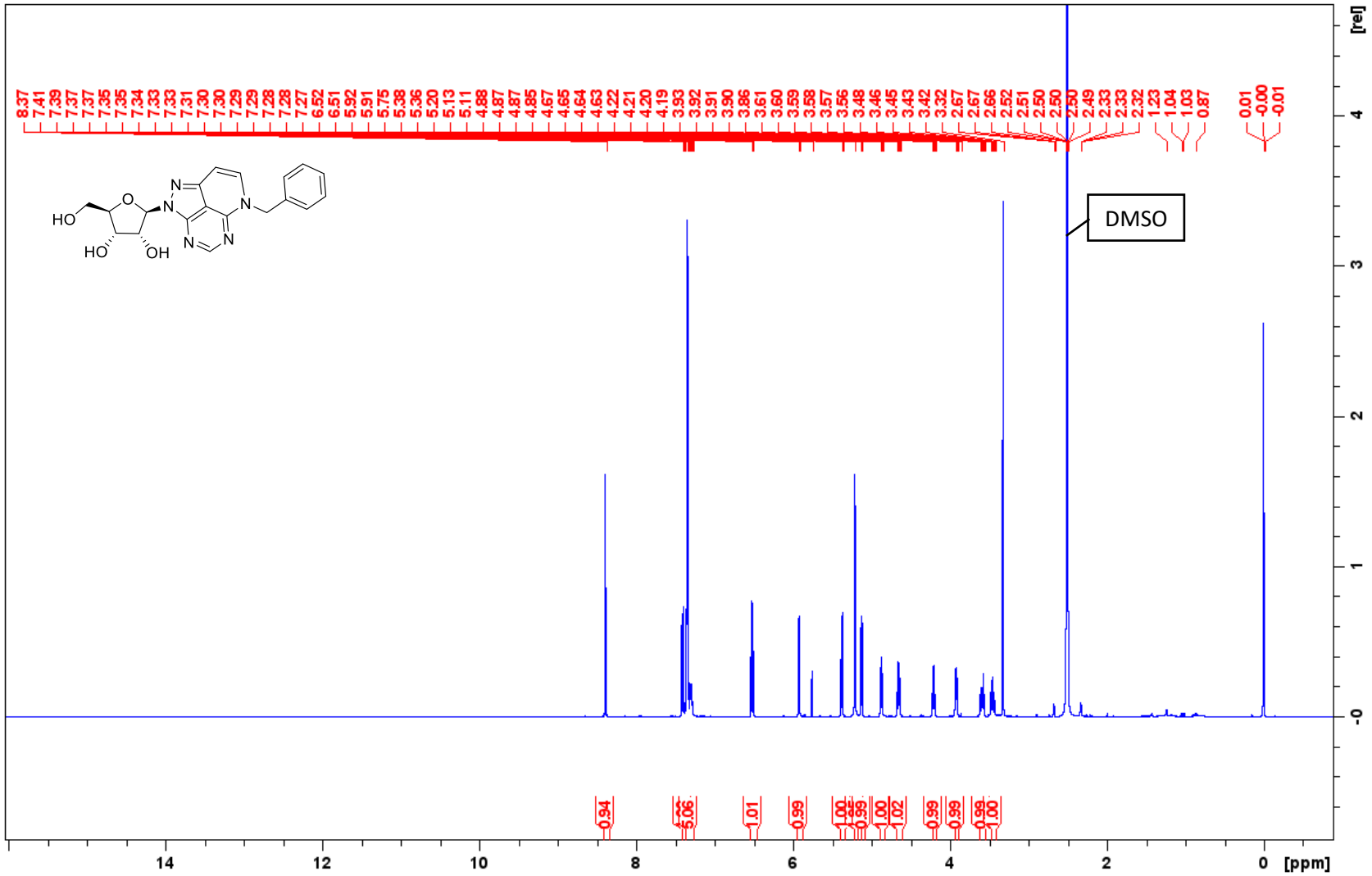

^{13}C NMR (DMSO-d6, 100MHz)

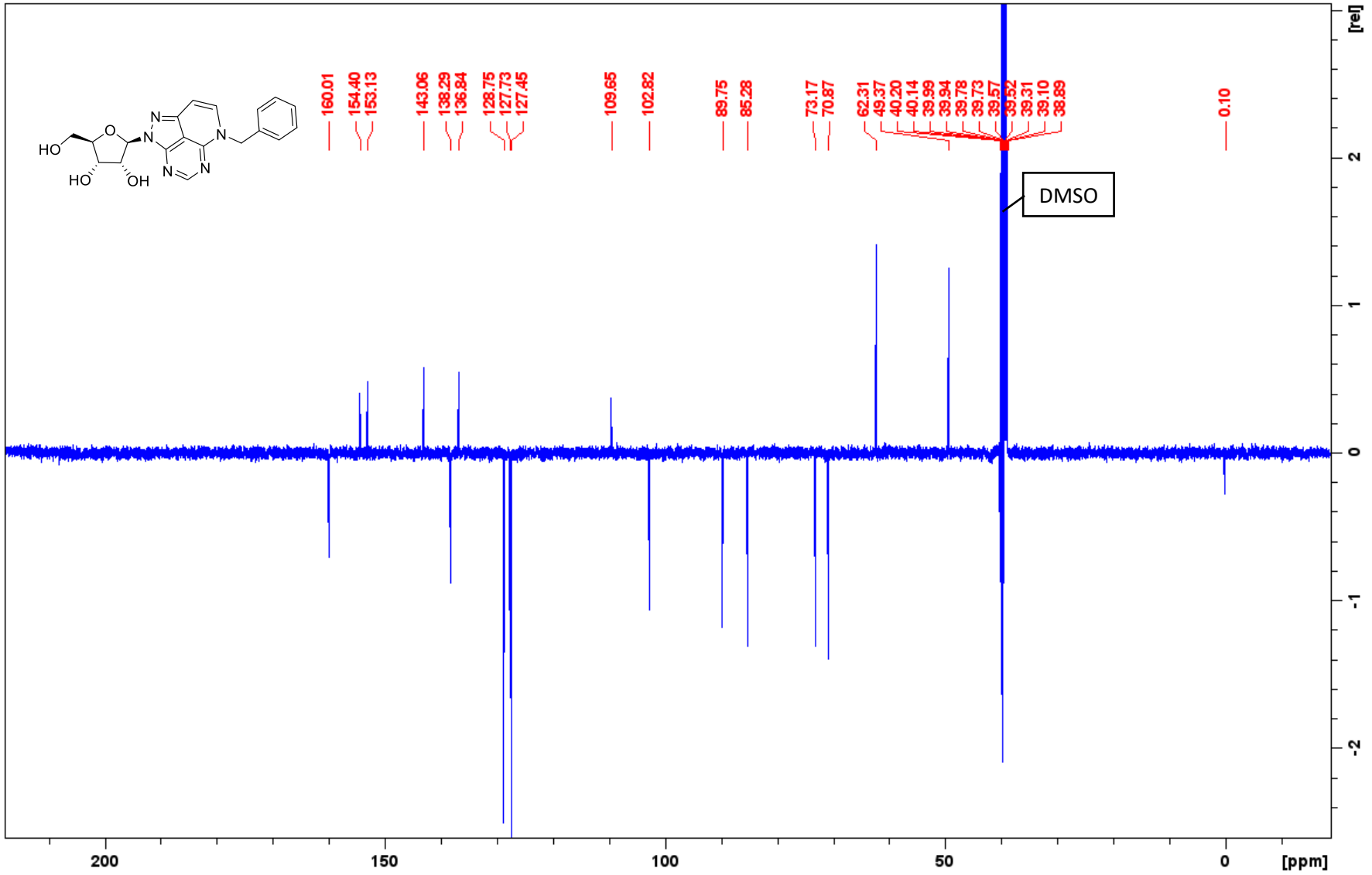

Compound **5-cyclpentyl-1-(β-D-ribofuranosyl)-1,2,5,6,8-pentazaacenaphtylene (15b)**

^{1}H NMR (DMSO-d6, 400MHz)

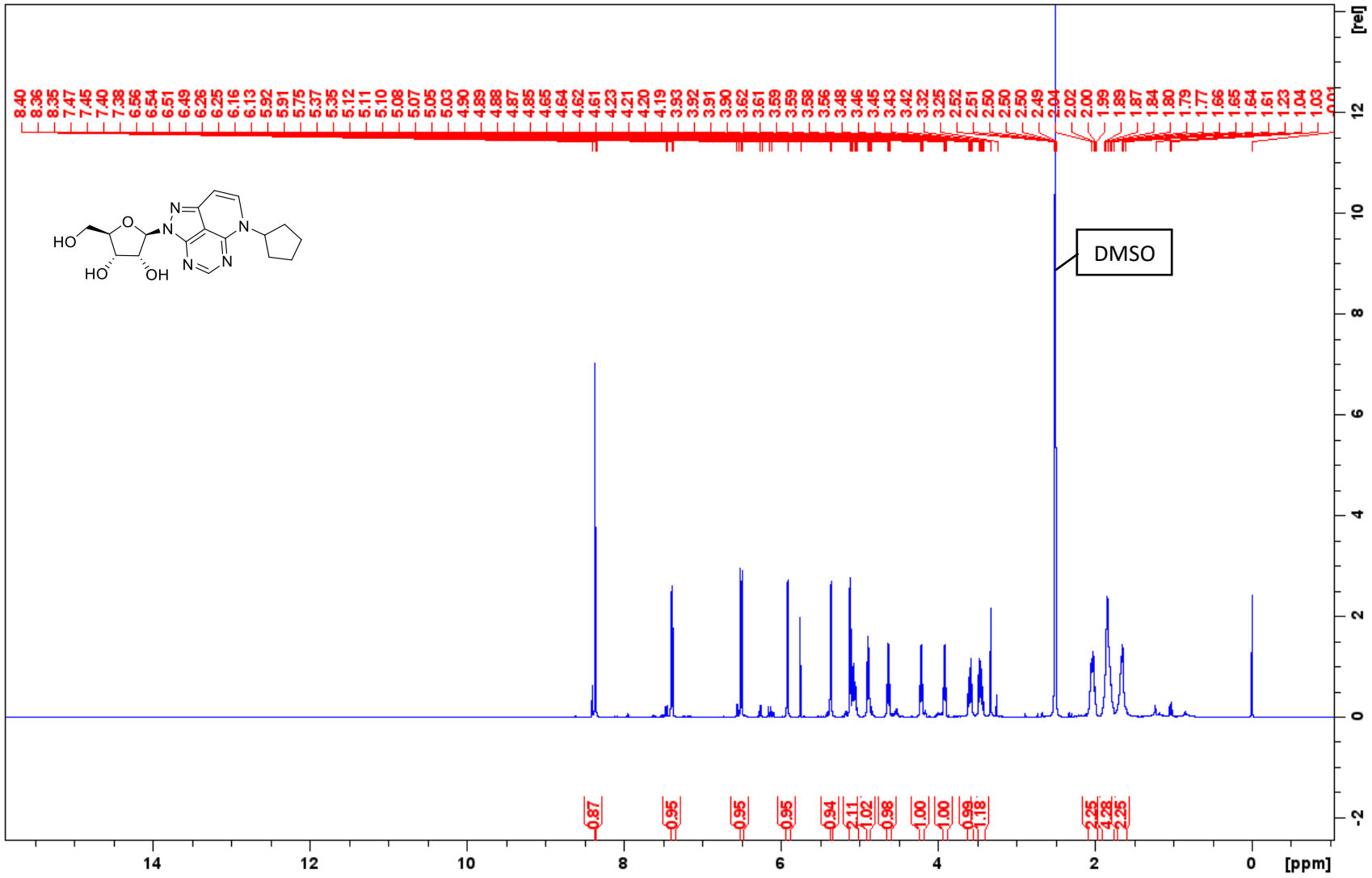

^{13}C NMR (DMSO-d6, 100MHz)

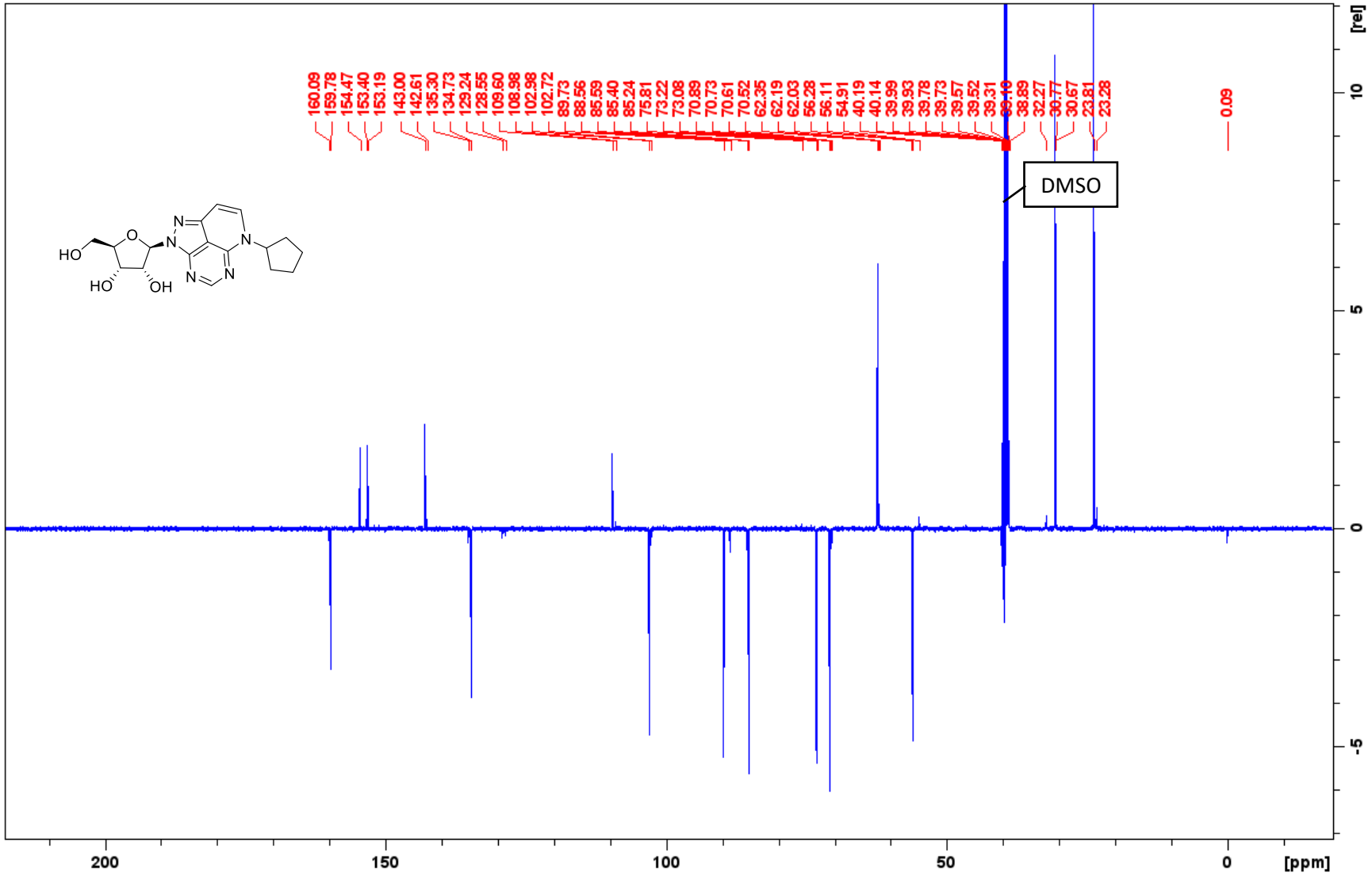

Compound **5-(4-methoxybenzyl)-1-(β-D-ribofuranosyl)-1,2,5,6,8-pentazaacenaphtylene (15c)**

^{1}H NMR (DMSO-d6, 400MHz)

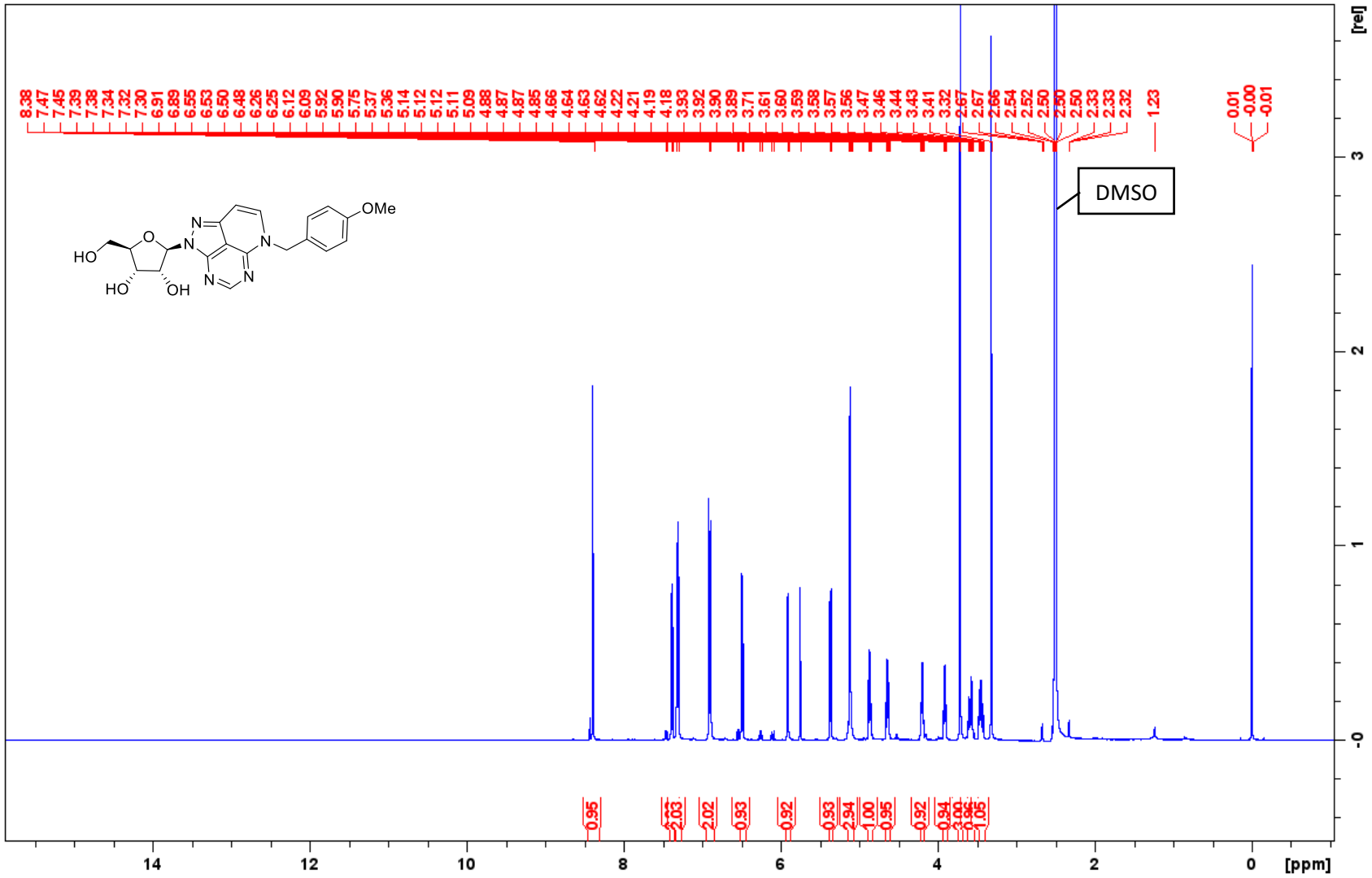

^{13}C NMR (DMSO-d6, 100MHz)

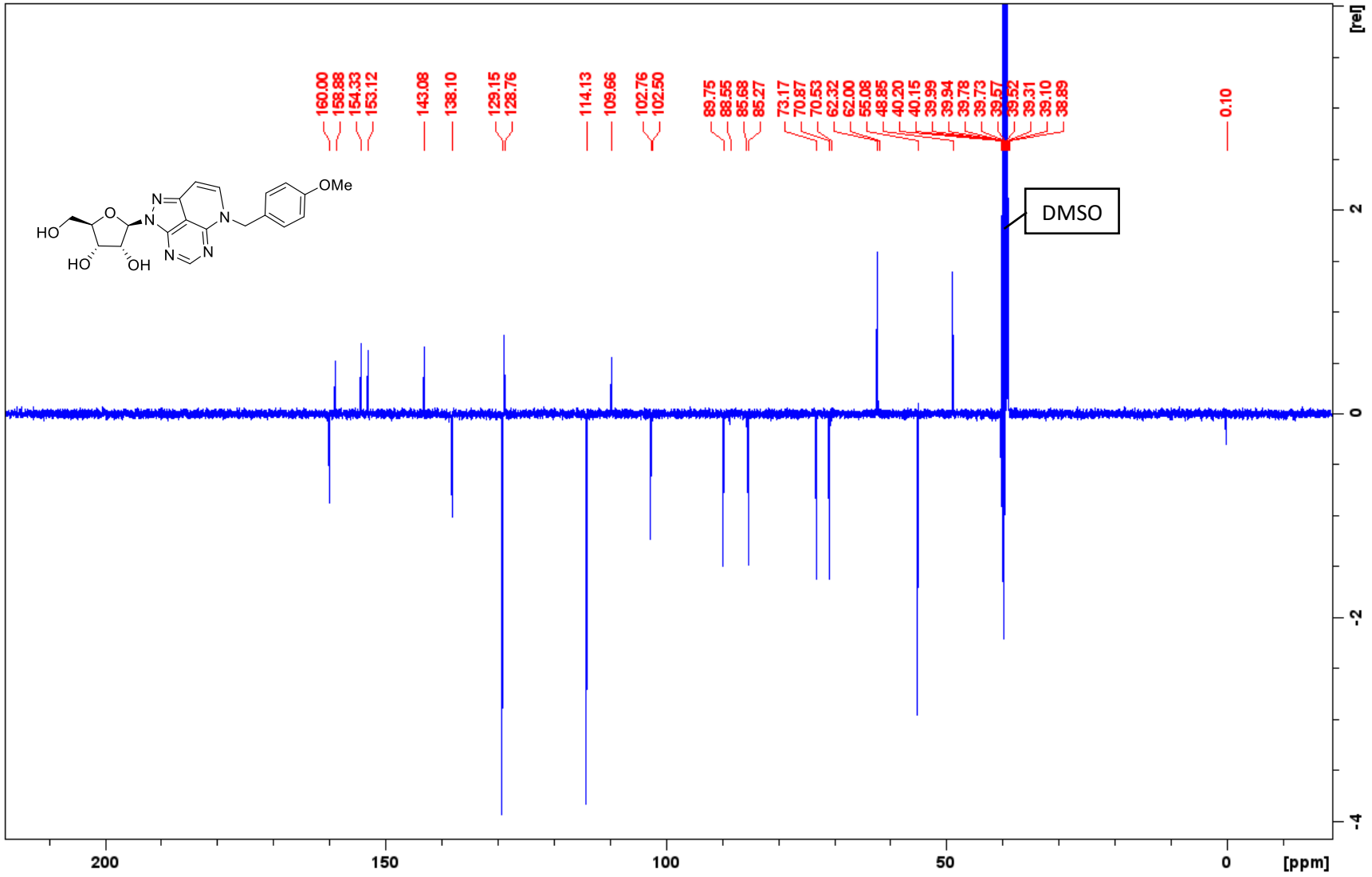

Compound **5-methyl-1-(β-D-ribofuranosyl)-1,2,5,6,8-pentazaacenaphtylene (15d)**

^{1}H NMR (DMSO-d6, 400MHz)

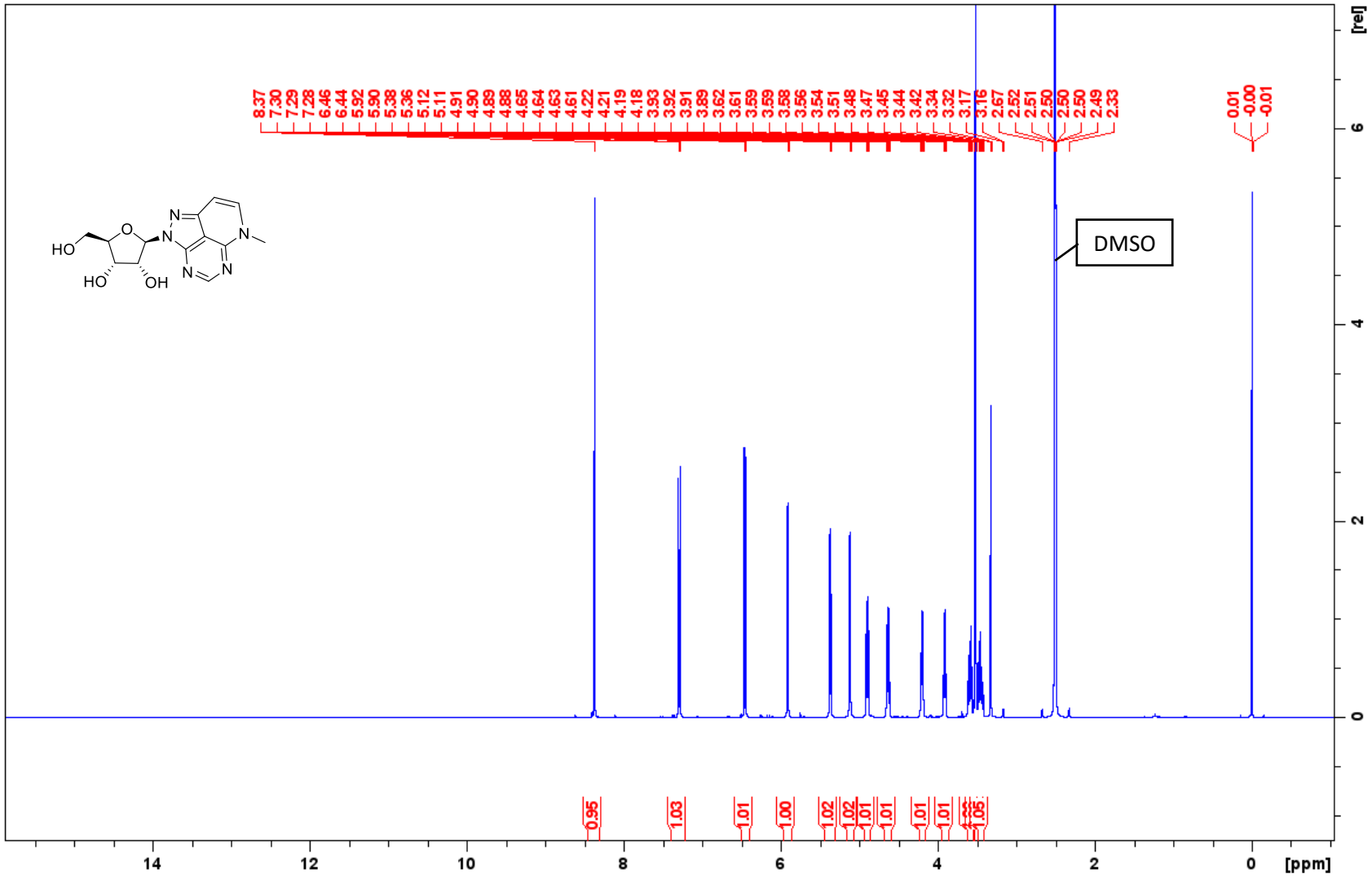

^{13}C NMR (DMSO-d6, 100MHz)

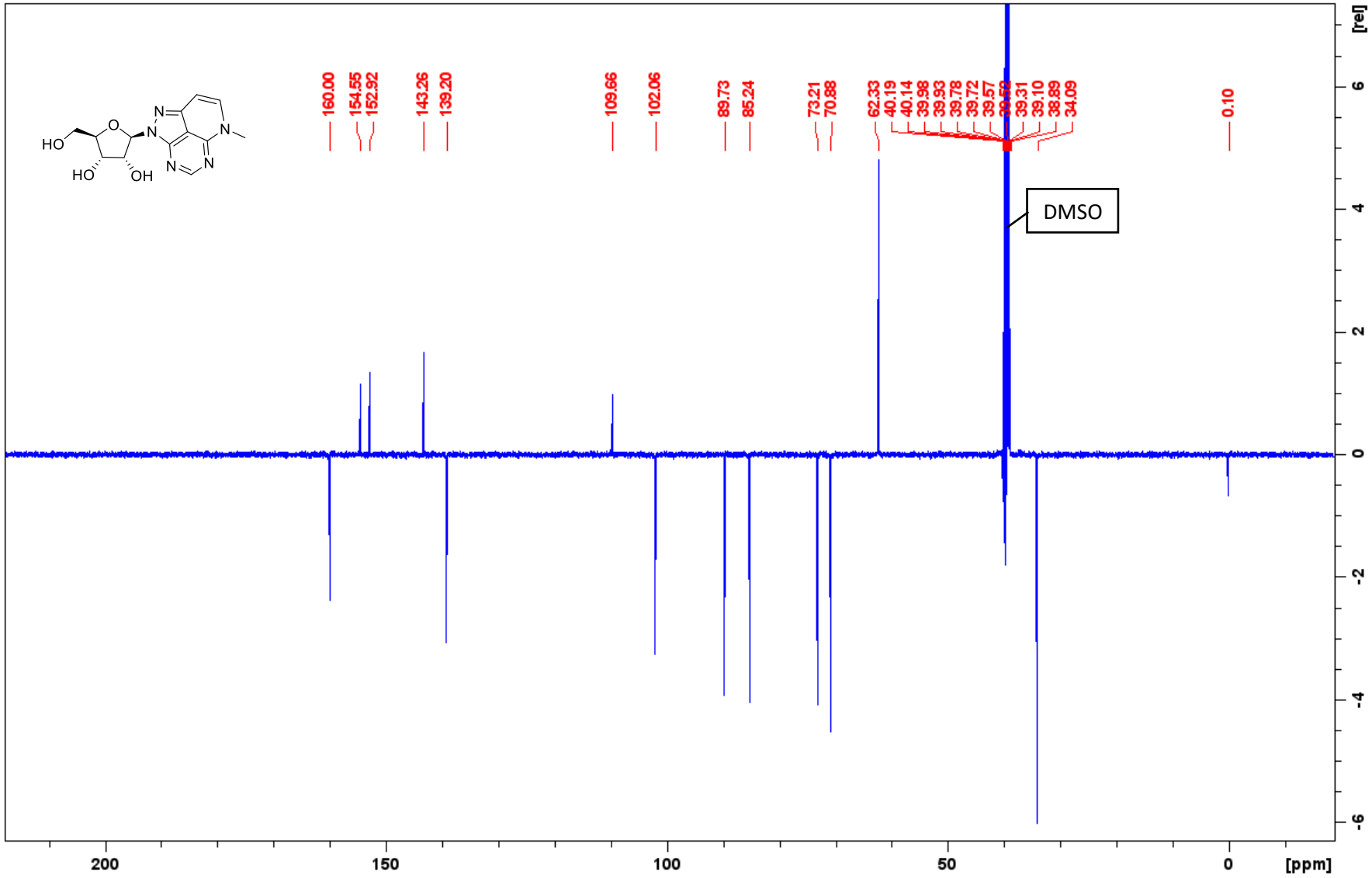

Compound **1-(β-D-ribofuranosyl)-5-thia-1,2,6,8-tetraazaacenaphtylene (29)**

^{1}H NMR (DMSO-d6, 400MHz)

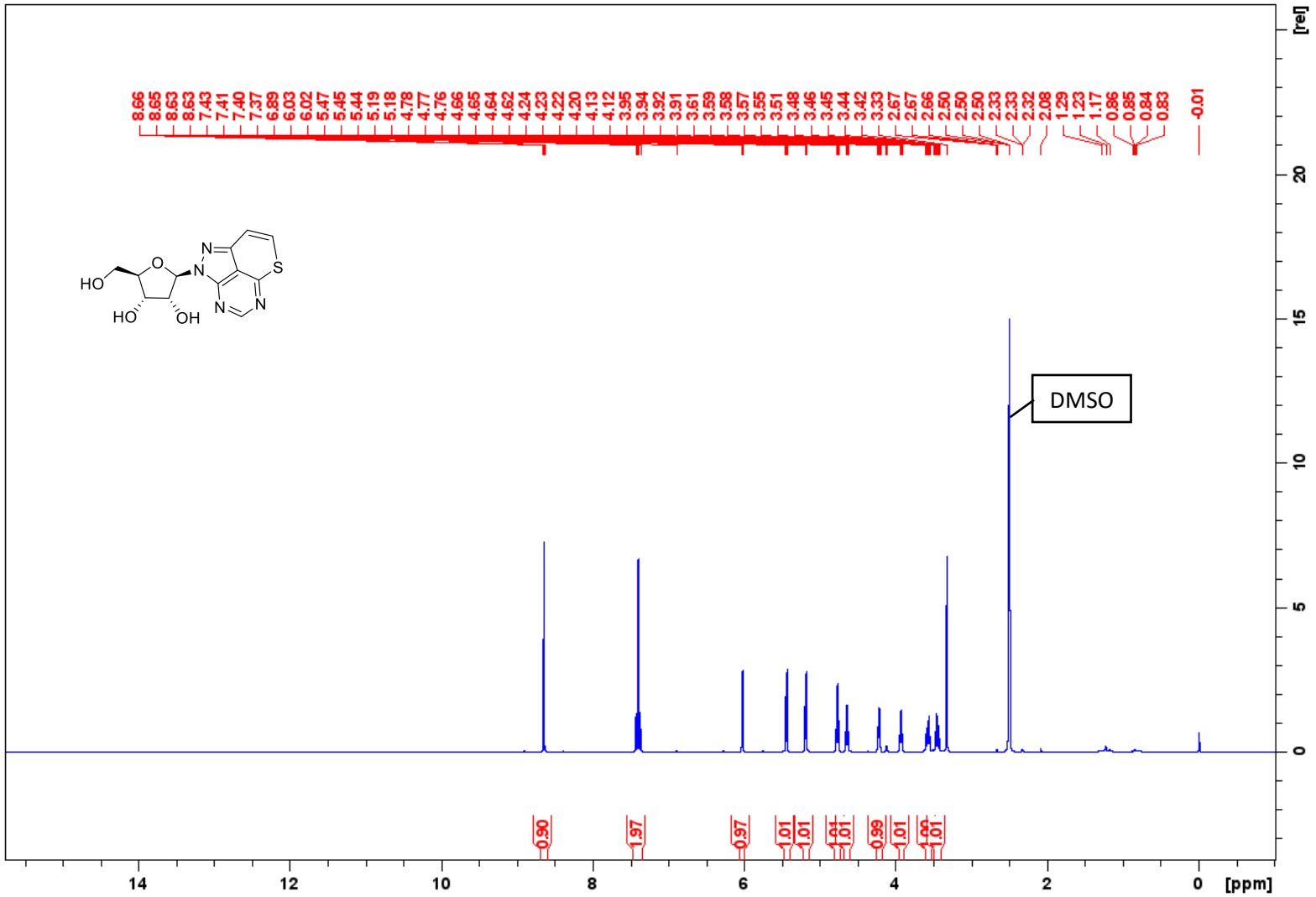

^{13}C NMR (DMSO-d6, 100MHz)

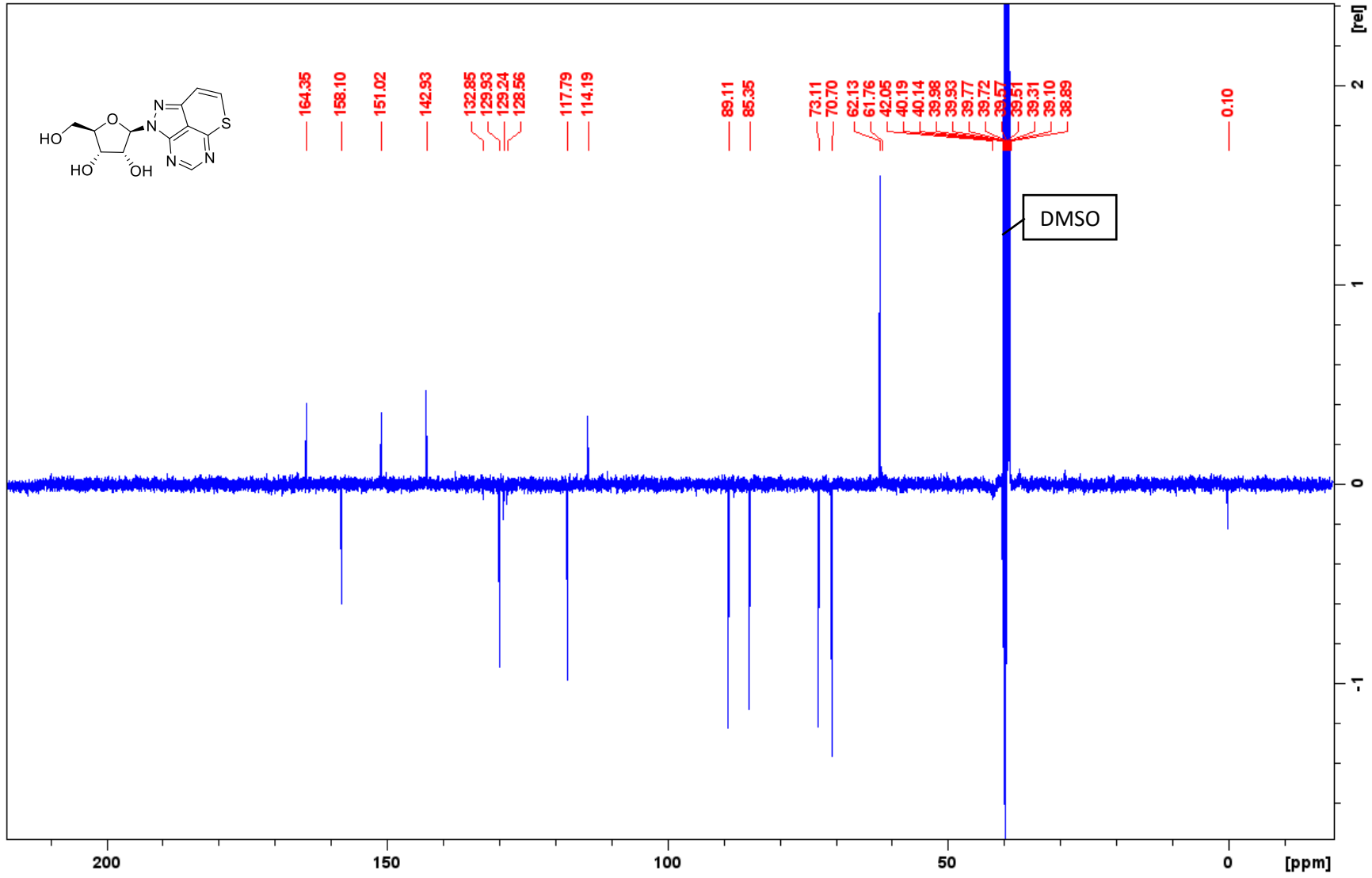

LCMS-traces of final compounds

Compound **7a**

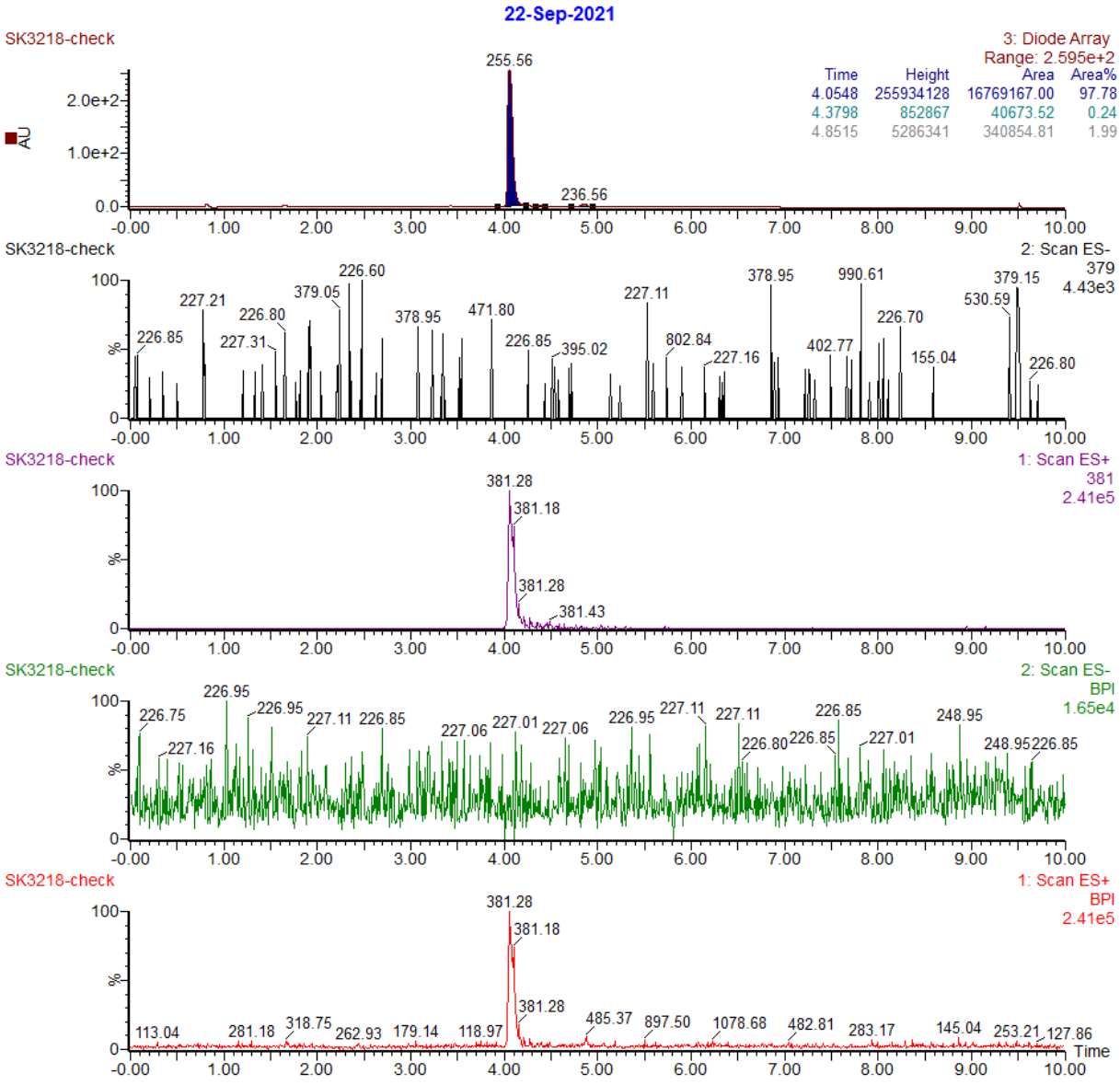

Compound **7b**

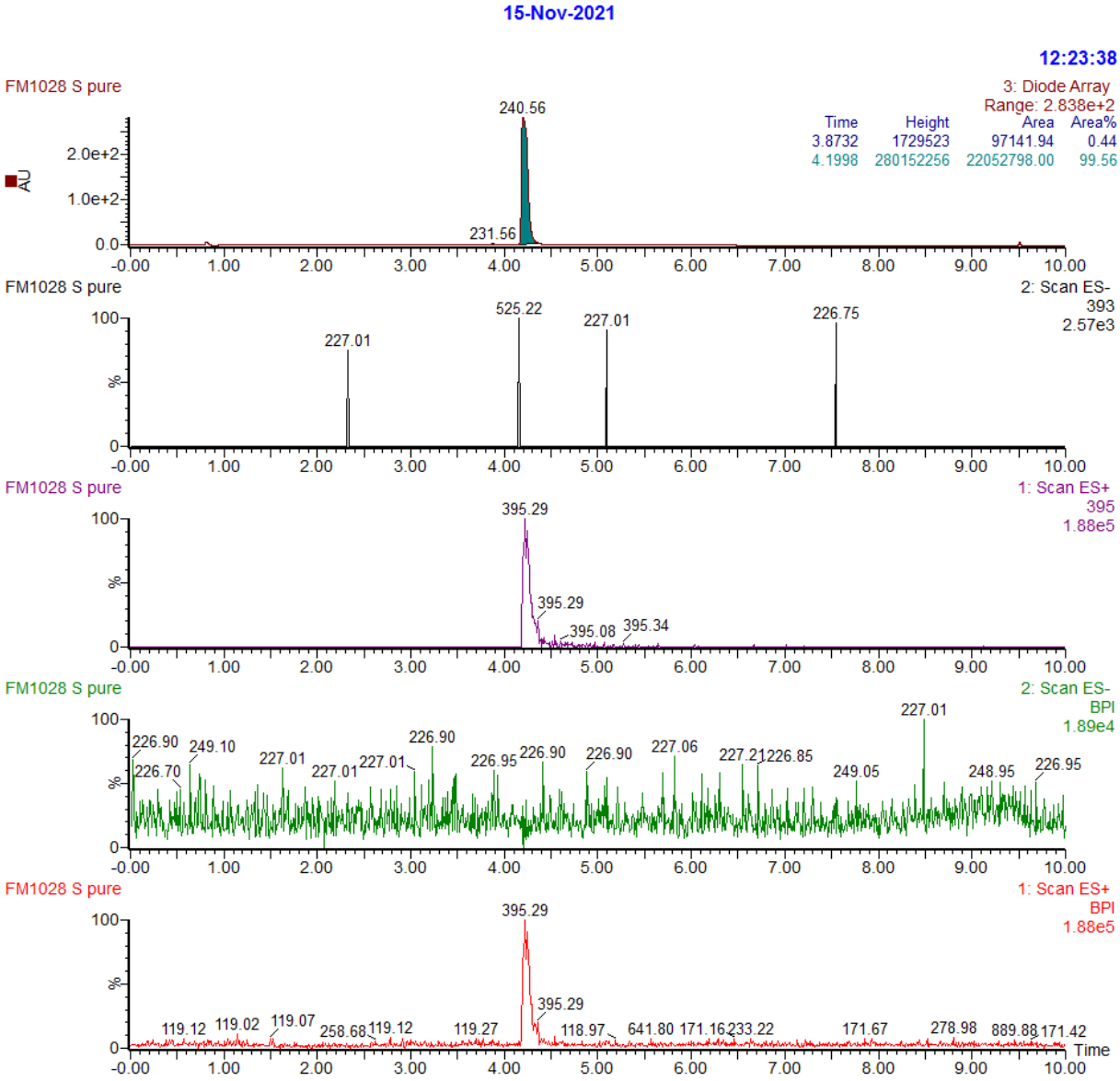
15-Nov-2021
12:23:38
FM1028 S pure
3: Diode Array
Range: 2.838e+2
Time Height Area Area%
3.8732 1729523 97141.94 0.44
4.1998 280152256 22052798.00 99.56
240.56
231.56
AU
FM1028 S pure
2: Scan ES-
393
2.57e3
525.22
227.01
227.01
226.75
FM1028 S pure
1: Scan ES+
395
1.88e5
395.29
395.29
395.08
395.34
FM1028 S pure
2: Scan ES-
BPI
1.89e4
227.01
226.90
249.10
226.70
227.01
227.01
227.01
226.90
226.95
226.90
226.90
227.06
227.21
226.85
249.05
248.95
226.95
FM1028 S pure
1: Scan ES+
BPI
1.88e5
395.29
395.29
119.12
119.02
119.07
258.68
119.12
119.27
118.97
641.80
171.16
233.22
171.67
278.98
889.88
171.42
Time

Compound **7c**

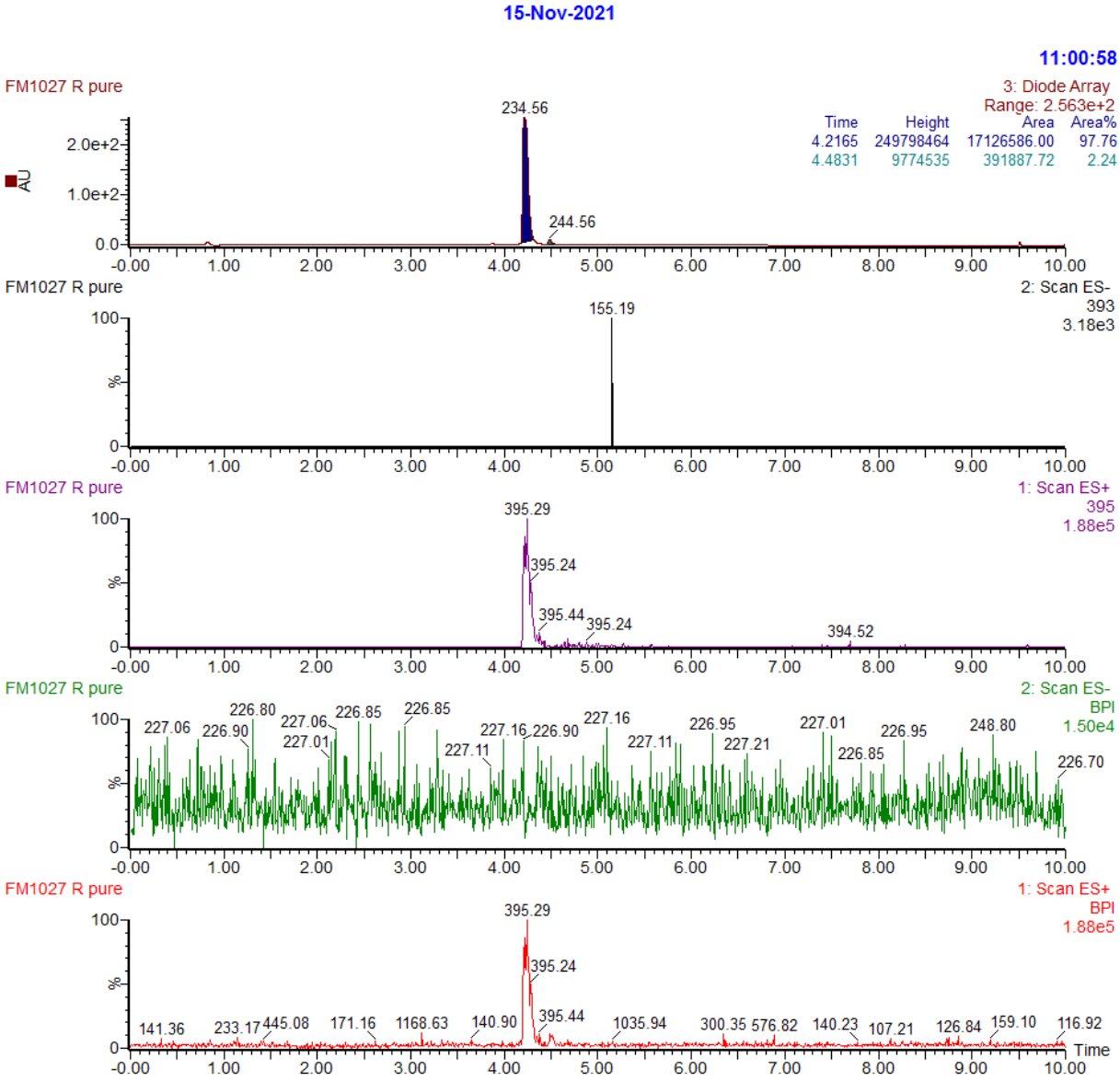
15-Nov-2021
11:00:58
FM1027 R pure
3: Diode Array
Range: 2.563e+2
Time Height Area Area%
4.2165 249798464 17126586.00 97.76
4.4831 9774535 391887.72 2.24
234.56
244.56
AU
FM1027 R pure
2: Scan ES-
393
3.18e3
155.19
FM1027 R pure
1: Scan ES+
395
1.88e5
395.29
395.24
395.44
395.24
394.52
FM1027 R pure
2: Scan ES-
BPI
1.50e4
227.06
226.90
226.80
227.06
227.01
226.85
226.85
227.11
227.16
226.90
227.16
227.11
226.95
227.21
227.01
226.85
226.95
248.80
226.70
FM1027 R pure
1: Scan ES+
BPI
1.88e5
395.29
395.24
395.44
141.36
233.17
445.08
171.16
1168.63
140.90
1035.94
300.35
576.82
140.23
107.21
126.84
159.10
116.92
Time

Compound **7d**

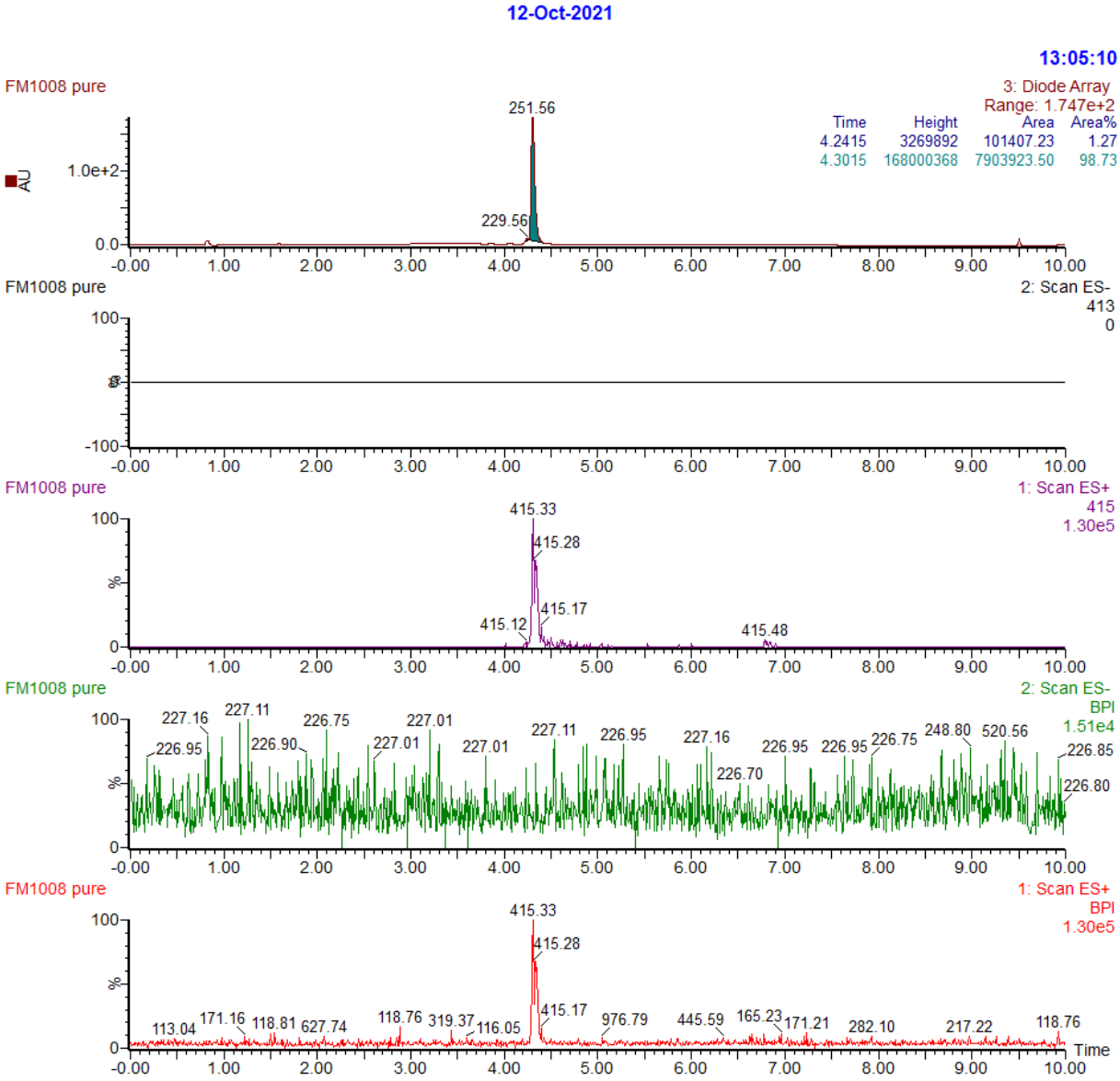
12-Oct-2021
13:05:10
FM1008 pure
3: Diode Array
Range: 1.747e+2
Time Height Area Area%
4.2415 3269892 101407.23 1.27
4.3015 168000368 7903923.50 98.73
AU
1.0e+2
0.0
251.56
229.56
FM1008 pure
2: Scan ES-
413
0
100
%
-100
FM1008 pure
1: Scan ES+
415
1.30e5
415.33
415.28
415.17
415.12
415.48
FM1008 pure
2: Scan ES-
BPI
1.51e4
227.16
227.11
226.95
226.90
226.75
227.01
227.01
227.01
227.11
226.95
227.16
226.70
226.95
226.95
226.75
248.80
520.56
226.85
226.80
FM1008 pure
1: Scan ES+
BPI
1.30e5
415.33
415.28
415.17
113.04
171.16
118.81
627.74
118.76
319.37
116.05
976.79
445.59
165.23
171.21
282.10
217.22
118.76
Time
-0.00 1.00 2.00 3.00 4.00 5.00 6.00 7.00 8.00 9.00 10.00

Compound **7g**

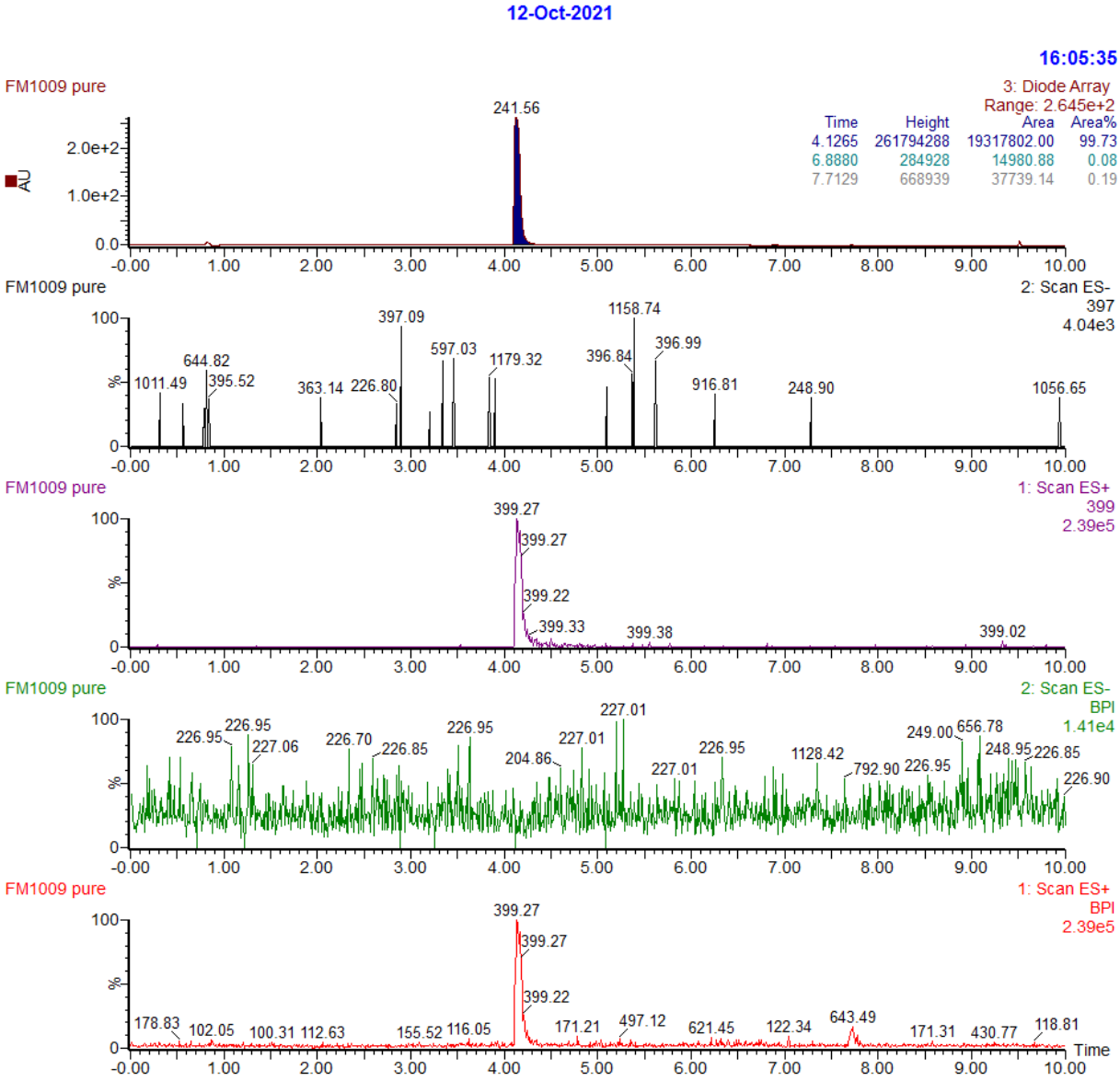
12-Oct-2021
16:05:35
FM1009 pure
3: Diode Array
Range: 2.645e+2
Time Height Area Area%
4.1265 261794288 19317802.00 99.73
6.8880 284928 14980.88 0.08
7.7129 668939 37739.14 0.19
241.56
AU
FM1009 pure
2: Scan ES-
397
4.04e3
397.09
1158.74
597.03
644.82
1179.32
396.84
396.99
1011.49
395.52
363.14
226.80
916.81
248.90
1056.65
FM1009 pure
1: Scan ES+
399
2.39e5
399.27
399.27
399.22
399.33
399.38
399.02
FM1009 pure
2: Scan ES-
BPI
1.41e4
227.01
226.95
226.95
227.06
226.70
226.85
226.95
204.86
227.01
226.95
227.01
1128.42
249.00
656.78
792.90
226.95
248.95
226.85
226.90
FM1009 pure
1: Scan ES+
BPI
2.39e5
399.27
399.27
399.22
178.83
102.05
100.31
112.63
155.52
116.05
171.21
497.12
621.45
122.34
643.49
171.31
430.77
118.81
Time

Compound **7j**

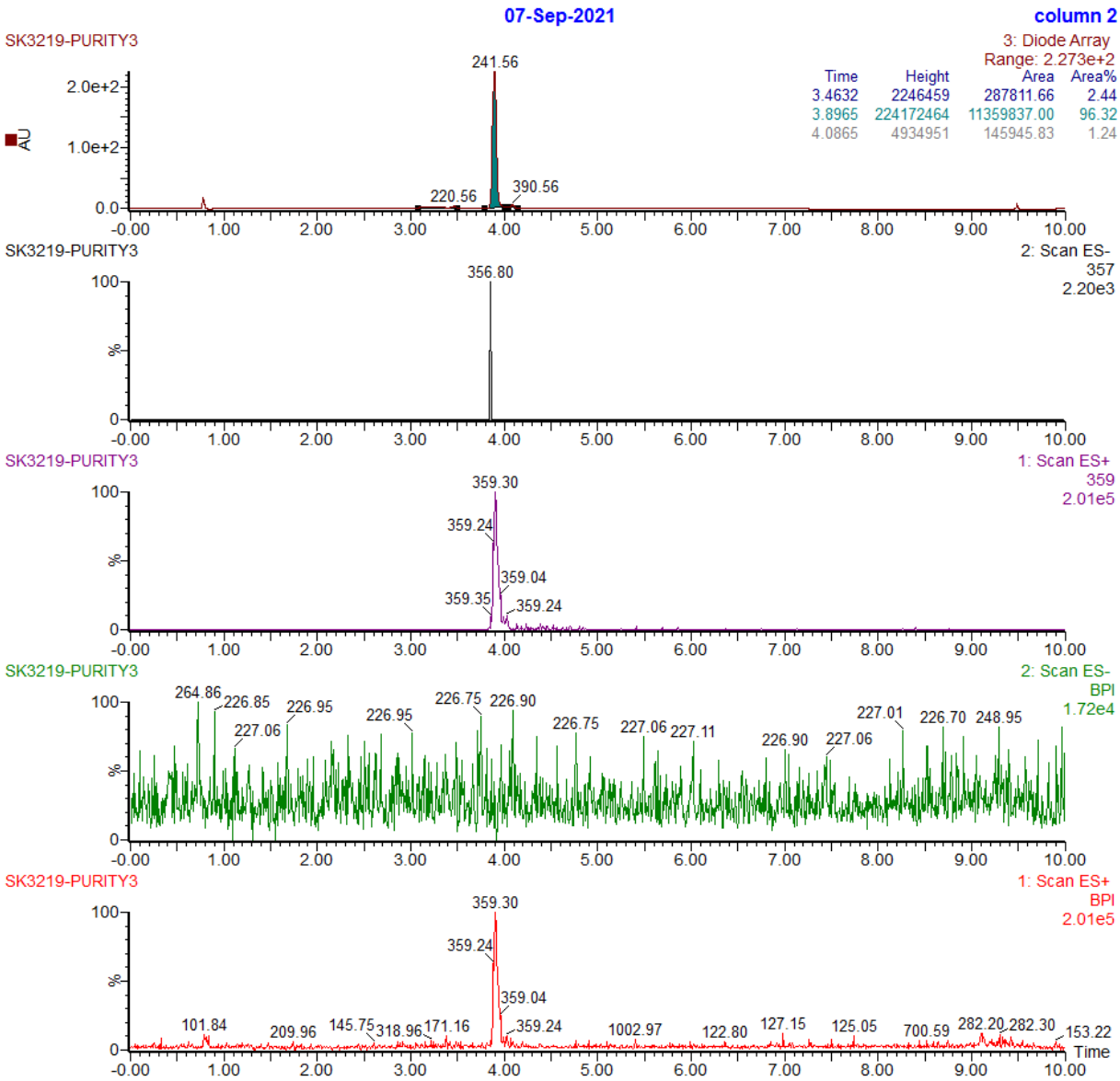
07-Sep-2021
column 2
SK3219-PURITY3
3: Diode Array
Range: 2.273e+2
Time Height Area Area%
3.4632 2246459 287811.66 2.44
3.8965 224172464 11359837.00 96.32
4.0865 4934951 145945.83 1.24
241.56
220.56
390.56
AU
SK3219-PURITY3
2: Scan ES-
357
2.20e3
356.80
SK3219-PURITY3
1: Scan ES+
359
2.01e5
359.30
359.24
359.04
359.35
359.24
SK3219-PURITY3
2: Scan ES-
BPI
1.72e4
264.86
226.85
227.06
226.95
226.95
226.75
226.90
226.75
227.06
227.11
226.90
227.06
227.01
226.70
248.95
SK3219-PURITY3
1: Scan ES+
BPI
2.01e5
359.30
359.24
359.04
101.84
209.96
145.75
318.96
171.16
359.24
1002.97
122.80
127.15
125.05
700.59
282.20
282.30
153.22
Time

Compound **8a**

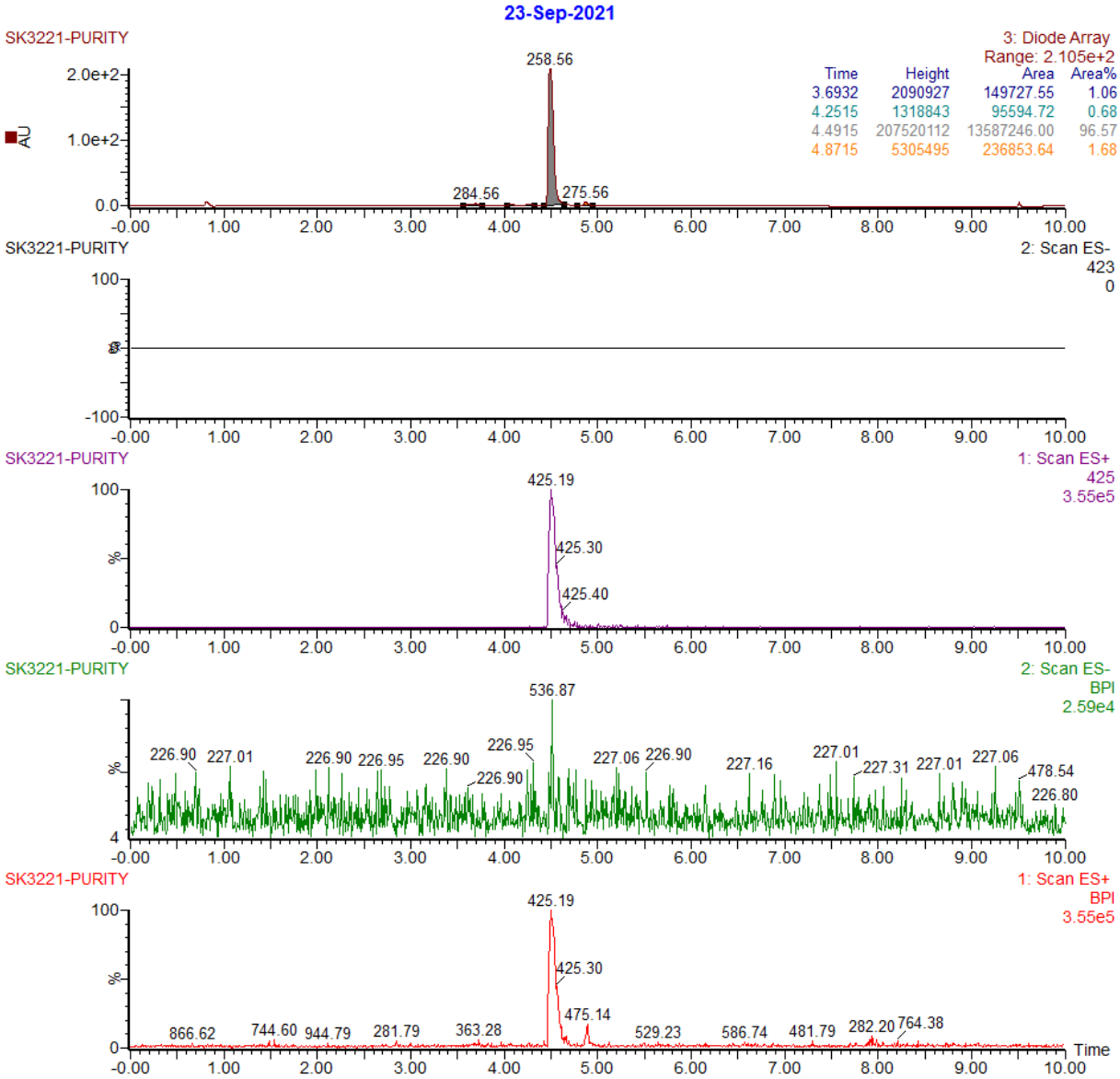
23-Sep-2021
SK3221-PURITY
3: Diode Array
Range: 2.105e+2
Time Height Area Area%
3.6932 2090927 149727.55 1.06
4.2515 1318843 95594.72 0.68
4.4915 207520112 13587246.00 96.57
4.8715 5305495 236853.64 1.68
258.56
284.56
275.56
AU
SK3221-PURITY
2: Scan ES-
423
0
SK3221-PURITY
1: Scan ES+
425
3.55e5
425.19
425.30
425.40
SK3221-PURITY
2: Scan ES-
BPI
2.59e4
536.87
SK3221-PURITY
1: Scan ES+
BPI
3.55e5
425.19
425.30
475.14
Time

Compound **8b**

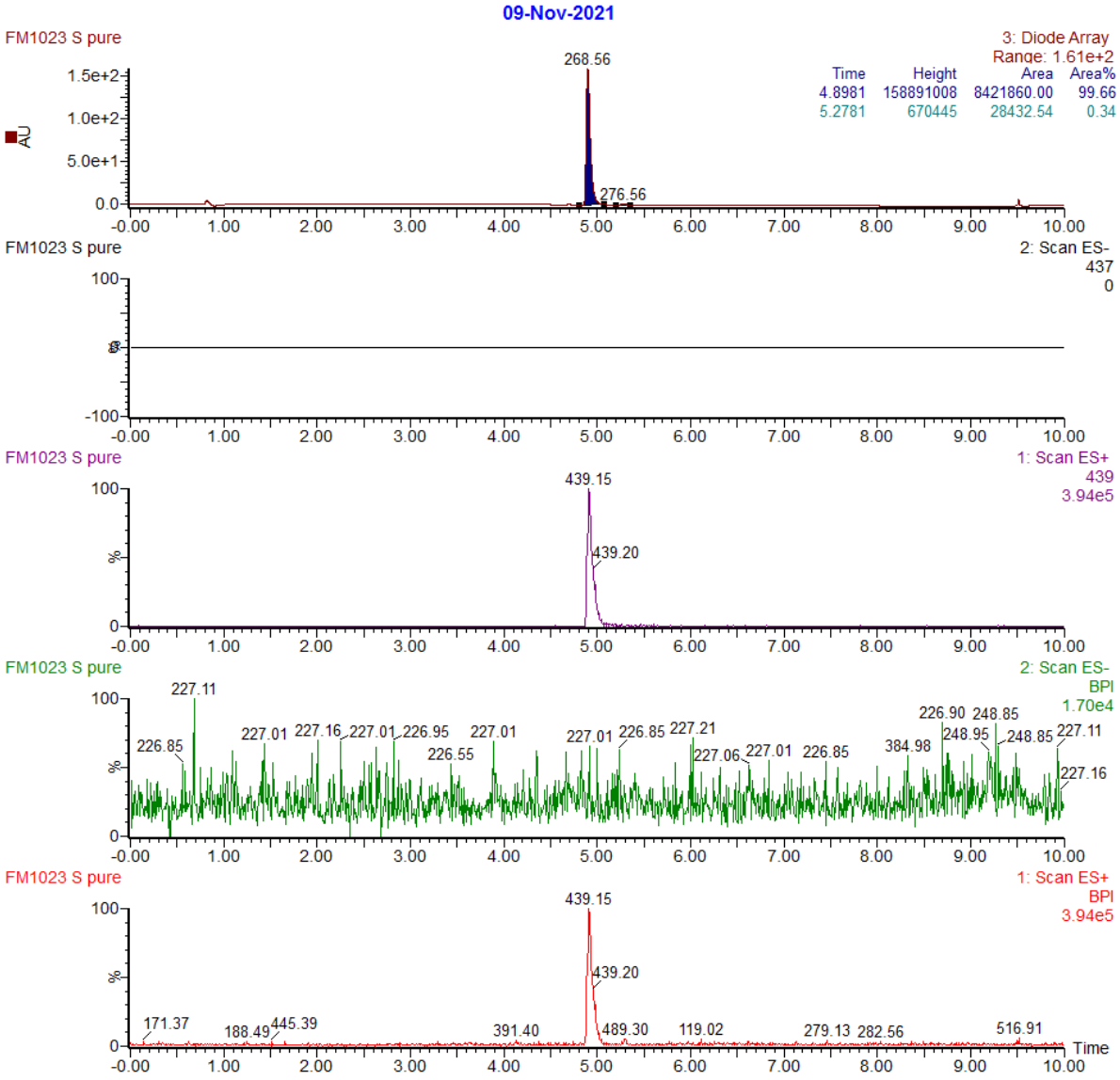
09-Nov-2021
FM1023 S pure
3: Diode Array
Range: 1.61e+2
Time Height Area Area%
4.8981 158891008 8421860.00 99.66
5.2781 670445 28432.54 0.34
268.56
276.56
AU
FM1023 S pure
2: Scan ES-
437
0
FM1023 S pure
1: Scan ES+
439
3.94e5
439.15
439.20
FM1023 S pure
2: Scan ES-
BPI
1.70e4
227.11
226.85
227.01
227.16
227.01
226.95
226.55
227.01
227.01
226.85
227.21
227.06
227.01
226.85
384.98
226.90
248.85
248.95
248.85
227.11
227.16
FM1023 S pure
1: Scan ES+
BPI
3.94e5
439.15
439.20
171.37
188.49
445.39
391.40
489.30
119.02
279.13
282.56
516.91
Time

Compound **8c**

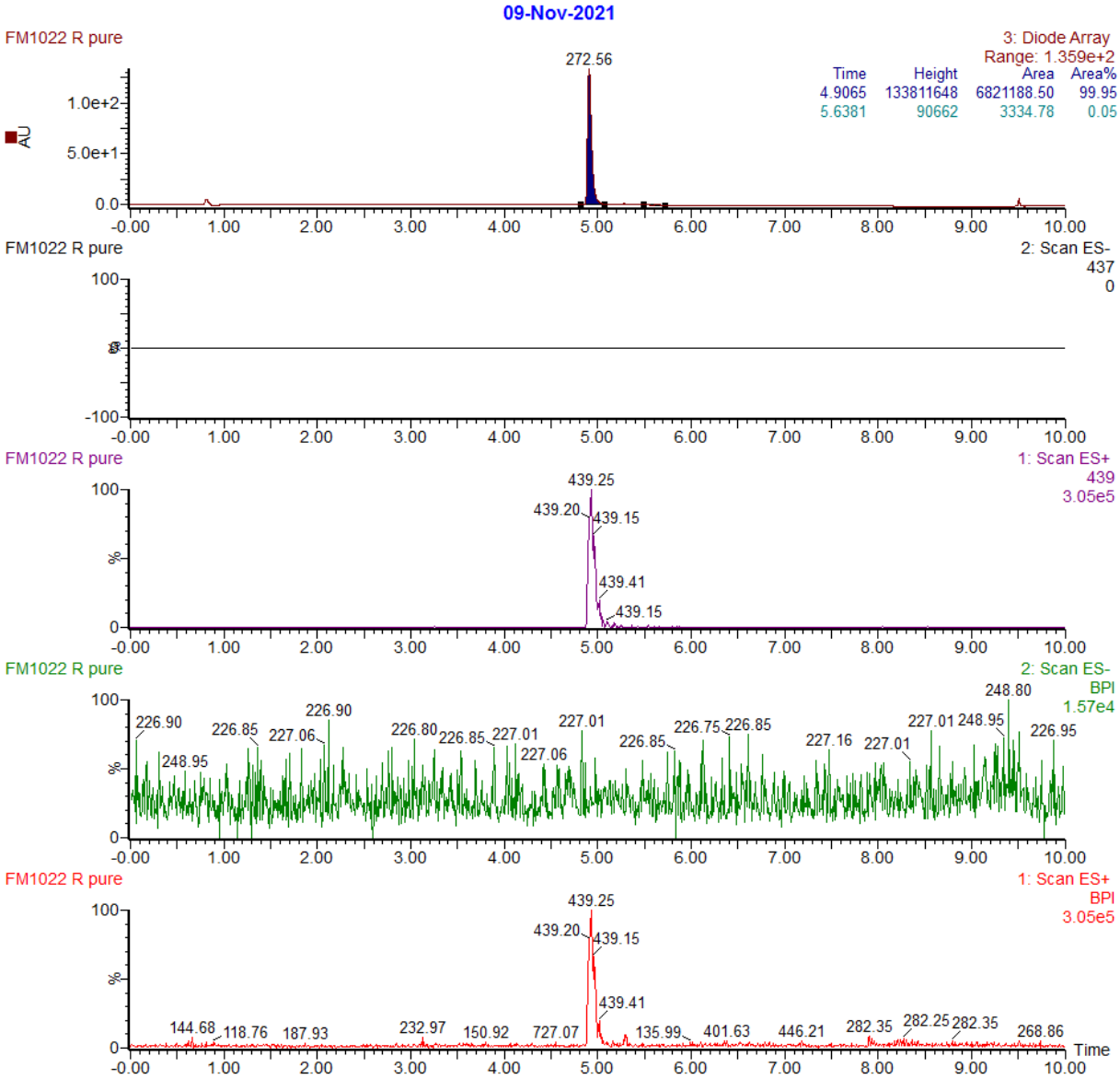
09-Nov-2021
FM1022 R pure
3: Diode Array
Range: 1.359e+2
272.56
Time Height Area Area%
4.9065 133811648 6821188.50 99.95
5.6381 90662 3334.78 0.05
AU
FM1022 R pure
2: Scan ES-
437
0
FM1022 R pure
1: Scan ES+
439
3.05e5
439.25
439.20
439.15
439.41
439.15
FM1022 R pure
2: Scan ES-
BPI
1.57e4
248.80
226.90
226.85
227.06
226.90
226.80
226.85
227.01
227.01
227.06
226.85
226.75
226.85
227.16
227.01
227.01
248.95
226.95
248.95
FM1022 R pure
1: Scan ES+
BPI
3.05e5
439.25
439.20
439.15
439.41
144.68
118.76
187.93
232.97
150.92
727.07
135.99
401.63
446.21
282.35
282.25
282.35
268.86
Time

Compound **8d**

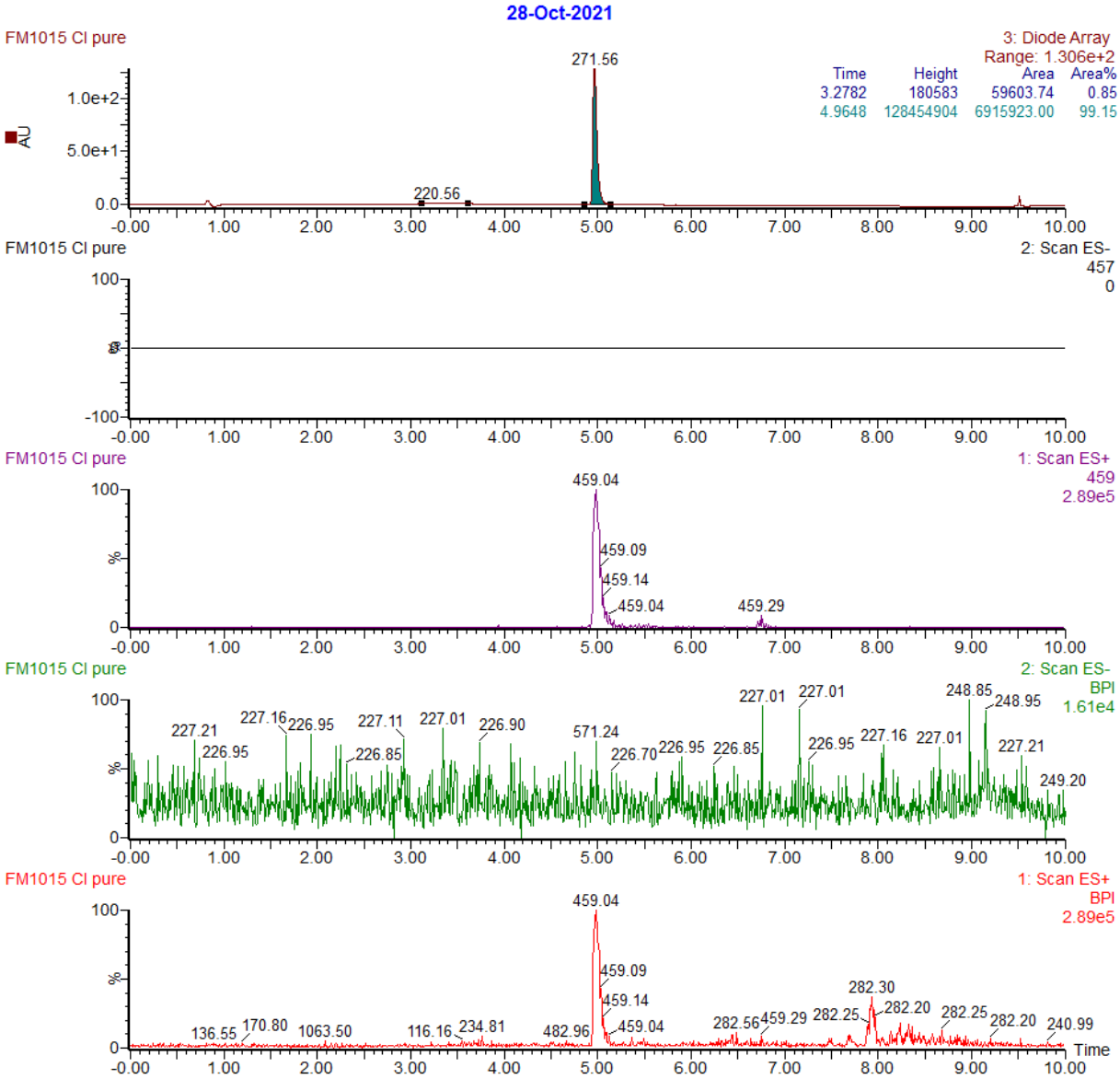
28-Oct-2021
FM1015 Cl pure
3: Diode Array
Range: 1.306e+2
Time Height Area Area%
3.2782 180583 59603.74 0.85
4.9648 128454904 6915923.00 99.15
271.56
220.56
AU
FM1015 Cl pure
2: Scan ES-
457
0
FM1015 Cl pure
1: Scan ES+
459
2.89e5
459.04
459.09
459.14
459.29
FM1015 Cl pure
2: Scan ES-
BPI
1.61e4
227.21
227.16
226.95
227.11
227.01
226.90
571.24
226.70
226.85
248.85
248.95
249.20
FM1015 Cl pure
1: Scan ES+
BPI
2.89e5
459.04
459.09
459.14
459.29
282.30
282.20
282.25
240.99
Time

Compound **8e**

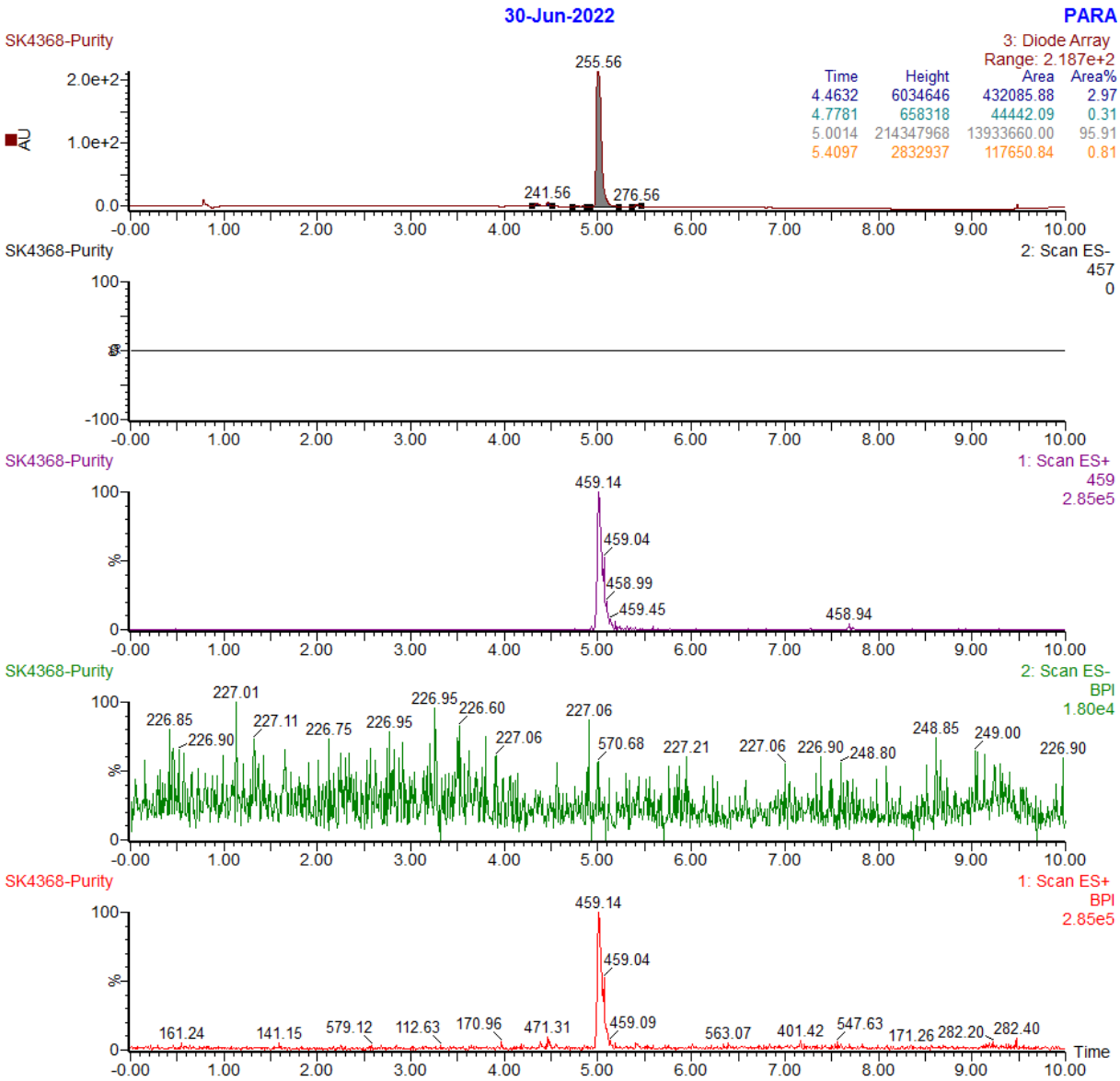
30-Jun-2022
PARA
SK4368-Purity
3: Diode Array
Range: 2.187e+2
Time Height Area Area%
4.4632 6034646 432085.88 2.97
4.7781 658318 44442.09 0.31
5.0014 214347968 13933660.00 95.91
5.4097 2832937 117650.84 0.81
255.56
241.56
276.56
AU
SK4368-Purity
2: Scan ES-
457
0
SK4368-Purity
1: Scan ES+
459
2.85e5
459.14
459.04
458.99
459.45
458.94
SK4368-Purity
2: Scan ES-
BPI
1.80e4
227.01
226.85
226.90
227.11
226.75
226.95
226.95
226.60
227.06
227.06
570.68
227.21
227.06
226.90
248.80
248.85
249.00
226.90
SK4368-Purity
1: Scan ES+
BPI
2.85e5
459.14
459.04
161.24
141.15
579.12
112.63
170.96
471.31
459.09
563.07
401.42
547.63
171.26
282.20
282.40
Time

Compound **8f**

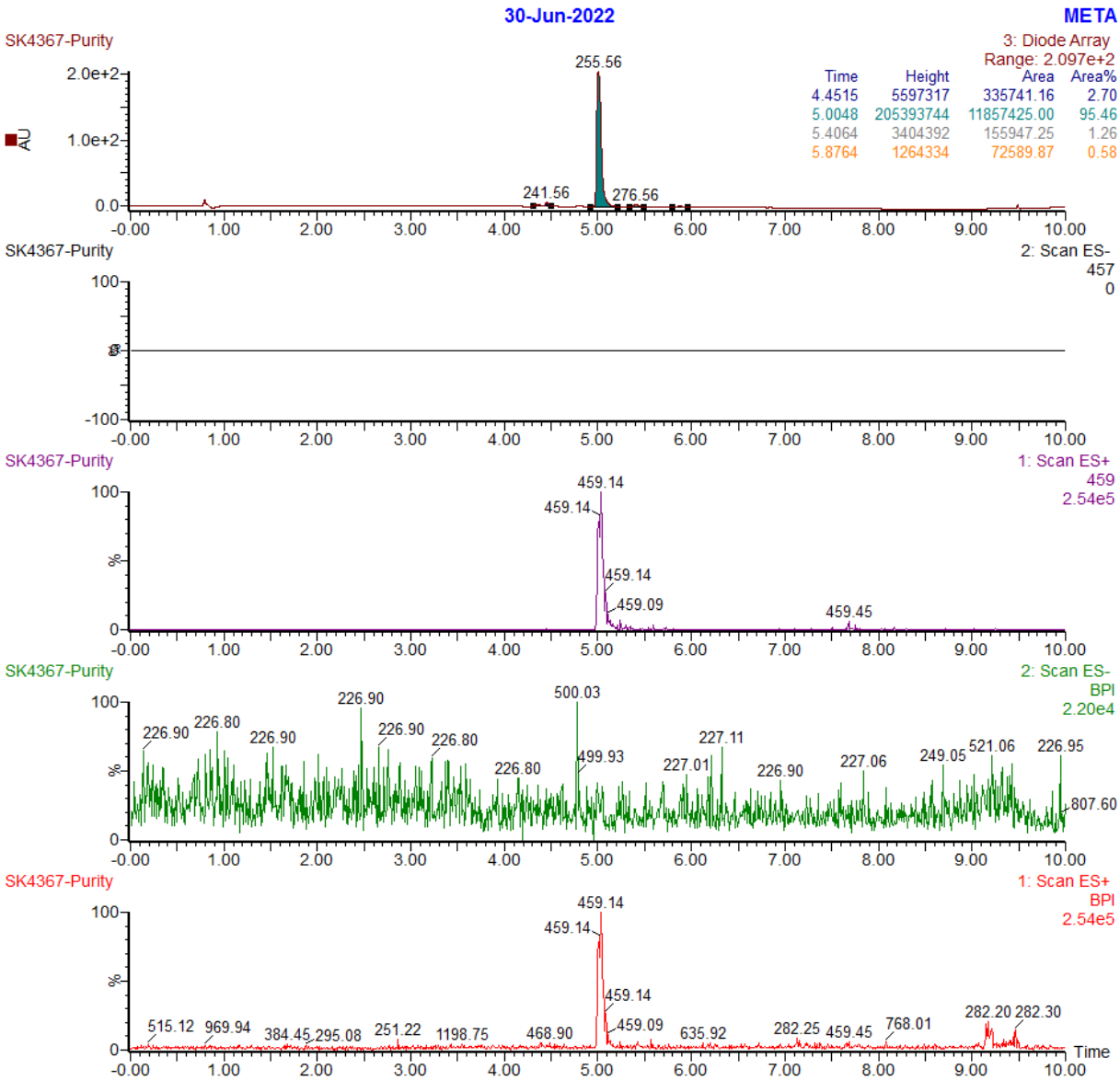
30-Jun-2022
META
SK4367-Purity
3: Diode Array
Range: 2.097e+2
Time Height Area Area%
4.4515 5597317 335741.16 2.70
5.0048 205393744 11857425.00 95.46
5.4064 3404392 155947.25 1.26
5.8764 1264334 72589.87 0.58
255.56
241.56
276.56
AU
SK4367-Purity
2: Scan ES-
457
0
SK4367-Purity
1: Scan ES+
459
2.54e5
459.14
459.14
459.14
459.09
459.45
SK4367-Purity
2: Scan ES-
BPI
2.20e4
226.90
226.80
226.90
226.90
226.80
226.80
500.03
499.93
227.01
227.11
226.90
227.06
249.05
521.06
226.95
807.60
SK4367-Purity
1: Scan ES+
BPI
2.54e5
459.14
459.14
459.14
459.09
515.12
969.94
384.45
295.08
251.22
1198.75
468.90
635.92
282.25
459.45
768.01
282.20
282.30
Time

Compound **8g**

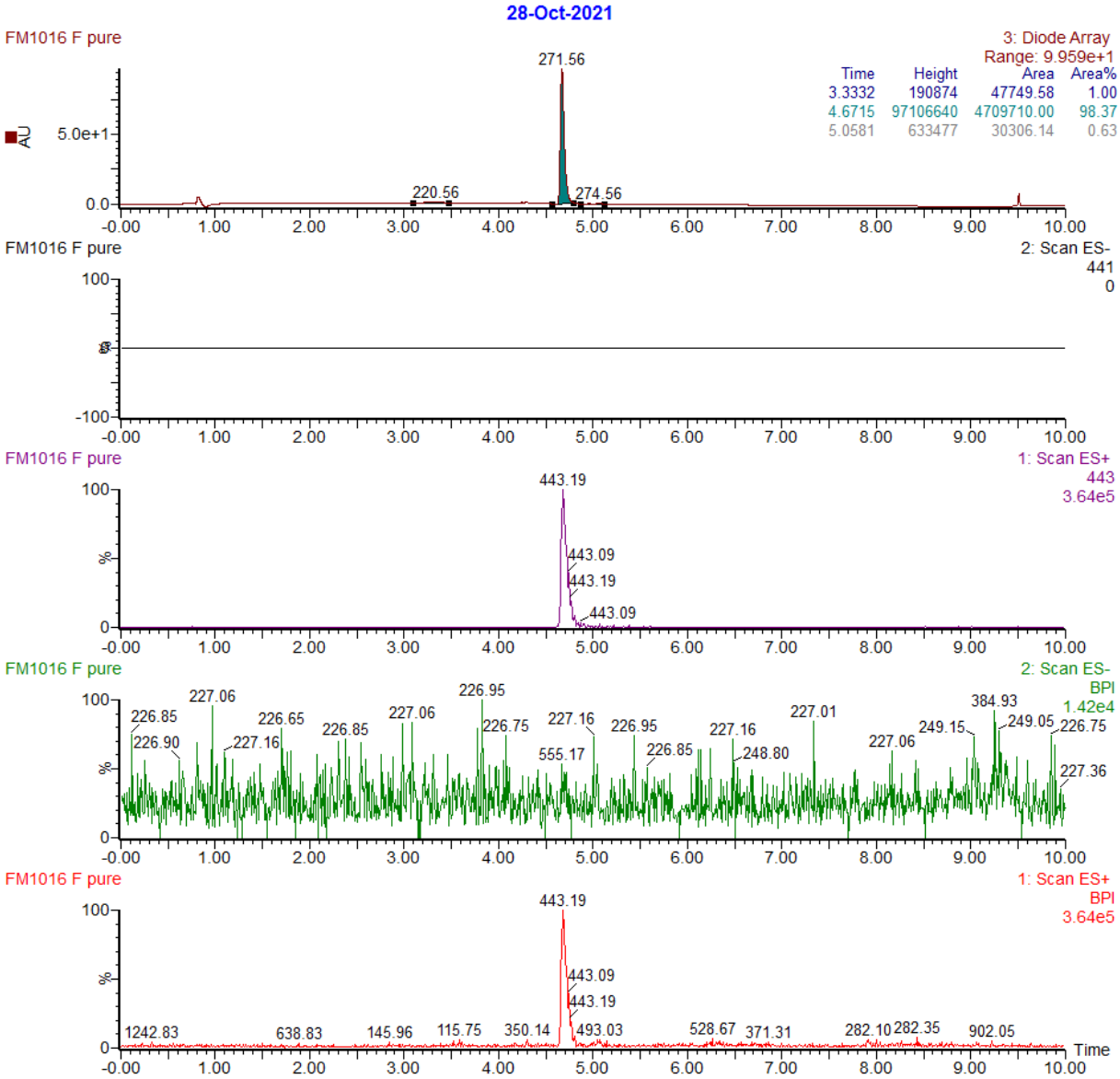
28-Oct-2021
FM1016 F pure
3: Diode Array
Range: 9.959e+1
Time Height Area Area%
3.3332 190874 47749.58 1.00
4.6715 97106640 4709710.00 98.37
5.0581 633477 30306.14 0.63
271.56
220.56
274.56
AU
5.0e+1
0.0
FM1016 F pure
2: Scan ES-
441
0
FM1016 F pure
1: Scan ES+
443
3.64e5
443.19
443.09
443.19
443.09
FM1016 F pure
2: Scan ES-
BPI
1.42e4
226.85
227.06
226.90
227.16
226.65
226.85
227.06
226.95
226.75
227.16
555.17
226.95
226.85
227.16
248.80
227.01
227.06
249.15
384.93
249.05
226.75
227.36
FM1016 F pure
1: Scan ES+
BPI
3.64e5
443.19
443.09
443.19
1242.83
638.83
145.96
115.75
350.14
493.03
528.67
371.31
282.10
282.35
902.05
Time

Compound **8h**

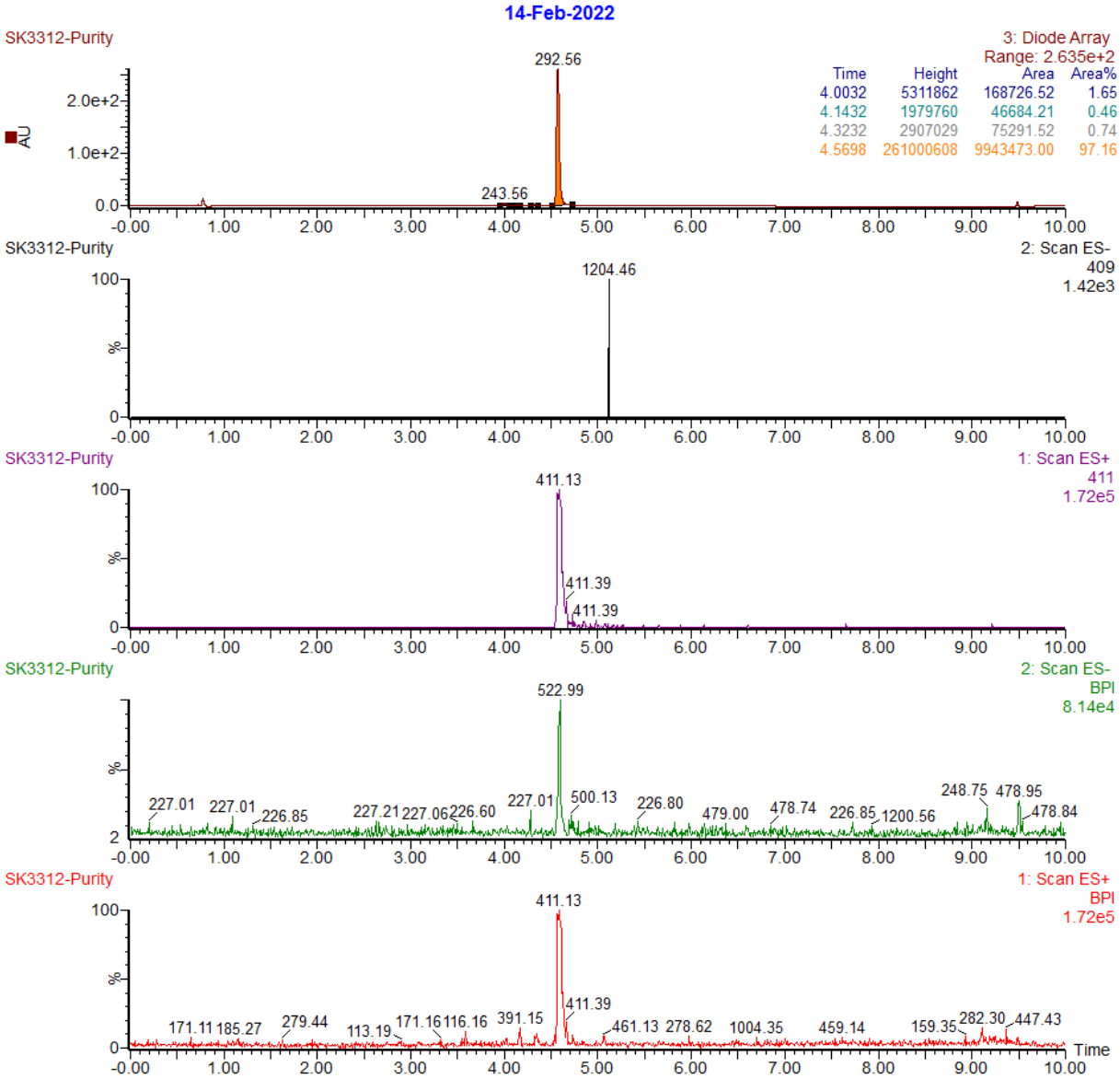
14-Feb-2022
SK3312-Purity
3: Diode Array
Range: 2.635e+2
Time Height Area Area%
4.0032 5311862 168726.52 1.65
4.1432 1979760 46684.21 0.46
4.3232 2907029 75291.52 0.74
4.5698 261000608 9943473.00 97.16
292.56
243.56
AU
2.0e+2
1.0e+2
0.0
SK3312-Purity
2: Scan ES-
409
1.42e3
1204.46
SK3312-Purity
1: Scan ES+
411
1.72e5
411.13
411.39
411.39
SK3312-Purity
2: Scan ES-
BPI
8.14e4
522.99
227.01
227.01
226.85
227.21
227.06
226.60
227.01
500.13
226.80
479.00
478.74
226.85
1200.56
248.75
478.95
478.84
SK3312-Purity
1: Scan ES+
BPI
1.72e5
411.13
411.39
171.11
185.27
279.44
113.19
171.16
116.16
391.15
461.13
278.62
1004.35
459.14
159.35
282.30
447.43
Time
%
100
0
2
-0.00
1.00
2.00
3.00
4.00
5.00
6.00
7.00
8.00
9.00
10.00

Compound **8i**

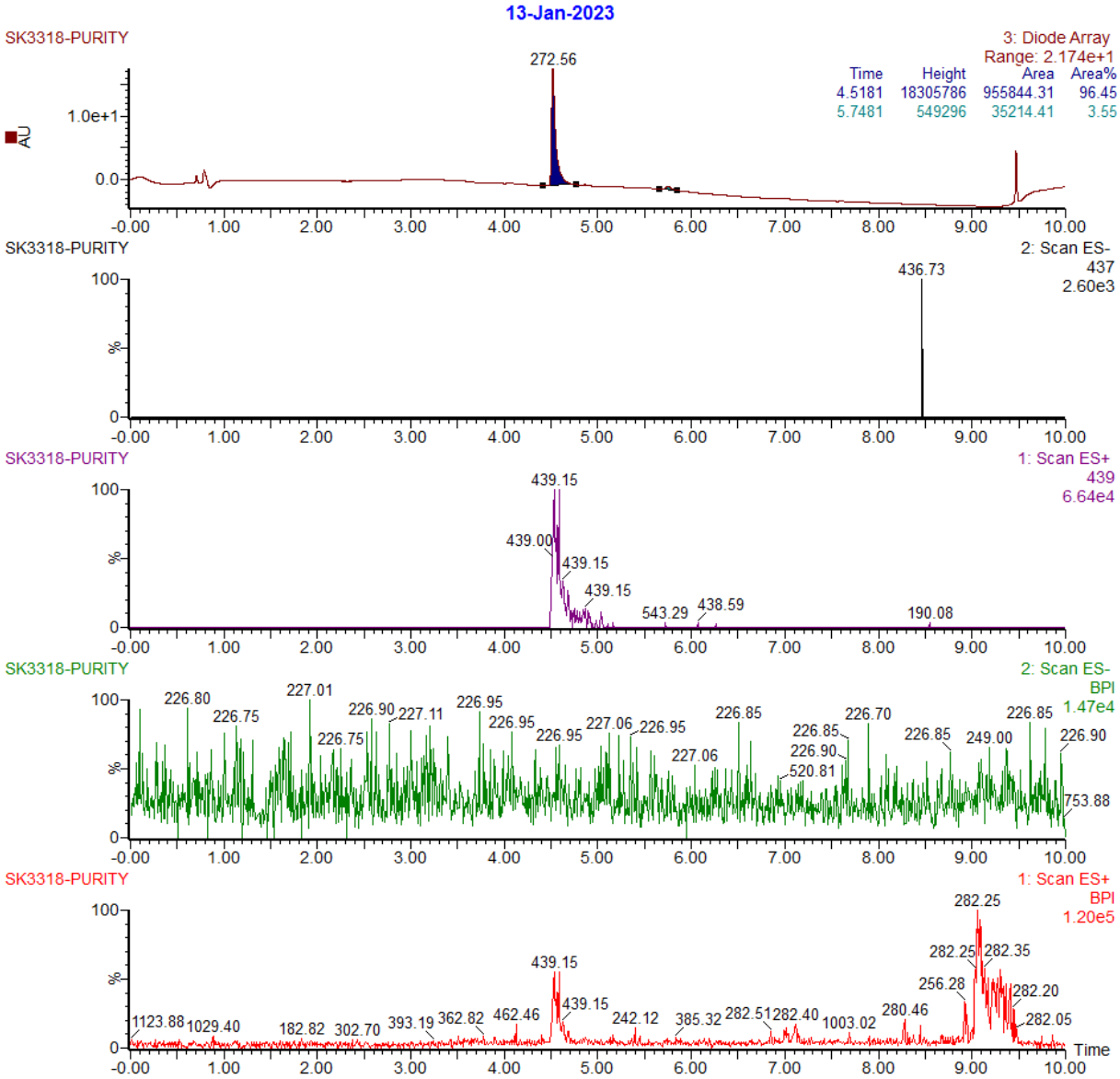
13-Jan-2023
SK3318-PURITY
3: Diode Array
Range: 2.174e+1
Time Height Area Area%
4.5181 18305786 955844.31 96.45
5.7481 549296 35214.41 3.55
272.56
AU
1.0e+1
0.0
SK3318-PURITY
2: Scan ES-
437
2.60e3
436.73
SK3318-PURITY
1: Scan ES+
439
6.64e4
439.15
439.00
439.15
439.15
543.29
438.59
190.08
SK3318-PURITY
2: Scan ES-
BPI
1.47e4
226.80
226.75
227.01
226.75
226.90
227.11
226.95
226.95
226.95
227.06
226.95
227.06
226.85
226.85
226.90
520.81
226.70
226.85
249.00
226.85
226.90
753.88
SK3318-PURITY
1: Scan ES+
BPI
1.20e5
282.25
282.25
282.35
256.28
282.20
282.05
439.15
439.15
1123.88
1029.40
182.82
302.70
393.19
362.82
462.46
242.12
385.32
282.51
282.40
1003.02
280.46
Time

Compound **8j**

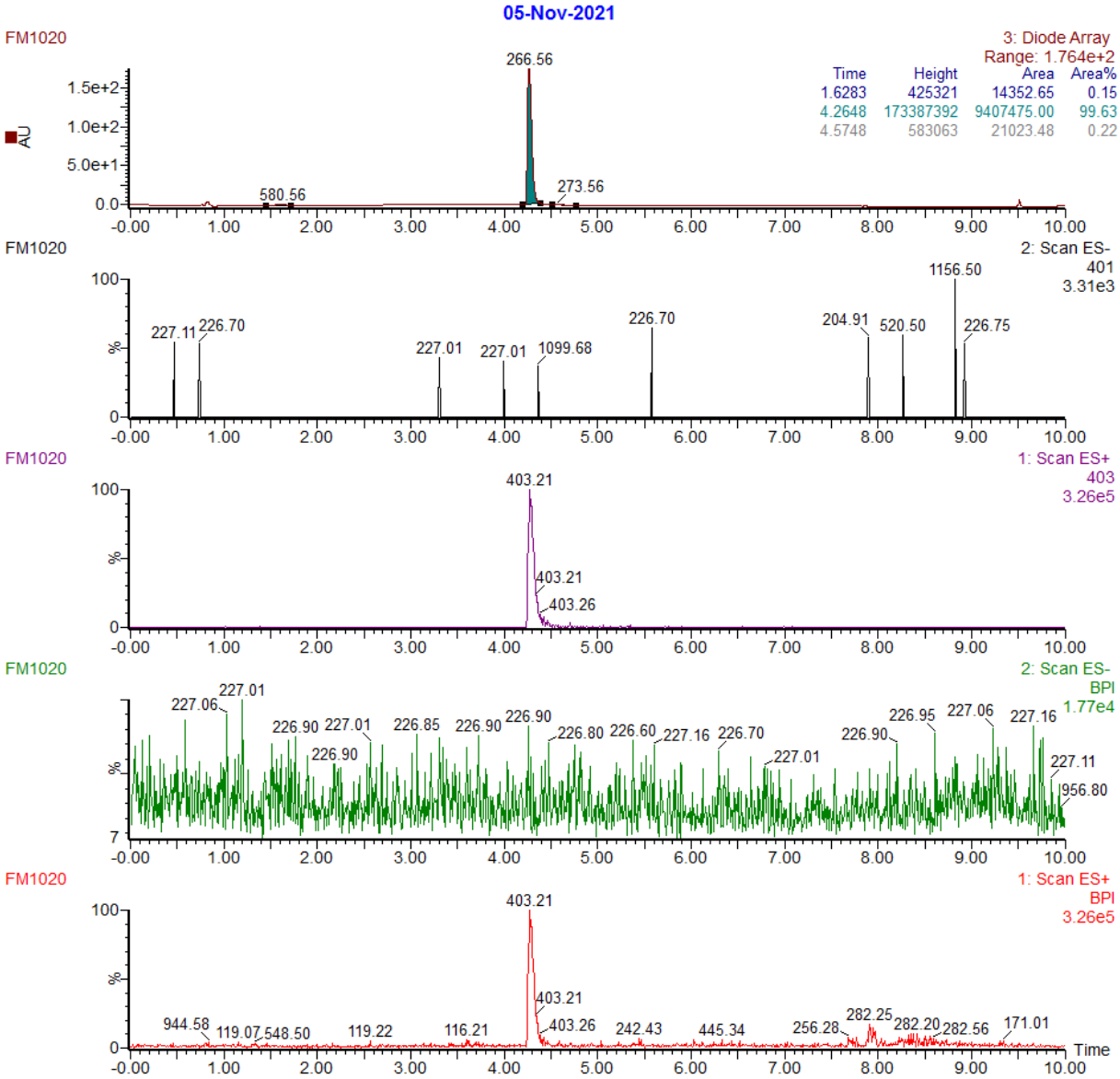
05-Nov-2021
FM1020
3: Diode Array
Range: 1.764e+2
Time Height Area Area%
1.6283 425321 14352.65 0.15
4.2648 173387392 9407475.00 99.63
4.5748 583063 21023.48 0.22
AU
266.56
580.56
273.56
FM1020
2: Scan ES-
401
3.31e3
227.11 226.70 227.01 227.01 1099.68 226.70 204.91 520.50 1156.50 226.75
FM1020
1: Scan ES+
403
3.26e5
403.21 403.21 403.26
FM1020
2: Scan ES-
BPI
1.77e4
227.06 227.01 226.90 227.01 226.85 226.90 226.90 226.80 226.60 227.16 226.70 227.01 226.90 226.95 227.06 227.16 227.11 956.80
FM1020
1: Scan ES+
BPI
3.26e5
403.21 403.21 403.26 944.58 119.07 548.50 119.22 116.21 242.43 445.34 256.28 282.25 282.20 282.56 171.01
Time

Compound **15a**

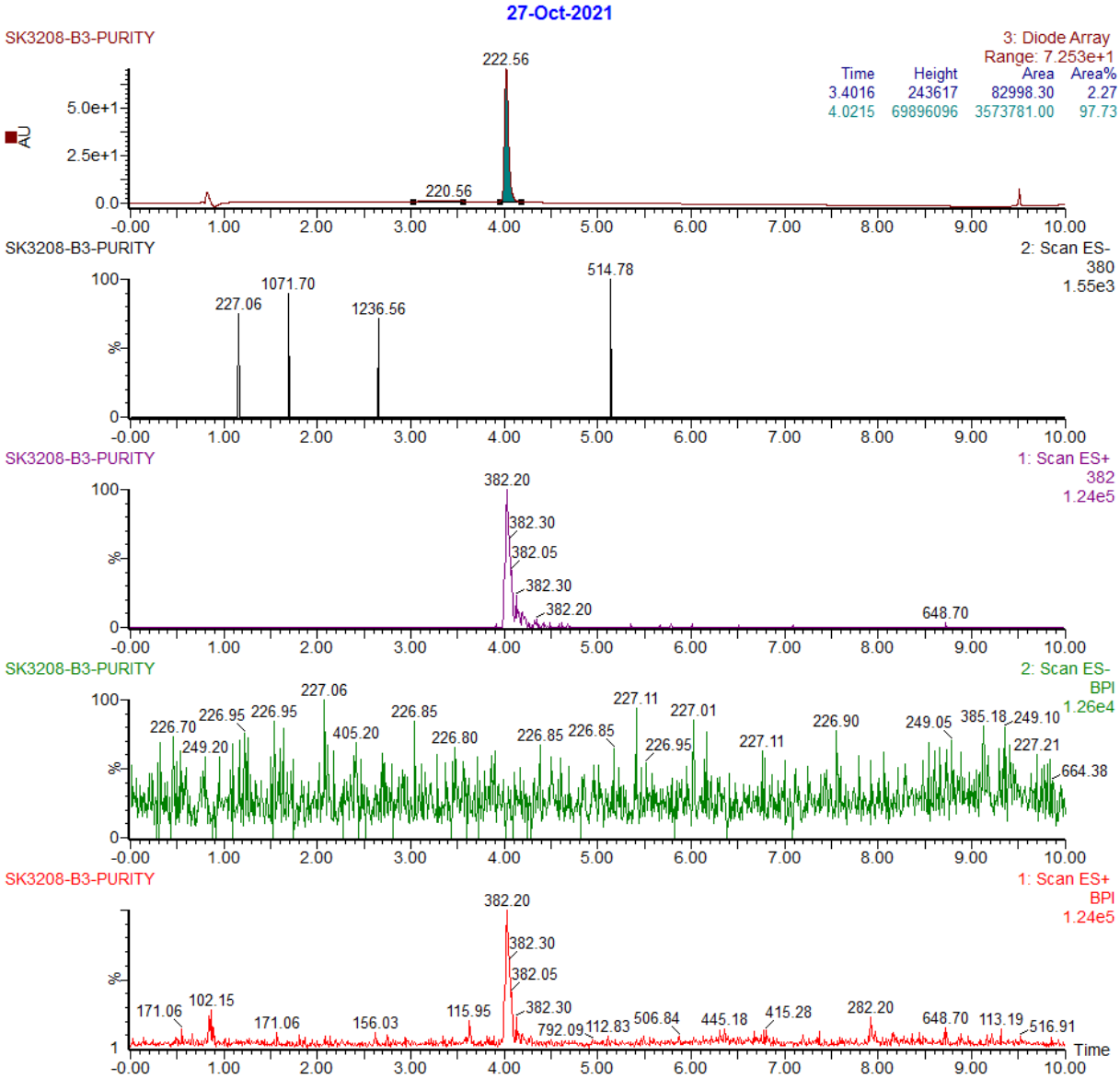

Compound **15b**

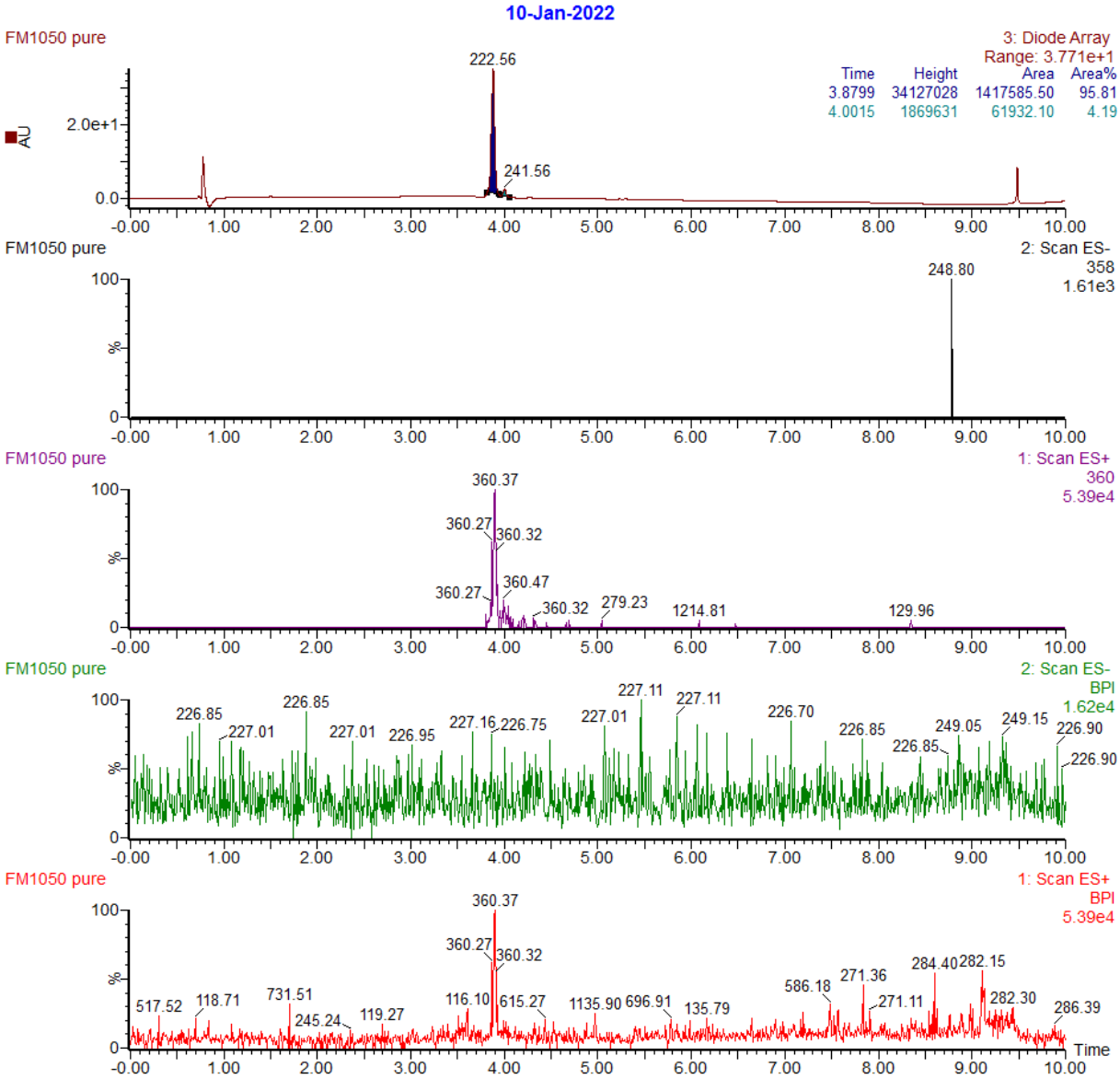

Compound **15c**

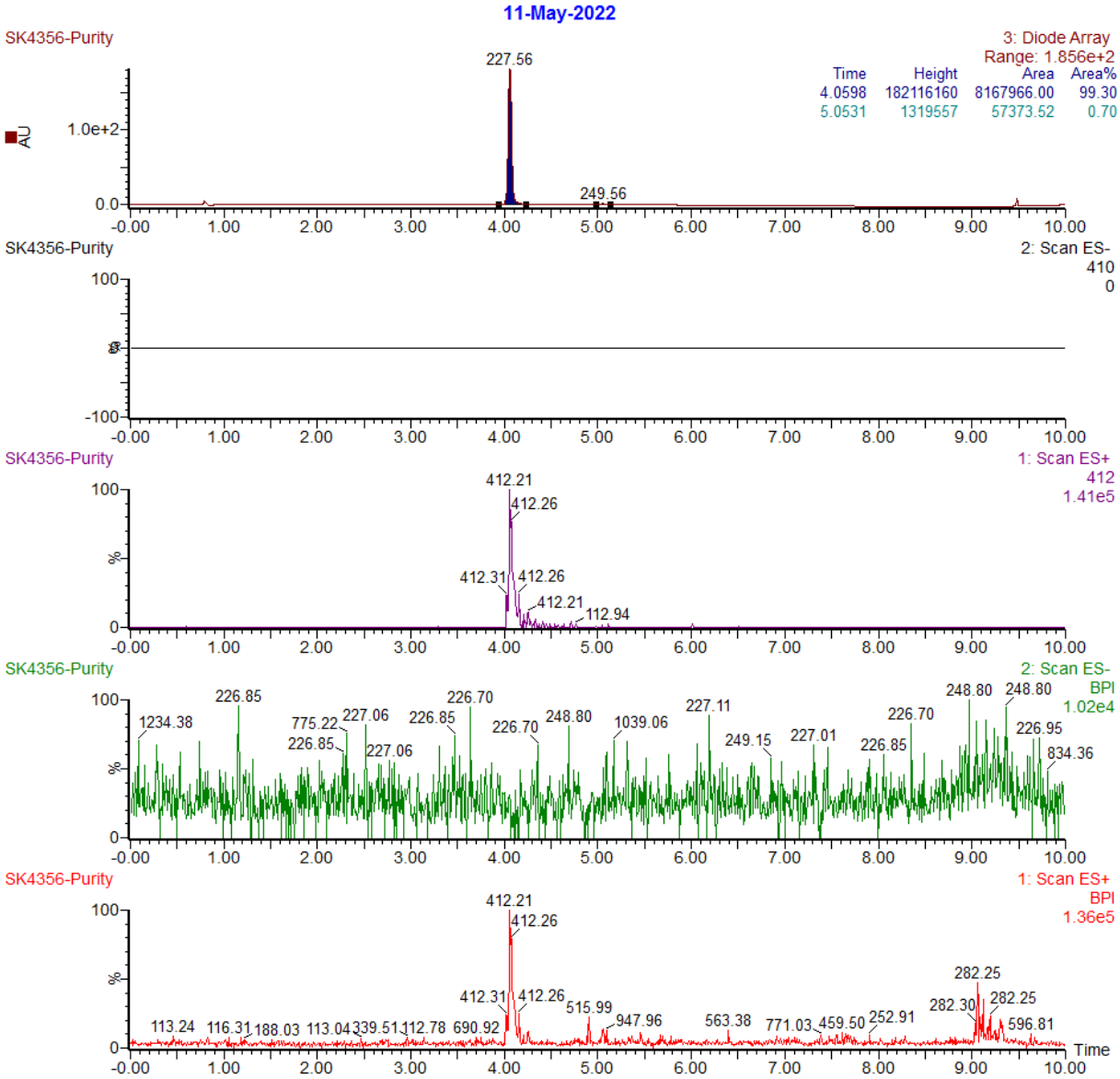

Compound **15d**

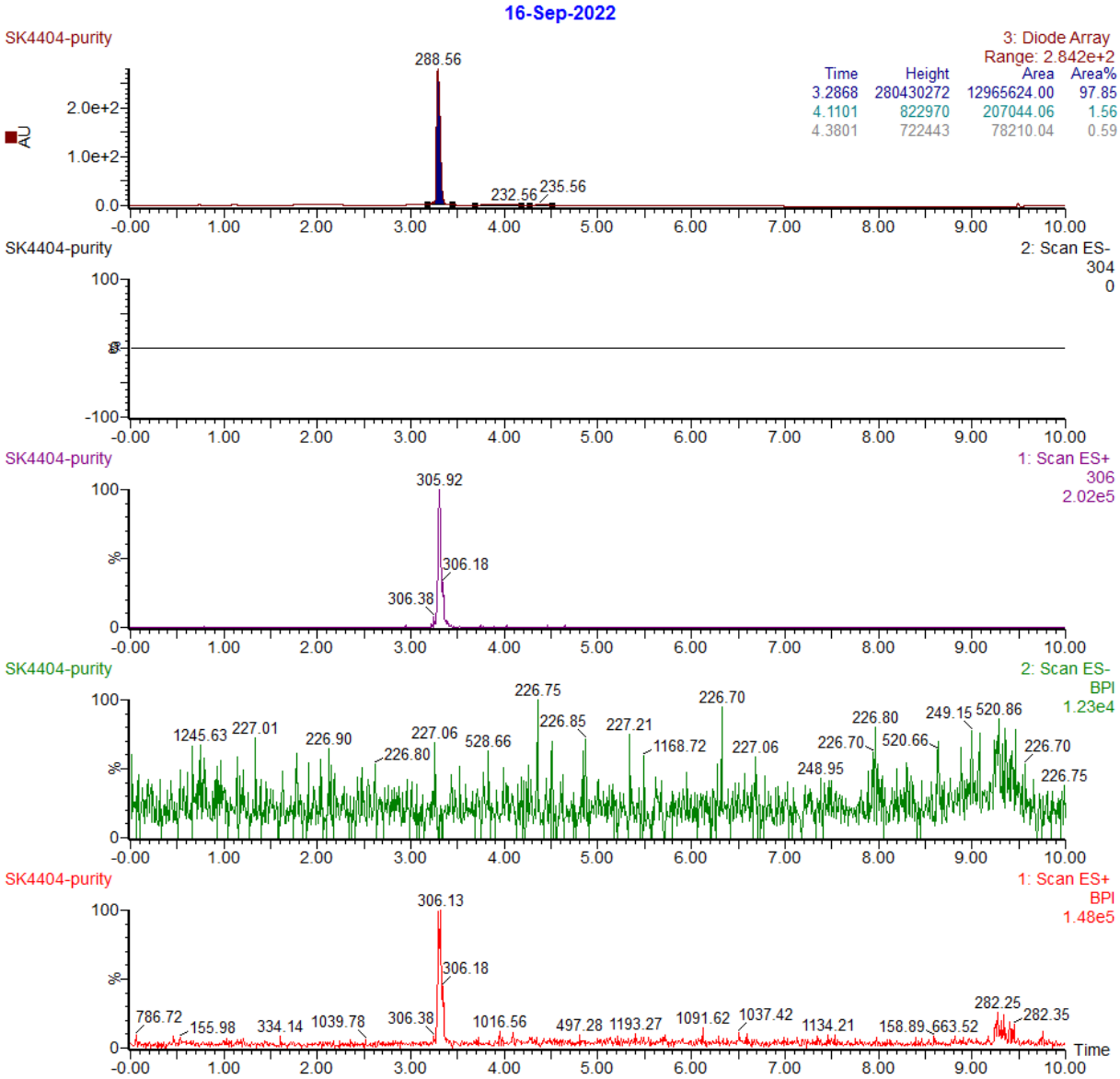

Compound **29**

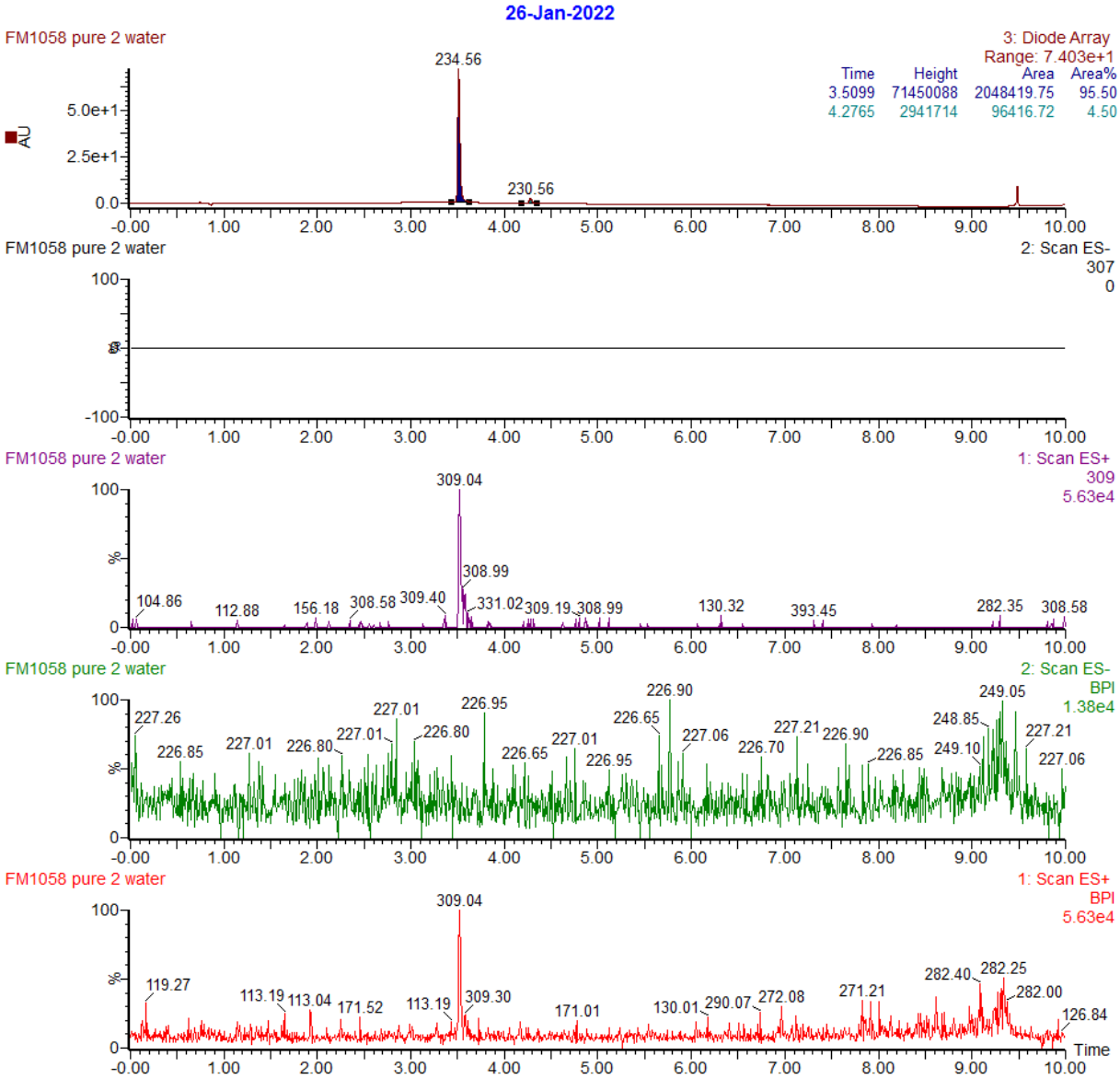
26-Jan-2022
FM1058 pure 2 water
3: Diode Array
Range: 7.403e+1
Time Height Area Area%
3.5099 71450088 2048419.75 95.50
4.2765 2941714 96416.72 4.50
234.56
230.56
AU
FM1058 pure 2 water
2: Scan ES-
307
0
FM1058 pure 2 water
1: Scan ES+
309
5.63e4
309.04
308.99
FM1058 pure 2 water
2: Scan ES-
BPI
1.38e4
FM1058 pure 2 water
1: Scan ES+
BPI
5.63e4
309.04
Time

References

[1] Rigaku Oxford Diffraction, (2020), CrysAlisPro Software system, version 1.171.41.93a, Rigaku Corporation, Oxford, UK.

[2] O.V. Dolomanov, L.J. Bourhis, R.J. Gildea, J.A.K. Howard, H. Puschmann, J. Appl. Crystallogr. 42 (2009) 339-341.

[3] G.M. Sheldrick, Acta Crystallogr. Sect. A71 (2015) 3-8.

[4] G.M. Sheldrick, Acta Crystallogr. Sect. C71 (2015) 3-8.